213038US22

IN THE UNITED STATES PATENT & TRADEMARK OFFICE

IN RE APPLICATION OF: WILLIS ET AL.	:
	: GROUP ART UNIT: **3746** (ANTICIPATED)
SERIAL NO.: NEW APPLICATION	:
FILED: HEREWITH	: EXAMINER: **LOUIS J. CASAREGOLA** (REQUESTED)

FOR: INTEGRATED TURBINE POWER GENERATION SYSTEM HAVING LOW PRESSURE SUPPLEMENTAL CATALYTIC REACTOR

ASSISTANT COMMISSIONER FOR PATENTS
WASHINGTON, D.C. 20231

SIR:

REQUEST FOR SPECIFIC EXAMINER REGARDING *COPIED CLAIMS*

I request that this application be assigned to Primary Examiner ***LOUIS J. CASAREGOLA***, in group art unit 3764 because (1) he examined **the exact same claims** as claims 1-2 presented herein when he examined and allowed United States patent No. 6,205,768 and (2) because this application raises interference issues requiring the attention of a primary examiner knowledgeable in this technology.

Claims 1-3 in this application are identical copies of (1) claims 1 and 2 in United States patent No. 6,205,768, issued March 27, 2001, naming Robert W.Dibble and Rajiv K.Mongia as

inventors, and assigned at issue to Solo Energy Corporation, and (2) claim 1 in United States patent No. 6,109,693 isued August 22, 2000, naming Rajiv K. Mongia, George L. Touchon, Robert W. Dibble, and Martin L. Lagod as inventors, and assigned at issue to Solo Energy Corporation. This application supports the limitations defined in claims 1-3; see for example Figure 3 showing separate air and fuel lines 18, 46, the compressor 4, the recuperator 12, the primary catalytic converer 14, the turbine 10, and the low pressure catalytic converter 16.

In addition, claims 4-9 are modeled after the three claims identified above in the '768 and '693 patents.

I intend to file a 37 CFR 1.607 interference request with those two patents as soon as practicable after filing this application.

Since this application raises interference issues, ***it should be placed on the examiner's special cases docket.***

Respectfully submitted,

Richard A. Neifeld
Registration No. 35,299
Presumptive Attorney of Record (pending filing of Power)
Tel(direct): (703) 412-6492
Fax: (703) 413-2220
Email: rneifeld@oblon.com

Oblon, Spivak, McClelland, Maier & Neustadt, P.C.
Crystal Square Five - Fourth Floor
1755 Jefferson Davis Highway
Arlington, Virginia 22202

I:\atty\RAN\clients\Capstone\213038\ReqForExaminerandCopiedClaims.010821.wpd

Appendix A

POWER CONTROLLER

REFERENCE TO RELATED APPLICATION

This application claims the benefit of U.S. Provisional Application No. 60/080,457, filed on April 2, 1998.

BACKGROUND OF THE INVENTION

1. Field of the Invention

This invention relates generally to power generation and processing systems and in particular to distributed generation power systems.

2. Description of the Prior Art

Conventional power generation and distribution systems are configured to maximize the specific hardware used. In the case of a turbine power motor, for example, the output or bus voltage in a conventional power distribution system varies with the speed of the turbine. In such systems, the turbine speed must be regulated to control the output or bus voltage. Consequently, the engine cannot be run too low in speed else the bus voltage would not be high enough to generate some of the voltages that are needed. As a result, the turbine would have to be run at higher speeds and lower temperatures, making it less efficient.

What is needed therefore is a power generation and distribution system where the bus voltage is regulated by a bi-directional controller independent of turbine speed.

SUMMARY OF THE INVENTION

The present invention provides in a first aspect, a power controller which provides a distributed generation power networking system in which bi-directional power converters are used with a common DC bus for permitting compatibility

between various energy components. Each power converter operates essentially as a customized bi-directional switching converter configured, under the control of the power controller, to provide an interface for a specific energy component to the DC bus. The power controller controls the way in which each energy component, at any moment, will sink or source power, and the manner in which the DC bus is regulated. In this way, various energy components can be used to supply, store and/or use power in an efficient manner. The various energy components include energy sources, loads, storage devices and combinations thereof.

In another aspect, the present invention provides a turbine system including a turbine engine, a load, a power controller, an energy reservoir for providing transient power to the DC bus and an energy reservoir controller, in communication with the power controller for providing control to the energy reservoir. The power controller includes an engine power conversion in communication with the turbine engine, an utility power conversion in communication with the load and a DC bus.

These and other features and advantages of this invention will become further apparent from the detailed description and accompanying figures that follow. In the figures and description, numerals indicate the various features of the invention, like numerals referring to like features throughout both the drawing figures and the written description.

BRIEF DESCRIPTION OF THE DRAWINGS

FIG. 1 is a block diagram of a power controller according to the present invention.

FIG. 2 is a detailed block diagram of a power converter in the power controller illustrated in FIG. 1.

FIG. 3 is a simplified block diagram of a turbine system including the power architecture of the power controller illustrated in FIG. 1.

FIG. 4 is a block diagram of the power architecture of a typical implementation of the power controller illustrated in FIG. 1.

FIG. 5 is a schematic diagram of the internal power architecture of the power controller illustrated in FIG. 1.

FIG. 6 is a functional block diagram of an interface between load/utility grid and turbine generator using the power controller according to the present invention.

FIG. 7 is a functional block diagram of an interface between load/utility grid and turbine generator using the power controller for a stand-alone application according to the present invention.

FIG. 8 is a schematic diagram of an interface between a load/utility grid and turbine generator using the power controller according to the present invention.

FIG. 9 is a block diagram of the software architecture for the power controller including external interfaces.

FIG. 10 is a block diagram of an EGT control mode loop for regulating the temperature of the turbine.

FIG. 11 is a block diagram of a speed control mode loop for regulating the rotating speed of the turbine.

FIG. 12 is a block diagram of a power control mode loop for regulating the power producing potential of the turbine.

FIG. 13 is a state diagram showing various operating states of the power controller.

FIG. 14 is a block diagram of the power controller interfacing with a turbine and fuel device.

FIG. 15 is a block diagram of the power controller in multi-pack configuration.

FIG. 16 is a block diagram of a utility grid analysis system for the power controller according to the present invention.

FIG. 17 is a graph of voltage against time for the utility grid analysis system illustrated in FIG. 16.

FIG. 18 is a diagram of the power controller shown in FIG. 16, including brake resistor.

DETAILED DESCRIPTION OF THE PREFERRED EMBODIMENT(S)

Referring to FIG.1, power controller 10 provides a distributed generation power networking system in which bi-directional (i.e. reconfigurable) power converters are

used with a common DC bus for permitting compatibility between one or more energy components. Each power converter operates essentially as a customized bi-directional switching converter configured, under the control of power controller 10, to provide an interface for a specific energy component to DC bus 24. Power controller 10 controls the way in which each energy component, at any moment, will sink or source power, and the manner in which DC bus 24 is regulated. In this way, various energy components can be used to supply, store and/or use power in an efficient manner.

One skilled in the art will recognize that the particular configurations shown herein are for illustrative purposes only. In particular, the present invention is not limited to the use of three bi-directional converters as shown in FIG. 1. Rather, the number of power converters is dependent on various factors, including but not limited to, the number of energy components and the particular power distribution configuration desired. For example, as illustrated in FIGS. 5 and 6, power controller 10 can provide a distributed generation power system with as few as two power converters.

The energy components, as shown in FIG. 1, include energy source 12, utility/load 18 and storage device 20. The present invention is not limited to the distribution of power between energy source 12, energy storage device 20 and utility/load 18, but rather may be adapted to provide power distribution in an efficient manner for any combination of energy components.

Energy source 12 may be a gas turbine, photovoltaics, wind turbine or any other conventional or newly developed source. Energy storage device 20 may be a flywheel, battery, ultracap or any other conventional or newly energy storage device. Load 18 may be an utility grid, dc load, drive motor or any other conventional or newly developed utility/load 18.

Referring now to FIG. 2, a detailed block diagram of power converter 14 in power controller 10, shown in FIG. 1, is illustrated. Energy source 12 is connected to DC bus 24 via power converter 14. Energy source 12 may be, for example, a gas turbine driving an AC generator to produce AC which is applied to power converter 14. DC bus 24 connects power converter 14 to utility/load 18 and additional energy components 36. Power converter 14 includes input filter 26, power switching system

28, output filter 34, signal processor 30 and main CPU 32. In operation, energy source 12 applies AC to input filter 26 in power converter 14. The filtered AC is then applied to power switching system 28 which may conveniently be a series of insulated gate bipolar transistor (IGBT) switches operating under the control of signal processor (SP) 30 which is controlled by main CPU 32. One skilled in the art will recognize that other conventional or newly developed switches may be utilized as well. The output of the power switching system 28 is applied to output filter 34 which then applies the filtered DC to DC bus 24.

In accordance with the present invention, each power converter 14, 16 and 22 operates essentially as a customized, bi-directional switching converter under the control of main CPU 32, which uses SP 30 to perform its operations. Main CPU 32 provides both local control and sufficient intelligence to form a distributed processing system. Each power converter 14, 16 and 22 is tailored to provide an interface for a specific energy component to DC bus 24. Main CPU 32 controls the way in which each energy component 12, 18 and 20 sinks or sources power, and DC bus 24 is regulated at any time. In particular, main CPU 32 reconfigures the power converters 14, 16 and 22 into different configurations for different modes of operation. In this way, various energy components 12, 18 and 20 can be used to supply, store and/or use power in an efficient manner. In the case of a turbine power generator, for example, a conventional system regulates turbine speed to control the output or bus voltage. In the power controller, the bi-directional controller independently of turbine speed regulates the bus voltage.

Operating Modes

FIG. 1 shows the system topography in which DC bus 24, regulated at 800 v DC for example, is at the center of a star pattern network. In general, energy source 12 provides power to DC bus 24 via power converter 14 during normal power generation mode. Similarly, during the power generation mode, power converter 16 converts the power on DC bus 24 to the form required by utility/load 18, which may be any type of load including a utility web. During other modes of operation, such as utility start up, power converters 14 and 16 are controlled by the main processor to operate in different manners.

For example, energy is needed to start the turbine. This energy may come from load/utility grid 18 (utility start) or from energy storage 20 (battery start), such as a battery, flywheel or ultra-cap. During a utility start up, power converter 16 is required to apply power from load 18 to DC bus 24 for conversion by power converter 14 into the power required by energy source 12 to startup. During utility start, energy source or turbine 12 is controlled in a local feedback loop to maintain the turbine revolutions per minute (RPM). Energy storage or battery 20 is disconnected from DC bus 24 while load/utility grid 10 regulates V_{DC} on DC bus 24.

Similarly, in the battery start mode, the power applied to DC bus 24 from which energy source 12 is started may be provided by energy storage 20 which may be a flywheel, battery or similar device. Energy storage 20 has its own power conversion circuit in power converter 22, which limits the surge current into DC bus 24 capacitors, and allows enough power to flow to DC Bus 24 to start energy source 12. In particular, power converter 16 isolates DC bus 24 so that power converter 14 can provide the required starting power from DC bus 24 to energy source 12.

Electronics Architecture

Referring to FIG. 3, a simplified block diagram of a turbine system 50 using the power controller electronics architecture of the present invention is illustrated. The turbine system 50 includes a fuel metering system 42, turbine engine 58, power controller 52, energy reservoir conversion 62, energy/reservoir 64 and load/utility grid 60. The fuel metering system 42 is matched to the available fuel and pressure. The power controller 52 converts the electricity from turbine engine 58 into regulated DC then converts it to utility grade AC electricity. By separating the engine control from the converter that creates the utility grade power, greater control of both processes is realized. All of the interconnections are comprised of a communications bus and a power connection.

The power controller 52 includes an engine power conversion 54 and utility power conversion 56 which provides for the two power conversions that take place between the turbine 58 and the load/utility grid 60. One skilled in the art will recognize that the power controller 52 can provide a distributed generation power system with as few as two power converters 54 and 56. The bi-directional (i.e. reconfigurable) power

converters 54 and 56 are used with a common regulated DC bus 66 for permitting compatibility between the turbine 58 and load/utility grid 60. Each power converter 54 and 56 operates essentially as a customized bi-directional switching converter configured, under the control of the power controller 10, to provide an interface for a specific energy component 58 or 60 to the DC bus 66. The power controller 10 controls the way in which each energy component, at any moment, will sink or source power, and the manner in which the DC bus 66 is regulated. Both of these power conversions 54 and 56 are capable of operating in a forward or reverse direction. This allows starting the turbine 58 from either the energy reservoir 64 or the load/utility grid 60. The regulated DC bus 66 allows a standardized interface to energy reservoirs such as batteries, flywheels, and ultra-caps. The architecture of the present invention permits the use of virtually any technology that can convert its energy to/from electricity. Since the energy may flow in either direction to or from the energy reservoir 64, transients may be handled by supplying energy or absorbing energy. Not all systems will need the energy reservoir 64. The energy reservoir 64 and its energy reservoir conversion 62 are not contained inside the power controller 52.

Referring to FIG. 4, the power architecture 68 of a typical implementation of the power controller 70 is shown. The power controller 70 includes a generator converter 72 and output converter 74 which provides for the two power conversions that take place between the turbine 76 and the load/utility grid 78. In particular, the generator converter 72 provides for AC to DC power conversion and the output converter 74 provides for DC to AC power conversion. Both of these power converters 72 and 74 are capable of operating in a forward or reverse direction. This allows starting the turbine 76 from either the energy storage device 86 or the load/utility grid 78. Since the energy may flow in either direction to or from the energy storage device 86, transients may be handled by supplying energy or absorbing energy. The energy storage device 86 and its DC converter 84 are not contained inside the power controller 70. The DC converter 84 provides for DC to DC power conversion.

Referring to FIG. 5, a schematic 90 of a typical internal power architecture, such as that shown in FIG. 4, is shown. The turbine has an integral PMG that can be used as either a generator (for starting) or a generator (normal mode of operation).

Because all of the controls can be performed in the digital domain and all switching (except for one output contactor) is done with solid state switches, it is easy to shift the direction of the power flow as needed. This permits very tight control of the turbine during starting and stopping. In a typical configuration, the power output is a 480 VAC, 3-phase output. One skilled in the art will recognize that the present invention may be adapted to provide for other power output requirements such as a 3-phase, 400 VAC, and single-phase, 480 VAC.

Power controller 92 includes generator converter 94 and output converter 96. Generator converter 94 includes IGBT switches 94, such as a seven-pack IGBT module 94, driven by control logic 98, providing a variable voltage, variable frequency 3-phase drive to the PMG 100. Inductors 102 are utilized to minimize any current surges associated with the high frequency switching components which may affect the PMG 100 to increase operating efficiency.

IGBT module 94 is part of the electronics that controls the engine of the turbine. IGBT module 94 incorporates gate driver and fault sensing circuitry as well as a seventh IGBT used to dump power into a resistor. The gate drive inputs and fault outputs require external isolation. Four external, isolated power supplies are required to power the internal gate drivers. IGBT module 94 is typically used in a turbine system that generates 480 VAC at its output terminals delivering up to 30 kWatts to a freestanding or utility-connected load. During startup and cool down (and occasionally during normal operation), the direction of power flow through the seven-pack reverses. When the turbine is being started, power is supplied to the DC bus 112 from either a battery (not shown) or from the utility grid 108. The DC is converted to a variable frequency AC voltage to generator the turbine.

For utility grid connect operation, control logic 110 sequentially drives the solid state IGBT switches, typically configured in a six-pack IGBT module 96, associated with load converter 96 to boost the utility voltage to provide start power to the generator converter 94. The IGBT switches in load converter 96 are preferably operated at a high (15 kHz) frequency, and modulated in a pulse width modulation manner to provide four quadrant converter operation. Inductors 104 and AC filter

capacitors 106 are utilized to minimize any current surges associated with the high frequency switching components which may affect load 108.

Six-pack IGBT module 96 is part of the electronics that controls the converter of the turbine. IGBT module 96 incorporates gate driver and fault sensing circuitry. The gate drive inputs and fault outputs require external isolation. Four external, isolated power supplies are required to power the internal gate drivers. IGBT module 96 is typically used in a turbine system that generates 480 VAC at its output terminals delivering up to approximately 30 kWatts to a free-standing or utility-connected load. After the turbine is running, six-pack IGBT module 96 is used to convert the regulated DC bus voltage to the approximately 50 or 60 hertz utility grade power. When there is no battery (or other energy reservoir), the energy to run the engine during startup and cool down must come from utility grid 108. Under this condition, the direction of power flow through the six-pack IGBT module 96 reverses. DC bus 112 receives its energy from utility grid 108, using six-pack IGBT module 96 as a boost converter (the power diodes act as a rectifier). The DC is converted to a variable frequency AC voltage to generator the turbine. To accelerate the engine as rapidly as possible at first, current flows at the maximum rate through seven-pack IGBT module 94 and also six-pack IGBT module 96.

Dual IGBT module 114, driven by control logic 116, is used to provide an optional neutral to supply 3 phase, 4 wire loads.

Startup

Energy is needed to start the turbine. Referring to FIGS. 3 and 4, this energy may come from utility grid 60 or from energy reservoir 64, such as a battery, flywheel or ultra-cap. When utility grid 60 supplies the energy, utility grid 60 is connected to power controller 52 through two circuits. First is an output contactor that handles the full power (30 kWatts). Second is a "soft-start" or "pre-charge" circuit that supplies limited power (it is current limited to prevent very large surge currents) from utility grid 66 to DC bus 62 through a simple rectifier. The amount of power supplied through the soft-start circuit is enough to start the housekeeping power supply, power the control board, and run the power supplies for the IGBTs, and close the output contactor. When the contactor closes, the IGBTs are configured to create DC from the

AC waveform. Enough power is created to run the fuel metering circuit 42, start the engine, and close the various solenoids (including the dump valve on the engine).

When energy reservoir 64 supplies the energy, energy reservoir 64 has its own power conversion circuit 62 that limits the surge circuit into DC bus capacitors. Energy reservoir 64 allows enough power to flow to DC bus 62 to run fuel-metering circuit 42, start the engine, and close the various solenoids (including the dump valve on the engine). After the engine becomes self-sustaining, the energy reservoir starts to replace the energy used to start the engine, by drawing power from DC bus 62. In addition to the sequences described above, power controller senses the presence of other controllers during the initial power up phase. If another controller is detected, the controller must be part of a multi-pack, and proceeds to automatically configure itself for operation as part of a multi-pack.

System Level Operation

Referring to FIG. 6, a functional block diagram 130 of an interface between utility grid 132 and turbine generator 148 using power controller 136 of the present invention is shown. In this example, power controller 136 includes two bi-directional converters 138 and 140. Permanent magnet generator converter 140 starts turbine 148 (using the generator as a generator) from utility or battery power. Load converter 138 then produces AC power using an output from generator converter 140 to draw power from high-speed turbine generator 148. Power controller 136 also regulates fuel to turbine 148 and provides communications between units (in paralleled systems) and to external entities.

During a utility startup sequence, utility 132 supplies starting power to turbine 148 by "actively" rectifying the line via load converter 138, and then converting the DC to variable voltage, variable frequency 3-phase power in generator converter 136. As is illustrated in FIG. 7, for stand-alone applications 150, the start sequence is the same as the utility start sequence shown in FIG. 6 with the exception that the start power comes from battery 170 under the control of an external battery controller. Load 152 is then fed from the output terminals of load converter 158.

Referring to FIG. 8, a schematic illustration 180 of an interface between utility grid 132 and turbine generator 148 using the power controller is illustrated. Control

logic 184 also provides power to fuel cutoff solenoids 198, fuel control valve 200 and igniter 202. An external battery controller (not shown), if used, connects directly to DC bus 190. In accordance with an alternative embodiment of the invention, a fuel system (not shown) involving a compressor (not shown) operated from a separate variable speed drive can also derive its power directly from DC bus 190.

In operation, control and start power comes from either the external battery controller (for battery start applications) or from the utility, which is connected to a rectifier using inrush limiting techniques to slowly charge internal bus capacitor 190. For utility grid connect operation, control logic 184 sequentially drives solid state IGBT switches 214 associated with load converter 192 to boost the utility voltage to provide start power to generator converter 186. Switches 214 are preferably operated at a high (15 kHz) frequency, and modulated in a pulse width modulation manner to provide four quadrant converter operation. In accordance with the present invention, load converter 192 either sources power from DC bus 190 to utility grid 222 or from utility grid 222 to DC bus 190. A current regulator (not shown) may achieve this control. Optionally, two of the switches 214 serve to create an artificial neutral for stand-alone applications (for stand-alone applications, start power from an external DC supply (not shown) associated with external DC converter 220 is applied directly to DC bus 190).

Solid state (IGBT) switches 214 associated with generator converter 186 are also driven from control logic 184, providing a variable voltage, variable frequency 3-phase drive to generator 218 to start turbine 208. Control logic 184 receives feedback via current sensors I_{sens} as turbine 206 is ramped up in speed to complete the start sequence. When turbine 206 achieves a self sustaining speed of, for example, approx. 40,000 RPM, generator converter 186 changes its mode of operation to boost the generator output voltage and provide a regulated DC bus voltage.

PMG filter 188 associated with generator converter 186 includes three inductors to remove the high frequency switching component from permanent magnet generator 208 to increase operating efficiency. Output AC filter 194 associated with load converter 192 includes three or optionally four inductors (not shown) and AC

filter capacitors (not shown) to remove the high frequency switching component. Output contactor 210 disengages load converter 192 in the event of a unit fault.

During a start sequence, control logic 184 opens fuel cutoff solenoid 198 and maintains it open until the system is commanded off. Fuel control 200 may be a variable flow valve providing a dynamic regulating range, allowing minimum fuel during start and maximum fuel at full load. A variety of fuel controllers, including but not limited to, liquid and gas fuel controllers, may be utilized. One skilled in the art will recognize that the fuel control can be by various configurations, including but not limited to a single or dual stage gas compressor accepting fuel pressures as low as approximately ¼ psig. Igniter 202, a spark type device similar to a spark plug for an internal combustion engine, is operated only during the start sequence.

For stand-alone operation, turbine 206 is started using external DC converter 220 which boosts voltage from a battery (not shown), and connects directly to the DC bus 190. Load converter 192 is then configured as a constant voltage, constant frequency (for example, approximately 50 or 60 Hz) source. One skilled in the art will recognize that the output is not limited to a constant voltage, constant frequency source, but rather may be a variable voltage, variable frequency source. For rapid increases in output demand, external DC converter 220 supplies energy temporarily to DC bus 190 and to the output. The energy is restored after a new operating point is achieved.

For utility grid connect operation, the utility grid power is used for starting as described above. When turbine 206 has reached a desired operating speed, converter 192 is operated at utility grid frequency, synchronized with utility grid 222, and essentially operates as a current source converter, requiring utility grid voltage for excitation. If utility grid 222 collapses, the loss of utility grid 222 is sensed, the unit output goes to zero (0) and disconnects. The unit can receive external control signals to control the desired output power, such as to offset the power drawn by a facility, but ensure that the load is not backfed from the system.

Power Controller Software

Referring to FIG. 9, power controller 230 includes main CPU 232, generator SP 234 and converter SP 236. Main CPU software program sequences events which occur

inside power controller 230 and arbitrates communications to externally connected devices. Main CPU 232 is preferably a MC68332 microprocessor, available from Motorola Semiconductor, Inc. of Phoenix, Arizona. Other suitable commercially available microprocessors may be used as well. The software performs the algorithms that control engine operation, determine power output and detect system faults.

Commanded operating modes are used to determine how power is switched through the major converts in the controller. The software is responsible for turbine engine control and issuing commands to other SP processors enabling them to perform the generator converter output converter power switching. The controls also interface with externally connected energy storage devices (not shown) that provide black start and transient capabilities.

Generator SP 234 and converter SP 236 are connected to power controller 230 via serial peripheral interface (SPI) bus 238 to perform generator and converter control functions. Generator SP 234 is responsible for any switching which occurs between DC bus 258 and the output to generator. Converter SP 236 is responsible for any switching which occurs between DC bus 258 and output to load. As illustrated in FIG. 5, generator SP 234 and converter SP 236 operate IGBT modules.

Local devices, such as a smart display 242, smart battery 244 and smart fuel control 246, are connected to main CPU 232 in power controller 230 via intracontroller bus 240, which may be a RS485 communications link. Smart display 242, smart battery 244 and smart fuel control 246 performs dedicated controller functions, including but not limited to display, energy storage management, and fuel control functions.

Main CPU 232 in power controller 230 is coupled to user port 248 for connection to a computer, workstation, modem or other data terminal equipment which allows for data acquisition and/or remote control. User port 248 may be implemented using a RS232 interface or other compatible interface.

Main CPU 232 in power controller 230 is also coupled to maintenance port 250 for connection to a computer, workstation, modem or other data terminal equipment which allows for remote development, troubleshooting and field upgrades.

Maintenance port 250 may be implemented using a RS232 interface or other compatible interface.

The main CPU processor software communicates data through a TCP/IP stack over intercontroller bus 252, typically an Ethernet 10 Base 2 interface, to gather data and send commands between power controllers (as shown and discussed in detail with respect to FIG. 15). In accordance with the present invention, the main CPU processor software provides seamless operation of multiple paralleled units as a single larger generator system. One unit, the master, arbitrates the bus and sends commands to all units.

Intercontroller bus 254, which may be a RS485 communications link, provides high-speed synchronization of power output signals directly between converter SPs, such as converter SP 236. Although the main CPU software is not responsible for communicating on the intercontroller bus 254, it informs converter SPs, including converter SP 236, when main CPU 232 is selected as the master.

External option port bus 256, which may be a RS485 communications link, allows external devices, including but not limited to power meter equipment and auto disconnect switches, to be connected to generator SP 234.

In operation, main CPU 232 begins execution with a power on self-test when power is applied to the control board. External devices are detected providing information to determine operating modes the system is configured to handle. Power controller 230 waits for a start command by making queries to external devices. Once received, power controller 230 sequences up to begin producing power. As a minimum, main CPU 232 sends commands to external smart devices 242, 244 and 246 to assist with bringing power controller 230 online. If selected as the master, the software may also send commands to initiate the sequencing of other power controllers (FIG. 15) connected in parallel. A stop command will shutdown the system bringing it offline.

System I/O

The main CPU 232 software interfaces with several electronic circuits (not shown) on the control board to operate devices that are universal to all power controllers 230. Interface to system I/O begins with initialization of registers within

power controller 230 to configure internal modes and select external pin control. Once initialized, the software has access to various circuits including discrete inputs/outputs, analog inputs/outputs, and communication ports. These external devices may also have registers within them that require initialization before the device is operational.

Each of the following sub-sections provides a brief overview that defines the peripheral device the software must interface with. The contents of these sub-sections do not define the precise hardware register initialization required.

Communications

Referring to FIG. 9, main CPU 232 is responsible for all communication systems in power controller 230. Data transmission between a plurality of power controllers 230 is accomplished through intercontroller bus 252. Main CPU 232 initializes the communications hardware attached to power controller 230 for intercontroller bus 252.

Main CPU 232 provides control for external devices, including smart devices 242, 244 and 246, which share information to operate. Data transmission to external devices, including smart display 242, smart battery 244 and smart fuel control 246 devices, is accomplished through intracontroller communications bus 240. Main CPU 232 initializes any communications hardware attached to power controller 230 for intracontroller communications bus 240 and implements features defined for the bus master on intracontroller communications bus 240.

Communications between devices such as switch gear and power meters used for master control functions exchange data across external equipment bus 246. Main CPU 232 initializes any communications hardware attached to power controller 230 for external equipment port 246 and implements features defined for the bus master on external equipment bus 246.

Communications with a user computer is accomplished through user interface port 248. Main CPU 232 initializes any communications hardware attached to power controller 230 for user interface port 248. In a typical configuration, at power up, the initial baud rate will be selected to 19200 baud, 8 data bits, 1 stop, and no parity. The user has the ability to adjust and save the communications rate setting via user interface port 248 or optional smart external display 242. The saved communications rate is

used the next time power controller 230 is powered on. Main CPU 232 communicates with a modem (not shown), such as a Hayes compatible modem, through user interface port 248. Once communications are established, main CPU 232 operates as if were connected to a local computer and operates as a slave on user interface port 248 (it only responds to commands issued).

Communications to service engineers, maintenance centers, and so forth are accomplished through maintenance interface port 250. Main CPU 232 initializes the communications to any hardware attached to power controller 230 for maintenance interface port 250. In a typical implementation, at power up, the initial baud rate will be selected to 19200 baud, 8 data bits, 1 stop, and no parity. The user has the ability to adjust and save the communications rate setting via user port 248 or optional smart external display 242. The saved communications rate is used the next time power controller 230 is powered on. Main CPU 232 communicates with a modem, such as a Hayes compatible modem, through maintenance interface port 250. Once communications are established, main CPU 232 operates as if it were connected to a local computer and operates as a slave on maintenance interface port 250 (it only responds to commands issued).

Controls

Referring to FIG. 9, main CPU 232 orchestrates operation for motor, converter, and engine controls for power controller 230. The main CPU 232 does not directly perform motor and converter controls. Rather, generator and converter SP processors 234 and 236 perform the specific control algorithms based on data communicated from main CPU 232. Engine controls are performed directly by main CPU 232 (see FIG. 14).

Main CPU 232 issues commands via SPI communications bus 238 to generator SP 234 to execute the required motor control functions. Generator SP 234 will operate the motor (not shown) in either a DC bus mode or a RPM mode as selected by main CPU 232. In the DC bus voltage mode, generator SP 234 uses power from the motor to maintain the DC bus at the setpoint. In the RPM mode, generator SP 234 uses power from the motor to maintain the engine speed at the setpoint. Main CPU 232 provides Setpoint values.

Main CPU 232 issues commands via SPI communications bus 238 to converter SP 236 to execute required converter control functions. Converter SP 236 will operate the converter (not shown) in a DC bus mode, output current mode, or output voltage mode as selected by main CPU 232. In the DC bus voltage mode, converter SP 236 regulates the utility power provided by power controller 230 to maintain the internal bus voltage at the setpoint. In the output current mode, converter SP 236 uses power from the DC bus to provide commanded current out of the converter. In the output voltage mode, converter SP 236 uses power from the DC bus to provide commanded voltage out of the converter. Main CPU 232 provides Setpoint values.

Referring to FIGS. 10-12, control loops 260, 282 and 300 are used to regulate engine controls. These loops include exhaust gas temperature (EGT) control (FIG. 10), speed control (FIG. 11) and power control (FIG. 12). All three of the control loops 260, 282 and 300 are used individually and collectively by main CPU 232 to provide the dynamic control and performance required of power controller 230. These loops are joined together for different modes of operation.

The open-loop light off control algorithm is a programmed command of the fuel device used to inject fuel until combustion begins. In a typical configuration, main CPU 232 takes a snap shot of the engine EGT and begins commanding the fuel device from about 0% to 25% of full command over about 5 seconds. Engine light is declared when the engine EGT rises about 28° C (50° F) from the initial snap shot.

Referring to FIG. 10, EGT control mode loop 260 provides various fuel output commands to regulate the temperature of the turbine. Engine speed signal 262 is used to determine the maximum EGT setpoint temperature 266 in accordance with predetermined setpoint temperature values. EGT setpoint temperature 266 is compared by comparator 268 against feedback EGT signal 270 to determine error signal 272, which is then applied to a proportional-integral (PI) algorithm 274 for determining the fuel command required to regulate EGT at the setpoint. Maximum/minimum fuel limits 278 are used to limit EGT control algorithm fuel command output 276 to protect from integrator windup. Resultant output signal 280 is regulated EGT signal fuel flow command. In operation, EGT control mode loop 260 operates at about a 100 ms rate.

Referring to FIG. 11, speed control mode loop 282 provides various fuel output commands to regulate the rotating speed of the turbine. Feedback speed signal 288 is read and compared by comparator 286 against setpoint speed signal 284 to determine error signal 290, which is then applied to PI algorithm 292 to determine the fuel command required to regulate engine speed at the setpoint. EGT control (FIG. 10) and maximum/minimum fuel limits are used in conjunction with the speed control algorithm 282 to protect output signal 294 from surge and flame out conditions. Resultant output signal 298 is regulated turbine speed fuel flow command. In a typical implementation, speed control mode loop 282 operates at about a 20ms rate.

Referring to FIG. 12, power control mode loop 300 regulates the power producing potential of the turbine. Feedback power signal 306 is read and compared by comparator 304 against setpoint power signal 302 to determine error signal 308, which is then applied to PI algorithm 310 to determine the speed command required to regulate output power at the setpoint. Maximum/minimum speed limits are used to limit the power control algorithm speed command output to protect output signal 312 from running into over speed and under speed conditions. Resultant output signal 316 is regulated power signal turbine speed command. In a typical implementation, the maximum operating speed of the turbine is generally 96,000 RPM and the minimum operating speed of the turbine is generally 45,000 RPM. The loop operates generally at about a 500 ms rate.

Start Only Battery

Referring to FIG. 14, energy storage device 470 may be a start only battery. In the DC bus voltage control mode, start only battery 470 provides energy to regulate voltage to the setpoint command. Main CPU 472 commands the bus voltage to control at different values depending on the configuration of power controller 478. In the state of charge (SOC) control mode, the start only battery system provides a recharging power demand when requested. Available recharging power is generally equivalent to maximum engine power less power being supplied to the output load and system parasitic loads. Main CPU 472 transmits a recharging power level that is the minimum of the original power demand and available recharging power.

Transient Battery

The transient battery provides the DC bus voltage control as described below as well as the state of charge (SOC) control mode described for the start only battery. The transient battery contains a larger energy storage device than the start only battery.

DC Bus Voltage Control

DC bus 462 supplies power for logic power, external components and system power output. TABLE 1 defines the setpoint the bus voltage is to be controlled at based on the output power configuration of power controller 478:

TABLE 1

B3 POWER OUTPUT	SETPOINT
480/400 VAC Output	800 Vdc
240/208 VAC Output	400 Vdc

In the various operating modes, power controller 478 will have different control algorithms responsible for managing the DC bus voltage level. Any of the battery options 470 as well as SPs 456 and 458 have modes that control power flow to regulate the voltage level of DC bus 462. Under any operating circumstances, only one device is commanded to a mode that regulates DC bus 462. Multiple algorithms would require sharing logic that would inevitably make system response slower and software more difficult to comprehend.

System States

Referring to FIG. 13, state diagram 320 showing various operating states of power controller 478 is illustrated. Sequencing the system through the entire operating procedure requires power controller to transition through the operating states defined in TABLE 2.

TABLE 2

STATE #	SYSTEM STATE	DESCRIPTION
0	Power Up	Performs activities of initializing and testing the system.
1	Stand By	Closer power to bus and continues system monitoring

			while waiting for a start command.
	2	Prepare to Start	Initializes any external devices preparing for the start procedure.
	3	Bearing Lift Off	Configures the system and commands the engine to be rotated to a predetermined RPM, such as 25,000 RPM.
	4	Open Loop Light Off	Turns on ignition system and commands fuel open loop to light the engine.
	5	Closed Loop Acceleration	Continues motoring and closed fuel control until the system reaches the no load state.
	6	Run	Engine operates in a no load self-sustaining state producing power only to operate the controller.
	7	Load	Converter output contactor is closed and system is producing power.
	8	Re-Charge	System operates off of fuel only and produces power for recharging energy storage device if installed.
	9	Cooldown	System is motoring engine to reduce EGT before shutting down.
	10	Re-Start	Reduces engine speed to begin open loop light when a start command is received in the cooldown state.
	11	Re-Light	Performs a turbine re-light in transition from the cooldown to warmdown state. Allows continued engine cooling when motoring is no longer possible.
	12	Warmdown	Sustains turbine operation with fuel at a predetermined RPM, such as 50,000 RPM, to cool when engine motoring is not possible.
	13	Shutdown	Reconfigures the system after a cooldown to enter the stand by state.
	14	Fault	Turns off all outputs when presence of fault which disables power conversion exists. Logic power is still available for interrogating system faults.
	15	Disable	Fault has occurred where processing may no longer

be possible. All system operation is disabled.

Main CPU 472 begins execution in the "power up" state 322 after power is applied. Transition to the "stand by" state 324 is performed upon successfully completing the tasks of the "power up" state 322. Initiating a start cycle transitions the system to the "prepare to start" state 326 where all system components are initialized for an engine start. The engine then sequences through start states and onto the "run/load" state 328. To shutdown the system, a stop command which sends the system into either "warm down" or "cool down" state 332 is initiated. Systems that have a battery may enter the "re-charge" state 334 prior to entering the "warm down" or "cool down" state 332. When the system has finally completed the "warm down" or "cool down" process 332, a transition through the "shut down" state 330 will be made before the system re-enters the "standby" state 324 awaiting the next start cycle. During any state, detection of a fault with a system severity level indicating the system should not be operated will transition the system state to "fault" state 334. Detection of faults that indicate a processor failure has occurred will transition the system to the "disable" state 336.

One skilled in the art will recognize that in order to accommodate each mode of operation, the state diagram is multidimensional to provide a unique state for each operating mode. For example, in the "prepare to start" state 326, control requirements will vary depending on the selected operating mode. Therefore, the presence of a stand-alone "prepare to start" state 326, stand-alone transient "prepare to start" state 326, utility grid connect "prepare to start" state 326 and utility grid connect transient "prepare to start" state 326 will be required. Each combination is known as a system configuration (SYSCON) sequence. Main CPU 472 identifies each of the different system configuration sequences in a 16-bit word known as a SYSCON word, which is a bit-wise construction of an operating mode and system state number. In a typical configuration, the system state number is packed in bits 0 through 11. The operating mode number is packed in bits 12 through 15. This packing method provides the system with the capability of sequence through 4096 different system states in 16 different operating modes.

Separate "power up" 322, "re-light" 338, "warm down" 332, "fault" 334 and "disable" 336 states are not required for each mode of operation. The contents of these states are mode independent.

"Power Up" State

Operation of the system begins in the "power up" state 322 once application of power activates main CPU 472. Once power is applied to power controller 478, all the hardware components will be automatically reset by hardware circuitry. Main CPU 472 is responsible for ensuring the hardware is functioning correctly and configure the components for operation. Main CPU 472 also initializes its own internal data structures and begins execution by starting the Real-Time Operating System (RTOS). Successful completion of these tasks directs transition of the software to the "stand by" state 324. Main CPU 472 performs these procedures in the following order:

1. Initialize main CPU 472
2. Perform RAM Test
3. Perform FLASH Checksum
4. Start RTOS
5. Run Remaining POST
6. Initialize SPI Communications
7. Verify Generator SP Checksum
8. Verify Converter SP Checksum
9. Initialize IntraController Communications
10. Resolve External Device Addresses
11. Look at Input Line Voltage
12. Determine Mode
13. Initialize Maintenance Port
14. Initialize User Port
15. Initialize External Option Port
16. Initialize InterController
17. Chose Master/Co-Master
18. Resolve Addressing
19. Transition to Stand By State (depends on operating mode)

"Stand By" State

Main CPU 472 continues to perform normal system monitoring in the "stand by" state 324 while it waits for a start command signal. Main CPU 472 commands either energy storage device 470 or utility 468 to provide continuous power supply. In operation, main CPU 472 will often be left powered on waiting to be start or for troubleshooting purposes. While main CPU 472 is powered up, the software continues to monitor the system and perform diagnostics in case any failures should occur. All communications will continue to operate providing interface to external sources. A start command will transition the system to the "prepare to start" state 326.

"Prepare to Start" State

Main CPU 472 prepares the control system components for the engine start process. Many external devices may require additional time for hardware initialization before the actual start procedure can commence. The "prepare to start" state 326 provides those devices the necessary time to perform initialization and send acknowledgment to the main CPU 472 that the start process can begin. Once also systems are ready to go, the software shall transition to the "bearing lift off" state 328.

"Bearing Lift Off" State

Main CPU 472 commands generator SP 456 to motor the engine 454 from typically about 0 to 25,000 RPM to accomplish the bearing lift off procedure. A check is performed to ensure the shaft is rotating before transition to the next state occurs.

"Open Loop Light Off" State

Once the motor 452 reaches its liftoff speed, the software commences and ensures combustion is occurring in the turbine. In a typical configuration, main CPU 472 commands generator SP 456 to motor the engine 454 to a dwell speed of about 25,000 RPM. Execution of the open loop light off state 340 starts combustion. Main CPU 472 then verifies that the engine 454 has not met the "fail to light" criteria before transition to the "closed loop accel" state 342.

"Closed Loop Accel" State

Main CPU 472 sequences engine 454 through a combustion heating process to bring the engine 454 to a self-sustaining operating point. In a typical configuration, commands are provided to generator SP 456 commanding an increase in engine speed

to about 45,000 RPM at a rate of about 4000 RPM/sec. Fuel controls are executed to provide combustion and engine heating. When engine 454 reaches "no load" (requires no electrical power to motor), the software transitions to "run" state 344.

"Run" State

Main CPU 472 continues operation of control algorithms to operate the engine at no load. Power may be produced from engine 454 for operating control electronics and recharging any energy storage device 470 for starting. No power is output from load converter 458. A power enable signal transitions the software into "load" state 346. A stop command transitions the system to begin shutdown procedures (may vary depending on operating mode).

"Load" State

Main CPU 472 continues operation of control algorithms to operate the engine 454 at the desired load. Load commands are issued through the communications ports, display or system loads. A stop command transitions main CPU 472 to begin shutdown procedures (may vary depending on operating mode). A power disable signal can transition main CPU 472 back to "run" state 344.

"Re-charge" State

Systems that have an energy storage option may be required to charge energy storage device 470 to maximum capacity before entering the "warmdown" 348 or "cooldown" 332 states. During the "re-charge" state 334 of operation, main CPU 472 continues operation of the turbine producing power for battery charging and controller supply. No out power is provided. When the energy storage device 470 has charged, the system transitions to either the "cooldown" 332 or "warmdown" 348 state depending on system fault conditions.

"Cool Down" State

"Cool down" state 332 provides the ability to cool the turbine after operation and a means of purging fuel from the combustor. After normal operation, software sequences the system into "cool down" state 332. In a typical configuration, engine 454 is motored to a cool down speed of about 45,000 RPM. Airflow continues to move through engine 454 preventing hot air from migrating to mechanical components in the cold section. This motoring process continues until the engine EGT falls below

a cool down temperature of about 193°C (380°F). Cool down may be entered at much lower than the final cool down temperature when engine 454 fails to light. The engine's combustor requires purging of excess fuel which may remain. The software always operates the cool down cycle for a minimum purge time of 60 seconds. This purge time ensures remaining fuel is evacuated from the combustor. Completion of this process transitions the system into the "shutdown" state 330. For user convenience, the system does not require a completion of the enter "cooldown" state 332 before being able to attempt a restart. Issuing a start command transitions the system into the "restart" state 350.

"Restart" State

Engine 454 is configured from the "cool down" state 332 before engine 454 can be restart. In a typical configuration, the software lowers the engine speed to about 25,000 RPM at a rate of 4,000 RPM/sec. Once the engine speed has reached this level, the software transitions the system into the "open loop light off" state to perform the actual engine start.

"Shutdown" State

During the "shutdown" state 330, the engine rotor is brought to rest and system outputs are configured for idle operation. In a typical configuration, the software commands the rotor to rest by lowering the engine speed at a rate of 2,000 RPM/sec or no load condition, whichever is faster. Once the speed reaches about 14,000 RPM, the generator SP is commanded to reduce the shaft speed to about 0 RPM in less than 1 second.

"Re-light" State

When a system fault occurs where no power is provided from the utility or energy storage device 470, the software re-ignites combustion to perform a warm down. The generator SP is configured to regulate voltage (power) for the internal DC bus. Fuel is added as defined in the open loop light off fuel control algorithm to ensure combustion occurs. Detection of engine light will transition the system to "warm down" state 348.

"Warm Down" State

Fuel is provided when no electric power is available to operate engine 454 at a no load condition to lower the operating temperature in "warm down" state 348. In a typical configuration, engine speed is operated at about 50,000 RPM by supplying fuel through the speed control algorithm. Engine temperatures less than about 343°C (650°F) causes the system to transition to "shutdown" state 330.

"Fault" State

The present invention disables all outputs placing the system in a safe configuration when faults that prohibit safe operation of the turbine system are present. Operation of system monitoring and communications will continue if the energy is available.

"Disable" State

The system disables all outputs placing the system in a safe configuration when faults that prohibit safe operation of the turbine system are present. System monitoring and communications will most likely not continue.

Modes of Operation

The turbine works in two major modes – utility grid-connect and stand-alone. In the utility grid-connect mode, the electric power distribution system i.e., the utility grid, supplies a reference voltage and phase, and the turbine supplies power in synchronism with the utility grid. In the stand-alone mode, the turbine supplies its own reference voltage and phase, and supplies power directly to the load. The power controller switches automatically between the modes.

Within the two major modes of operation are sub-modes. These modes include stand-alone black start, stand-alone transient, utility grid connect and utility grid connect transient. The criteria for selecting an operating mode is based on numerous factors, including but not limited to, the presence of voltage on the output terminals, the black start battery option, and the transient battery option.

Referring to FIG. 14, generator converter 456 and load converter 458 provide an interface for energy source 460 and utility 468, respectively, to DC bus 462. For illustrative purposes, energy source 460 is a turbine including engine 454 and generator 452. Fuel device 474 provides fuel via fuel line 476 to engine 454. Generator converter 456 and load converter 458 operate as customized bi-directional switching

converters under the control of controller 472. In particular, controller 472 reconfigures the generator converter 456 and load converter 458 into different configurations to provide for the various modes of operation. These modes include stand-alone black start, stand-alone transient, utility grid connect and utility grid connect transient as discussed in detail below. Controller 472 controls the way in which generator 452 and utility 468 sinks or sources power, and DC bus 462 is regulated at any time. In this way, energy source 460, utility/load 468 and energy storage device 470 can be used to supply, store and/or use power in an efficient manner. Controller 472 provides command signals via line 479 to engine 454 to determine the speed of turbine 460. The speed of turbine 460 is maintained through generator 452. Controller 472 also provides command signals via control line 480 to fuel device 474 to maintain the EGT of the engine 454 at its maximum efficiency point. Generator SP 456 is responsible for maintaining the speed of the turbine 460, but putting current into generator 452 or pulling current out of generator 452.

Stand-alone Black Start

Referring to FIG. 14, in the stand-alone black start mode, energy storage device 470, such as battery, is provided for starting purposes while energy source 460, such as turbine including engine 454 and generator 452, supplies all transient and steady state energy. Referring to TABLE 3, controls for a typical stand-alone black start mode are shown.

TABLE 3

SYSTEM STATE	ENGINE CONTROLS	MOTOR CONTROLS	CONVERTER CONTROLS	ENERGY STORAGE CONTROLS
Power Up	-	-	-	-
Stand By	-	-	-	DC Bus
Prepare to Start	-	-	-	DC Bus
Bearing Lift Off	-	RPM	-	DC Bus
Open Loop Light Off	Open Loop Light	RPM	-	DC Bus
Closed Loop Accel	EGT	RPM	-	DC Bus
Run	Speed	DC Bus	-	SOC
Load	Speed	DC Bus	Voltage	SOC

Recharge	Speed	DC Bus	-	SOC
Cool Down	-	RPM	-	DC Bus
Restart	-	RPM	-	DC Bus
Shutdown	-	RPM	-	DC Bus
Re-light	Speed	DC Bus	-	-
Warm Down	Speed	DC Bus	-	-
Fault	-	-	-	-
Disable	-	-	-	-

Stand-alone Transient

In the stand-alone transient mode, storage device 479 is provided for the purpose of starting and assisting the energy source 460, in this example the turbine, to supply maximum rated output power during transient conditions. Storage device 479, typically a battery, is always attached to DC bus 462 during operation, supplying energy in the form of current to maintain the voltage on DC bus 462. Converter/SP 458 provides a constant voltage source when producing output power. As a result, load 468 is always supplied the proper AC voltage value that it requires. Referring to TABLE 4, controls for a typical stand-alone transient mode are shown.

TABLE 4

SYSTEM STATE	ENGINE CONTROLS	MOTOR CONTROLS	CONVERTER CONTROLS	ENERGY STORAGE CONTROLS
Power Up	-	-	-	-
Stand By	-	-	-	DC Bus
Prepare to Start	-	-	-	DC Bus
Bearing Lift Off	-	RPM	-	DC Bus
Open Loop Light Off	Open Loop Light	RPM	-	DC Bus
Closed Loop Accel	EGT	RPM	-	DC Bus
Run	Power & EGT	RPM	-	DC Bus
Load	Power & EGT	RPM	Voltage	DC Bus
Recharge	Power & EGT	RPM	-	DC Bus
Cool Down	-	RPM	-	DC Bus
Restart	-	RPM	-	DC Bus

	Shutdown	-	RPM	-	DC Bus
	Re-light	Speed	DC Bus	-	-
	Warm Down	Speed	DC Bus	-	-
	Fault	-	-	-	-
5	Disable	-	-	-	-

Utility Grid Connect

Referring to FIG. 14, in the utility grid connect mode, the energy source 460, in this example the turbine is connected to the utility grid 468 providing load leveling and management where transients are handled by the utility grid 468. The system operates as a current source, pumping current into utility 468. Referring to TABLE 5, controls for a typical utility grid connect mode are shown.

TABLE 5

	SYSTEM STATE	ENGINE CONTROLS	MOTOR CONTROLS	CONVERTER CONTROLS	ENERGY STORAGE CONTROLS
	Power Up	-	-	-	N/A
	Stand By	-	-	-	N/A
20	Prepare to Start	-	-	DC Bus	N/A
	Bearing Lift Off	-	RPM	DC Bus	N/A
	Open Loop Light Off	Open Loop Light	RPM	DC Bus	N/A
	Closed Loop Accel	EGT	RPM	DC Bus	N/A
25	Run	Power & EGT	RPM	DC Bus	N/A
	Load	Power & EGT	RPM	DC Bus	N/A
	Recharge	N/A	N/A	N/A	N/A
	Cool Down	-	RPM	DC Bus	N/A
	Restart	-	RPM	DC Bus	N/A
30	Shutdown	-	RPM	DC Bus	N/A
	Re-light	Speed	DC Bus	-	N/A
	Warm Down	Speed	DC Bus	-	N/A
	Fault	-	-	-	N/A
	Disable	-	-	-	N/A

Utility Grid Connect Transient

In the utility grid connect transient mode, the energy source 460, in this example the turbine, is connected to the utility grid 468 providing load leveling and management. The turbine that is assisted by energy storage device 470, typically a battery, handles transients. The system operates as a current source, pumping current into utility 468 with the assistance of energy storage device 470. Referring to TABLE 6, controls for a typical utility grid connect transient mode are shown.

TABLE 6

SYSTEM STATE	ENGINE CONTROLS	MOTOR CONTROLS	CONVERTER CONTROLS	ENERGY STORAGE CONTROLS
Power Up	-	-	-	-
Stand By	-	-	-	DC Bus
Prepare to Start	-	-	-	DC Bus
Bearing Lift Off	-	RPM	-	DC Bus
Open Loop Light Off	Open Loop Light	RPM	-	DC Bus
Closed Loop Accel	EGT	RPM	-	DC Bus
Run	Power & EGT	RPM	-	DC Bus
Load	Power & EGT	RPM	Current	DC Bus
Recharge	Power & EGT	RPM	-	DC Bus
Cool Down	-	RPM	-	DC Bus
Restart	-	RPM	-	DC Bus
Shutdown	-	RPM	-	DC Bus
Re-light	Speed	DC Bus	-	-
Warm Down	Speed	DC Bus	-	-
Fault	-	-	-	-
Disable	-	-	-	-

Multi-pack Operation

In accordance with the present invention, the power controller can operate in a single or multi-pack configuration. In particular, power controller, in addition to being

a controller for a single turbogenerator, is capable of sequencing multiple systems as well. Referring to FIG. 15, for illustrative purposes, multi-pack system 510 including three power controllers 518, 520 and 522 is shown. The ability to control multiple controllers 518, 520 and 522 is made possible through digital communications interface and control logic contained in each controllers main CPU (not shown).

Two communications busses 530 and 534 are used to create the intercontroller digital communications interface for multi-pack operation. One bus 534 is used for slower data exchange while the other bus 530 generates synchronization packets at a faster rate. In a typical implementation, for example, an IEEE-502.3 bus links each of the controllers 518, 520 and 522 together for slower communications including data acquisition, start, stop, power demand and mode selection functionality. An RS485 bus links each of the systems together providing synchronization of the output power waveforms.

One skilled in the art will recognize that the number of power controllers that can be connected together is not limited to three, but rather any number of controllers can be connected together in a multi-pack configuration. Each power controller 518, 520 and 522 includes its own energy storage device 524, 526 and 528, respectively, such as a battery. In accordance with another embodiment of the invention, power controllers 518, 520 and 522 can all be connected to the same single energy storage device (not shown), typically a very large energy storage device which would be rated too big for an individual turbine. Distribution panel, typically comprised of circuit breakers, provides for distribution of energy.

Multi-pack control logic determines at power up that one controller is the master and the other controllers become slave devices. The master is in charge of handling all user-input commands, initiating all inter-system communications transactions, and dispatching units. While all controllers 518, 520 and 522 contain the functionality to be a master, to alleviate control and bus contention, one controller is designated as the master.

At power up, the individual controllers 518, 520 and 522 determine what external input devices they have connected. When a controller contains a minimum number of input devices it sends a transmission on intercontroller bus 530 claiming to

be master. All controllers 518, 520 and 522 claiming to be a master begin resolving who should be master. Once a master is chosen, an address resolution protocol is executed to assign addresses to each slave system. After choosing the master and assigning slave addresses, multi-pack system 510 can begin operating.

A co-master is also selected during the master and address resolution cycle. The job of the co-master is to act like a slave during normal operations. The co-master should receive a constant transmission packet from the master indicating that the master is still operating correctly. When this packet is not received within a safe time period, 20 ms for example, the co-master may immediately become the master and take over master control responsibilities.

Logic in the master configures all slave turbogenerator systems. Slaves are selected to be either utility grid-connect (current source) or standalone (voltage source). A master controller, when selected, will communicate with its output converter logic (converter SP) that this system is a master. The converter SP is then responsible for transmitting packets over the intercontroller bus 530, synchronizing the output waveforms with all slave systems. Transmitted packets will include at least the angle of the output waveform and error-checking information with transmission expected every quarter cycle to one cycle.

Master control logic will dispatch units based on one of three modes of operation: (1) peak shaving, (2) load following, or (3) base load. Peak shaving measures the total power consumption in a building or application using a power meter, and the multi-pack system 510 reduces the utility consumption of a fixed load, thereby reducing the utility rate schedule and increasing the overall economic return of the turbogenerator. Load following is a subset of peak shaving where a power meter measures the total power consumption in a building or application and the multi-pack system 10 reduces the utility consumption to zero load. In base load, the multi-pack system 10 provides a fixed load and the utility supplements the load in a building or application. Each of these control modes require different control strategies to optimize the total operating efficiency.

A minimum number of input devices are typically desired for a system 510 to claim it is a master during the master resolution process. Input devices that are looked

for include a display panel, an active RS232 connection and a power meter connected to the option port. Multi-pack system 510 typically requires a display panel or RS232 connection for receiving user-input commands and power meter for load following or peak shaving.

In accordance with the present invention, the master control logic dispatches controllers based on operating time. This would involve turning off controllers that have been operating for long periods of time and turning on controllers with less operating time, thereby reducing wear on specific systems.

Utility Grid Analysis and Transient Ride Through

Referring to FIGS. 16-18, transient handling system 580 for power controller 620 is illustrated. Transient handling system 580 allows power controller 620 to ride through transients which are associated with switching of correction capacitors on utility grid 616 which causes voltage spikes followed by ringing. Transient handling system 580 also allows ride through of other faults, including but not limited to, short circuit faults on utility grid 616, which cleared successfully, cause voltage sags. Transient handling system 580 is particularly effective towards handling transients associated with digital controllers, which generally have a slower current response rate due to A/D conversion sampling. During a transient, a large change in the current can occur in between A/D conversions. The high voltage impulse caused by transients typically causes an over current in digital power controllers.

As is illustrated in FIG. 17, a graph 590 showing transients typically present on utility grid 616 is shown. The duration of a voltage transient, measured in seconds, is shown on the x-axis and its magnitude, measured in volts, is shown on the y-axis. A capacitor switching transient, such as shown at 592, which is relatively high in magnitude (up to about 200%) and short in duration (somewhere between 1 and 20 milliseconds) could be problematic to operation of a power controller.

Referring to FIGS. 16-18, changes on utility grid 616 are reflected as changes in the magnitude of the voltage. In particular, the type and seriousness of any fault or event on utility grid 616 can be determined by magnitude estimator 584, which monitors the magnitude and duration of any change on utility grid 616.

In accordance with the present invention, the effect of voltage transients can be minimized by monitoring the current such that when it exceeds a predetermined level, switching is stopped so that the current can decay, thereby preventing the current from exceeding its predetermined level. The present invention thus takes advantage of analog over current detection circuits that have a faster response than transient detection based on digital sampling of current and voltage. Longer duration transients indicate abnormal utility grid conditions. These must be detected so power controller 620 can shut down in a safe manner. In accordance with the present invention, algorithms used to operate power controller 620 provide protection against islanding of power controller 620 in the absence of utility-supplied grid voltage. Near short or near open islands are detected within milliseconds through loss of current control. Islands whose load is more closely matched to the power controller output will be detected through abnormal voltage magnitudes and frequencies as detected by magnitude estimator 584.

In particular, referring to FIG. 18, power controller 620 includes brake resistor 612 connected across DC bus 622. Brake resistor 612 acts as a resistive load, absorbing energy when converter SP 608 is turned off. In operation, when converter SP 608 is turned off, power is no longer exchanged with utility grid 616, but power is still being received from the turbine, which is absorbed by brake resistor 612. The present invention detects the DC voltage between generator and converter SPs 606 and 608. When the voltage starts to rise, brake resistor 612 is turned on to allow it to absorb energy.

In a typical configuration, AC motor 618 produces three phases of AC at variable frequencies. AC/DC converter 602 under the control of motor SP 606 converts the AC to DC which is then applied to DC bus 622 (regulated for example at 800 vDC) which is supported by capacitor 610 (for example, at 800 microfarads with two milliseconds of energy storage). AC/DC converter 604, under the control of converter SP 608, converts the DC into three-phase AC, and applies it to utility grid 616. In accordance with the present invention, current from DC bus 622 can by dissipated in brake resistor 612 via modulation of switch 614 operating under the control of motor SP 606. Switch 614 may be an IGBT switch, although one skilled in

the art will recognize that other conventional or newly developed switches may be utilized as well.

Motor SP 606 controls switch 614 in accordance to the magnitude of the voltage on DC bus 622. The bus voltage of DC bus 622 is typically maintained by converter SP 608, which shuttles power in and out of utility grid 616 to keep DC bus 622 regulated at, for example, 800 vDC. When converter SP 608 is turned off, it no longer is able to maintain the voltage of DC bus 622, so power coming in from the motor causes bus voltage of DC bus 622 to rise quickly. The rise in voltage is detected by motor SP 606, which turns on brake resistor 612 and modulates it on and off until the bus voltage is restored to its desired voltage, for example, 800 vDC. Converter SP 608 detects when the utility grid transient has dissipated, i.e., AC current has decayed to zero

and restarts the converter side of power controller 620. Brake resistor 612 is sized so that it can ride through the transient and the time taken to restart converter.

Referring to FIGS. 18 and 20, in accordance with the present invention, both the voltage and zero crossings (to determine where the AC waveform of utility grid 616 crosses zero) are monitored to provide an accurate model of utility grid 616. Utility grid analysis system includes angle estimator 582, magnitude estimator 584 and phase locked loop 586. The present invention continuously monitors utility grid voltage and based on these measurements, estimates the utility grid angle, thus facilitating recognition of under/over voltages and sudden transients. Current limits are set to disable DC/AC converter 604 when current exceeds a maximum and wait until current decays to an acceptable level. The result of measuring the current and cutting it off is to allow DC/AC converter 604 to ride through transients better. Thus when DC/AC converter 608 is no longer exchanging power with utility grid 616, power is dissipated in brake resistor 612.

In accordance with the present invention, converter SP 608 is capable of monitoring the voltage and current at utility grid 616 simultaneously. In particular, power controller 620 includes a utility grid analysis algorithm. One skilled in the art will recognize that estimates of the utility grid angle and magnitude may be derived via conventional algorithms or means. The true utility grid angle θ_{AC}, which is the angle

of the generating source, cycles through from 0 to 2π and back to 0 at a rate of 60 hertz. The voltage magnitude estimates of the three phases are designated $V_{1\ mag}$, $V_{2\ mag}$ and $V_{3\ mag}$ and the voltage measurement of the three phases are designated V_1, V_2 and V_3.

A waveform, constructed based upon the estimates of the magnitude and angle for each phase, indicates what a correct measurement would look like. For example, using the first of the three phase voltages, the cosine of the true utility grid angle θ_{AC} is multiplied by the voltage magnitude estimate $V_{1\ mag}$, with the product being a cosine-like waveform. Ideally, the product would be voltage measurement V_1.

Feedback loop 588 uses the difference between the absolute magnitude of the measurement of V_1 and of the constructed waveform to adjusts the magnitude of the magnitude estimate $V_{1\ mag}$. One skilled in the art will recognize that the other two phases of three-phase signal can be adjusted similarly, with different angle templates corresponding to different phases of the signal. Thus, magnitude estimate $V_{1\ mag}$ and angle estimate θ_{EST} are used to update magnitude estimate $V_{1\ mag}$. Voltage magnitude estimates $V_{1\ mag}$, $V_{2\ mag}$ and $V_{3\ mag}$ are steady state values used in a feedback configuration to track the magnitude of voltage measurements V_1, V_2 and V_3. By dividing the measured voltages V_1 by the estimates of the magnitude $V_{1\ mag}$, the cosine of the angle for the first phase can be determined (similarly, the cosine of the angles of the other signals will be similarly determined).

In accordance with the present invention, the most advantageous estimate for the cosine of the angle, generally the one that is changing the most rapidly, is chosen to determine the instantaneous measured angle. In most cases, the phase that has an estimate for the cosine of an angle closest to zero is selected since it yields the greatest accuracy. Utility grid analysis system 580 thus includes logic to select which one of the cosines to use. The angle chosen is applied to angle estimator 582, from which an estimate of the instantaneous angle θ_{EST} of utility grid 616 is calculated and applied to phase locked loop 586 to produce a filtered frequency. The angle is thus differentiated to form a frequency that is then passed through a low pass filter (not shown). Phase locked loop 586 integrates the frequency and also locks the phase of the estimated

instantaneous angle θ_{EST}, which may have changed in phase due to differentiation and integration, to the phase of true utility grid angle θ_{AC}.

In a typical operation, when the phase changes suddenly on measured voltage V_I, the algorithm of the present invention compares the product of the magnitude estimate $V_{I\ mag}$ and the cosine of true utility grid angle θ_{AC} against the real magnitude multiplied by the cosine of a different angle. A sudden jump in magnitude would be realized.

Thus, three reasonably constant DC voltage magnitude estimates are generated. A change in one of those voltages indicates whether the transient present on utility grid 616 is substantial or not. One skilled in the art will recognize that there are a number of ways to determine whether a transient is substantial or not, i.e. whether abnormal conditions exist on the utility grid system, which require power controller 620 to shut down. A transient can be deemed substantial based upon the size of the voltage magnitude and duration. Examples of the criteria for shutting down power controller 620 are shown in FIG. 17. Detection of abnormal utility grid behavior can also be determined by examining the frequency estimate.

On detecting abnormal utility grid behavior, a utility grid fault shutdown is initiated. When system controller 620 initiates a utility grid fault shutdown, output contactor is opened within a predetermined period of time, for example, 100 msec, and the main fuel trip solenoid (not shown) is closed, removing fuel from the turbogenerator. A warm shutdown ensues during which control power is supplied from generator 618 as it slows down. In a typical configuration, the warm-down lasts about 1-2 minutes before the rotor (not shown) is stopped. The control software does not allow a restart until utility grid voltage and frequency are within permitted limits.

Having now described the invention in accordance with the requirements of the patent statutes, those skilled in this art will understand how to make changes and modifications in the present invention to meet their specific requirements or conditions. For example, the power controller, while described generally, may be implemented in an analog or digital configuration. In the preferred digital configuration, one skilled in the art will recognize that various terms utilized in the invention are generic to both analog and digital configurations of power controller. For example, converters

referenced in the present application is a general term which includes inverters, signal processors referenced in the present application is a general term which includes digital signal processors, and so forth. Correspondingly, in a digital implementation of the present invention, inverters and digital signal processors would be utilized. Such changes and modifications may be made without departing from the scope and spirit of the invention as set forth in the following claims.

ABSTRACT OF THE DISCLOSURE

POWER CONTROLLER

A power controller provides a distributed generation power networking system in which bi-directional power converters are used with a common DC bus for permitting compatibility between various energy components. Each power converter operates essentially as a customized bi-directional switching converter configured, under the control of the power controller, to provide an interface for a specific energy component to the DC bus. The power controller controls the way in which each energy component, at any moment, will sink or source power, and the manner in which the DC bus is regulated. In this way, various energy components can be used to supply, store and/or use power in an efficient manner. The various energy components include energy sources, loads, storage devices and combinations thereof.

WHAT IS CLAIMED IS:

1. A power controller for distributing power among a plurality of energy components, comprising:

a DC bus; and

a plurality of power converters, each of which is connected between one of said energy components and said DC bus and is responsive to said power controller, wherein said power controller provides a distributed generation power system by controlling the way each energy component sinks or sources power and said DC bus is regulated.

2. A power controller claimed in claim 1, wherein each of said power converters operates as a customized bi-directional switching converter configured, under the control of said power controller, to provide an interface for said energy component to said DC bus.

3. The power controller claimed in claim 1, wherein each of said power converters comprises:

a power switching system; and

a processing system for providing control to said power switching system.

4. The power controller claimed in claim 3, wherein said processing system further comprises:

a signal processor; and

a central processing unit for providing control to said signal processor.

5. The power controller claimed in claim 3, wherein said central processing unit reconfigures said power converter into different configurations for different modes of operation.

6. The power controller claimed in claim 3, wherein said power switching system comprises a plurality of insulated gate bipolar transistor switches.

7. The power controller claimed in claim 1, wherein said plurality of energy components includes an energy source.

8. The power controller claimed in claim 7, wherein said energy source comprises a gas turbine.

9. The power controller claimed in claim 8, wherein said gas turbine drives an AC generator to produce AC which is applied to said power converter.

10. The power controller claimed in claim 9, wherein said controller regulates DC bus voltage independently of turbine speed.

11. The power controller claimed in claim 1, wherein said plurality of energy components includes an energy storage device.

12. The power controller claimed in claim 11, wherein said energy storage device comprises a flywheel.

13. The power controller claimed in claim 11, wherein said energy storage device comprises a battery.

14. The power controller claimed in claim 11, wherein said energy storage device comprises an ultracap.

15. The power controller claimed in claim 1, wherein said plurality of energy components includes a load.

16. The power controller claimed in claim 15, wherein said load comprises an AC utility.

17. The power controller claimed in claim 16, wherein said load comprises a DC load.

18. The power controller claimed in claim 16, wherein said load comprises a drive motor.

19. The power controller claimed in claim 1, wherein said plurality of energy components includes an energy source, a load and a storage device.

20. The power controller claimed in claim 19, wherein during a utility start up mode of operation, one of said power converters applies power from said load to said DC bus for conversion by another of said power converters into power required by said energy source to startup and said storage device is disconnected from said DC bus while said load regulates DC voltage on said DC bus.

21. The power controller claimed in claim 20, wherein said energy source comprises a turbine and is controlled in a local feedback loop to maintain said turbine revolutions per minute (RPM).

22. The power controller claimed in claim 19, wherein during a utility start up mode of operation, one of said power converters isolates said DC bus so that another of said power converters provides the required starting power from said DC bus to said energy source.

23. The power controller claimed in claim 1, wherein said power converters comprise a generator converter and output converter.

24. The power controller claimed in claim 23, wherein said power controller is digital, said generator converter is a generator inverter and said output converter is an output inverter.

25. The power controller claimed in claim 4, wherein said central processing unit sequences events which occur inside said power controller and arbitrates communications to externally connected devices.

26. The power controller claimed in claim 4, wherein said central processing unit is a Motorola MC68332 microprocessor.

27. The power controller claimed in claim 19, wherein said energy source comprises a turbogenerator, said energy storage device comprises a battery and said load comprises a utility grid.

28. The power controller claimed in claim 19, wherein said energy source comprises a turbogenerator, said energy storage device comprises a capacitive device and said load comprises a utility grid.

29. The power controller claimed in claim 19 wherein said energy source comprises a turbogenerator, and said load comprises a utility grid.

30. The power controller claimed in claim 1, wherein said plurality of energy components comprises a turbogenerator and a load.

31. A turbine system, comprising:

a turbine engine;

a load; and

a power controller for converting electricity from said turbine engine into regulated DC and then to AC electricity, wherein said power controller includes an engine power conversion in communication with said turbine engine, an utility power conversion in communication with said load and a DC bus.

32. The turbine system claimed in claim 31, further comprising:

a fuel metering system in communication with an energy reservoir controller and said power controller.

33. The turbine system claimed in claim 31, wherein said power controller provides a distributed generation power system utilizing said engine power conversion and said utility power conversion.

34. The turbine system claimed in claim 31, wherein said engine power conversion and said utility power conversion operate as a customized bi-directional switching converters, under control of said power controller, to provide an interface for said turbine engine and said load to said DC bus.

35. A method for controlling the distribution of power among a plurality of energy components, comprising the steps of:

connecting a power converter between a DC bus and each of said energy components;

controlling the way each of said energy components sinks or sources power; and

controlling the way said DC bus is regulated responsive to operation of each of said energy components.

36. The method claimed in claim 35, wherein said step of controlling the way each of said energy components sinks or sources power, further comprises the step of:

controlling the way each of said power converters is configured.

37. The method claimed in claim 35, wherein said step of controlling the way each of said energy components sinks or sources power, further comprises the step of:

controlling said power converters such that they operate as customized, bi-directional switching converters configured to provide an interface for said energy components to said DC bus.

38. The method claimed in claim 36, wherein said each of said power converters comprises a power switching system and said step of controlling the way each of said power converters is configured, further comprises the step of:

providing control to said power switching system.

39. The method claimed in claim 35, wherein said step of controlling the way each of said power converters is configured, further comprises the step of:

reconfiguring said each of said power converters into different configurations for different modes of operation.

40. The method claimed in 35, wherein said plurality of energy components include an energy source, a load and a storage device.

41. The method claimed in claim 40, wherein said energy source comprises a turbogenerator, said energy storage device comprises a battery and said load comprises a utility grid.

42. The method claimed in claim 40, wherein said energy source comprises a turbogenerator, said energy storage device comprises a capacitive device and said load comprises a utility grid.

43. The method claimed in claim 40, further comprising the steps of:

during a utility start up mode of operation, utilizing one of said power converters to apply power from said load to said DC bus for conversion by another of said power converters into power required by said energy source to startup;

disconnecting said storage device from said DC bus while said load regulates DC voltage on said DC bus.

44. The method claimed in claim 43, wherein said energy source comprises a turbine and further comprising the step of:

utilizing a local feedback loop to maintain said revolutions per minute (RPM) of said turbine.

45. The method claimed in claim 40 further comprising the steps of:

during a utility start up mode of operation, isolating one of said power converters from said DC bus so that another of said power converters provides the required starting power from said DC bus to said energy source.

46. The method claimed in claim 35, wherein said power converters comprise a generator converter and output converter.

47. The method claimed in claim 46, wherein said distribution of power is controlled digitally, said generator converter is a generator inverter and said output converter is an output inverter.

48. The method claimed in claim 35, further comprising the steps of:

sequencing events which occur; and

arbitrating communications to externally connected devices.

49. A power control system, comprising:

a plurality of power controllers for distributing power among a plurality of energy components; and

a first bus for providing communication between said plurality of power controllers.

50. The power control system claimed in claim 49, further comprising:

a second bus for providing communication between said plurality of power controllers.

51. The power control system claimed in claim 50, wherein said first bus provides for data exchange at a first rate and said second bus provides for data exchange at a second rate.

52. The power control system claimed in claim 51, wherein said first bus provides for sychronization of output power waveforms.

53. The power control system claimed in claim 52, wherein said second bus provides for data acquisition.

54. The power control system claimed in claim 52, wherein said second bus provides for start and stop operation of said system.

55. The power control system claimed in claim 52, wherein said second bus provides mode selection.

56. The power control system claimed in claim 49, wherein each of said plurality of power controllers comprises:

a DC bus; and

a plurality of power converters, one of said plurality of power converters connected between one of said plurality of energy components and said DC bus and is responsive to said power controller, wherein said power controller provides a distributed generation power system by controlling the way each energy component sinks or sources power and said DC bus is regulated.

57. The power control system claimed in claim 52, wherein each of said power converters operates as a customized bi-directional switching converter configured, under the control of said power controller, to provide an interface for said energy component to said DC bus.

58. The power control system claimed in claim 49, wherein said plurality of power controllers includes a master controller with remainder of said plurality of power controllers being slave controllers..

59. The power control system claimed in claim 58, wherein said master controller handles user-input commands.

60. The power control system claimed in claim 58, wherein said master controller initiates inter-system communication transactions.

61. The power control system claimed in claim 58, wherein said master controller dispatches said slave controllers.

62. The power control system claimed 58, wherein said system determines a master controller and assigns addresses to said slave controllers.

63. The power control system claimed in claim 58, wherein said slave controllers includes a co-master controller for monitoring operation of said master controller.

64. The power control system claimed in claim 63, wherein said co-master controller receives a signal from said master controller indicating that said master controller is operating correctly.

65. The power control system claimed in claim 58, wherein said slave controllers are selected to be either a current source or standalon

66. The power control system claimed in 58, wherein said master controller further comprises:

a signal processor; and

a central processing unit for providing control to said signal processor.

67. The power control system claimed in claim 58, wherein said signal processor is digital.

68. The power control system claimed in claim 66, wherein said master controller communicates with said signal processor that it is a master controller.

69. The power control system claimed in claim 66, wherein said signal processor transmits packets over said first bus for synchronizing output waveforms with said slave controllers.

70. The power control system claimed in claim 69, wherein said packets include an angle of said output waveforms.

71. The power control system claimed in claim 69, wherein said packets include error-checking information.

72. The power control system claimed in claim 58, wherein said master controller measures total power consumption and said system, in response to said measurement, adjusts utility consumption to a fixed load.

73. The power control system claimed in claim 59, wherein said master controller adjusts utility consumption to a zero load.

74. The power control system claimed in claim 58, wherein said system provides a fixed load and utility supplements said load in an application.

75. The power control system claimed in claim 58, wherein said master controller dispatches slave controllers based on operating time.

76. The power control system claimed in claim 75, wherein said master controller turns off slave controllers that have been operating for long periods of time and turning on slave controllers with less operating time by reducing wear on specific slave controllers.

77. The power control system claimed in claim 49, wherein system provides for multi-turbogenerator control.

78. The power control system claimed in claim 77, further comprising:

a plurality of turbine engines;

a plurality of loads;

wherein said plurality of power controllers convert electricity from said plurality of turbine engines into regulated DC and then to AC electricity, wherein said plurality of power controllers include an engine power conversion in communication with said plurality of turbine enginee, an utility power conversion in communication with said plurality of loads and a DC bus.

79. A digital power controller for distributing power among a plurality of energy components, comprising:

a DC bus; and

a plurality of power inverters, each of which is connected between said energy component and said DC bus and is responsive to said power controller, wherein said power controller provides a distributed generation power system by controlling the way each energy component sinks or sources power and said DC bus is regulated,

wherein said energy components include an energy source, energy storage device and load.

80. The digital power controller claimed in claim 79, wherein said controller operates in a first and second mode.

81. The digital power controller claimed in claim 80, wherein in said first mode, said load supplies a reference voltage and phase, and said energy source supplies power in synchronism with said load.

82. The digital power controller claimed in claim 80, wherein in said second mode, said energy source supplies its own reference voltage and phase, and supplies power directly to said load.

83. The digital power controller claimed in claim 79, wherein said energy source comprises a turbine and said load comprises a grid.

84. The digital power controller claimed in claim 80, wherein said controller switches automatically between said first and second modes.

85. The digital power controller claimed in claim 80, wherein each of said first and second modes comprises a plurality of sub-modes.

86. The digital power controller claimed in claim 85, wherein in a first sub-mode, said energy storage device provides for starting and said energy source supplies transient and steady state energy.

87. The digital power controller claimed in claim 85, wherein in a second sub-mode, said storage device starts and assists said energy source to supply maximum output power during transient conditions.

88. The digital power controller claimed in claim 87, wherein said storage device is always attached to said DC bus during operation, supplying energy to maintain voltage on said DC bus.

89. The digital power controller claimed in claim 85, wherein in a third sub-mode, said energy source is connected to said load providing load leveling and management and said load handles transients.

90. The digital power controller claimed in claim 85, wherein in a fourth sub-mode, said energy source is connected to said load providing load leveling and management and said energy storage device handles transients.

91. A method of controlling the distribution of power among a plurality of energy components using a computer including a digital signal processor comprising the steps of:

interfacing a plurality of power inverters between a DC bus and each of said energy components;

controlling the way each of said energy components sinks or sources power; and

controlling the way said DC bus is regulated responsive to operation of each of said energy components, wherein said energy components include an energy source, a load and a storage device.

92. The method claimed in claim 91, further comprising the steps of:

applying power to said power inverters for start up;

error checking said power inverters;

initializing internal data structures; and

starting operating system.

93. The method claimed in claim 92, further comprising the steps of:

monitoring said system and performing diagnostics should failures occur; and

commanding either energy storage device or load to provide continuous power supply.

94. The method claimed in claim 93, further comprising the steps of:
initializing external devices; and
acknowledging start process can begin.

95. The method claimed in claim 94, further comprising the steps of:
commanding signal processor to motor said energy source; and
ensuring said energy source is rotating.

96. The method claimed in claim 95, further comprising the step of:
once said energy source reaches a predetermined speed, ensuring combustion is occurring.

97. The method claimed in claim 96, further comprising the step of:
sequencing said energy source through a heating process to bring said energy source to a self-sustaining operating point.

98. The method claimed in claim 97, further comprising the step of:
continuing operation of control algorithms to operate said energy source at no load.

99. The method claimed in claim 98, further comprising the step of:
continuing operation of control algorithms to operate said energy source at a desired load.

100. The method claimed in claim 99, further comprising the step of:
charging energy storage device to maximum capacity.

101. The method claimed in claim 100, further comprising the steps of:
cooling said energy source after operation; and
purging fuel.

102. The method claimed in claim 101, further comprising the step of:
configuring said energy source before said energy source is restarted.

103. The method claimed in claim 102, further comprising the steps of:
resting said energy source; and
configuring system outputs for idle operation.

104. The method claimed in claim 102, further comprising the step of:

re-igniting combustion to perform a warm down when a system fault occurs where no power is provided from load or energy storage device.

105. The method claimed in claim 104, further comprising the step of:

providing fuel when no electric power is available to operate said energy source at a no load condition to lower operating temperature in warm down state.

106. The method claimed in claim 105, further comprising the step of:

monitoring said system for faults.

107. The method claimed in claim 106, further comprising the step of:

disabling all outputs so that said system is placed in a safe configuration when faults that prohibit safe operation occur.

108. A method of controlling the distribution of power in a system including a turbine, among a plurality of energy components, using a computer including a digital signal processor comprising the steps of:

interfacing a plurality of power inverters between a DC bus and each of said energy components;

controlling the way each of said energy components sinks or sources power; and

controlling the way said DC bus is regulated responsive to operation of each of said energy components, wherein said energy components include an energy source, a load and a energy storage device.

109. The method claimed in claim 108, further comprising the step of:

varying a speed command to regulate power of said system.

110. The method claimed in claim 108, further comprising the step of:

varying a fuel flow command to regulate speed of said turbine.

111. The method claimed in claim 108, further comprising the step of:

varying a fuel flow command to regulate exhaust gas temperature of said turbine.

112. The method claimed in claim 108, wherein said power inverters include first and second power inverters under the control of first and second signal processors, respectively.

113. The method claimed in claim 112, further comprising the step of:

varying a current command associated with said first signal processor to regulate a speed of said turbine.

114. The method claimed in claim 112, further comprising the step of:

varying a current command associated with said second signal processor to regulate voltage of said DC bus.

115. The method claimed in claim 112, further comprising the step of:

varying a current command associated with said first signal processor to regulate voltage of said DC bus.

116. The method claimed in claim 112, further comprising the step of:

providing power from said DC bus in accordance with said second signal processor to provide a constant AC voltage output.

117. The method claimed in claim 108, further comprising the step of:

providing power bi-directionally from said energy storage device to regulate voltage of said DC bus.

118. The method claimed in claim 108, further comprising the step of:

providing power from said DC bus in accordance with said second signal processor to provide a constant AC current output.

119. The method claimed in claim 108, further comprising the step of:

varying an AC current command to said second signal processor to regulate a constant turbine EGT.

120. The method claimed in claim 108, further comprising the step of:

providing power bi-directionally from said energy storage device to regulate a device state of charge.

121. A method of controlling the distribution of power in a system including a turbine, among a plurality of energy components, using a computer including a digital signal processor comprising the steps of:

interfacing a plurality of power inverters between a DC bus and each of said energy components;

controlling the way each of said energy components sinks or sources power; and

controlling the way said DC bus is regulated responsive to operation of each of said energy components, wherein said energy components include an energy source, a load and a energy storage device.

122. The method claimed in claim 121, further comprising the step of:

varying a speed command to regulate power of said system.

123. The method claimed in claim 122, further comprising the step of:

varying a fuel flow command to regulate speed of said turbine.

124. The method claimed in claim 123, further comprising the step of:

varying a fuel flow command to regulate exhaust gas temperature of said turbine.

125. The method claimed in claim 124, wherein said power inverters include first and second power inverters under the control of first and second signal processors, respectively.

126. The method claimed in claim 125, further comprising the step of:

varying a current command associated with said first signal processor to regulate a speed of said turbine.

127. The method claimed in claim 126, further comprising the step of:

varying a current command associated with said second signal processor to regulate voltage of said DC bus.

128. The method claimed in claim 127, further comprising the step of:

varying a current command associated with said first signal processor to regulate voltage of said DC bus.

129. The method claimed in claim 128, further comprising the step of:

providing power from said DC bus in accordance with said second signal processor to provide a constant AC voltage output.

130. The method claimed in claim 129, further comprising the step of:

providing power bi-directionally from said energy storage device to regulate voltage of said DC bus.

131. The method claimed in claim 130, further comprising the step of:

providing power from said DC bus in accordance with said second signal processor to provide a constant AC current output.

132. The method claimed in claim 131, further comprising the step of:

varying an AC current command to said second signal processor to regulate a constant turbine EGT.

133. The method claimed in claim 132, further comprising the step of:
providing power bi-directionally from said energy storage device to regulate a device state of charge.

134. A power controller for distributing power among a plurality of energy components, comprising:
a DC bus;
a plurality of power converters, each of which is connected between one of said energy components and said DC bus and is responsive to said power controller, wherein said power controller provides a distributed generation power system by controlling the way each energy component sinks or sources power and said DC bus is regulated; and
means for detecting transients associated with one of said energy components.

135. The power controller claimed in claim 134, further comprising:
means for suspending power transfer between one of said energy components and one of said power converters.

136. The power controller claimed in claim 135, further comprising:
means for resuming power transfer between one of said energy components and one of said power converters once current in said one of said energy components has decayed to near zero.

137. The power controller claimed in claim 136, further comprising:
means for dissipating via a resistive load said power fed into said DC bus by said other one of said energy components.

138. The power controller claimed in claim 134, further comprising:
means for estimating phase voltage magnitudes and grid phase angle in a feedback process, in conjunction with measurements of actual phase voltages to improve estimated peak voltage magnitudes;
means for estimating an instantaneous angle of each phase of an utility grid based on said estimated peak voltage magnitudes and measured phase voltages;
means for utilizing most accurate angle estimate to calculate an estimate of an instantaneous phase angle of said grid;

means for differentiating and filtering to form an estimate of grid frequency;

means for integrating said grid frequency to produce an estimated grid phase angle; and

means for correcting said estimated grid phase angle to converge in phase with an estimate of an instantaneous phase angle of said grid.

139. A method for controlling the distribution of power among a plurality of energy components, comprising the steps of:

connecting a power converter between a DC bus and each of said energy components;

controlling the way each of said energy components sinks or sources power;

controlling the way said DC bus is regulated responsive to operation of each of said energy components; and

detecting transients associated with one of said energy components.

140. The method claimed in claim 139, further comprising the step of:

suspending power transfer between one of said energy components and one of said power converters.

141. The method claimed in claim 140, further comprising the step of:

resuming power transfer between one of said energy components and one of said power converters once current in said one of said energy components has decayed to near zero.

142. The method claimed in claim 141, further comprising the step of:

dissipating via a resistive load said power fed into said DC bus by said other one of said energy components.

143. The method claimed in claim 139, further comprising the steps of:

estimating phase voltage magnitudes and grid phase angle in a feedback process, in conjunction with measurements of actual phase voltages to improve estimated peak voltage magnitudes;

estimating an instantaneous angle of each phase of an utility grid based on said estimated peak voltage magnitudes and measured phase voltages;

utilizing most accurate angle estimate to calculate an estimate of an instantaneous phase angle of said grid;

differentiating and filtering to form an estimate of grid frequency;

means for integrating said grid frequency to produce an estimated grid phase angle; and

correcting said estimated grid phase angle to converge in phase with an estimate of an instantaneous phase angle of said grid.

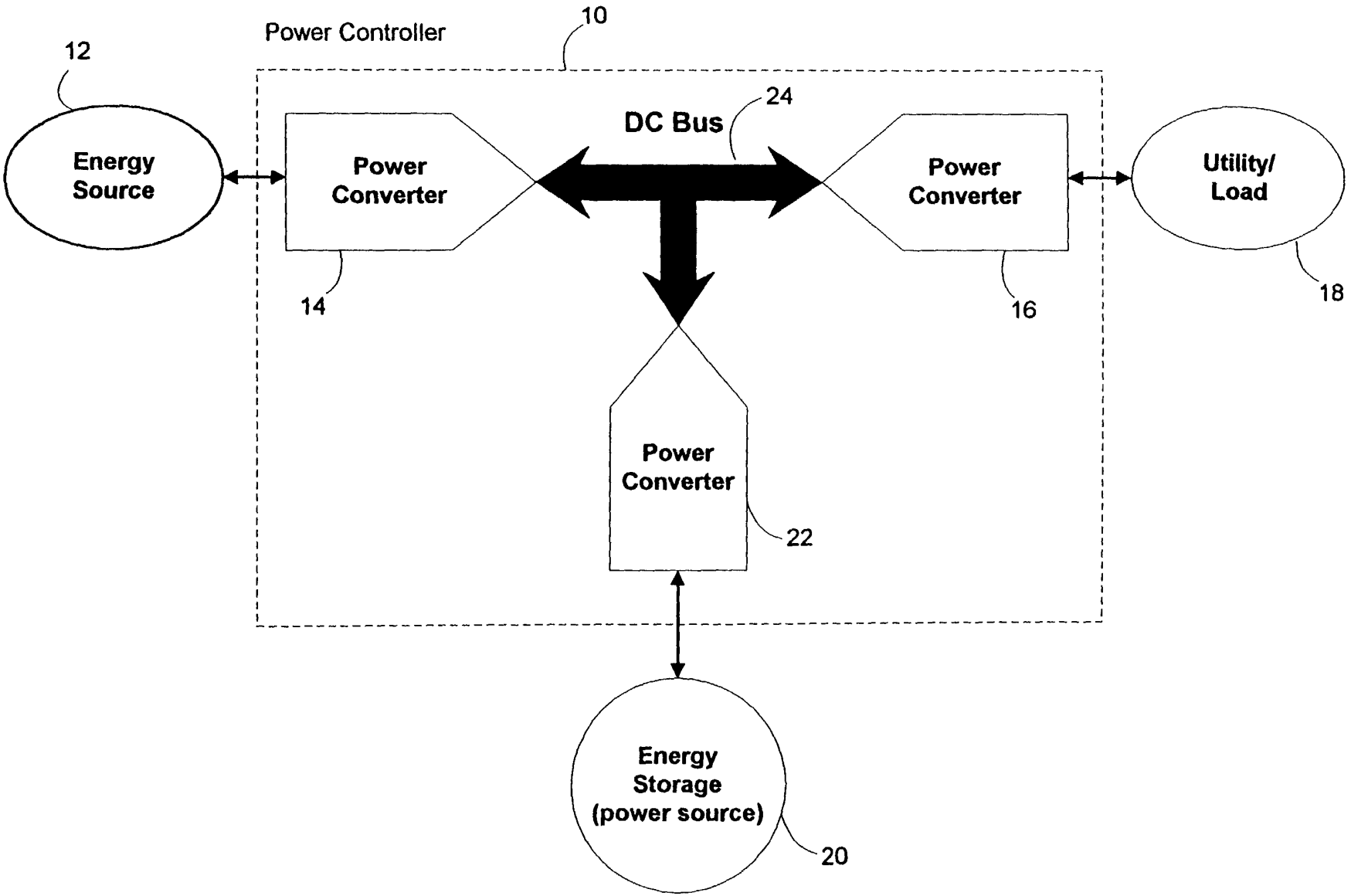

FIG. 1

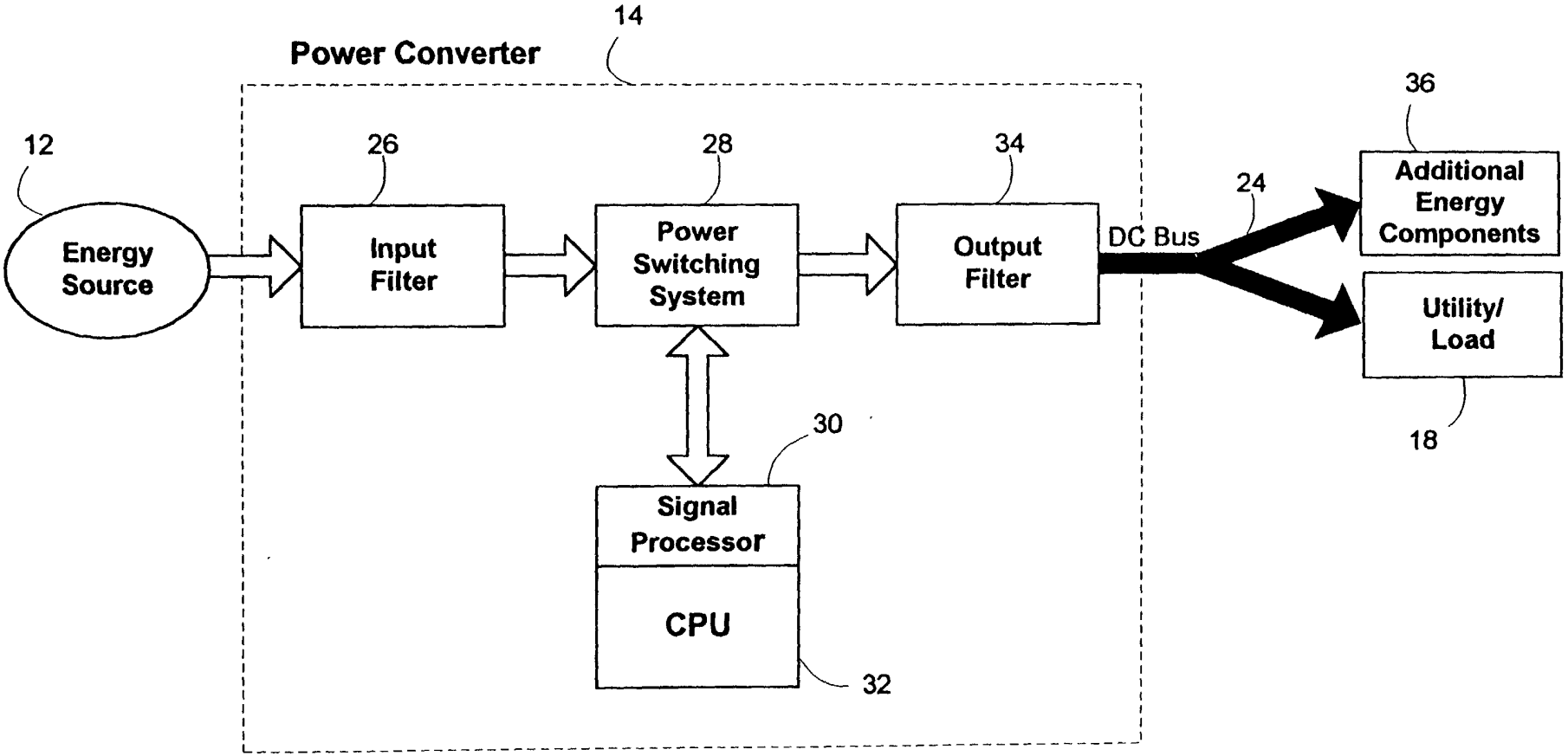

FIG. 2

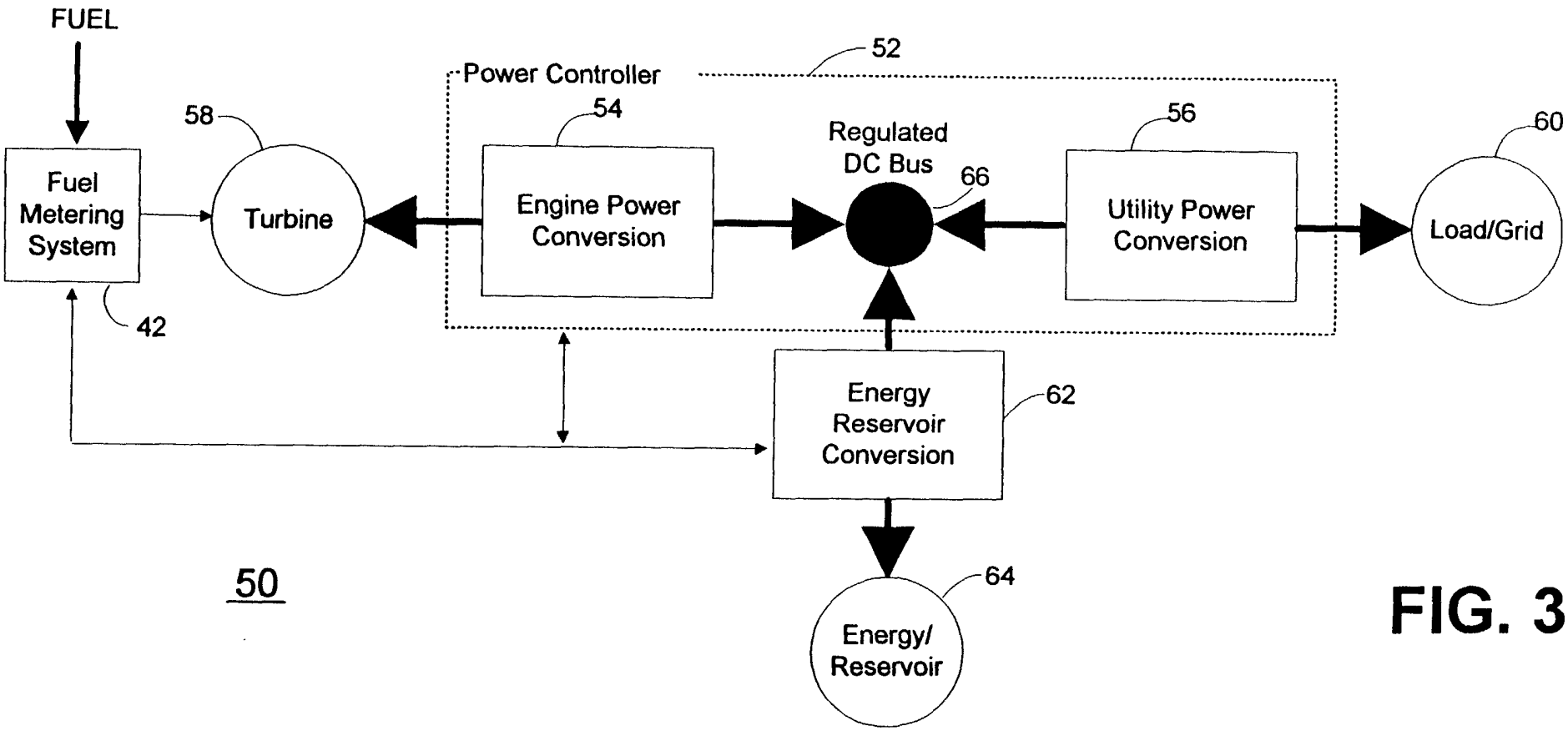
FUEL
Power Controller
52
58
54
56
60
Regulated
DC Bus
66
Fuel
Metering
System
Turbine
Engine Power
Conversion
Utility Power
Conversion
Load/Grid
42
Energy
Reservoir
Conversion
62
64
Energy/
Reservoir
50

FIG. 3

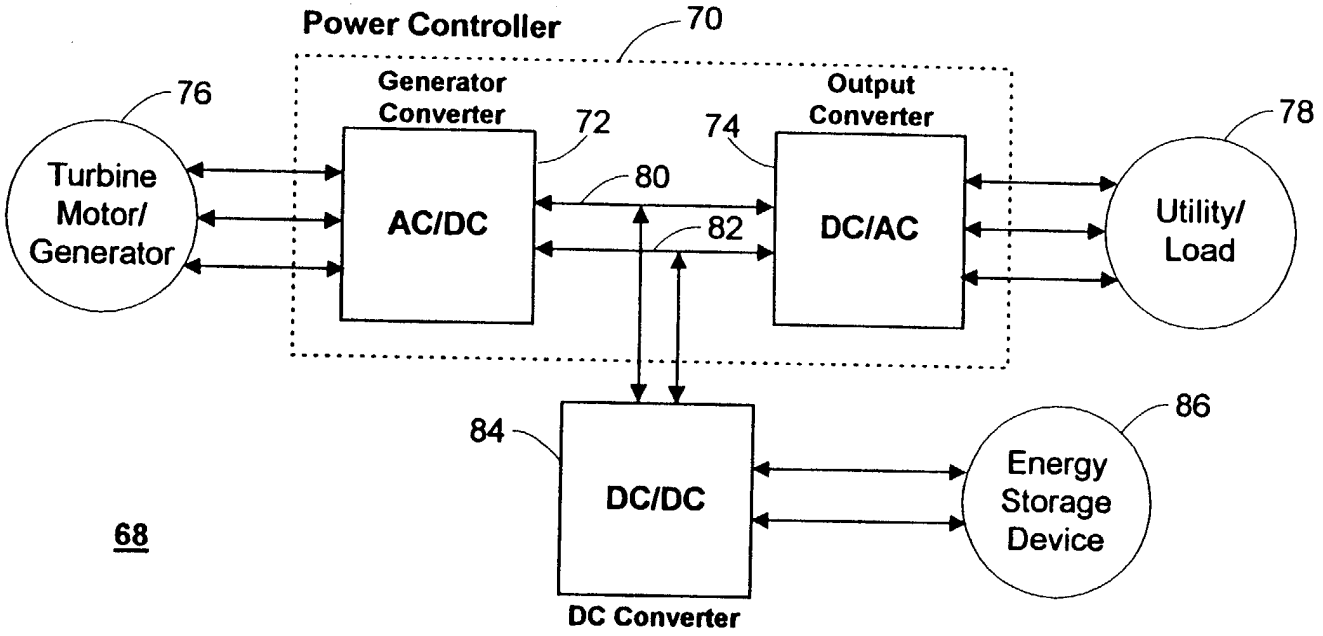

FIG. 4

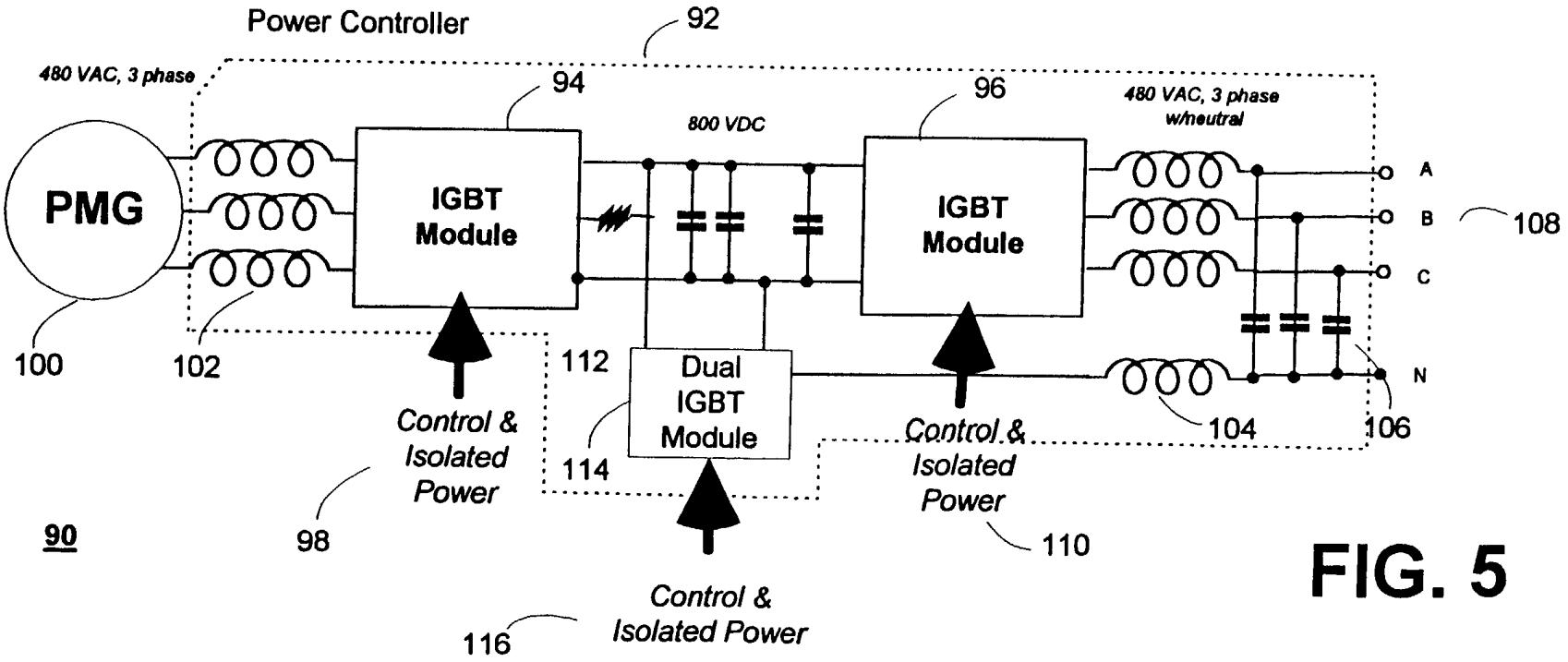

FIG. 5

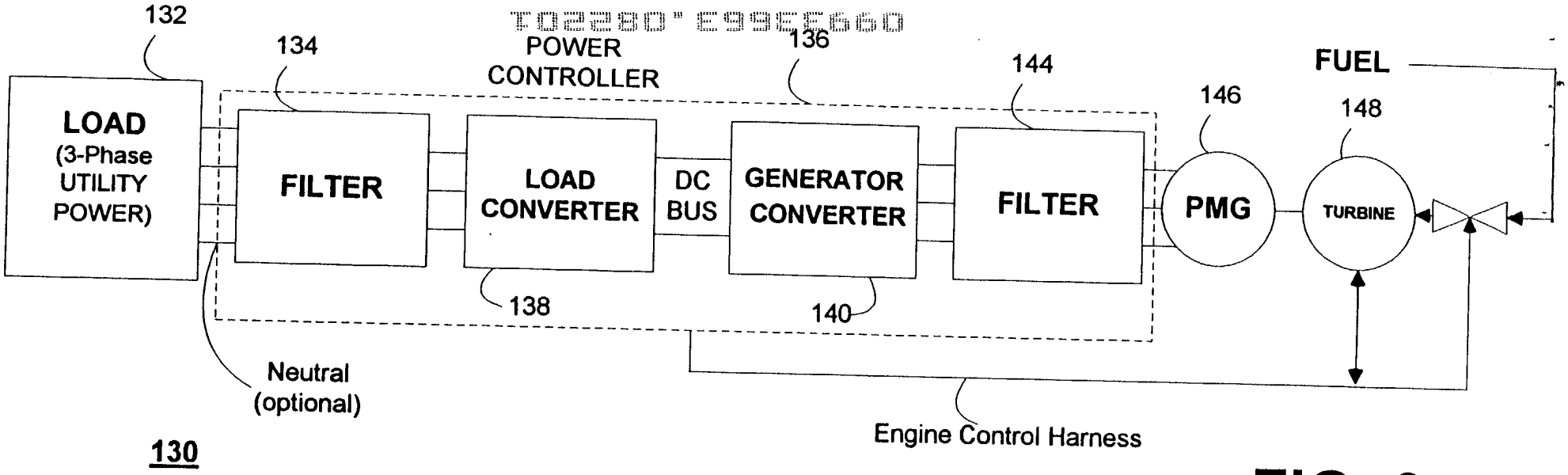
132
134
POWER CONTROLLER
136
144
FUEL
146
148
LOAD
(3-Phase UTILITY POWER)
FILTER
LOAD CONVERTER
DC BUS
GENERATOR CONVERTER
FILTER
PMG
TURBINE
138
140
Neutral (optional)
Engine Control Harness
130

FIG. 6

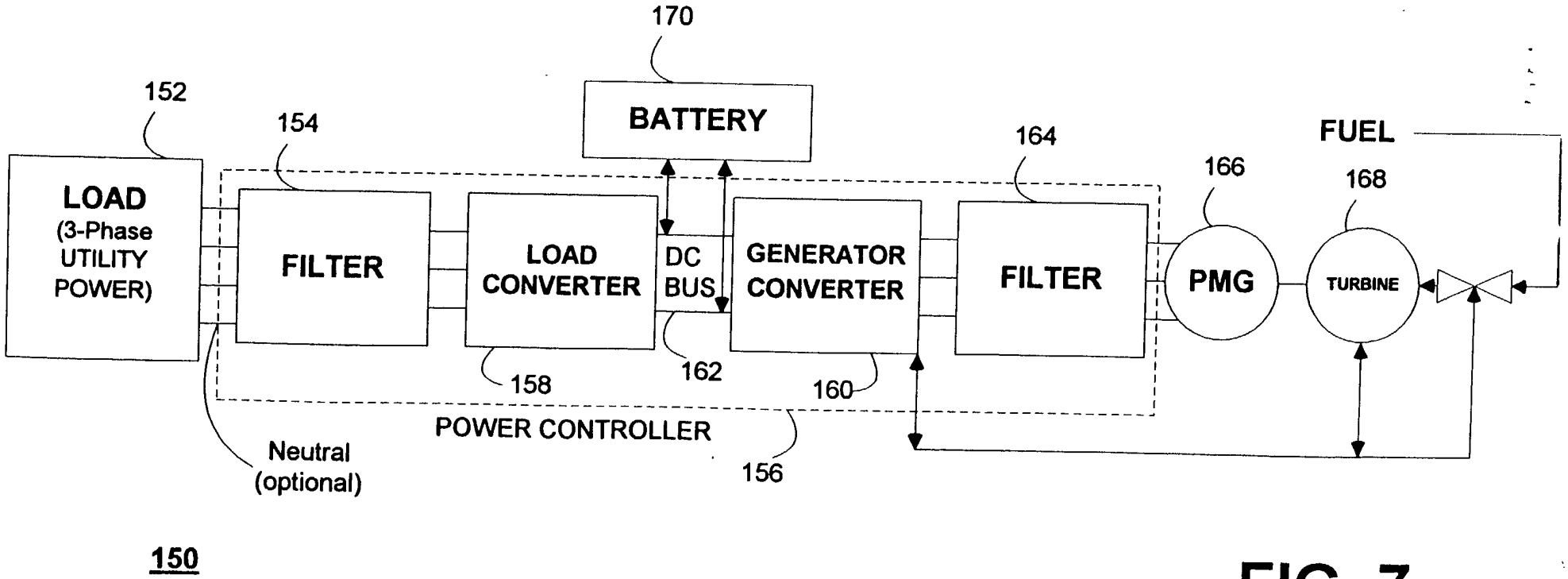
170
BATTERY
152
154
164
FUEL
166
168
LOAD
(3-Phase UTILITY POWER)
FILTER
LOAD CONVERTER
DC BUS
GENERATOR CONVERTER
FILTER
PMG
TURBINE
158
162
160
POWER CONTROLLER
Neutral (optional)
156
150

FIG. 7

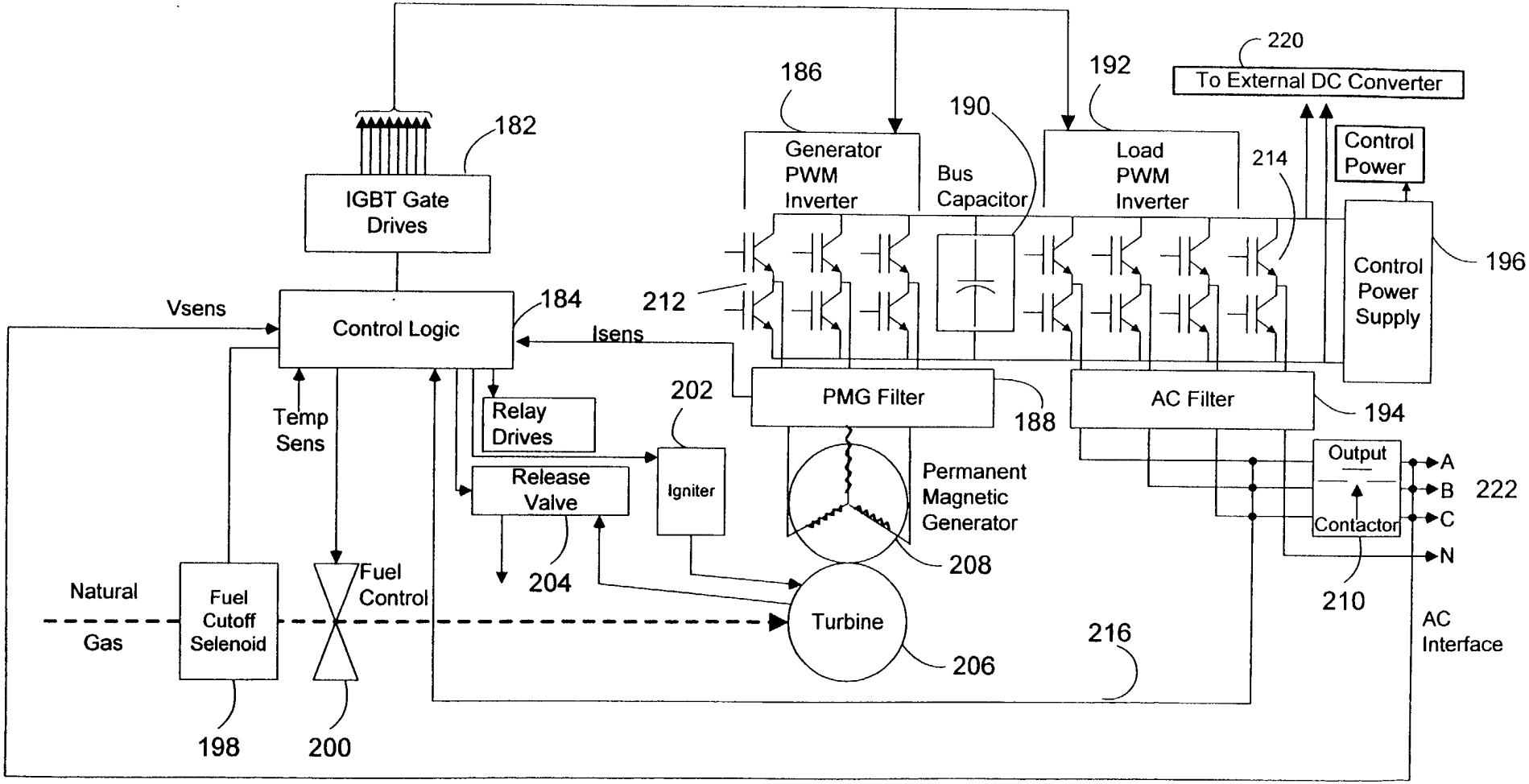
220
To External DC Converter
186
192
190
182
Generator PWM Inverter
Bus Capacitor
Load PWM Inverter
214
Control Power
IGBT Gate Drives
196
Control Power Supply
Vsens
184
212
Control Logic
Isens
202
PMG Filter
188
AC Filter
194
Temp Sens
Relay Drives
Output
A
B
C
222
Release Valve
Igniter
Permanent Magnetic Generator
Contactor
N
208
204
210
Natural Gas
Fuel Cutoff Selenoid
Fuel Control
Turbine
216
AC Interface
206
198
200

180

FIG. 8

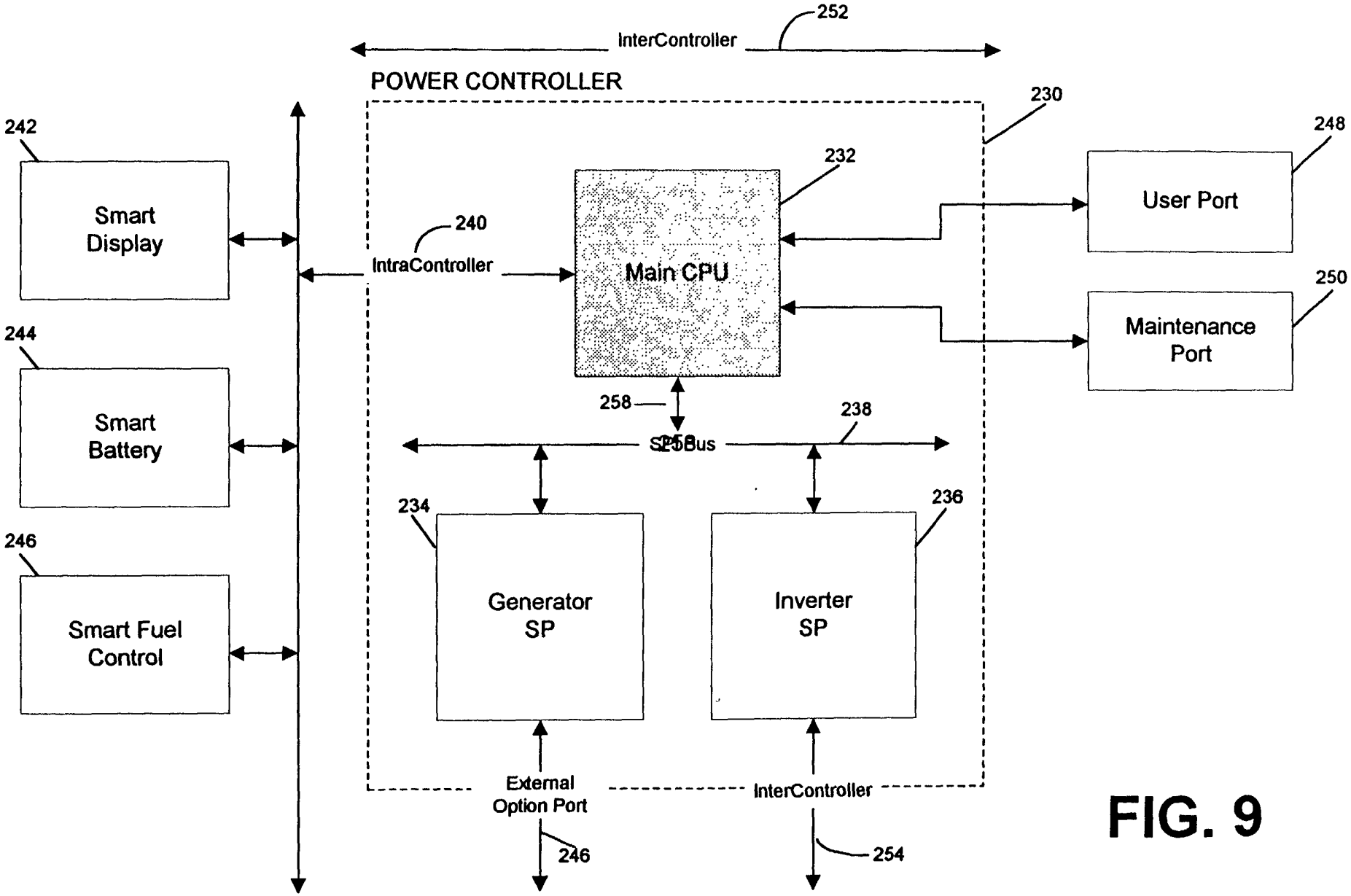

FIG. 9

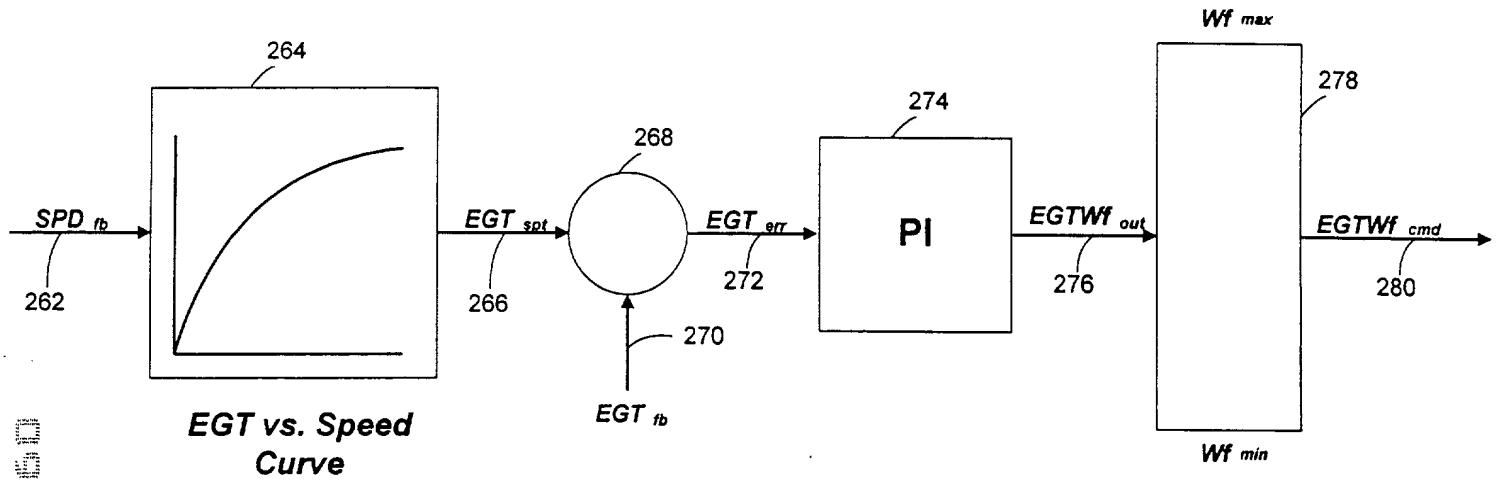

260

FIG. 10

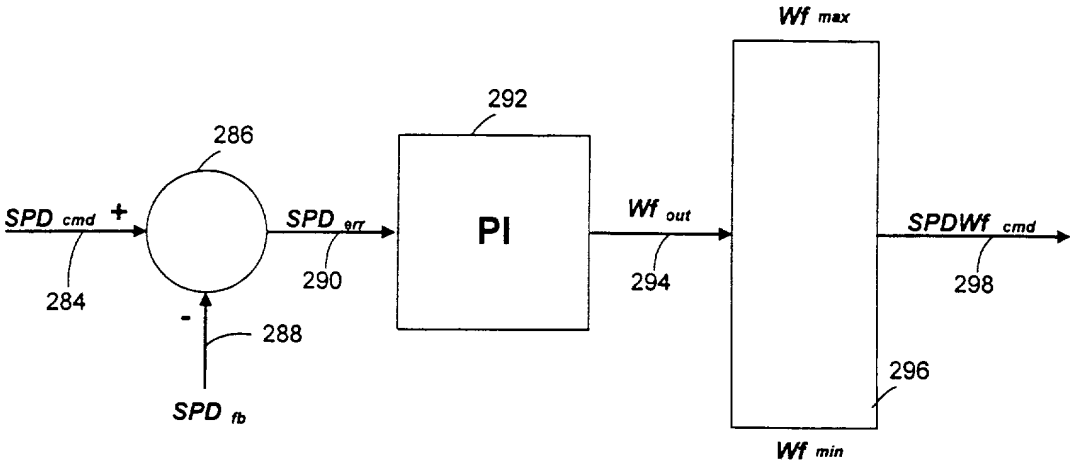
Wf max
292
286
SPD cmd
+
SPD err
PI
Wf out
SPDWf cmd
284
290
294
298
-
288
296
SPD fb
Wf min

282

FIG. 11

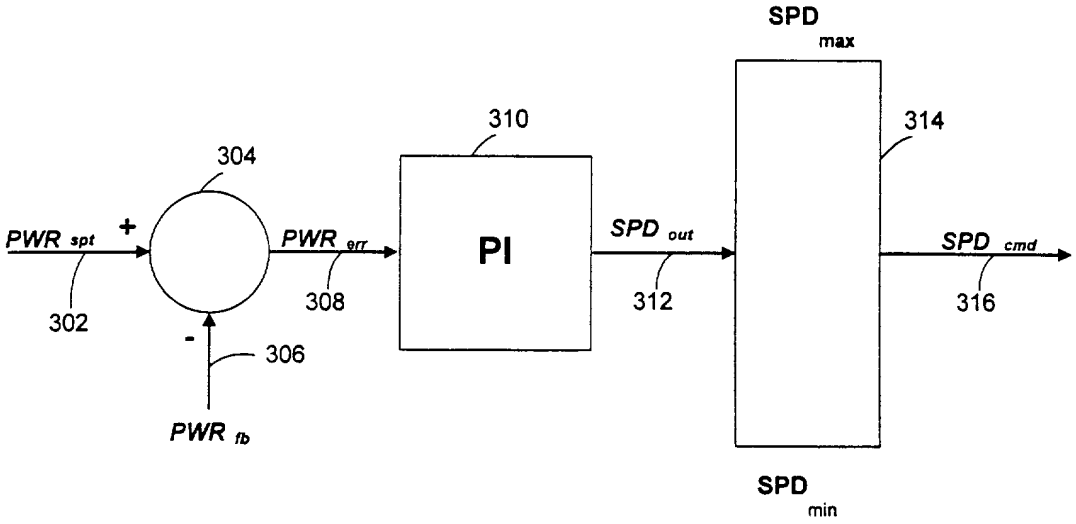
SPD max
310
314
304
PWR spt
+
PWR err
PI
SPD out
SPD cmd
302
308
312
316
-
306
PWR fb
SPD min

300

FIG. 12

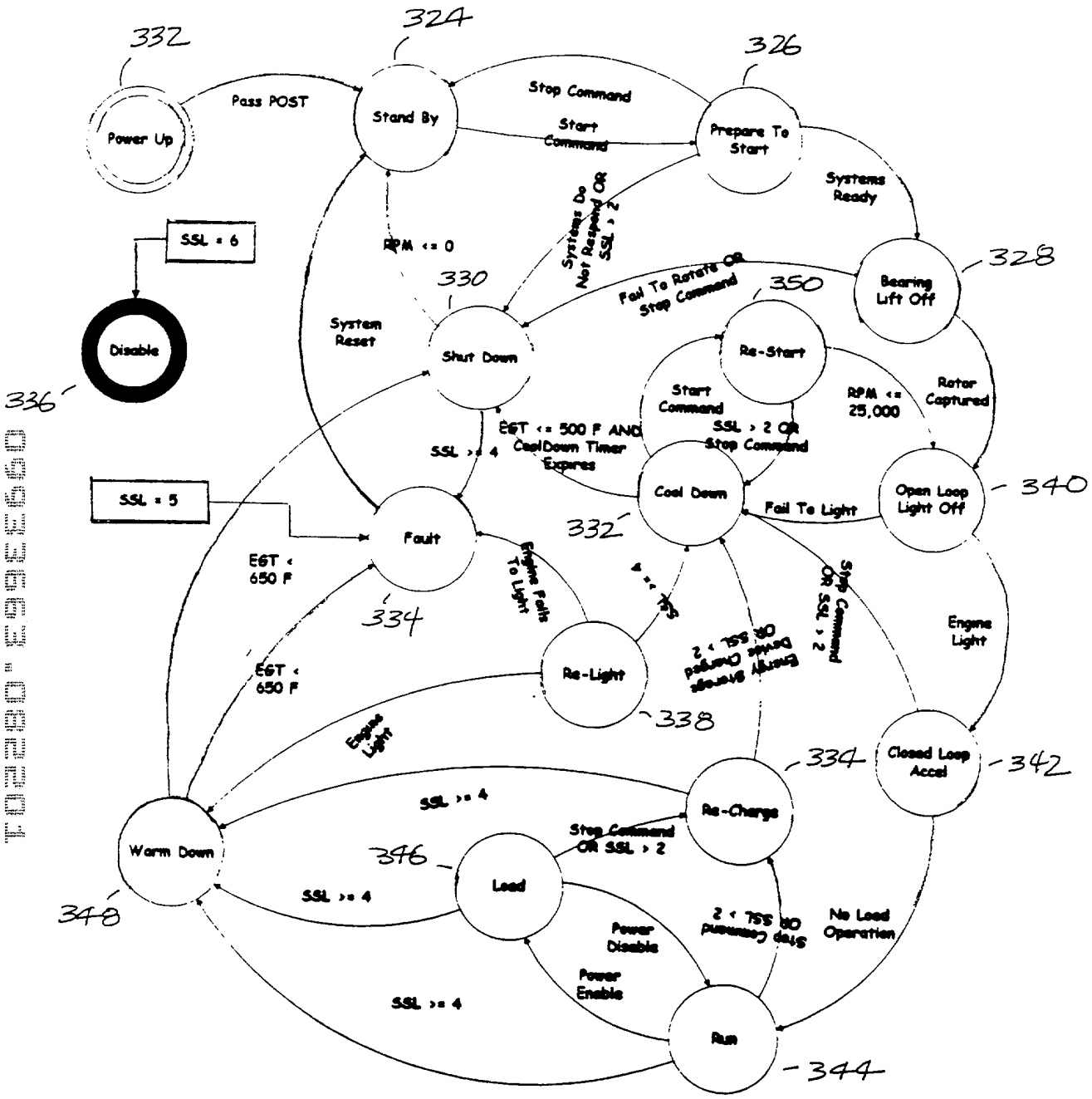
332
324
326
Power Up
Pass POST
Stand By
Stop Command
Start Command
Prepare To Start
Systems Ready
SSL = 6
Disable
336
RPM <= 0
330
Systems Do Not Respond OR SSL > 2
Fail To Rotate OR Stop Command
350
Bearing Lift Off
328
System Reset
Shut Down
Re-Start
Start Command
SSL > 2 OR Stop Command
RPM <= 25,000
Rotor Captured
EGT <= 500 F AND CoolDown Timer Expires
SSL >= 4
Cool Down
Open Loop Light Off
340
SSL = 5
Fault
332
Fail To Light
EGT < 650 F
334
Engine Fails To Light
Re-Light
338
Engine Light
Closed Loop Accel
342
334
Re-Charge
SSL >= 4
Stop Command OR SSL > 2
Warm Down
346
Load
SSL >= 4
Power Disable
No Load Operation
348
Power Enable
SSL >= 4
Run
344

FIG. 13

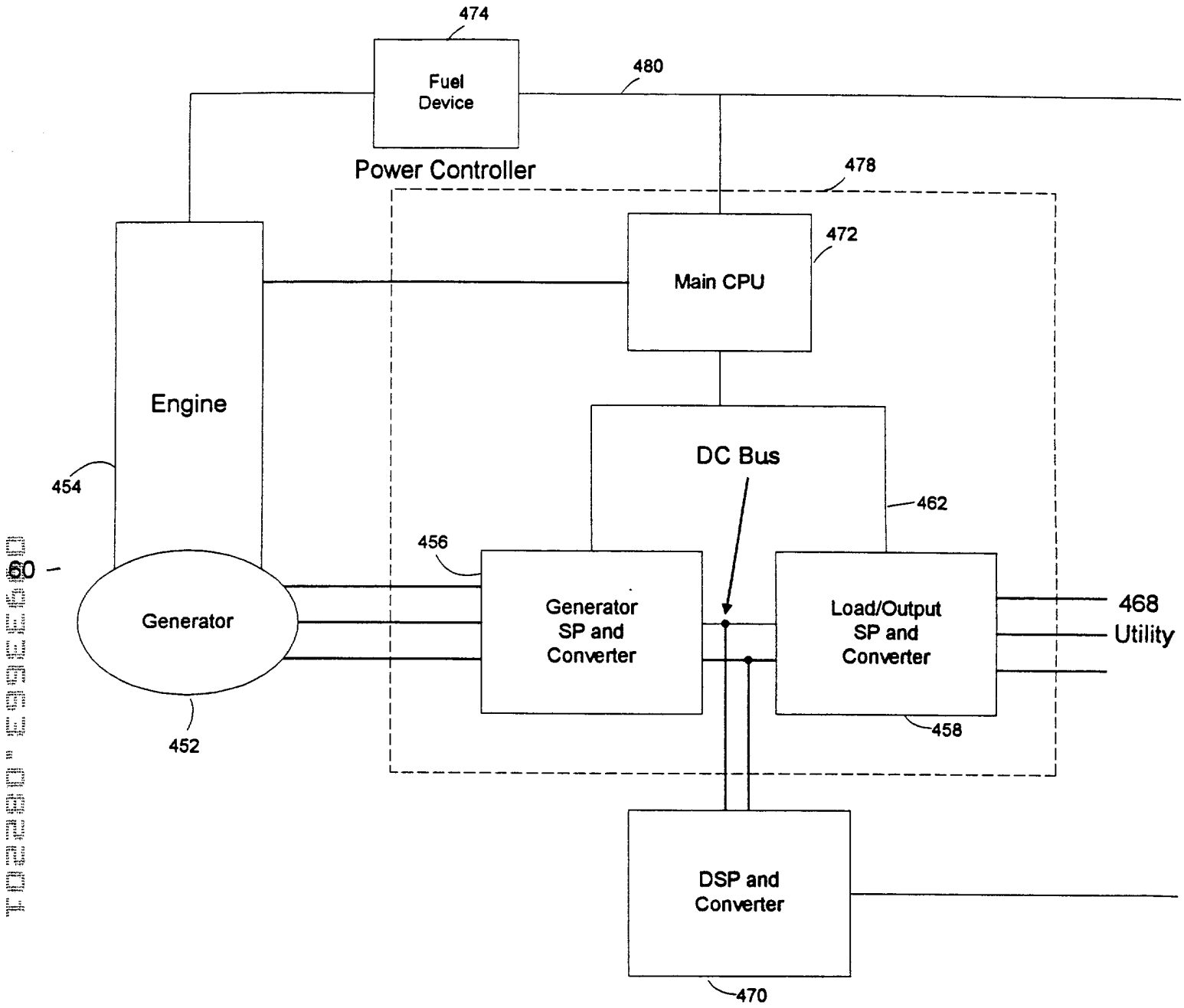
474
Fuel Device
480
Power Controller
478
472
Main CPU
Engine
DC Bus
454
462
456
60
Generator
Generator SP and Converter
Load/Output SP and Converter
468
Utility
452
458
DSP and Converter
470

450

FIG. 14

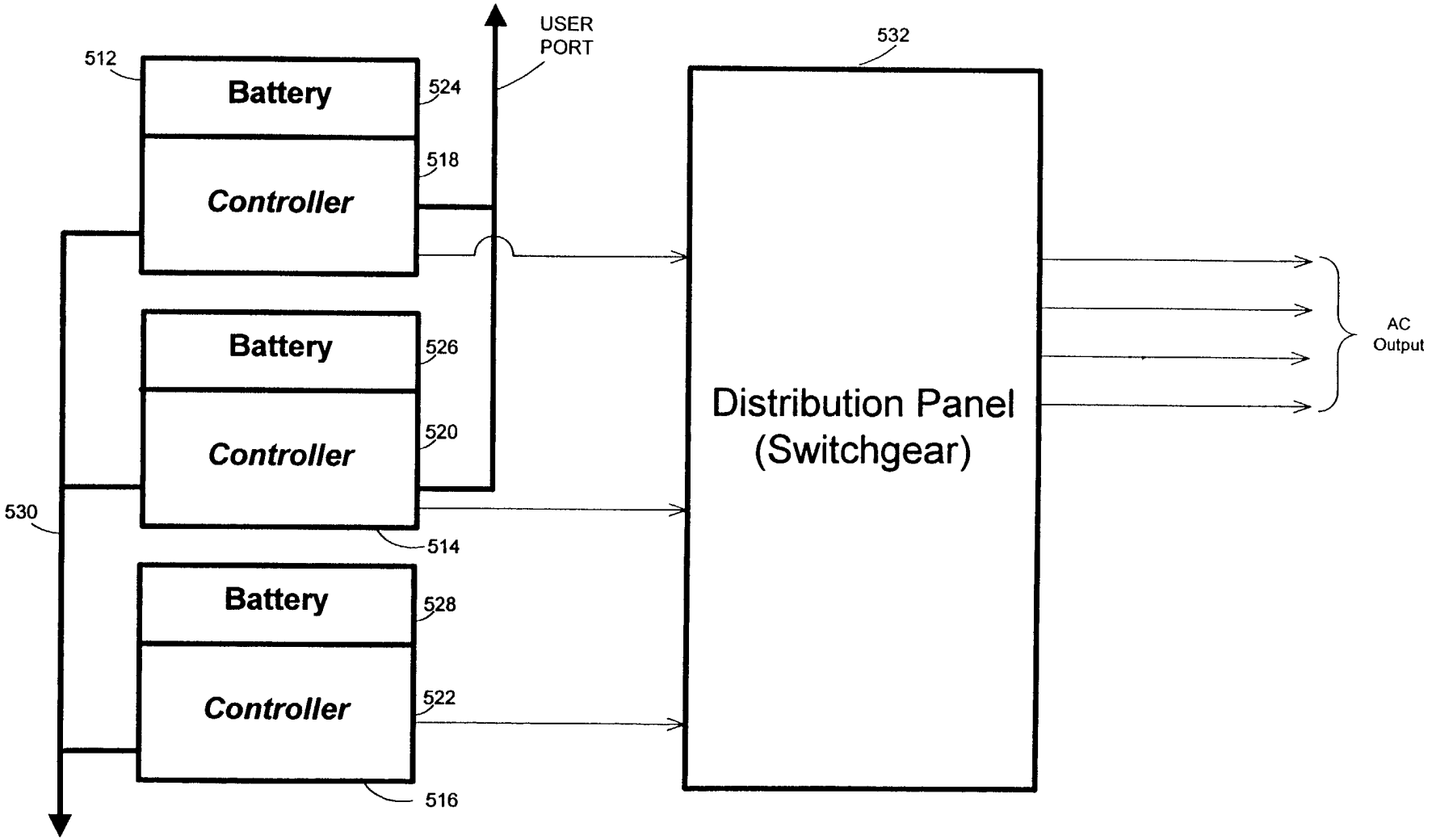

FIG. 15

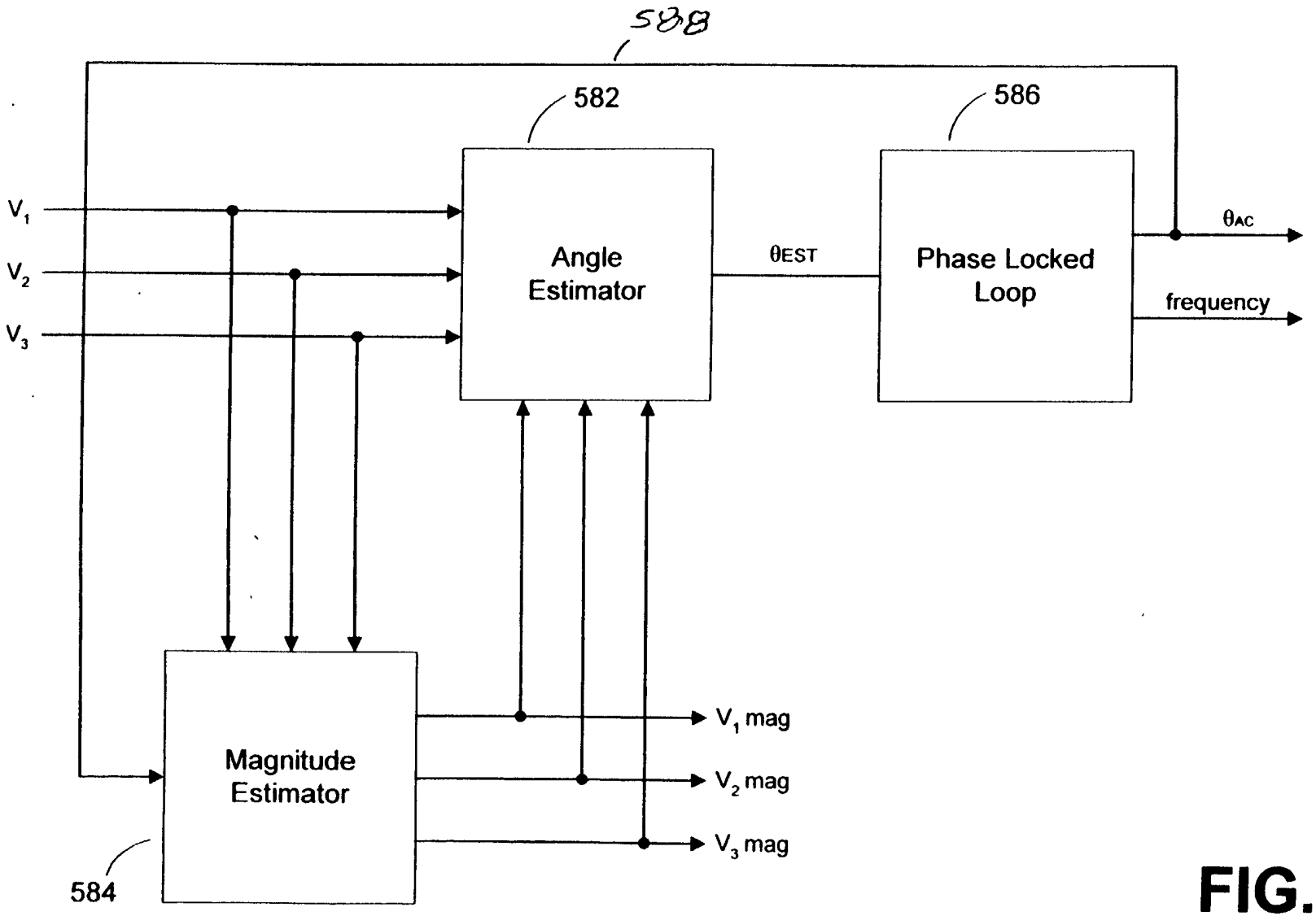
588
582
586
V1
V2
V3
Angle Estimator
θEST
Phase Locked Loop
θAC
frequency
Magnitude Estimator
V1 mag
V2 mag
V3 mag
584
580

FIG. 16

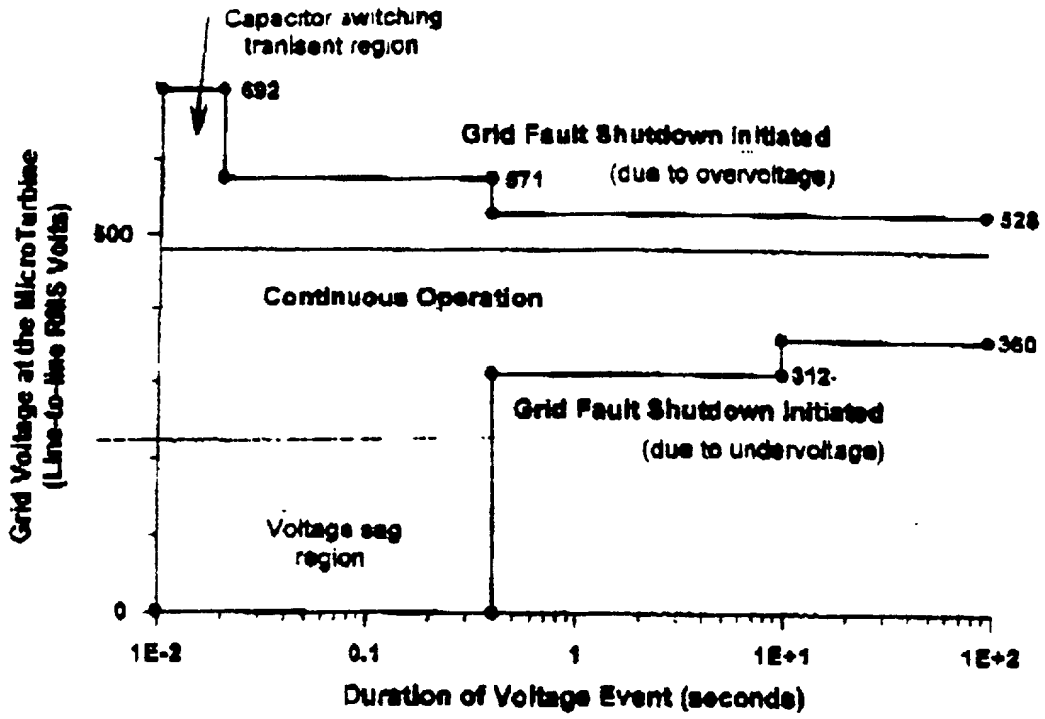
Capacitor switching transient region
692
Grid Fault Shutdown initiated
(due to overvoltage)
571
528
500
Continuous Operation
360
312
Grid Fault Shutdown initiated
(due to undervoltage)
Voltage sag region
0
1E-2
0.1
1
1E+1
1E+2
Duration of Voltage Event (seconds)
Grid Voltage at the MicroTurbine (Line-to-line RMS Volts)

FIG. 17

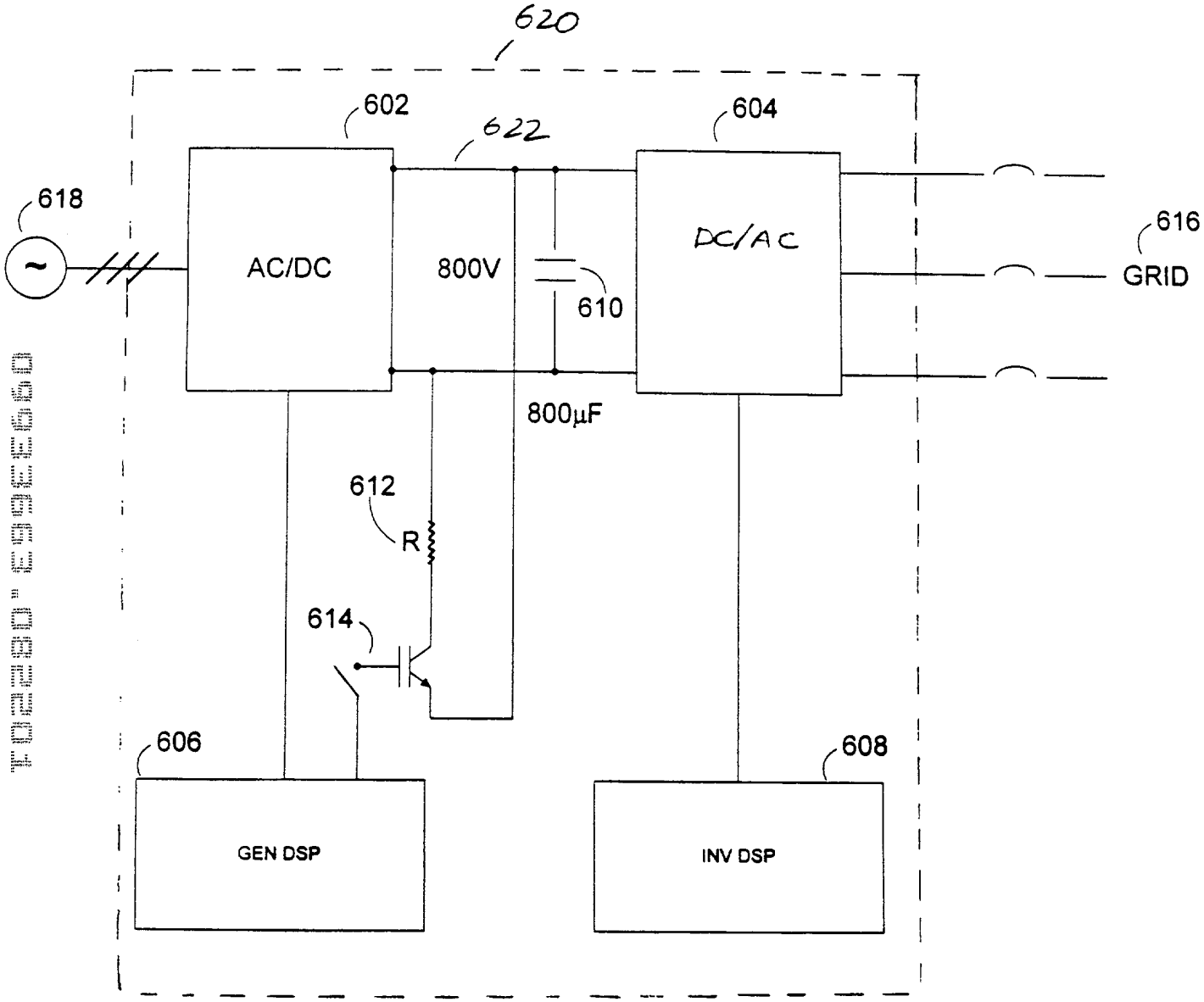
620
602
622
604
618
AC/DC
800V
610
DC/AC
616
GRID
800µF
612
R
614
606
608
GEN DSP
INV DSP

600

FIG. 18

Appendix B

ANALYSIS OF EMISSION CONTROL BY A CATALYTIC RECUPERATOR AND BY UPSTREAM MONOLITHS

INTRODUCTION

[redacted] using post turbine catalytic monoliths and catalytically active exhaust-side recuperator surfaces to remove hydrocarbon and carbon monoxide emissions from the Capstone turbogenerators. [redacted] This report represents the detailed analysis, calculations, results, and conclusions. Also attached are the MathSoft Mathcad™ 6+ documents comprising the analyses and an Excel 5.0 spreadsheet of the findings.

TRANSPORT AND KINETIC ANALYSIS OF THE RECUPERATOR AND MONOLITHS

The analysis of the conversion of heptene (C_7H_{14}), methane (CH_4), and carbon monoxide (CO), were completed for several configurations of a recuperator and honeycomb catalytic converters. The method used was a MATHCAD program, and the procedures were similar to the document sent to Capstone [redacted] (CAPSTONE.MCD document).

The analyses consist of the following features (see printouts for ~~CPSTONE5.MCD and~~ CPSTONE6.MCD):

Gas Properties

- The properties of the gases used in the combustion mixture are described on pages 1-8.
- The gas compositions both for complete combustion air with fuel equivalence ratio 0.1 in moist (2 vol% water vapor) air, as specified in the problem statement, and also for an adiabatic temperature rise from 1000° to 1511_F using heptene are defined on page 2. The difference in properties between these two compositions is insignificant.
- Essential transport properties, such as the diffusivities of the added gases are determined on pages 3-4.
- Mixture properties such as viscosity, thermal conductivity, heat capacity, and various dimensionless transport numbers such as the Prandtl and Schmidt numbers are defined and calculated on pages 5-8.

[redacted]

B1

Recuperator and Converter Dimensions and Operating Conditions

- The dimensions of the honeycomb sizes from 100 to 800 cells/in.^{2} are defined on page 9 along with the size and dimensions of the recuperator and the upstream monolith converters.
- The five operating combustion conditions representing the different power level cases for the turbogenerator are specified on pages 9-10.
- The pressure drop for the 600 or 800 cells/in^2 recuperator is determined on page 11, and the analysis of heat transfer within the recuperator is described on page 12.

Recuperator Performance

- Mass transfer rates to the wall of the recuperator (assuming very fast conversion kinetics at the wall) are described on pages 13-14 for all three added components (C_7H_{14}, CH_4, and CO). These calculations used average temperatures to determine an integrated formula for fuel conversion.
- An alternative form of conversion was developed by looking at local Nusselt number (modified for the square channel configuration). This analysis is described on pages 15 and 16. The two methods show good agreement for C_7H_{14}conversion.
- Catalytic properties and functions are defined on pages 17-18, and the specific rate expression for oxidation of dilute CH_4 by supported palladium oxide (PdO) is described on page 19.
- Slow (in CPSTONE5.MCD and related to the rate of CH_4 oxidation) and moderate (in CPSTONE6.MCD and related to the rate of C_3H_6 oxidation) rate constants for C_7H_{14} oxidation are described on p. 19.
- The performance of the recuperator for conversion with temperature-dependent mass transfer properties and specific catalytic rates for C_7H_{14} and CH_4 are described on pages 20-21.

Performance of Upstream Monoliths

- The operating conditions for 200, 400, and 600 cells/in.^{2} honeycombs is described on pages 22-25.
- The pressure drop for three honeycombs (200, 400, and 600 cells/in.^{2}) is described on pages 22-23, and matched to the maximum specified conditions. From of these calculations, two honeycomb converter configurations, 400 cells/in.^{2} by 4 in. length and 600 cells/in.^{2} by 3.5 in. length, were chosen for mass transfer calculations.
- The effluent concentrations of added components are calculated for the constant temperature monoliths (400 cells/in.^{2} in CPSTONE5.MCD and 600 cells/in.^{2} in CPSTONE6.MCD) for the five operating conditions (cases) on pages 24-25, assuming very fast catalytic rates.
- Finally, on pages 25-27, the conversion of C_7H_{14} and CH_4 using finite catalytic rates are described for the honeycomb converters (400 cells/in.^{2} in CPSTONE5.MCD and 600 cells/in.^{2} in CPSTONE6.MCD).

RESULTS OF THE ANALYSIS

The principal results of the analysis of post turbine fuel component conversion are shown in the attached spreadsheet tables (CAPSTN5.XLS) and Mathcad documents (CPSTONE5.MCD and CPSTONE6.MCD). The main results of the analyses are summarized as follows:

Catalytic Recuperator

- The ΔP/P calculations seem to very closely fit your measured values. [redacted] We chose as the best calculation of pressure drop an 800 cells/in^2 x 7-in. with 10% additional added length to describe the chevron geometry of the recuperator foils.
- The estimated averaged wall temperatures, or skin temperatures, within the recuperator seemed a little low (< 50°F) based on [redacted] discussions of recuperator thermal efficiency. As a consequence, the cell size was increased to 600 cells/in^2 keeping the length the same (7 in. x 1.1) for a conservative calculation of mass transfer rates.
- For the mass transfer limited cases (assuming fast kinetics), virtually complete conversion CH_4 and CO is predicted (see Table of Results 1). Except at the highest power level, conversion of CH_4 and CO was essentially complete within the first inch or two of entry into the recuperator.
- For the transport-limited cases with C_7H_{14}, maximum conversions are low only for Case 5 (full power). Even in this case, 50 ppm would be converted to < 1 ppm (0.2 ppm) while concentrations entering the recuperator above 250 ppm would exit at levels above 1 ppm (500 ppm ⇒ 2.1 ppm). The situation improves for the other cases (e.g., Case 4 gives 500 ppm ⇒ 0.02 ppms while 5000 ppm ⇒ 0.17 ppm) .
- Conversions would be much higher for transport limited conversion in a the 800 cells/in.^{2} recuperator, as calculations with this cell size were found reproduce the observed pressure drop. In this case, the logarithm of the inlet concentration divided by the outlet concentration for all added components would be ~35 % greater with the smaller cell size.
- The step-wise calculation which includes the temperature on flow velocity and transport properties showed reasonably good agreement with the integrated calculation using average properties. This method gave lower overall conversion than the averaged property formulas, but the results were close. Perhaps the higher property values at the inlet, particularly the greater velocity, more than offset the lower transport values at the outlet side.
- CH_4 conversion is catalytically rate limited under all conditions (see Table of Results 1). Conversions were calculated to be very low, with a maximum conversion of ~66% under Case 1 and ~32% conversion under Case 5. These conversions would increase somewhat, perhaps by a factor of 2, with the use of a thicker coating (e.g., 25 μm vs. 10 μm).
- CO conversion is likely to exceed 99% in all operating conditions for the recuperator. This is because the kinetics of CO conversion are probably much faster than CH_4 and may well be close to the transport-limited case, at least through the (hotter) first several inches of the recuperator where most of the CO would be consumed.

[redacted]

- The catalytic recuperator, C_7H_{14} rate determines its conversion in the recuperator conditions (see Table of Results 1). For the slower rates (derived from the rates for CH_4 oxidation) using the 600 cells/in.^{2} value for recuperator cell size, we find a range from 99.4% conversion under Case 1 to about 85.6% under Case 5. If twice the rate of combustion of propane is extrapolated to the higher temperatures of the recuperator, much higher C_7H_{14} conversions result, 99.98% under Case 1, and 96.4% under Case 5.

Catalytic Monoliths

- The pressure drop reaches maximum specifications for the 400 cells/in.^{2} honeycomb at 4-in. length. Maximum pressure drop would be reached in a shorter (~3.5 in. length) 600 cells/in.^{2} monolith. Both configurations were chosen for analysis (CPSTONE5.MCD for 400 cells/in.^{2} and CPSTONE6.MCD for 600 cells/in.^{2}).
- Transport-limited conversion shows excellent performance for methane and CO in all cases, including the full-power case, for both honeycomb configurations (see Table of Results 2).
- As for the recuperator, methane conversion is again reaction rate limited (see Table of Results 3), with conversions range from 93.8% under Case 1 with the 600 cells/in.^{2} monolith to only 31% conversion under Case 5 for the 400 cells/in.^{2} monolith.
- C_7H_{14} conversions under transport-limited conditions depends on the specific configuration (see Table of Results 2). For the 600 cells/in.^{2} monolith conversions are very high for Case 1, but fall to about 92% for Case 5. With the 400 cells/in.^{2} configuration, these fast kinetic transport-limited conversions fall to 87% conversion under Case 5.
- The reaction rate of C_7H_{14} strongly affects its conversion in either honeycomb monolith (see Table of Results 3). For the extrapolated propane kinetics at 600 cells/in.^{2}, 98% conversion is expected under Case 5, whereas the 400 cells/in.^{2} using the more conservative extrapolation using PdO methane kinetics, 86% conversion is expected under Case 5.

Effect of Washcoat Thermal Conductivity in a Recuperator

- The application of a thin washcoat of porous alumina gives a very slight *increase* in the overall heat transfer coefficient [redacted] CPSNALT2.MCD). The thermal conductivity of the washcoat, while significantly less than that of stainless 321, is greater than that of the gas phase boundary. Because the washcoat displaces the gas phase (creating a narrower channel) it causes a slight increase in overall heat transfer coefficient.

[redacted]

OVERALL CONCLUSIONS AND RECOMMENDATIONS

The conclusions and recommendations drawn from the results of the analysis is listed below:

1) The actual C_7H_{14} outlet concentration from the turbine are needed to assess the effluent emissions in the high-power case (Case 5) for either control strategy. Provided that fast catalytic rates can be provided in washcoats on either the recuperator or upstream monoliths, maximum conversions for C_7H_{14} under full power range from 99.6% (for an effective cell size of 600 cells/in^2) to > 99.9% (if the effective cell size is 800 cells/in^2).

2) The two methods (averaged properties and integrated formulas vs. local temperature dependent properties and finite difference integration) show good agreement for recuperator performance with infinitely fast catalytic reactions at the wall.

3) Clearly, it will be necessary to apply and measure specific catalytic rates for C_7H_{14} or gasoline to be sure that these estimated conversions could be achieved under actual operating conditions for either the catalytic recuperator or the upstream honeycomb monoliths.

4) Thin wash coats (< 20 μm) should have minimal effect on the transport of heat through the recuperator given the much greater resistance of the gas phase boundary layers.

5) For the current operating conditions, use of a standard 400 cells/in^2 x 4-in length catalytic monolith upstream of the recuperator is recommended.

6) If the recuperator temperature can be raised (~ 200°F) high conversions of CO, C_7H_{14}, and even CH_4 can be expected under all flow conditions. In this case it is possible that only the first 3 to 4 inches of the recuperator be wash coated with catalyst because the downstream wall temperatures are too cool to be effective.

[redacted]

Inlet (added component) conc(ppm)	Recuperator - Transport only (assumes fast reaction kinetics) at 600 cells/in2														
	Case-1			Case-2			Case-3			Case-4			Case-5		
	CH4	C7H14	CO	CH4	C7H14	CO	CH4	C7H14	CO	CH4	C7H14	CO	CH4	C7H14	CO
5000	2.011E-25	3.554E-05	5.555E-23	3.704E-19	0.002197	3.002E-17	1.373E-15	0.022964	5.542E-14	1.470E-12	0.1687	3.276E-11	2.818E-05	20.8392	1.467E-04
2000	8.046E-26	1.422E-05	2.222E-23	1.481E-19	8.787E-04	1.201E-17	5.492E-16	0.009186	2.217E-14	5.880E-13	0.0674683	1.310E-11	1.127E-05	8.2557	5.870E-05
1000	4.023E-26	7.108E-06	1.111E-23	7.407E-20	4.393E-04	6.003E-18	2.746E-16	0.004593	1.108E-14	2.940E-13	0.0337341	6.552E-12	5.637E-06	4.1278	2.935E-05
500	2.011E-26	3.554E-06	5.555E-24	3.704E-20	2.197E-04	3.002E-18	1.373E-16	0.002296	5.542E-15	1.470E-13	0.0168671	3.276E-12	2.818E-06	2.0639	1.467E-05
200	8.046E-27	1.422E-06	2.222E-24	1.481E-20	8.787E-05	1.201E-18	5.492E-17	9.186E-04	2.217E-15	5.880E-14	0.0067468	1.310E-12	1.127E-06	0.8256	5.870E-06
100	4.023E-27	7.108E-07	1.111E-24	7.407E-21	4.393E-05	6.003E-19	2.746E-17	4.593E-04	1.108E-15	2.940E-14	0.0033734	6.552E-13	5.637E-07	0.4128	2.935E-06
50	2.011E-27	3.554E-07	5.555E-25	3.704E-21	2.197E-05	3.002E-19	1.373E-17	2.296E-04	5.542E-16	1.470E-14	0.0016867	3.276E-13	2.818E-07	0.2064	1.467E-06
20	8.046E-28	1.422E-07	2.222E-25	1.481E-21	8.787E-06	1.201E-19	5.492E-18	9.186E-05	2.217E-16	5.880E-15	6.747E-04	1.310E-13	1.127E-07	0.082557	5.870E-07
10	4.023E-28	7.108E-08	1.111E-25	7.407E-22	4.393E-06	6.003E-20	2.746E-18	4.593E-05	1.108E-16	2.940E-15	3.373E-04	6.552E-14	5.637E-08	0.041278	2.935E-07
5	2.011E-28	3.554E-08	5.555E-26	3.704E-22	2.197E-06	3.002E-20	1.373E-18	2.296E-05	5.542E-17	1.470E-15	1.687E-04	3.276E-14	2.818E-08	0.020639	1.467E-07
2	8.046E-29	1.422E-08	2.222E-26	1.481E-22	8.787E-07	1.201E-20	5.492E-19	9.186E-06	2.217E-17	5.880E-16	6.747E-05	1.310E-14	1.127E-08	0.008256	5.870E-08
1	4.023E-29	7.108E-09	1.111E-26	7.407E-23	4.393E-07	6.003E-21	2.746E-19	4.593E-06	1.108E-17	2.940E-16	3.373E-05	6.552E-15	5.637E-09	0.004128	2.935E-08

Recuperator - C7H14 without reaction with T-dependence (step) and CH4and C7H14 with finite catalytic reaction rates at the wall (C7H14 rate = 10 x CH4 Rate - slow kinetics)

Inlet conc(ppm)	Case-1			Case-2			Case-3			Case-4			Case-5		
	C7H14step	CH4react	C7H14react	C7H14step	CH4react	C7H14react	C7H14step	CH4react	C7H14react	C7H14step	CH4react	C7H14react	C7H14step	CH4react	C7H14react
5000	3.201E-04	1675.00	31.5850	0.012075	2065.00	82.9500	0.094050	2310.00	139.15	0.5350	2545.00	217.85	34.8400	3420.00	707.50
2000	1.280E-04	670.00	12.6340	0.004830	826.00	33.1800	0.037620	924.00	55.6600	0.2140	1018.00	87.1400	13.9360	1368.00	283.00
1000	6.402E-05	335.00	6.3170	0.002415	413.00	16.5900	0.018810	462.00	27.8300	0.1070	509.00	43.5700	6.9680	684.00	141.50
500	3.201E-05	167.50	3.1585	0.001208	206.50	8.2950	0.009405	231.00	13.9150	0.053500	254.50	21.7850	3.4840	342.00	70.7500
200	1.280E-05	67.0000	1.2634	0.000483	82.6000	3.3180	0.003762	92.4000	5.5660	0.021400	101.80	8.7140	1.3936	136.80	28.3000
100	6.402E-06	33.5000	0.6317	0.000242	41.3000	1.6590	0.001881	46.2000	2.7830	0.010700	50.9000	4.3570	0.6968	68.4000	14.1500
50	3.201E-06	16.7500	0.3159	0.000121	20.6500	0.8295	9.405E-04	23.1000	1.3915	0.005350	25.4500	2.1785	0.3484	34.2000	7.0750
20	1.280E-06	6.7000	0.1263	0.000048	8.2600	0.3318	3.762E-04	9.2400	0.5566	0.002140	10.1800	0.8714	0.1394	13.6800	2.8300
10	6.402E-07	3.3500	0.063170	2.415E-05	4.1300	0.1659	1.881E-04	4.6200	0.2783	0.001070	5.0900	0.4357	0.069680	6.8400	1.4150
5	3.201E-07	1.6750	0.031585	1.208E-05	2.0650	0.082950	9.405E-05	2.3100	0.1392	5.350E-04	2.5450	0.2179	0.034840	3.4200	0.7075
2	1.280E-07	0.6700	0.012634	4.830E-06	0.8260	0.033180	3.762E-05	0.9240	0.055660	2.140E-04	1.0180	0.0871	0.013936	1.3680	0.2830
1	6.402E-08	0.3350	0.006317	2.415E-06	0.4130	0.016590	1.881E-05	0.4620	0.027830	1.070E-04	0.5090	0.0436	0.006968	0.6840	0.1415

	ln(yout/yin)				
Case# :	1	2	3	4	5
CH4:	-65.383	-50.957	-42.739	-35.763	-18.994
C7H14	-18.762	-14.638	-12.291	-10.297	-5.49
CO	-59.762	-46.562	-39.041	-32.659	-17.344
C7H14step	-16.56407	-12.933811	-10.88112	-9.142682	-4.966427
CH4react	-1.0936247	-0.8843077	-0.77219	-0.675307	-0.379797
C7H14react	-5.0645109	-4.0989552	-3.581641	-3.133386	-1.955456

BL transport only with averaged intergated values
BL transport only with averaged intergated values
BL transport only with averaged intergated values
BL transport only with T-dependent properties and step-wise integration
BL transport-restricted catalytic rates with T-dependent properties and step-wise integration
BL transport-restricted catalytic rates with T-dependent properties and step-wise integration

B2

Table of Results 2

[redacted]

Inlet (added component) conc(ppm)		Transport only (assumes fast reaction kinetics) for a 600 cells/in2 x 3.5-in length square honeycomb monolith														
		Case-1			Case-2			Case-3			Case-4			Case-5		
	CH4	C7H14	CO	CH4	C7H14	CO	CH4	C7H14	CO	CH4	C7H14	CO	CH4	C7H14	CO	
5000	7.960E-25	4.179E-04	2.470E-22	2.069E-18	0.017928	1.708E-16	9.839E-15	0.1545	3.802E-13	1.170E-11	0.9353	2.395E-10	2.773E-04	70.3859	0.001222	
2000	3.184E-25	1.672E-04	9.878E-23	8.276E-19	0.007171	6.831E-17	3.936E-15	0.061810	1.521E-13	4.678E-12	0.3741	9.582E-11	1.109E-04	28.1544	4.890E-04	
1000	1.592E-25	8.359E-05	4.939E-23	4.138E-19	0.003586	3.415E-17	1.968E-15	0.030905	7.604E-14	2.339E-12	0.1871	4.791E-11	5.546E-05	14.0772	2.445E-04	
500	7.960E-26	4.179E-05	2.470E-23	2.069E-19	0.001793	1.708E-17	9.839E-16	0.015452	3.802E-14	1.170E-12	0.093528	2.395E-11	2.773E-05	7.0386	1.222E-04	
200	3.184E-26	1.672E-05	9.878E-24	8.276E-20	0.000717	6.831E-18	3.936E-16	0.006181	1.521E-14	4.678E-13	0.037411	9.582E-12	1.109E-05	2.8154	4.890E-05	
100	1.592E-26	8.359E-06	4.939E-24	4.138E-20	0.000359	3.415E-18	1.968E-16	0.003090	7.604E-15	2.339E-13	0.018706	4.791E-12	5.546E-06	1.4077	2.445E-05	
50	7.960E-27	4 179E-06	2.470E-24	2.069E-20	0.000179	1.708E-18	9.839E-17	0.001545	3.802E-15	1.170E-13	0.009353	2.395E-12	2.773E-06	0.7039	1 222E-05	
20	3.184E-27	1.672E-06	9 878E-25	8.276E-21	7 171E-05	6 831E-19	3.936E-17	6 181E-04	1.521E-15	4 678E-14	0.003741	9.582E-13	1.109E-06	0.2815	4.890E-06	
10	1.592E-27	8 359E-07	4 939E-25	4 138E-21	3 586E-05	3.415E-19	1.968E-17	3.090E-04	7.604E-16	2.339E-14	0.001871	4.791E-13	5.546E-07	0.1408	2.445E-06	
5	7.960E-28	4.179E-07	2.470E-25	2.069E-21	1.793E-05	1.708E-19	9.839E-18	1.545E-04	3.802E-16	1.170E-14	9.353E-04	2.395E-13	2.773E-07	0.070386	1 222E-06	
2	3.184E-28	1.672E-07	9 878E-26	8.276E-22	7.171E-06	6.831E-20	3.936E-18	6.181E-05	1.521E-16	4.678E-15	3.741E-04	9.582E-14	1.109E-07	0.028154	4.890E-07	
1	1.592E-28	8.359E-08	4.939E-26	4.138E-22	3.586E-06	3.415E-20	1.968E-18	3.090E-05	7.604E-17	2.339E-15	1.871E-04	4.791E-14	5.546E-08	0.014077	2 445E-07	
		Transport only (assumes fast reaction kinetics) for a 400 cells/in2 x 4-in length square honeycomb monolith														
Inlet conc(ppm)		Case-1			Case-2			Case-3			Case-4			Case-5		
	CH4	C7H14	CO	CH4	C7H14	CO	CH4	C7H14	CO	CH4	C7H14	CO	CH4	C7H14	CO	
5000	3.307E-18	0.003426	2.617E-16	2.551E-13	0.090292	7.363E-12	1.616E-10	0.5882	2.615E-09	3.558E-08	2.81565014	3.550E-07	0.01476631	119.35	0.045698	
2000	1.323E-18	0.001370	1.047E-16	1 021E-13	0.036117	2.945E-12	6.463E-11	0.2353	1.046E-09	1.423E-08	1.12626006	1.420E-07	0.00590653	47.7559	0.018279	
1000	6.613E-19	6.852E-04	5.234E-17	5.103E-14	0.018058	1.473E-12	3.231E-11	0.1176	5.230E-10	7.115E-09	0.56313003	7 100E-08	0.00295326	23.8779	0.009140	
500	3.307E-19	3.426E-04	2 617E-17	2.551E-14	0.009029	7.363E-13	1.616E-11	0.058825	2.615E-10	3.558E-09	0.28156501	3.550E-08	0.00147663	11.9390	0.004570	
200	1.323E-19	1.370E-04	1.047E-17	1.021E-14	0.003612	2.945E-13	6.463E-12	0.023530	1.046E-10	1.423E-09	0.11262601	1.420E-08	5.907E-04	4.7756	0.001828	
100	6.613E-20	6.852E-05	5.234E-18	5.103E-15	0.001806	1.473E-13	3.231E-12	0.011765	5.230E-11	7.115E-10	0.056313	7.100E-09	2.953E-04	2.3878	9.140E-04	
50	3.307E-20	3.426E-05	2.617E-18	2.551E-15	9.029E-04	7.363E-14	1.616E-12	0.005882	2.615E-11	3.558E-10	0.0281565	3.550E-09	1.477E-04	1.1939	4 570E-04	
20	1.323E-20	1.370E-05	1.047E-18	1.021E-15	3.612E-04	2.945E-14	6.463E-13	0.002353	1.046E-11	1.423E-10	0.0112626	1.420E-09	5.907E-05	0.4776	1.828E-04	
10	6.613E-21	6.852E-06	5.234E-19	5.103E-16	1.806E-04	1.473E-14	3.231E-13	0.001176	5.230E-12	7.115E-11	0.0056313	7.100E-10	2.953E-05	0.2388	9 140E-05	
5	3.307E-21	3.426E-06	2.617E-19	2.551E-16	9.029E-05	7.363E-15	1.616E-13	5.882E-04	2.615E-12	3.558E-11	0.00281565	3.550E-10	1.477E-05	0.1194	4.570E-05	
2	1.323E-21	1.370E-06	1.047E-19	1.021E-16	3.612E-05	2.945E-15	6.463E-14	2.353E-04	1.046E-12	1.423E-11	0.00112626	1.420E-10	5.907E-06	0.047756	1 828E-05	
1	6.613E-22	6.852E-07	5.234E-20	5.103E-17	1.806E-05	1 473E-15	3.231E-14	1.176E-04	5.230E-13	7.115E-12	5.631E-04	7 100E-11	2 953E-06	0.023878	9.140E-06	
				ln(yout/yin)												
	Case# :	1	2	3	4	5										
	CH4-600	-64.0074	-49.2367	-40.7696	-33.689	-16.7076		BL transport only with averaged intergated values								
	C7H14-600	-16.2974	-12.5386	-10.3846	-8.5841	-4.2632		BL transport only with averaged intergated values								
	CO-600	-58.27	-44.8234	-37.1153	-30.6695	-15.2241		BL transport only with averaged intergated values								
	CH4-400	-48.7678	-37.5142	-31.0633	-25.6688	-12.7326		BL transport only with averaged intergated values								
	C7H14-400	-14.1935	-10.9219	-9.0478	-7.482	-3.7348		BL transport only with averaged intergated values								
	CO-400	-44.3966	-34.1518	-28.2792	-23 3684	-11.6029		BL transport only with averaged intergated values								

[redacted]

Inlet (added component)		C7H14 with finite catalytic reaction rates at the wall (slow C7H14 rate = 10 x CH4 rate; moderate C7H14 rate = 2 x C3H8 rate)														
		Case-1			Case-2			Case-3			Case-4			Case-5		
conc(ppm)	Recup-m	600cpi-m	400cpi-s	Recup-m	600cpi-m	400cpi-s	Recup-m	600cpi-m	400cpi-s	Recup-m	600cpi-m	400cpi-s	Recup-m	600cpi-m	400cpi-s	
5000	1.1680	0.001005	1.7905	5.7100	0.035610	11.1500	13.35	0.2715	31.6500	27.6200	14.9700	75.7500	180.18	99.6500	726.00	
2000	0.4672	4.020E-04	0.7162	2.2840	0.014244	4.4600	5.3400	0.1086	12.6760	11.1280	5.9880	30.3000	72.0600	39.8600	291.20	
1000	0.2336	2.010E-04	0.3581	1.1420	0.007122	2.2300	2.6700	0.054290	6.3380	5.5640	2.9940	15.1500	36.0300	19.9300	145.60	
500	0.1168	1.005E-04	0.1791	0.5710	0.003561	1.1150	1.3350	0.027145	3.1690	2.7820	1.4970	7.5750	18.0150	9.9650	72.8000	
200	0.046720	4.020E-05	0.071620	0.2284	0.001424	0.4460	0.5340	0.010858	1.2676	1.1128	0.5988	3.0300	7.2060	3.9860	29.1200	
100	0.023360	2.010E-05	0.035810	0.1142	7.122E-04	0.2230	0.2670	0.005429	0.6338	0.5564	0.2994	1.5150	3.6030	1.9930	14.5600	
50	0.011680	1.005E-05	0.017905	0.057100	3.561E-04	0.1115	0.1335	0.002715	0.3169	0.2782	0.1497	0.7575	1.8015	0.9965	7.2800	
20	0.004672	4.020E-06	0.007162	0.022840	1.424E-04	0.044600	0.053400	0.001086	0.1268	0.1113	0.059880	0.3030	0.7206	0.3986	2.9120	
10	0.002336	2.010E-06	0.003581	0.011420	7.122E-05	0.022300	0.026700	5.429E-04	0.063380	0.055640	0.029940	0.1515	0.3603	0.1993	1.4560	
5	0.001168	1.005E-06	0.001791	0.005710	3.561E-05	0.011150	0.013350	2.715E-04	0.031690	0.027820	0.014970	0.075750	0.1802	0.099650	0.7280	
2	4.672E-04	4.020E-07	7.162E-04	0.002284	1.424E-05	0.004460	0.005340	1.086E-04	0.012676	0.011128	0.005988	0.030300	0.072060	0.039860	0.2912	
1	2.336E-04	2.010E-07	3.581E-04	0.001142	7.122E-06	0.002230	0.002670	5.429E-05	0.006338	0.005564	0.002994	0.015150	0.036030	0.019930	0.1456	
		C7H14 without reaction and CH4 with finite catalytic reaction rates at the wall														
Inlet		Case-1			Case-2			Case-3			Case-4			Case-5		
conc(ppm)	C7H14	CH4H600	CH4H400	C7H14	CH4H600	CH4H400	C7H14	CH4H600	CH4H400	C7H14	CH4H600	CH4H400	C7H14	CH4H600	CH4H400	
5000	3.201E-04	310.00	391.30	0.012075	590.60	705.80	0.094050	882.60	988.50	0.5350	1180.00	1310.50	34.8400	2646.60	2979.50	
2000	1.280E-04	124.00	156.52	0.004830	236.00	282.20	0.037620	341.00	385.40	0.2140	464.00	524.20	13.9360	1138.60	1191.80	
1000	6.402E-05	62.0000	78.2600	0.002415	118.00	141.10	0.018810	170.50	197.70	0.1070	232.00	262.10	6.9680	569.30	595.90	
500	3.201E-05	31.0000	39.1300	0.001208	59.0090	70.5500	0.009405	85.2500	98.8500	0.053500	116.00	131.05	3.4840	284.65	297.95	
200	1.280E-05	12.4000	15.6520	4.830E-04	23.6000	28.2200	0.003762	34.1000	39.5400	0.021400	46.4000	52.4200	1.3936	113.86	119.18	
100	6.402E-06	6.2000	7.8260	2.415E-04	11.8000	14.1100	0.001881	17.0500	19.7700	0.010700	23.2000	26.2100	0.6968	56.9300	59.5900	
50	3.201E-06	3.1000	3.9130	1.208E-04	5.9000	7.0550	9.405E-04	8.5250	9.8850	0.005350	11.6000	13.1050	0.3484	28.4650	29.7950	
20	1.280E-06	1.2400	1.5652	4.830E-05	2.3600	2.8220	3.762E-04	3.4100	3.9540	0.002140	4.6400	5.2420	0.1394	11.3860	11.9180	
10	6.402E-07	0.6200	0.7826	2.415E-05	1.1800	1.4110	1.881E-04	1.7050	1.9770	0.001070	2.3200	2.6210	0.069680	5.6930	5.9590	
5	3.201E-07	0.3100	0.3913	1.208E-05	0.5900	0.7055	9.405E-05	0.8525	0.9885	5.350E-04	1.1600	1.3105	0.034840	2.8465	2.9795	
2	1.280E-07	0.1240	0.1565	4.830E-06	0.2360	0.2822	3.762E-05	0.3410	0.3954	2.140E-04	0.4640	0.5242	0.013936	1.1386	1.1918	
1	6.402E-08	0.062000	0.078260	2.415E-06	0.1180	0.1411	1.881E-05	0.1705	0.1977	1.070E-04	0.2320	0.2621	0.006968	0.5693	0.5959	
				ln(yout/yin)												
	Case# :	1	2	3	4	5										
	C7H14Rs	2.34E-04	1.14E-03	2.67E-03	5.56E-03	3.60E-02		BL transport-restricted slower catalytic rates with T-dependent properties and step-wise integration								
	C7H14H600f	2.01E-07	7.12E-06	5.43E-05	2.99E-03	1.99E-02		BL transport-restricted moderate catalytic rates with T-dependent properties and step-wise integration								
	C7H14H400s	3.58E-04	2.23E-03	6.34E-03	1.52E-02	1.46E-01		BL transport-restricted slower catalytic rates with T-dependent properties and step-wise integration								
	C7H14R	-16.56407	-12.933811	-10.881122	-9.1426817	-4.966427		BL transport only with T-dependent properties and step-wise integration								
	CH4H600	0.062	0.118	0.1705	0.232	0.5693		BL transport-restricted catalytic rates with T-dependent properties and step-wise integration								
	CH4H400	0.07826	0.1411	0.1977	0.2621	0.5959		BL transport-restricted catalytic rates with T-dependent properties and step-wise integration								

Gas Properties and Constants

$cm = 0.01 \cdot m$ $J = kg \cdot m^2 \cdot sec^{-2}$ $W = J \cdot sec^{-1}$ $Pref = 1 \cdot atm$

$N = kg \cdot m \cdot sec^{-2}$ $Pa \equiv N \cdot m^{-2}$ $atm = 101300 \cdot Pa$ $\mu m = 0.000001 \cdot m$

$R = 8.3143 \cdot \frac{J}{K}$ $Rc = 8.3143 \cdot J \cdot mole^{-1} \cdot K^{-1}$

n	Gas	MolWt	σ(LJ)	ε(LJ)
0	CH4	$MW_0 = 16.044 \cdot gm$	$\sigma_0 = 3.785 \cdot 10^{-10} \cdot m$	$\varepsilon_0 = 148.6 \cdot K$
1	O2	$MW_1 = 31.999 \cdot gm$	$\sigma_1 = 3.464 \cdot 10^{-10} \cdot m$	$\varepsilon_1 = 106.7 \cdot K$
2	N2	$MW_2 = 28.018 \cdot gm$	$\sigma_2 = 3.798 \cdot 10^{-10} \cdot m$	$\varepsilon_2 = 71.4 \cdot K$
3	CO2	$MW_3 = 44.010 \cdot gm$	$\sigma_3 = 3.941 \cdot 10^{-10} \cdot m$	$\varepsilon_3 = 195.2 \cdot K$
4	H2O	$MW_4 = 18.015 \cdot gm$	$\sigma_4 = 2.641 \cdot 10^{-10} \cdot m$	$\varepsilon_4 = 809.1 \cdot K$

5 C7H14 methyl-cyclohexane $Tc7 = 572.2 \cdot K$ $Tb7 = 374.1 \cdot K$ $Pc7 = 3.47 \cdot 10^6 \cdot Pa$ $Vc7 = 368$

$\varepsilon_5 = \frac{Tc7}{1.2593}$ $\sigma_5 = Vc7^{\frac{1}{3}} \cdot 10^{-10} \cdot m$

$MW_5 = 98.189 \cdot gm$ $\sigma_5 = 7.1661 \cdot 10^{-10} \cdot m$ $\varepsilon_5 = 454.3794 \cdot K$

6 CO	$MW_6 = 28.01 \cdot gm$	$\sigma_6 = 3.69 \cdot 10^{-10} \cdot m$	$\varepsilon_6 = 91.7 \cdot K$

Define constants for transport integrals:

$\sigma\mu a_0 = 1.16145$	$\sigma\mu b_0 = 0.14874$	$\sigma Da_0 = 1.06036$	$\sigma Db_0 = 0.1561$
$\sigma\mu a_1 = 0.52487$	$\sigma\mu b_1 = 0.7732$	$\sigma Da_1 = 0.193$	$\sigma Db_1 = 0.47635$
$\sigma\mu a_2 = 2.16178$	$\sigma\mu b_2 = 2.43787$	$\sigma Da_2 = 1.03587$	$\sigma Db_2 = 1.52996$
		$\sigma Da_3 = 1.76474$	$\sigma Db_3 = 3.89411$

Define transport integrals:

$$\Omega\mu(T) = \sigma\mu a_0 \cdot \exp\left(-\sigma\mu b_0 \cdot \ln(T)\right) + \sum_{i\mu=1}^{2} \sigma\mu a_{i\mu} \cdot \exp\left(\sigma\mu b_{i\mu} \cdot T\right) \qquad \Omega\mu(3) = 1.0394$$

$$\Omega D(T) = \sigma Da_0 \cdot \exp\left(\sigma Db_0 \cdot \ln(T)\right) + \sum_{i\mu=1}^{3} \sigma Da_{i\mu} \cdot \exp\left(\sigma Db_{i\mu} \cdot T\right) \qquad \Omega D(3) = 0.95002$$

B3

****

Set Inlet Conditions: $P := 1 \cdot atm$

$\phi := 0.1$ $\quad yadc7 := 0.0021859$

This value for yadc7 was determined via enthalpy functions [redacted] for temperature rise from 1000F to 1511F.

$yeqc7 := \phi \cdot \frac{0.205}{14}$ $\quad \phi eq := \phi \cdot \frac{yadc7}{yeqc7}$

The value for yeq was determine for a given equilvalence ratio of 0.1 in moist air

$yeqc7 = 0.001464$ $\quad \phi eq = 0.149281$

Define gas composition with C7H14 fuel using moist (2%) air:

$$y7(y0,x) := \frac{\begin{bmatrix} 0 \\ (1-y0)\cdot 0.205 - 10.5\cdot y0\cdot x \\ (1-y0)\cdot 0.775 \\ 7\cdot(y0\cdot x) \\ (1-y0)\cdot 0.02 + 7\cdot y0\cdot x \\ y0\cdot(1-x) \\ 0 \end{bmatrix}}{1 + 2.5\cdot y0\cdot x}$$

$yeq := y7(yeqc7, 1)$ $\quad yeq = \begin{bmatrix} 0 \\ 0.188634 \\ 0.771043 \\ 0.010213 \\ 0.03011 \\ 0 \\ 0 \end{bmatrix}$

$yad := y7(yadc7, 1)$ $\quad yad = \begin{bmatrix} 0 \\ 0.180613 \\ 0.769103 \\ 0.015218 \\ 0.035066 \\ 0 \\ 0 \end{bmatrix}$

****

Define functions for evaluation of mixture properties (ideal gas) for complete fuel conversion and a given temperature.

Density and average molecular weight:

$$\rho mix(T) := \left(\sum_{kk=0}^{6} yeq_{kk} \cdot MW_{kk} \right) \cdot \frac{P}{R \cdot T} \qquad MWmix := \left(\sum_{kk=0}^{6} yeq_{kk} \cdot MW_{kk} \right)$$

$\rho mix(300 \cdot K) = 1.162787 \cdot kg \cdot m^{-3}$ $\quad MWmix = 28.631 \cdot gm$

****

****

Define diffusion coefficients for specific binary diffusion pairs:

$$Diff(n,m,T) := 1.8829\cdot10^{-27}\cdot\frac{\left[\left(\frac{1}{MW_n}+\frac{1}{MW_m}\right)\cdot T^3\right]^{0.5}}{\left(\frac{\sigma_n+\sigma_m}{2}\right)^2\cdot\Omega D\left[\frac{T}{(\varepsilon_n\cdot\varepsilon_m)^{0.5}}\right]\cdot\frac{P}{Pref}}\cdot10^8\cdot gm^{0.5}\cdot cm^4\cdot sec^{-1}\cdot K^{1.5}$$

$Diff(0,2,300\cdot K) = 0.2225\cdot sec^{-1}\cdot cm^2$

$Diff(2,6,300\cdot K) = 0.207\cdot sec^{-1}\cdot cm^2$

Define functions for use with various fuel-air mixtures:

$$Dch4(T) := \frac{1}{\sum_{jgas=1}^{4}\frac{yeq_{jgas}}{Diff(0,jgas,T)}}$$

$Dch4(298\cdot K) = 2.1912\cdot10^{-5}\cdot m^2\cdot sec^{-1}$

$$Dc7h14(T) := \frac{1}{\sum_{jgas=1}^{4}\frac{yeq_{jgas}}{Diff(5,jgas,T)}}$$

$Dc7h14(298\cdot K) = 5.8372\cdot10^{-6}\cdot m^2\cdot sec^{-1}$

$$Dco(T) := \frac{1}{\sum_{jgas=1}^{4}\frac{yeq_{jgas}}{Diff(6,jgas,T)}}$$

$Dco(298\cdot K) = 2.0451\cdot10^{-5}\cdot m^2\cdot sec^{-1}$

****

Display gas mixture properties

$Tin := \left[(1000-32)\cdot\frac{5}{9}+273.15\right]\cdot K$ $Tin = 810.9278\cdot K$

$idsp := 0..9$

$Tdsp_{idsp} := (750+50\cdot idsp)\cdot K$ $Tout := \left[(1511-32)\cdot\frac{5}{9}+273.15\right]\cdot K$ $Tout = 1094.8167\cdot K$

****

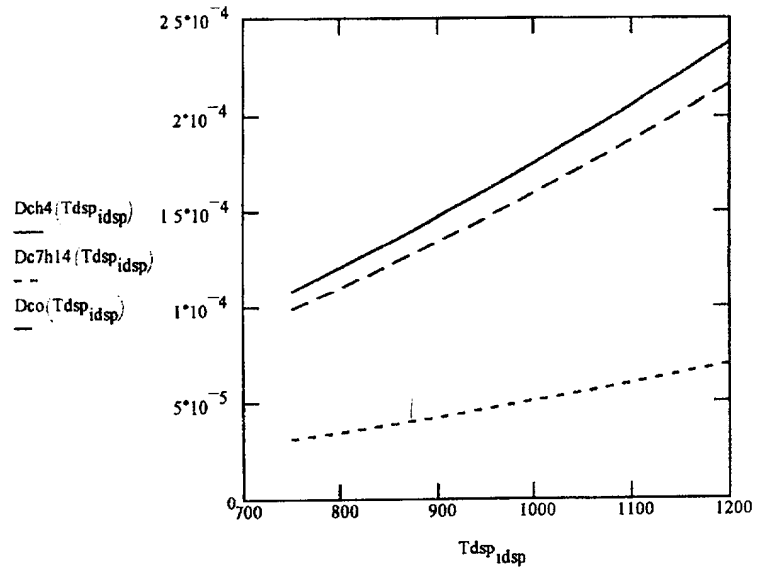

$Tdsp_{idsp}$	$Dch4(Tdsp_{idsp})$	$Dc7h14(Tdsp_{idsp})$	$Dco(Tdsp_{idsp})$
$7.5\cdot10^2\cdot K$	$1.082\cdot10^{-4}\cdot m^2\cdot sec^{-1}$	$3.1097\cdot10^{-5}\cdot m^2\cdot sec^{-1}$	$9.8836\cdot10^{-5}\cdot m^2\cdot sec^{-1}$
$8\cdot10^2\cdot K$	$1.2064\cdot10^{-4}\cdot m^2\cdot sec^{-1}$	$3.4776\cdot10^{-5}\cdot m^2\cdot sec^{-1}$	$1.101\cdot10^{-4}\cdot m^2\cdot sec^{-1}$
$8.5\cdot10^2\cdot K$	$1.3359\cdot10^{-4}\cdot m^2\cdot sec^{-1}$	$3.8613\cdot10^{-5}\cdot m^2\cdot sec^{-1}$	$1.2184\cdot10^{-4}\cdot m^2\cdot sec^{-1}$
$9\cdot10^2\cdot K$	$1.4705\cdot10^{-4}\cdot m^2\cdot sec^{-1}$	$4.2603\cdot10^{-5}\cdot m^2\cdot sec^{-1}$	$1.3402\cdot10^{-4}\cdot m^2\cdot sec^{-1}$
$9.5\cdot10^2\cdot K$	$1.61\cdot10^{-4}\cdot m^2\cdot sec^{-1}$	$4.6743\cdot10^{-5}\cdot m^2\cdot sec^{-1}$	$1.4665\cdot10^{-4}\cdot m^2\cdot sec^{-1}$
$1\cdot10^3\cdot K$	$1.7543\cdot10^{-4}\cdot m^2\cdot sec^{-1}$	$5.1031\cdot10^{-5}\cdot m^2\cdot sec^{-1}$	$1.5972\cdot10^{-4}\cdot m^2\cdot sec^{-1}$
$1.05\cdot10^3\cdot K$	$1.9033\cdot10^{-4}\cdot m^2\cdot sec^{-1}$	$5.5462\cdot10^{-5}\cdot m^2\cdot sec^{-1}$	$1.7322\cdot10^{-4}\cdot m^2\cdot sec^{-1}$
$1.1\cdot10^3\cdot K$	$2.057\cdot10^{-4}\cdot m^2\cdot sec^{-1}$	$6.0035\cdot10^{-5}\cdot m^2\cdot sec^{-1}$	$1.8714\cdot10^{-4}\cdot m^2\cdot sec^{-1}$
$1.15\cdot10^3\cdot K$	$2.2152\cdot10^{-4}\cdot m^2\cdot sec^{-1}$	$6.4746\cdot10^{-5}\cdot m^2\cdot sec^{-1}$	$2.0148\cdot10^{-4}\cdot m^2\cdot sec^{-1}$
$1.2\cdot10^3\cdot K$	$2.378\cdot10^{-4}\cdot m^2\cdot sec^{-1}$	$6.9593\cdot10^{-5}\cdot m^2\cdot sec^{-1}$	$2.1624\cdot10^{-4}\cdot m^2\cdot sec^{-1}$

Define interpolation formulas for Dch4, Dc7h14, and Dco vs. T(K) via Jandel Scientific's Tablecurve program

$$Dch4T(T) := \exp\left(-10.623294 + 1.6259688\cdot\ln\left(\frac{T}{K}\right) - \frac{46.41736\cdot K}{T}\right)\cdot\frac{cm^2}{sec}$$

$Dch4(1000\cdot K) = 1.75426\cdot sec^{-1}\cdot cm^2$

$Dch4T(1000\cdot K) = 1.75432\cdot sec^{-1}\cdot cm^2$

$$Dc7h14T(T) := \exp\left(11.822189 + 1.6260138\cdot\ln\left(\frac{T}{K}\right) - \frac{82.65375\cdot K}{T}\right)\cdot\frac{cm^2}{sec}$$

$Dc7h14(1000\cdot K) = 0.51031\cdot sec^{-1}\cdot cm^2$

$Dc7h14T(1000\cdot K) = 0.51031\cdot sec^{-1}\cdot cm^2$

$$DcoT(T) := \exp\left(10.831955 + 1.6394196\cdot\ln\left(\frac{T}{K}\right) - 24.53899\cdot\frac{K}{T}\right)\cdot cm^2\cdot sec^{-1}$$

$Dco(1000\cdot K) = 1.59722\cdot sec^{-1}\cdot cm^2$

$DcoT(1000\cdot K) = 1.59714\cdot sec^{-1}\cdot cm^2$

Define viscosity functions for major constituents:

$$\mu(T) := \begin{bmatrix} 2.6693\cdot10^{-26}\cdot\dfrac{(MW_0\cdot T)^{0.5}}{(\sigma_0)^2\cdot\Omega\mu\left(\frac{T}{\varepsilon_0}\right)}\cdot\dfrac{10^5\cdot cm}{sec}\cdot\left(\dfrac{gm}{K}\right)^{0.5} \\ \dfrac{(MW_1\cdot T)^{0.5}}{(\sigma_1)^2\cdot\Omega\mu\left(\frac{T}{\varepsilon_1}\right)}\cdot\left[2.6693\cdot10^{-26}\cdot\left(\dfrac{10^5\cdot cm}{sec}\right)\cdot\left(\dfrac{gm}{K}\right)^{0.5}\right] \\ \dfrac{(MW_2\cdot T)^{0.5}}{(\sigma_2)^2\cdot\Omega\mu\left(\frac{T}{\varepsilon_2}\right)}\cdot\left[2.6693\cdot10^{-26}\cdot\left(\dfrac{10^5\cdot cm}{sec}\right)\cdot\left(\dfrac{gm}{K}\right)^{0.5}\right] \\ \dfrac{(MW_3\cdot T)^{0.5}}{(\sigma_3)^2\cdot\Omega\mu\left(\frac{T}{\varepsilon_3}\right)}\cdot\left[2.6693\cdot10^{-26}\cdot\left(\dfrac{10^5\cdot cm}{sec}\right)\cdot\left(\dfrac{gm}{K}\right)^{0.5}\right] \\ \dfrac{1.116\cdot(MW_4\cdot T)^{0.5}}{(3.115\cdot10^{-8}\cdot cm)^2\cdot\Omega\mu\left(\frac{T}{514\cdot K}\right)}\cdot\left[2.6693\cdot10^{-26}\cdot\left(\dfrac{10^5\cdot cm}{sec}\right)\cdot\left(\dfrac{gm}{K}\right)^{0.5}\right] \end{bmatrix}$$

$$\mu(300\cdot K) = \begin{bmatrix} 1.10281\cdot10^{-5} \\ 2.0603\cdot10^{-5} \\ 1.76981\cdot10^{-5} \\ 1.51851\cdot10^{-5} \\ 1.06784\cdot10^{-5} \end{bmatrix}\cdot kg\cdot m^{-1}\cdot sec^{-1}$$

$$\mu mix(T) := \sum_{n=1}^{4}\frac{yeq_n\cdot\mu(T)_n}{\sum_{m=1}^{4}yeq_m\cdot\left[\dfrac{\left[1+\left(\frac{\mu(T)_n}{\mu(T)_m}\right)^{0.5}\cdot\left(\frac{MW_m}{MW_n}\right)^{0.25}\right]^2}{\left[8\cdot\left(1+\frac{MW_n}{MW_m}\right)\right]^{0.5}}\right]}$$

$$yeq = \begin{bmatrix} 0 \\ 0.1886 \\ 0.771 \\ 0.0102 \\ 0.0301 \\ 0 \\ 0 \end{bmatrix}$$

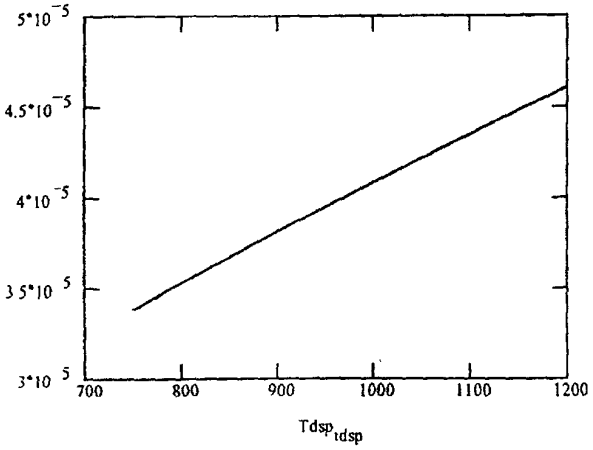

$Tdsp_{idsp}$	$\mu mix(Tdsp_{idsp})$
750·K	$3.3875\cdot10^{-5}\cdot kg\cdot m^{-1}\cdot sec^{-1}$
800·K	$3.5348\cdot10^{-5}\cdot kg\cdot m^{-1}\cdot sec^{-1}$
850·K	$3.6787\cdot10^{-5}\cdot kg\cdot m^{-1}\cdot sec^{-1}$
900·K	$3.8194\cdot10^{-5}\cdot kg\cdot m^{-1}\cdot sec^{-1}$
950·K	$3.9573\cdot10^{-5}\cdot kg\cdot m^{-1}\cdot sec^{-1}$
1000·K	$4.0926\cdot10^{-5}\cdot kg\cdot m^{-1}\cdot sec^{-1}$
1050·K	$4.2254\cdot10^{-5}\cdot kg\cdot m^{-1}\cdot sec^{-1}$
1100·K	$4.356\cdot10^{-5}\cdot kg\cdot m^{-1}\cdot sec^{-1}$
1150·K	$4.4844\cdot10^{-5}\cdot kg\cdot m^{-1}\cdot sec^{-1}$
1200·K	$4.6108\cdot10^{-5}\cdot kg\cdot m^{-1}\cdot sec^{-1}$

$$\mu mixT(T) := \exp\left(-0.6984944 - 0.640549\cdot\ln\left(\frac{T}{K}\right) + \frac{-14.50559\cdot K}{T}\right)\cdot 10^{-6}\cdot kg\cdot m^{-1}\cdot sec^{-1}$$

$\mu mix(1000\cdot K) = 4.0926\cdot 10^{-5}\ \cdot kg\cdot m^{-1}\cdot sec^{-1}$ $\mu mixT(1000\cdot K) = 4.09256\cdot 10^{-5}\ \cdot kg\cdot m^{-1}\cdot sec^{-1}$

****

Define thermal conductivity functions for light molecules

$igas := 0, 1 .. 4$

$$a\lambda := \begin{bmatrix} -1.869 \\ -.3273 \\ 0.3919 \\ -7.215 \\ 7.341 \end{bmatrix} \quad b\lambda := \begin{bmatrix} 0.08727 \\ 0.09966 \\ 0.09816 \\ 0.08015 \\ -0.01013 \end{bmatrix} \quad c\lambda := \begin{bmatrix} 1.179\cdot 10^{-4} \\ -(3.743\cdot 10^{-5}) \\ -(5.067\cdot 10^{-5}) \\ 5.477\cdot 10^{-6} \\ 1.801\cdot 10^{-4} \end{bmatrix} \quad d\lambda := \begin{bmatrix} -(3.614\cdot 10^{-8}) \\ 9.732\cdot 10^{-9} \\ 1.504\cdot 10^{-8} \\ -(1.053\cdot 10^{-8}) \\ -(9.1\cdot 10^{-8}) \end{bmatrix}$$

CH4
O2
N2
CO2
H2O

$$\lambda(i,T) := \left[a\lambda_i + b\lambda_i\cdot\frac{T}{K} + c\lambda_i\cdot\left(\frac{T}{K}\right)^2 + d\lambda_i\cdot\left(\frac{T}{K}\right)^3\right]\cdot 0.00001\cdot\frac{W}{cm\cdot K}$$

$\lambda(igas, 1000\cdot K)$

$0.16716\cdot kg\cdot m\cdot sec^{-3}\cdot K^{-1}$
$0.07163\cdot kg\cdot m\cdot sec^{-3}\cdot K^{-1}$
$0.06292\cdot kg\cdot m\cdot sec^{-3}\cdot K^{-1}$
$0.06788\cdot kg\cdot m\cdot sec^{-3}\cdot K^{-1}$
$0.08631\cdot kg\cdot m\cdot sec^{-3}\cdot K^{-1}$

W/m/K

$$\lambda mix(T) := \sum_{i=1}^{4} \frac{yeq_i\cdot\lambda(i,T)}{\sum_{j=1}^{4} yeq_j\cdot\left[\frac{\left[1+\left(\frac{\mu(T)_i}{\mu(T)_j}\right)^{0.5}\cdot\left(\frac{MW_j}{MW_i}\right)^{0.25}\right]^2}{\left[8\cdot\left(1+\frac{MW_i}{MW_j}\right)\right]^{0.5}}\right]}$$

$\lambda mix(1000\cdot K) = 0.000653\cdot\frac{W}{cm\cdot K}$

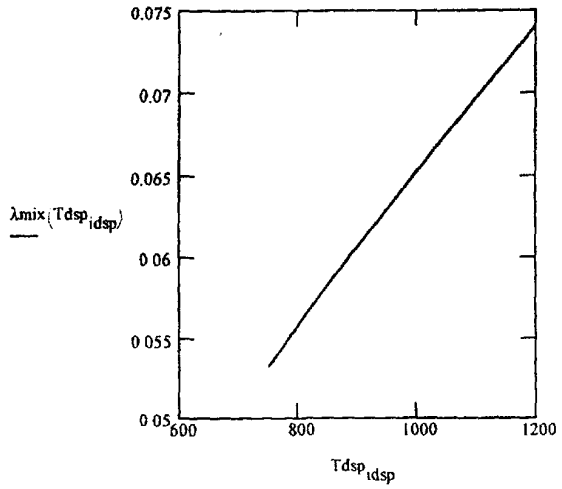

$Tdsp_{idsp}$	$\lambda mix(Tdsp_{idsp})$
$7.5\cdot 10^2\cdot K$	$0.05323\cdot kg\cdot m\cdot sec^{-3}\cdot K^{-1}$
$8\cdot 10^2\cdot K$	$0.055775\cdot kg\cdot m\cdot sec^{-3}\cdot K^{-1}$
$8.5\cdot 10^2\cdot K$	$0.058242\cdot kg\cdot m\cdot sec^{-3}\cdot K^{-1}$
$9\cdot 10^2\cdot K$	$0.060641\cdot kg\cdot m\cdot sec^{-3}\cdot K^{-1}$
$9.5\cdot 10^2\cdot K$	$0.06298\cdot kg\cdot m\cdot sec^{-3}\cdot K^{-1}$
$1\cdot 10^3\cdot K$	$0.065268\cdot kg\cdot m\cdot sec^{-3}\cdot K^{-1}$
$1.05\cdot 10^3\cdot K$	$0.067512\cdot kg\cdot m\cdot sec^{-3}\cdot K^{-1}$
$1.1\cdot 10^3\cdot K$	$0.069721\cdot kg\cdot m\cdot sec^{-3}\cdot K^{-1}$
$1.15\cdot 10^3\cdot K$	$0.071904\cdot kg\cdot m\cdot sec^{-3}\cdot K^{-1}$
$1.2\cdot 10^3\cdot K$	$0.074069\cdot kg\cdot m\cdot sec^{-3}\cdot K^{-1}$

$\lambda mixT(T) := \exp\left(-7.073383 + 0.6397005\cdot\ln\left(\frac{T}{K}\right) - \frac{65.2387\cdot K}{T}\right)\cdot W\cdot m^{-1}\cdot K^{-1}$

$\lambda mix(1000\cdot K) = 0.0653\cdot m^{-1}\cdot K^{-1}\cdot W$ $\lambda mixT(1000\cdot K) = 0.0659\cdot m^{-1}\cdot K^{-1}\cdot W$

****

Define heat capacities:

$$Cpcoef := \begin{bmatrix} 19.25 & .05213 & 0.00001197 & -0.00000001132 \\ 28.11 & -0.000368 & 0.00001746 & -0.00000001065 \\ 31.15 & -0.01357 & 0.0000268 & -0.00000001168 \\ 19.8 & 0.07344 & -0.00005602 & 0.00000001715 \\ 32.24 & 0.001924 & 0.00001055 & -0.000000003596 \\ -76.19 & 0.7867 & -0.0004204 & 0.00000007516 \end{bmatrix}$$

$$Cp(igas,T) := \sum_{jj=0}^{3} Cpcoef_{igas,jj}\cdot\left(\frac{T}{K}\right)^{jj}\cdot\frac{J}{K}$$

J/mol/K

$jj := 0..3$

$Cp(0,300\cdot K) = 35.6607\cdot K^{-1}\cdot J$ $Cp(5,300\cdot K) = 124.0133\cdot K^{-1}\cdot J$

$$Cpmix(T) := \sum_{jk=1}^{4} Cp(jk,T)\cdot yeq_{jk}$$ $Cpmix(998\cdot K) = 33.5144\cdot J\cdot K^{-1}$

$$Cpcfmix_{jj} := \sum_{jk=1}^{4} Cpcoef_{jk,jj}\cdot yeq_{jk}\cdot\frac{J}{K}$$

$$Cpcfmix = \begin{bmatrix} 30.493459 \\ -0.009725 \\ 2.370305\cdot 10^{-5} \\ -1.094786\cdot 10^{-8} \end{bmatrix}\cdot kg\cdot m^2\cdot sec^{-2}\cdot K^{-1}$$

$$CpmixT(T) := \sum_{jj=0}^{3} Cpcfmix_{jj}\cdot\left(\frac{T}{K}\right)^{jj}$$

$Cpmix(1000\cdot K) = 33.52413\cdot kg\cdot m^2\cdot sec^{-2}\cdot K^{-1}$

$CpmixT(1000\cdot K) = 33.52413\cdot kg\cdot m^2\cdot sec^{-2}\cdot K^{-1}$

$igas := 0,1..6$ $P = 1.013\cdot 10^5\cdot Pa$

****

****

Define momentum and thermal diffusivities:

$$\alpha(igas,T) := \frac{\lambda(igas,T)\cdot R\cdot T}{Cp(igas,T)\cdot P} \qquad \alpha(0,300\cdot K) = 0.2344\cdot sec^{-1}\cdot cm^2$$

$$\alpha mix(T) := \frac{\lambda mixT(T)\cdot R\cdot T}{CpmixT(T)\cdot P} \qquad \alpha mix(1000\cdot K) = 1.6132\cdot sec^{-1}\cdot cm^2$$

$$\upsilon mix(T) := \frac{\mu mixT(T)}{\rho mix(T)} \qquad \upsilon mix(1000\cdot K) = 1.1732\cdot sec^{-1}\cdot cm^2$$

$$\upsilon mixT(T) := \frac{\mu mixT(T)}{\rho mix(T)} \qquad \rho mix(1000\cdot K) = 3.48836\cdot 10^{-4}\cdot gm\cdot cm^{-3}$$

$$\rho mixT(T) := \rho mix(T)$$

$$Dch4T(1000\cdot K) = 1.7543\cdot sec^{-1}\cdot cm^2 \qquad Dc7h14T(1000\cdot K) = 0.5103\cdot sec^{-1}\cdot cm^2$$

Define Prandl, Schmidt, and Lewis numbers

$$Pr(T) := \frac{\upsilon mix(T)}{\alpha mix(T)} \qquad Pr(1000\cdot K) = 0.7272$$

$$Sc1T(T) := \frac{\upsilon mix(T)}{Dch4T(T)} \qquad Sc1T(1000\cdot K) = 0.6688 \qquad Sc7T(T) := \frac{\upsilon mix(T)}{Dc7h14T(T)} \qquad Sc7T(1000\cdot K) = 2.299$$

$$SccoT(T) := \frac{\upsilon mix(T)}{DcoT(T)} \qquad SccoT(1000\cdot K) = 0.7346$$

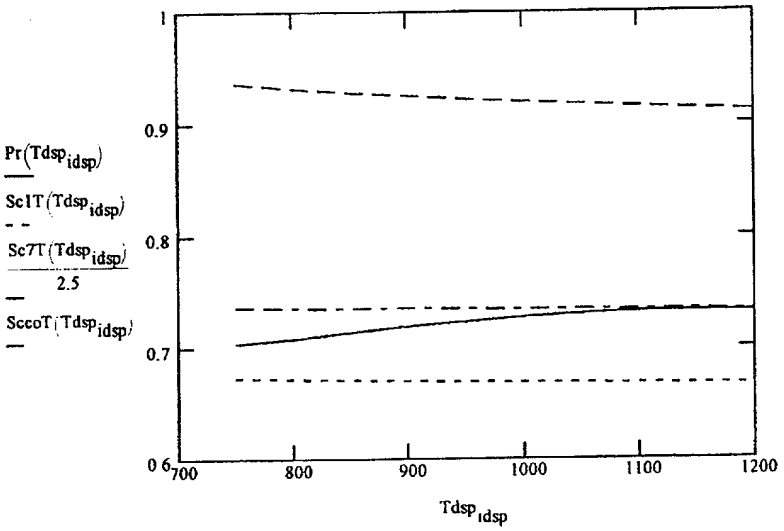

These relations have weak temperature dependence and (presumably) very weak dependence on composition

This ends the extended section that defines gas properties for the combustion mixtures.

****

Honeycombs: Represent as square channel metal alloy wall 0.003 mil, uncoated; 0.004 mil coated

dwalluc = 0.003·in dwalluc = 7.62·10^-5 ·m dwallc = 0.004·in dwallc = 1.016·10^-4 ·m

Cells1 = 100·in^-2 dwall1 = dwallc Cells2 = 200·in^-2 dwall2 = dwallc

dcell1 = (Cells1)^-0.5 - dwall1 dcell2 = (Cells2)^-0.5 - dwall2

dcell1 = 0.2438·cm ks1 = 0.002·cm dcell2 = 0.1694·cm ks2 = 0.002·cm

εcell1 = dcell1^2·Cells1 εcell1 = 0.9216 εcell2 = dcell2^2·Cells2 εcell2 = 0.89006

Cells4 = 400·in^-2 dwall4 = dwallc Cells6 = 600·in^-2 dwall6 = dwalluc

dcell4 = (Cells4)^-0.5 - dwall4 dcell4 = 0.1168·cm dcell6 = (Cells6)^-0.5 - dwall6 dcell6 = 0.0961·cm

dcell4 = 0.1168·cm ks4 = 0.001·cm dcell6 = 0.0961·cm ks6 = 0·cm

εcell4 = dcell4^2·Cells4 εcell4 = 0.8464 εcell6 = dcell6^2·Cells6 εcell6 = 0.85843

Cells8 = 800·in^-2 dwall8 = dwalluc

dcell8 = (Cells8)^-0.5 - dwall8 dcell8 = 0.0822·cm

dcell8 = 0.0822·cm ks8 = 0·cm

εcell8 = dcell8^2·Cells8 εcell8 = 0.83749

Define recuperator and monolith configurations:

dreco = 17·in dreco = 43.18·cm Lrec = 7·in

dreci = 6·in dreci = 15.24·cm Lrec = 17.78·cm

δd = 1.375·in **Add space for mounting and insulation?**

dhco = dreco - δd dhco = 39.6875·cm Lhc = 4·in

dhci = dreci + δd dhci = 18.7325·cm Lhc = 10.16·cm

$Shc = \pi \cdot \frac{dhco^2 - dhci^2}{4}$ Shc = 0.0961·m^2

Srecup = 0.0958·m^2 $\frac{Srecup}{Shc} = 0.9964$

Define initial combustion conditions

jcase = 0, 1 .. 4

case			
	0.2	1350	340
	0.26	1350	390
	0.314	1350	440
	0.38	1350	490
	0.72	1190	675

Mass flow (lb/sec)
Recup T inlet (F)
Recup T outlet (F)

$TKF(T) = \left(\frac{T}{K} - 273.15\right)\cdot\frac{9}{5} + 32$

$TFK(t) = \frac{(t - 32)\cdot 5\cdot K}{9} + 273.15\cdot K$

$Prec := 1 \cdot atm$ $Phc := 1 \cdot atm$

$mf_{jcase+1} := case_{jcase,0} \cdot 0.454 \cdot kg \cdot sec^{-1}$ $Trecin_{jcase+1} := TFK(case_{jcase,1})$ $Trecout_{jcase+1} := TFK(case_{jcase,2})$

$$mf = \begin{bmatrix} 0 \\ 0.0908 \\ 0.118 \\ 0.1426 \\ 0.1725 \\ 0.3269 \end{bmatrix} \cdot kg \cdot sec^{-1} \qquad Trecin = \begin{bmatrix} 0 \\ 1005.37 \\ 1005.37 \\ 1005.37 \\ 1005.37 \\ 916.48 \end{bmatrix} \cdot K \qquad Trecout = \begin{bmatrix} 0 \\ 444.26 \\ 472.04 \\ 499.82 \\ 527.59 \\ 630.37 \end{bmatrix} \cdot K$$

$$Urec_{jcase+1} := \frac{mf_{jcase+1}}{\rho mix(Trecin_{jcase+1}) \cdot \frac{Srecup}{2}} \qquad Urec = \begin{bmatrix} 0 \\ 5.4633 \\ 7.1023 \\ 8.5774 \\ 10.3803 \\ 17.929 \end{bmatrix} \cdot m \cdot sec^{-1} \qquad Grec_{jcase+1} := \frac{mf_{jcase+1}}{\left(\frac{Srecup}{2}\right)}$$

Only half of the recuperator cross section is available for exhuast gas flow

$$Uhc2_{jcase+1} := \frac{mf_{jcase+1}}{\rho mix(Trecin_{jcase+1}) \cdot Shc \cdot \varepsilon cell2} \qquad Uhc4_{jcase+1} := Uhc2_{jcase+1} \cdot \frac{\varepsilon cell2}{\varepsilon cell4} \qquad Uhc6_{jcase+1} := Uhc2_{jcase+1} \cdot \frac{\varepsilon cell2}{\varepsilon cell6}$$

$$Uhc2 = \begin{bmatrix} 0 \\ 3.058 \\ 3.9753 \\ 4.801 \\ 5.8101 \\ 10.0353 \end{bmatrix} \cdot m \cdot sec^{-1} \qquad Uhc4 = \begin{bmatrix} 0 \\ 3.2157 \\ 4.1804 \\ 5.0487 \\ 6.1098 \\ 10.553 \end{bmatrix} \cdot m \cdot sec^{-1}$$

$$Tavg := \frac{Trecin + Trecout}{2} \qquad Tavg = \begin{bmatrix} 0 \\ 724.8167 \\ 738.7056 \\ 752.5944 \\ 766.4833 \\ 773.4278 \end{bmatrix} \cdot K$$

Define average temperature etc/ for estimated ΔP and ΔT in the recuperator

$\rho mixrec(T) := \frac{MWmix \cdot Prec}{R \cdot T}$ $\rho mixrec(Tavg_1) = 0.4813 \cdot kg \cdot m^{-3}$

****

Evaluate Reynolds numbers for use in calculating the momentum, heat, and mass transfer functions:

$$Rerec6(G,T) := \frac{G \cdot dcell6}{\mu mixT(T)} \qquad Rerec6(Grec_1, Tavg_1) = 54.9906$$

$$Rerec8(G,T) := \frac{G \cdot dcell8}{\mu mixT(T)} \qquad Rerec8(Grec_1, Tavg_1) = 47.0389$$

For laminar flow with entrance effect (adapted from Kays & Crawford, "Convective Heat and Mass Transfer"):

$$cfricrec8(G,T,z) := \frac{14.227}{Rerec8(G,T)} \cdot \left[1 + 0.046263 \cdot \left(Rerec8(G,T) \cdot \frac{dcell8}{z}\right)\right]^{0.45363}$$

$$cfricrec6(G,T,z) := \frac{14.227}{Rerec6(G,T)} \cdot \left[1 + 0.046263 \cdot \left(Rerec6(G,T) \cdot \frac{dcell6}{z}\right)\right]^{0.45363}$$

Average coefficient of friction for a smooth square channel

Calculate monolith pressure drop in recuperator with entrance effect:

$$\Delta Prec8_{jcase+1} := 4 \cdot cfricrec8(Grec_{jcase+1}, Tavg_{jcase+1}, Lrec) \cdot \frac{\frac{(Urec_{jcase+1})^2}{2} \cdot \left[\rho mixrec(Trecin_{jcase+1}) + \rho mixrec(Trecout_{jcase+1}) \cdot \left(\frac{Trec}{Trec}\right.\right.}{2}$$

$$\Delta Prec6_{jcase+1} := 4 \cdot cfricrec6(Grec_{jcase+1}, Tavg_{jcase+1}, Lrec) \cdot \frac{\frac{(Urec_{jcase+1})^2}{2} \cdot \left[\rho mixrec(Trecin_{jcase+1}) + \rho mixrec(Trecout_{jcase+1}) \cdot \left(\frac{Trec}{Trec}\right.\right.}{2}$$

$$\frac{\Delta Prec8}{Prec} = \begin{bmatrix} 0 \\ 0.0097 \\ 0.013 \\ 0.0162 \\ 0.0203 \\ 0.0393 \end{bmatrix} \qquad \frac{\Delta Prec6}{Prec} = \begin{bmatrix} 0 \\ 0.0071 \\ 0.0095 \\ 0.0119 \\ 0.0149 \\ 0.0289 \end{bmatrix} \qquad \Delta Pobs\_P = \begin{bmatrix} 0 \\ 0.011 \\ 0.014 \\ 0.018 \\ 0.022 \\ 0.042 \end{bmatrix}$$

Chose 800 cells per in2 with 10% length factor in Lrec for chevrons

Averaged Nu for 800 cpi square channels (fully developed laminar flow) taken from Rosner:

$$Nuhavgrec8_{jcase+1} := 2.976 \cdot \left[1 + \left[\frac{7.6 \cdot (Lrec \cdot 1.1)}{Rerec8\left(Grec_{jcase+1}, Tavg_{jcase+1}\right) \cdot Pr\left(Tavg_{jcase+1}\right) \cdot dcell8}\right]^{\frac{8}{3}}\right]^{\frac{1}{8}}$$

$$Nuhavgrec8 = \begin{bmatrix} 0 \\ 2.976 \\ 2.976 \\ 2.976 \\ 2.976 \\ 2.9762 \end{bmatrix}$$

Entrance effect for heat transfer within the recuperator is only significant for the first half inch - average Nusselt No. = 2.976 for all cases

$$hrecavg_{jcase+1} := \frac{\lambda mix\left(Tavg_{jcase+1}\right) \cdot Nuhavgrec8_{jcase+1}}{dcell8} \qquad hrecavg = \begin{bmatrix} 0 \\ 188.0022 \\ 190.6356 \\ 193.2448 \\ 195.8307 \\ 197.1273 \end{bmatrix} \cdot kg \cdot sec^{-3} \cdot K^{-1}$$

W/m2/K

$$\Delta Tskin_{jcase+1} := \frac{Grec_{jcase+1} \cdot dcell8 \cdot \left(Cpmix\left(Trecout_{jcase+1}\right) \cdot Trecout_{jcase+1} - Cpmix\left(Trecin_{jcase+1}\right) \cdot Trecin_{jcase+1}\right)}{MWmix \cdot hrecavg_{jcase+1} \cdot 4 \cdot Lrec \cdot 1.1}$$

$$\Delta Tskin = \begin{bmatrix} 0 \\ -7.5657 \\ -9.274 \\ -10.5339 \\ -11.9549 \\ -13.635 \end{bmatrix} \cdot K \qquad \Delta Tskin \cdot 2 \cdot \frac{9}{5 \cdot K} = \begin{bmatrix} 0 \\ -27.2364 \\ -33.3864 \\ -37.9221 \\ -43.0378 \\ -49.0859 \end{bmatrix}$$

Approximate average ΔT (F) across wall in recuperator

ΔT seems low - more conservative calculation uses dcell for 600 cells/in2 - in this case ΔT maximum increases from 50F to about 70F

$$\Delta Tskin \cdot 2 \cdot \frac{9}{5 \cdot K} \cdot \left(\frac{dcell6}{dcell8}\right)^2 = \begin{bmatrix} 0 \\ -37.2231 \\ -45.628 \\ -51.8268 \\ -58.8182 \\ -67.0839 \end{bmatrix} \qquad \left(\frac{dcell6}{dcell8}\right)^2 = 1.3667$$

Use 600 cells/in2 in recuperator dimension for conservative calculation of CH4, C7H14, and CO conversions

Find mass transfer rates via Nusselt formulas:

$$Numavgrec6c1_{jcase+1} = 2.976\cdot\left[1+\left(\frac{7.6\cdot Lrec\cdot 1.1}{Rerec6\left(Grec_{jcase+1},Tavg_{jcase+1}\right)\cdot Sc1T\left(Tavg_{jcase+1}\right)\cdot dcell6}\right)^{\frac{8}{3}}\right]^{\frac{1}{8}} \quad Numavgrec6c1 = \begin{bmatrix} 0 \\ 2.976 \\ 2.976 \\ 2.9761 \\ 2.9761 \\ 2.9765 \end{bmatrix}$$

$$Numavgrec6c7_{jcase+1} = 2.976\cdot\left[1+\left(\frac{7.6\cdot Lrec\cdot 1.1}{Rerec6\left(Grec_{jcase+1},Tavg_{jcase+1}\right)\cdot Sc7T\left(Tavg_{jcase+1}\right)\cdot dcell6}\right)^{\frac{8}{3}}\right]^{\frac{1}{8}} \quad Numavgrec6c7 = \begin{bmatrix} 0 \\ 2.9765 \\ 2.977 \\ 2.9775 \\ 2.9784 \\ 2.9891 \end{bmatrix}$$

$$Numavgrec6co_{jcase+1} = 2.976\cdot\left[1+\left(\frac{7.6\cdot Lrec\cdot 1.1}{Rerec6\left(Grec_{jcase+1},Tavg_{jcase+1}\right)\cdot SccoT\left(Tavg_{jcase+1}\right)\cdot dcell6}\right)^{\frac{8}{3}}\right]^{\frac{1}{8}} \quad Numavgrec6co = \begin{bmatrix} 0 \\ 2.976 \\ 2.976 \\ 2.9761 \\ 2.9761 \\ 2.9766 \end{bmatrix}$$

Once again the entrance effects within the recuperator are negligible

The average (integral) Nusselt numbers at 1-atm show very little contribution of the thermal entry length, i.e. the flow velocities and heat and mass transfer coefficients have values close to those in long channels.

Now determine the maximum possible CH4, C7H14, and CO conversions in a 600 cells per in2 recuperator

$ych40 := 0.005 \qquad yc7h140 := 0.0005 \qquad yco0 := 0.005$

Start with maximum concentrations of added pollutants

$$ych4rec6_{jcase+1} = ych40\cdot\exp\left(\frac{-4\cdot Lrec\cdot 1.1\cdot Numavgrec6c1_{jcase+1}}{Rerec6\left(Grec_{jcase+1},Tavg_{jcase+1}\right)\cdot Sc1T\left(Tavg_{jcase+1}\right)\cdot dcell6}\right)$$

$$\frac{4\cdot Lrec\cdot 1.1\cdot Numavgrec6c1_{jcase+1}}{Rerec6\left(Grec_{jcase+1},Tavg_{jcase+1}\right)\cdot Sc1T\left(Tavg_{jcase+1}\right)\cdot dcell6} = \begin{bmatrix} 65.4083 \\ 50.9771 \\ 42.7552 \\ 35.7764 \\ 19.0017 \end{bmatrix}$$

$$\frac{ych4rec6}{ych40} = \begin{bmatrix} 0 \\ 0 \\ 0 \\ 0 \\ 0 \\ 5.5932\cdot 10^{-9} \end{bmatrix}$$

$$yc7h14rec6_{jcase+1} := yc7h140 \cdot \exp\left(\frac{-4 \cdot Lrec \cdot 1.1 \cdot Numavgrec6c7_{jcase+1}}{Rerec6\left(Grec_{jcase+1}, Tavg_{jcase+1}\right) \cdot Sc7T\left(Tavg_{jcase+1}\right) \cdot dcell6}\right)$$

$$yc7h14rec6 = \begin{bmatrix} 0 \\ 3.5287 \cdot 10^{-12} \\ 2.1834 \cdot 10^{-10} \\ 2.2859 \cdot 10^{-9} \\ 1.6805 \cdot 10^{-8} \\ 2.0597 \cdot 10^{-6} \end{bmatrix} \quad \frac{yc7h14rec6}{yc7h140} = \begin{bmatrix} 0 \\ 7.057 \cdot 10^{-9} \\ 4.367 \cdot 10^{-7} \\ 4.572 \cdot 10^{-6} \\ 3.361 \cdot 10^{-5} \\ 4.119 \cdot 10^{-3} \end{bmatrix} \quad \frac{-4 \cdot Lrec \cdot 1.1 \cdot Numavgrec6c7_{jcase+1}}{Rerec6\left(Grec_{jcase+1}, Tavg_{jcase+1}\right) \cdot Sc7T\left(Tavg_{jcase+1}\right) \cdot dcell6} = \begin{bmatrix} -18.7692 \\ -14.6441 \\ -12.2956 \\ -10.3007 \\ -5.492 \end{bmatrix}$$

$$ycorec6_{jcase+1} := yco0 \cdot \exp\left(\frac{-4 \cdot Lrec \cdot 1.1 \cdot Numavgrec6co_{jcase+1}}{Rerec6\left(Grec_{jcase+1}, Tavg_{jcase+1}\right) \cdot SccoT\left(Tavg_{jcase+1}\right) \cdot dcell6}\right)$$

$$ycorec6 = \begin{bmatrix} 0 \\ 0 \\ 0 \\ 0 \\ 0 \\ 1.457 \cdot 10^{-10} \end{bmatrix} \quad \frac{ycorec6}{yco0} = \begin{bmatrix} 0 \\ 0 \\ 0 \\ 0 \\ 6.4676 \cdot 10^{-15} \\ 2.914 \cdot 10^{-8} \end{bmatrix} \quad \frac{-4 \cdot Lrec \cdot 1.1 \cdot Numavgrec6co_{jcase+1}}{Rerec6\left(Grec_{jcase+1}, Tavg_{jcase+1}\right) \cdot SccoT\left(Tavg_{jcase+1}\right) \cdot dcell6} = \begin{bmatrix} -59.7854 \\ -46.5803 \\ -39.0561 \\ -32.672 \\ -17.3512 \end{bmatrix}$$

With 5000ppm C7H14 in turbine exhaust, exit concentration reaches 20 ppm at the highest power level for conservative 600 cells/in2 calculation. For 800 cells/in2, the exit concentration in this case would reach about 2 ppm. With only 500ppm C7H14 in the inlet, should get <2 ppm in the outlet of the recuperator assuming favorable catalytic rates at the wall. Also this calculation used averaged temperature and flow conditions - will compare below a 1-dimensional (axial) calculation that determines the effect of decreasing temperature on the kinetics and mass transport.

Maximum possible (transport-limited) CO and CH4 conversions in a 7 in. 600-800 cells/in2 recuperator are >99.99%, while cyclohexane conversion is >99.6%. The final CO and C7H14 levels are < 1 ppb and .2 ppm for post turbine concentrations of 1000 and 50 ppm, respectively.

An alternative method of calculating performance uses local Nusselt numbers for heat and mass transfer to determine the wall temperature and combustion rates at the wall. First we define the local Nu function then check conversion assuming fast kinetics and compare with the previous averaged (integrated) Nu formula.

Local Nu(x) taken from Kays & Crawford for hydro & thermal laminar flow entrance with circular channel (modified for square channel by a factor 2.96/3.66:

ncase := 5

$Numono(z) := (1 + \exp(-1.09689 - 0.381402\cdot\ln(z) - 8.287774\cdot z^{0.5}))\cdot 2.976$ $Numono(0.1152163) = 3.112$

$zzchar6c7_{jcase+1} := \frac{Rerec6(Grec_{jcase+1}, Trecin_{jcase+1})\cdot Sc7T(Trecin_{jcase+1})\cdot dcell6}{2}$ $\frac{Lrec}{zzchar6c7_{ncase}} = 0.9444$ **Case specific**

$zzchar6c1_{jcase+1} := \frac{Rerec6(Grec_{jcase+1}, Trecin_{jcase+1})\cdot Sc1T(Trecin_{jcase+1})\cdot dcell6}{2}$ $\frac{Lrec}{zzchar6c1_{ncase}} = 3.2574$ **Case specific**

$nz := 400$

$iz := 0..nz$

$Lrec = 17.78\cdot cm$ $dcell6 = 0.0961\cdot cm$

$zrec6_{iz} := iz\cdot\frac{Lrec}{nz} + dwall6$ $zz6c7_{iz} := \frac{zrec6_{iz}}{zzchar6c7_{ncase}}$ $zz6c1_{iz} := \frac{zrec6_{iz}}{zzchar6c1_{ncase}}$

$zzchar6c7 = \begin{bmatrix} 0 \\ 4.896 \\ 6.3647 \\ 7.6867 \\ 9.3023 \\ 18.8265 \end{bmatrix} \cdot cm$

$zzchar6c1 = \begin{bmatrix} 0 \\ 1.4244 \\ 1.8518 \\ 2.2364 \\ 2.7064 \\ 5.4583 \end{bmatrix} \cdot cm$

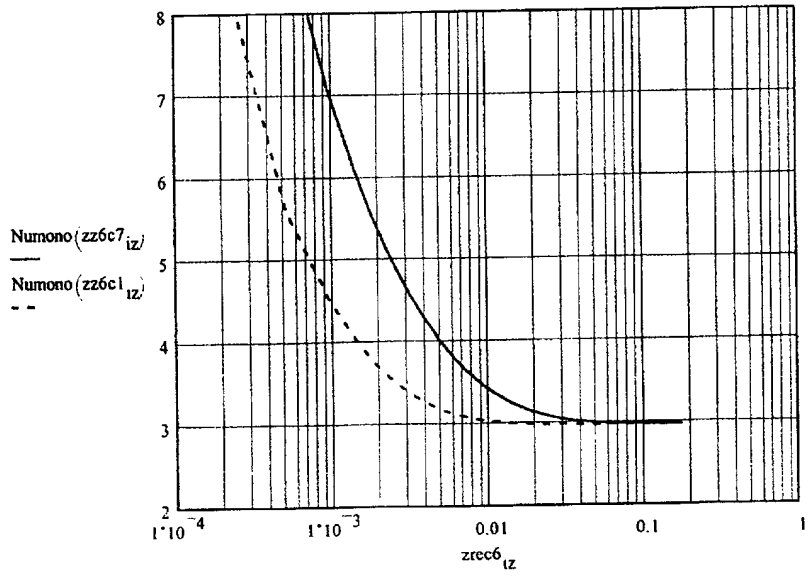

Case specific ncase = 5

Case specific ncase = 5

$$kgpbl6c7(T,z) := \frac{Dc7h14T(T)\cdot Numono\left(\frac{z}{zzchar6c7_{ncase}}\right)}{dcell6} \qquad kgpbl6c7(Trecin_{ncase}, Lrec) = 13.6159\cdot sec^{-1}\cdot cm$$

$$kgpbl6c1(T,z) := \frac{Dch4T(T)\cdot Numono\left(\frac{z}{zzchar6c1_{ncase}}\right)}{dcell6} \qquad kgpbl6c1(Trecin_{ncase}, Lrec) = 46.9581\cdot sec^{-1}\cdot cm$$

$$Trecz_{iz} := Trecin_{ncase} - \frac{Trecin_{ncase} - Trecout_{ncase}}{nz}\cdot iz \qquad Trecz_{nz} = 630.3722\cdot K \qquad Trecout_{ncase} = 630.3722\cdot K$$

****

Determine maximum conversion of fuels with very fast catalytic combustion rates (zero fuel concentration at the wall)

ncase = 5

$yzc7h14_0 := yc7h140$ $\qquad yzch4_0 := ych40$

$$yzc7h14_{iz+1} := \left(1 - kgpbl6c7(Trecz_{iz}, zrec6_{iz})\cdot\frac{Lrec}{nz}\cdot 1.1\cdot\frac{4}{dcell6}\cdot\frac{\varepsilon cell6}{Urec_{ncase}}\cdot\frac{Trecin_{ncase}}{Trecz_{iz}}\right)\cdot yzc7h14_{iz}$$ Case specific

$$yzch4_{iz+1} := \left(1 - kgpbl6c1(Trecz_{iz}, zrec6_{iz})\cdot\frac{Lrec}{nz}\cdot 1.1\cdot\frac{4}{dcell6}\cdot\frac{\varepsilon cell6}{Urec_{ncase}}\cdot\frac{Trecin_{ncase}}{Trecz_{iz}}\right)\cdot yzch4_{iz}$$ Case specific

$yzc7h14_{nz} = 3.385\cdot 10^{-6}$ $\qquad yzc7h14_0 = 0.0005$ $\qquad \frac{yzc7h14_{nz}}{yzc7h14_0} = 6.77\cdot 10^{-3}$ $\qquad \frac{yzch4_{nz}}{yzch4_0} = 4.3292\cdot 10^{-8}$

$yzch4_{nz} = 2.1646\cdot 10^{-10}$ $\qquad yzch4_0 = 0.005$

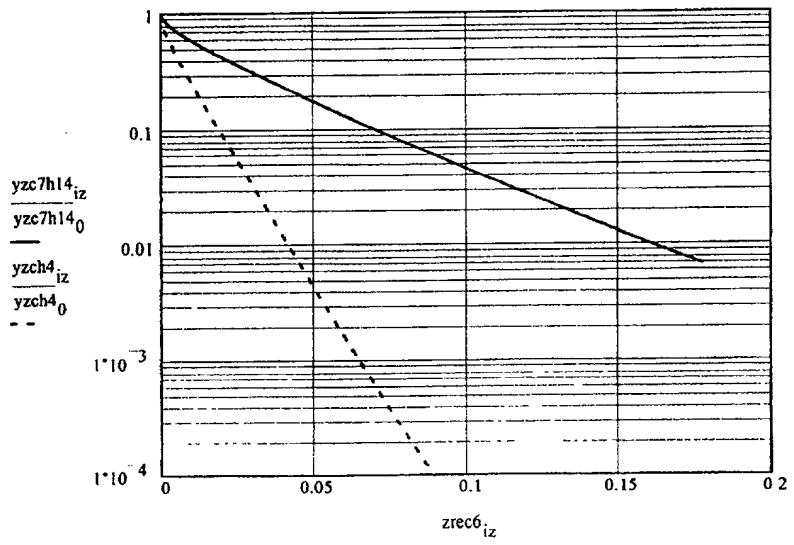

Case specific ncase = 5

Conversion of C7H14 under case 5 (full power) is 99.3% [vs. 99.6% via averaged integrated formulas] with about 1 inch entry length. Conversion of CH4 (and also CO) is very high (>99.99%) within 3.5 inches.

This result shows that the averaged integrated values for CH4, C7H14, and CO conversions are very good approximations and can be used for different values of fuel and CO concentrations.

****

****

Add finite rate kinetics for PdO/Al2O3 methane combustion catalyst
Begin by defining a few constants and catalyst functions

$R = 82.076 \cdot K^{-1} \cdot atm \cdot cm^3$ atm*cm3/mol*K

$Rcm := 83143000 \cdot gm \cdot cm^2 \cdot sec^{-2} \cdot K^{-1}$ TOL := 0.0001

Define Catalyst Functions:

$$\eta sph(\phi) := \frac{3}{\phi} \cdot \left(\frac{1}{\tanh(\phi)} - \frac{1}{\phi} \right)$$

$$\eta fpl(\phi) := \frac{\tanh(\phi)}{\phi}$$

Catalyst Physical Properties for Pd/Al2O3

$Scat := 85 \cdot m^2 \cdot gm^{-1}$ $\rho catpart = 2.5 \cdot gm \cdot cm^{-3}$

$V\mu pore := 0.15 \cdot cm^3 \cdot gm^{-1}$ dpcat = 0.0002·cm

$Lcat := 0.0020 \cdot cm$

$d\mu pore := 6 \cdot \frac{V\mu pore}{Scat}$ $\varepsilon\mu pore = 0.375$ $\tau\mu pore = 3.0$

$d\mu pore = 1.0588 \cdot 10^{-6} \cdot cm$

****

$$DeffCH4(T) := \frac{\frac{\varepsilon\mu pore}{\tau\mu pore}}{\frac{1}{Dch4T(T)} + \frac{3}{d\mu pore \cdot \sqrt{\frac{8}{\pi} \cdot \frac{R \cdot T}{MW_0}}}}$$

$$d\mu pore \cdot \sqrt{\frac{8}{\pi} \cdot \frac{R \cdot Tin}{MW_0}} = 0.1095 \cdot sec^{-1} \cdot cm^2$$

$DeffCH4(Tin) = 4.43271 \cdot 10^{3} \cdot sec^{1} \cdot cm^2$ $Dch4T(Tin) = 1.2343 \cdot sec^{1} \cdot cm^2$

$$DeffC7H14(T) := \frac{\varepsilon\mu pore}{\tau\mu pore}\left[\frac{1}{Dc7h14T(T)} + \frac{3}{d\mu pore\cdot\sqrt{\frac{8}{\pi}\cdot\frac{R\cdot T}{MW_6}}}\right] \qquad d\mu pore := \frac{8}{\pi}\cdot\frac{R\cdot Tin}{MW_6} = 0.0829\cdot sec^{-1}\cdot cm^2$$

$DeffC7H14(Tin) = 3.20528\cdot 10^{-3}\cdot sec^{-1}\cdot cm^2$ $\qquad Dc7h14(Tin) = 0.356\cdot sec^{-1}\cdot cm^2$

$$DmacCH4(T) := \frac{0.4}{2.5}\cdot Dch4T(T) \qquad DmacCH4(800\cdot K) = 0.193\cdot sec^{-1}\cdot cm^2$$

$$DmacC7H14(T) := \frac{0.4}{2.5}\cdot Dc7h14T(T) \qquad DmacC7H14(800\cdot K) = 0.0556\cdot sec^{-1}\cdot cm^2$$

$k0T := 1.0\cdot gm^{-1}\cdot sec^{-1}$ **Test value for k0T**

Microscopic Thiele Modulus for CH4

$$\phi\mu(k,T) := \sqrt{\left[\rho catpart\cdot\left(\frac{R\cdot T}{Pref}\right)\cdot\frac{k}{DeffCH4(T)}\right]}\cdot\frac{dpcat}{6} \qquad \phi\mu(k0T,Tin) = 0.2042$$

Macroscopic Thiele Modulus for CH4

$$\Phi mac(k,T) := \sqrt{\left[\rho catpart\cdot\left(\frac{R\cdot T}{Pref}\right)\cdot k\right]\cdot\frac{\eta sph(\phi\mu(k,T))}{DmacCH4(T)}}\cdot Lcat \qquad \Phi mac(k0T,Tin) = 1.8333$$

Microscopic Thiele Modulus for C7H14

$$\phi\mu7(k,T) := \sqrt{\left[\rho catpart\cdot\left(\frac{R\cdot T}{Pref}\right)\cdot\frac{k}{DeffC7H14(T)}\right]}\cdot\frac{dpcat}{6} \qquad \phi\mu7(k0T,Tin) = 0.2402$$

Macroscopic Thiele Modulus for C7H14

$$\Phi mac7(k,T) := \sqrt{\left[\rho catpart\cdot\left(\frac{R\cdot T}{Pref}\right)\cdot k\right]\cdot\frac{\eta sph(\phi\mu7(k,T))}{DmacC7H14(T)}}\cdot Lcat \qquad \Phi mac7(k0T,Tin) = 3.4117$$

$$RatekCH4(k,T) := \eta sph(\phi\mu(k,T))\cdot\eta fpl(\Phi mac(k,T))\cdot\left[\rho catpart\cdot\left(\frac{R\cdot T}{Pref}\right)\cdot k\right] \qquad RatekCH4(k0T,Tin) = 85999.4914\cdot sec^{-1}$$

$$RatekC7H14(k,T) := \eta sph(\phi\mu7(k,T))\cdot\eta fpl(\Phi mac7(k,T))\cdot\left[\rho catpart\cdot\left(\frac{R\cdot T}{Pref}\right)\cdot k\right] \qquad RatekC7H14(k0T,Tin) = 48479.296\cdot sec^{-1}$$

Defines transport restricted rate constant function given catalyst effective first order rate constant, k0T, methane or cyclohexane concentration, x, and surface temperature, T

PdO Catalyst Rate Constants

$Erpd0 := 12800 \cdot K$ $Erpd1 := 4900 \cdot K$ $Erpd3 := 15000 \cdot K$

Region0 - low T PdO to 625K ignores inhibition by H2O and CO2 | **Region1 - Intermediate T 625K to 909K** | **Region2 - Flat 909K to 1048K decomposition** | **Region3 - Pd metal**

$Apd0 := 2.4 \cdot 10^3 \cdot 200 \cdot gm^{-1} \cdot sec^{-1}$ $Apd1 := Apd0 \cdot \exp\left(-\frac{Erpd0}{625 \cdot K} + \frac{Erpd1}{625 \cdot K}\right)$

$Apd2 := Apd1 \cdot \exp\left(\frac{-Erpd1}{909.1 \cdot K}\right)$ $Apd3 := Apd2 \cdot \exp\left(\frac{Erpd3}{1048.1 \cdot K}\right)$

Interpolation formula for the four PdO+Pd rate constants

$$kpd(T) := \left[Apd3^2 \cdot \exp\left(-\frac{2 \cdot Erpd3}{T}\right) + \frac{1}{\left(Apd2^{-2} + Apd1^{-2} \cdot \exp\left(\frac{2 \cdot Erpd1}{T}\right) + Apd0^{-2} \cdot \exp\left(\frac{2 \cdot Erpd0}{T}\right)\right)} \right]^{0.5}$$

$nx := 0, 1 .. 41$ $T_{nx} := 500 \cdot K + nx \cdot 25 \cdot K$

CATALYTIC RATE CONSTANT vs TEMPERATURE (mol/atmCH4/s/gcat)

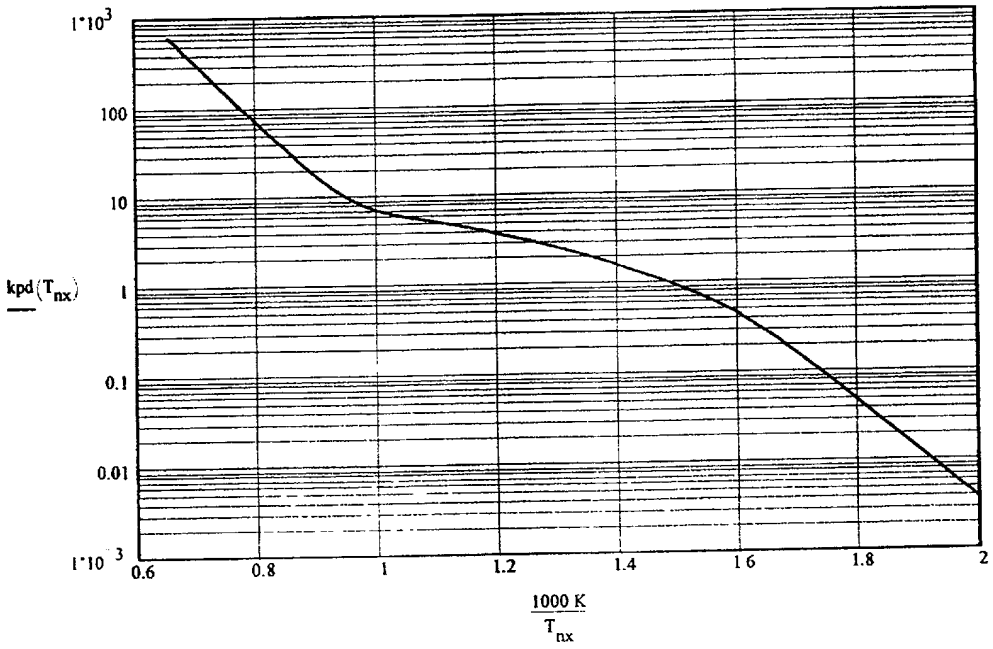

$$keffrec6c1(T,z) := \frac{1}{\left(\frac{1}{RatekCH4(kpd(T),T)\cdot Lcat}\right) + \frac{1}{kgpbl6c1(T,z)}} \qquad kgpbl6c1\left(Tavg_{ncase}, \frac{Lrec}{2}\right) = 35.3023\cdot sec^{-1}\cdot cm$$

$$keffrec6c1\left(Tavg_{ncase}, \frac{Lrec}{2}\right) = 0.7922\cdot sec^{-1}\cdot cm \qquad RatekCH4\left(kpd\left(Tavg_{ncase}\right), Tavg_{ncase}\right)\cdot Lcat = 0.8104\cdot sec^{-1}\cdot cm$$

$$keffrec6c7(T,z) := \frac{1}{\left(\frac{1}{RatekC7H14(10\cdot kpd(T),T)\cdot Lcat}\right) + \frac{1}{kgpbl6c7(T,z)}} \qquad kgpbl6c7\left(Tavg_{ncase}, \frac{Lrec}{2}\right) = 10.1756\cdot sec^{-1}\cdot cm$$

$$keffrec6c7\left(Tavg_{ncase}, \frac{Lrec}{2}\right) = 4.2778\cdot sec^{-1}\cdot cm \qquad RatekC7H14\left(10\cdot kpd\left(Tavg_{ncase}\right), Tavg_{ncase}\right)\cdot Lcat = 7.3807\cdot sec^{-1}\cdot cm$$

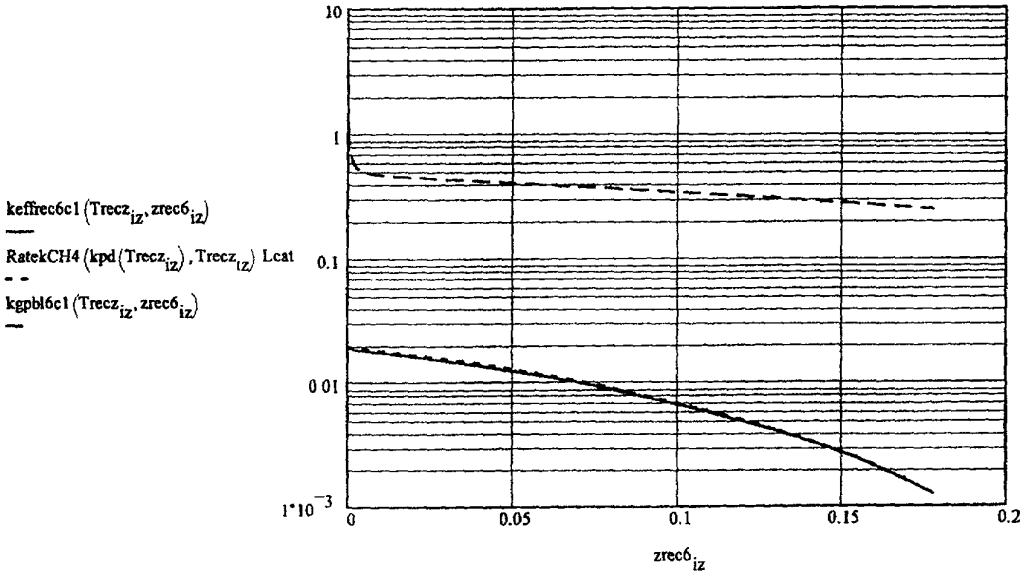

Case specific ncase = 5

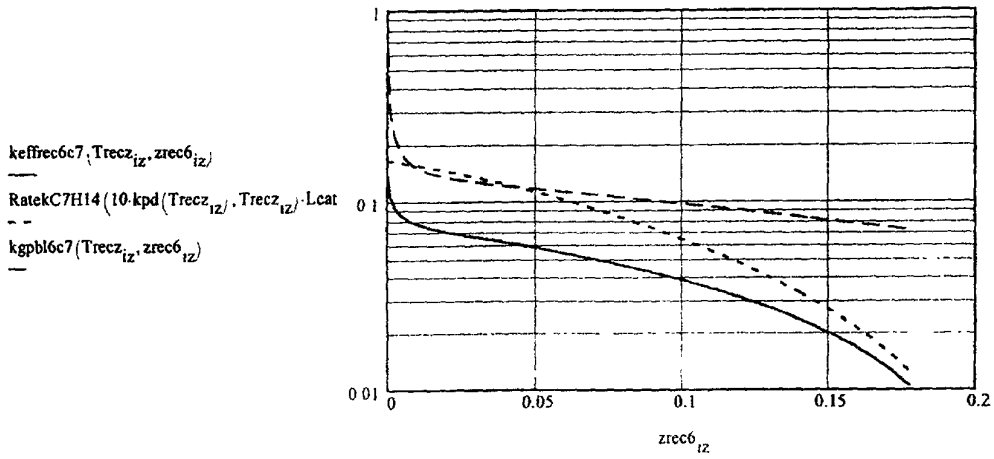

Determine conversion of fuels with transport-limited finite catalytic combustion rates:

Case specific ncase = 5

$Trecz_{iz} := Trecin_{ncase} - \frac{Trecin_{ncase} - Trecout_{ncase}}{nz} \cdot iz$ $Trecz_{nz} = 630.3722 \cdot K$ $Trecout_{ncase} = 630.3722 \cdot K$

$yzkc7h14_0 := yc7h140$ $yzkch4_0 := ych40$

$yzkc7h14_{iz+1} := \left(1 - keffrec6c7\left(Trecz_{iz}, zrec6_{iz}\right) \cdot \frac{Lrec}{nz} \cdot 1.1 \cdot \frac{4}{dcell6} \cdot \frac{\varepsilon cell6}{Urec_{ncase}} \cdot \frac{Trecin_5}{Trecz_{iz}}\right) \cdot yzkc7h14_{iz}$ **Case specific**

ncase = 5

$yzkch4_{iz+1} := \left(1 - keffrec6c1\left(Trecz_{iz}, zrec6_{iz}\right) \cdot \frac{Lrec}{nz} \cdot 1.1 \cdot \frac{4}{dcell6} \cdot \frac{\varepsilon cell6}{Urec_{ncase}} \cdot \frac{Trecin_5}{Trecz_{iz}}\right) \cdot yzkch4_{iz}$ **Case specific**

$yzkc7h14_{nz} = 7.036 \cdot 10^{-5}$ $yzkc7h14_0 = 0.0005$ $\frac{yzkc7h14_{nz}}{yzkc7h14_0} = 1.407 \cdot 10^{-1}$ $\frac{yzkch4_{nz}}{yzkch4_0} = 0.6838$

$yzkch4_{nz} = 0.0034$ $yzkch4_0 = 0.005$

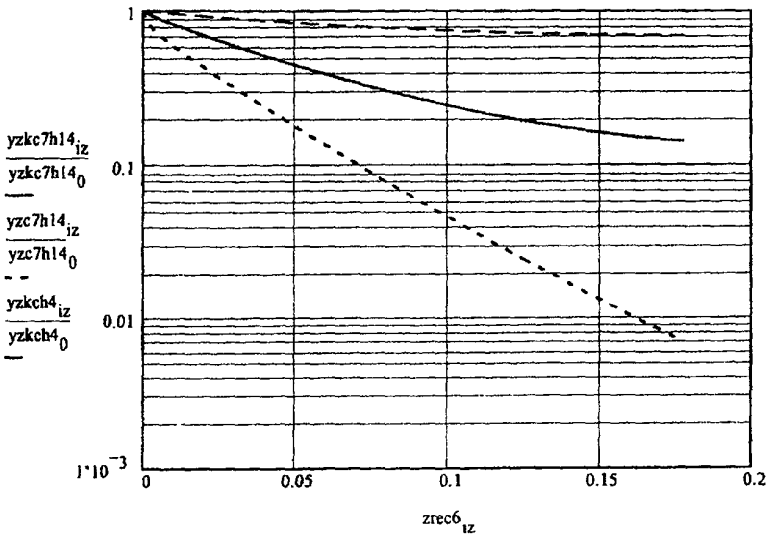

Case specific ncase = 5

Conversion of C7H14 under case 5 (full power) is 99.4% [vs. 99.3% for the maximum BL transport-limited conversion] with gradually decreasing (rate limited) conversion. Conversion of CH4 is very poor (35%). CO conversion is probably very high given higher catalytic and transport rates than with C7H14.

This result shows that the specific rates of catalytic oxidation of all added components needs to be measured as applied to a recuperator. The use of a recuperator for emission control would appear to be greatly enhanced with higher exhaust (recuperator) temperatures.

In the following section, the conversion of C7H14, CH4 and CO is considered for various honeycomb monliths

$Thc_{jcase+1} := Trecin_{jcase+1}$ $\rho mixhc_{jcase+1} := \rho mixrec(Trecin_{jcase+1})$

$Ghc2_{jcase+1} := \frac{mf_{jcase+1}}{Shc \cdot \varepsilon cell2}$ $Ghc4_{jcase+1} := \frac{mf_{jcase+1}}{Shc \cdot \varepsilon cell4}$ $Ghc6_{jcase+1} := \frac{mf_{jcase+1}}{Shc \cdot \varepsilon cell6}$

$$Uhc2 = \begin{bmatrix} 0 \\ 3.058 \\ 3.9753 \\ 4.801 \\ 5.8101 \\ 10.0353 \end{bmatrix} \cdot m \cdot sec^{-1} \qquad Uhc4 = \begin{bmatrix} 0 \\ 3.2157 \\ 4.1804 \\ 5.0487 \\ 6.1098 \\ 10.553 \end{bmatrix} \cdot m \cdot sec^{-1} \qquad Uhc6 = \begin{bmatrix} 0 \\ 3.1706 \\ 4.1218 \\ 4.9779 \\ 6.0242 \\ 10.4051 \end{bmatrix} \cdot m \cdot sec^{-1}$$

Evaluate Reynolds numbers for use in calculating the momentum, heat, and mass transfer functions:

$Rehc2_{jcase+1} := \frac{Ghc2_{jcase+1} \cdot dcell2}{\mu mixT(Thc_{jcase+1})}$ $Rehc4_{jcase+1} := \frac{Ghc4_{jcase+1} \cdot dcell4}{\mu mixT(Thc_{jcase+1})}$ $Rehc6_{jcase+1} := \frac{Ghc6_{jcase+1} \cdot dcell6}{\mu mixT(Thc_{jcase+1})}$

$$Rehc2 = \begin{bmatrix} 0 \\ 43.776 \\ 56.9088 \\ 68.7283 \\ 83.1744 \\ 167.4548 \end{bmatrix} \qquad Rehc4 = \begin{bmatrix} 0 \\ 31.7427 \\ 41.2655 \\ 49.836 \\ 60.3111 \\ 121.4242 \end{bmatrix} \qquad Rehc6 = \begin{bmatrix} 0 \\ 25.7355 \\ 33.4562 \\ 40.4048 \\ 48.8975 \\ 98.4453 \end{bmatrix}$$

$$cfrichc2(j,z) := \frac{14.227}{Rehc2_j} \cdot \left[1 + 0.046263 \cdot \left(Rehc2_j \cdot \frac{dcell2}{z}\right)\right]^{0.45363}$$

$$cfrichc4(j,z) := \frac{14.227}{Rehc4_j} \cdot \left[1 + 0.046263 \cdot \left(Rehc4_j \cdot \frac{dcell4}{z}\right)\right]^{0.45363}$$

Average coefficients of friction for smooth square channels

$$cfrichc6(j,z) := \frac{14.227}{Rehc6_j} \cdot \left[1 + 0.046263 \cdot \left(Rehc6_j \cdot \frac{dcell6}{z}\right)\right]^{0.45363}$$

Calculate monolith pressure drop in recuperator with entrance effect:

$$\Delta Phc2_{jcase+1} = 4\cdot cfrichc2(jcase+1, Lhc)\cdot \frac{Uhc2_{jcase+1}}{2}^2 \cdot \rho mixhc_{jcase+1}\cdot \frac{Lhc}{dcell2}$$

$$\Delta Phc4_{jcase+1} = 4\cdot cfrichc4(jcase+1, Lhc)\cdot \frac{Uhc4_{jcase+1}}{2}^2 \cdot \rho mixhc_{jcase+1}\cdot \frac{Lhc}{dcell4}$$

$$\Delta Phc6_{jcase+1} = 4\cdot cfrichc6(jcase+1, Lhc)\cdot \frac{Uhc6_{jcase+1}}{2}^2 \cdot \rho mixhc_{jcase+1}\cdot \frac{Lhc}{dcell6}$$

$$\frac{\Delta Phc2}{Phc} = \begin{bmatrix} 0 \\ 0.0013 \\ 0.0017 \\ 0.002 \\ 0.0024 \\ 0.0041 \end{bmatrix} \quad \frac{\Delta Phc4}{Phc} = \begin{bmatrix} 0 \\ 0.0028 \\ 0.0036 \\ 0.0044 \\ 0.0053 \\ 0.0088 \end{bmatrix} \quad \frac{\Delta Phc6}{Phc} = \begin{bmatrix} 0 \\ 0.004 \\ 0.0053 \\ 0.0064 \\ 0.0077 \\ 0.0127 \end{bmatrix} \quad \Delta Phcmax\_P = \begin{bmatrix} 0 \\ 0.003 \\ 0.004 \\ 0.005 \\ 0.006 \\ 0.011 \end{bmatrix}$$

Chose 400 cells per in2 honeycombs via estimated ΔP

Use 400 cells/in2 in honeycomb monolith for calculation of CH4, C7H14, and CO conversions

Find mass transfer rates via Nusselt formulas:

$$Numavghc4c1_{jcase+1} = 2.976\cdot\left[1 + \left(\frac{7.6\cdot Lhc}{Rehc4_{jcase+1}\cdot Sc1T\left(Thc_{jcase+1}\right)\cdot dcell4}\right)^{\frac{8}{3}}\right]^{\frac{1}{8}} \quad Numavghc4c1 = \begin{bmatrix} 0 \\ 2.976 \\ 2.9761 \\ 2.9761 \\ 2.9762 \\ 2.9774 \end{bmatrix}$$

$$Numavghc4co_{jcase+1} = 2.976\cdot\left[1 + \left(\frac{7.6\cdot Lhc}{Rehc4_{jcase+1}\cdot SccoT\left(Thc_{jcase+1}\right)\cdot dcell4}\right)^{\frac{8}{3}}\right]^{\frac{1}{8}} \quad Numavghc4co = \begin{bmatrix} 0 \\ 2.976 \\ 2.9761 \\ 2.9762 \\ 2.9763 \\ 2.9778 \end{bmatrix}$$

$$Numavghc4c7_{jcase+1} := 2.976\cdot\left[1+\left(\frac{7.6\cdot Lhc}{Rehc4_{jcase+1}\cdot Sc7T\left(Thc_{jcase+1}\right)\cdot dcell4}\right)^{\frac{8}{3}}\right]^{\frac{1}{8}} \qquad Numavghc4c7 = \begin{bmatrix} 0 \\ 2.977 \\ 2.9781 \\ 2.9795 \\ 2.9817 \\ 3.0123 \end{bmatrix}$$

Once again the entrance effects within monoliths are generally small

Now determine the maximum possible CH4, C7H14, and CO conversions in a 400 cells per in2 monolith

ych40 := 0.005 yc7h140 := 0.0005 yco0 := 0.005

$$ych4hc4_{jcase+1} := ych40\cdot\exp\left(\frac{-4\cdot Lhc\cdot Numavghc4c1_{jcase+1}}{Rehc4_{jcase+1}\cdot Sc1T\left(Thc_{jcase+1}\right)\cdot dcell4}\right)$$

$$\frac{-4\cdot Lhc\cdot Numavghc4c1_{jcase+1}}{Rehc4_{jcase+1}\cdot Sc1T\left(Thc_{jcase+1}\right)\cdot dcell4}$$

-48.7678
-37.5142
-31.0633
-25.6688
-12.7326

$$\frac{ych4hc4}{ych40} = \begin{bmatrix} 0 \\ 0 \\ 0 \\ 3.2315\cdot 10^{-14} \\ 7.1151\cdot 10^{-12} \\ 2.9532\cdot 10^{-6} \end{bmatrix}$$

$$ycohc4_{jcase+1} := yco0\cdot\exp\left(\frac{-4\cdot Lhc\cdot Numavghc4co_{jcase+1}}{Rehc4_{jcase+1}\cdot SccoT\left(Thc_{jcase+1}\right)\cdot dcell4}\right)$$

$$\frac{ycohc4}{yco0} = \begin{bmatrix} 0 \\ 0 \\ 1.4726\cdot 10^{-15} \\ 5.2301\cdot 10^{-13} \\ 7.0997\cdot 10^{-11} \\ 9.1398\cdot 10^{-6} \end{bmatrix}$$

$$\frac{-4\cdot Lhc\cdot Numavghc4co_{jcase+1}}{Rehc4_{jcase+1}\cdot SccoT\left(Thc_{jcase+1}\right)\cdot dcell4}$$

-44.3966
-34.1518
-28.2792
-23.3684
-11.6029

$$yc7h14hc4_{jcase+1} \quad yc7h140 \cdot \exp\left(\frac{4 \cdot Lhc \cdot Numavghc4c7_{jcase+1}}{Rehc4_{jcase+1} \cdot Sc7T\left(Thc_{jcase+1}\right) \cdot dcell4}\right) \qquad \frac{4 \cdot Lhc \cdot Numavghc4c7_{jcase+1}}{Rehc4_{jcase+1} \cdot Sc7T\left(Thc_{jcase+1}\right) \cdot dcell4}$$

-14.1935
-10.9219
9.0478
-7.482
-3.7348

$$\frac{yc7h14hc4}{yc7h140} = \begin{bmatrix} 0 \\ 6.8527 \cdot 10^{-7} \\ 1.8058 \cdot 10^{-5} \\ 0.0001 \\ 0.0006 \\ 0.0239 \end{bmatrix}$$

Only for C7H14 and only in case 5 (maximum power) does the BL transport-only calculated conversion (97.6%) fall below 99.9% with a 400 cells/in2 monolith. With 50 ppm C7H14 in the exhaust in this case, the exit concentration would be 1.2 ppm.

****

For the final analysis, consider the finite catalytic conversion of C7H14 and CH4 in a monolith: $mcase = 5$

$$zzcharhc4c7_{jcase+1} = \frac{Rehc4_{jcase+1} \cdot Sc7T\left(Thc_{jcase+1}\right) \cdot dcell4}{2} \qquad \frac{Lhc}{zzcharhc4c7_{mcase}} = 0.6199$$

$$zzcharhc4c1_{jcase+1} = \frac{Rehc4_{jcase+1} \cdot Sc1T\left(Trecin_{jcase+1}\right) \cdot dcell4}{2} \qquad \frac{Lhc}{zzcharhc4c1_{mcase}} = 2.1382$$

$nz = 400$ $\quad Lhc = 10.16 \cdot cm$ $\quad dcell4 = 0.1168 \cdot cm$

$$zhc4_{iz} = iz \cdot \frac{Lhc}{nz} + dwall4 \qquad zzhc4c7_{iz} = \frac{zhc4_{iz}}{zzcharhc4c7_{mcase}} \qquad zzhc4c1_{iz} = \frac{zhc4_{iz}}{zzcharhc4c1_{mcase}}$$

$$zzcharhc4c7 = \begin{bmatrix} 0 \\ 4.2621 \\ 5.5407 \\ 6.6914 \\ 8.0979 \\ 16.389 \end{bmatrix} \cdot cm$$

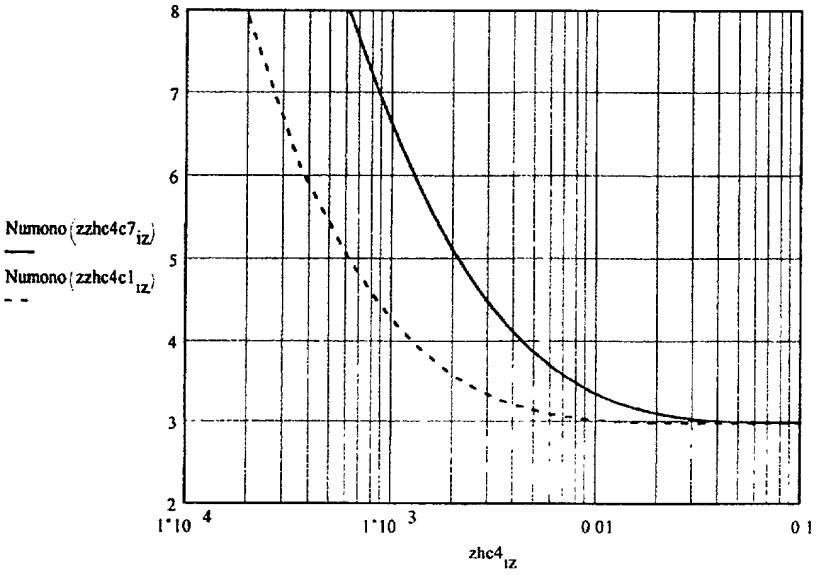

Case specific mcase = 5

$$kgpblhc4c7(T,z) := \frac{Dc7h14T(T)\cdot Numono\left(\frac{z}{zzcharhc4c7_{mcase}}\right)}{dcell4} \qquad kgpblhc4c7\left(Thc_{mcase}, Lhc\right) = 11.2014\cdot sec^{-1}\cdot cm$$

$$kgpblhc4c1(T,z) := \frac{Dch4T(T)\cdot Numono\left(\frac{z}{zzcharhc4c1_{mcase}}\right)}{dcell4} \qquad kgpblhc4c1\left(Thc_{mcase}, Lhc\right) = 38.6127\cdot sec^{-1}\cdot cm$$

$$keffhc4c1(T,z) := \frac{1}{\left(\frac{1}{RatekCH4(kpd(T),T)\cdot Lcat}\right) + \frac{1}{kgpblhc4c1(T,z)}} \qquad kgpblhc4c1\left(Thc_{mcase}, \frac{Lhc}{2}\right) = 38.615\cdot sec^{-1}\cdot cm$$

$$keffhc4c1\left(Thc_{mcase}, \frac{Lrec}{2}\right) = 1.8533\cdot sec^{-1}\cdot cm \qquad RatekCH4\left(kpd\left(Thc_{mcase}\right), Thc_{mcase}\right)\cdot Lcat = 1.9467\cdot sec^{-1}\cdot cm$$

$$keffhc4c7(T,z) := \frac{1}{\left(\frac{1}{RatekC7H14(10\cdot kpd(T),T)\cdot Lcat}\right) + \frac{1}{kgpblhc4c7(T,z)}} \qquad kgpblhc4c7\left(Thc_{mcase}, \frac{Lhc}{2}\right) = 11.2528\cdot sec^{-1}\cdot cm$$

$$keffhc4c7\left(Thc_{mcase}, \frac{Lhc}{2}\right) = 6.7062\cdot sec^{-1}\cdot cm \qquad RatekC7H14\left(10\cdot kpd\left(Thc_{mcase}\right), Thc_{mcase}\right)\cdot Lcat = 16.5977\cdot sec^{-1}\cdot cm$$

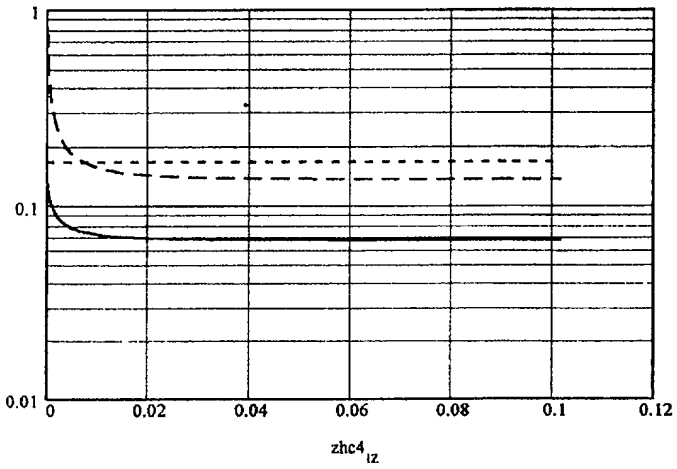

Determine conversion of fuels with transport-limited finite catalytic combustion rates:

Case specific mcase = 5

$yzkhc4c7h14_0 = yc7h140$ $yzkhc4ch4_0 = ych40$

$$Thc = \begin{bmatrix} 0 \\ 1005.3722 \\ 1005.3722 \\ 1005.3722 \\ 1005.3722 \\ 916.4833 \end{bmatrix} \cdot K$$

$$yzkhc4c7h14_{iz+1} = \left(1 - keffhc4c7\left(Thc_{mcase}, zhc4_{iz}\right) \cdot \frac{Lhc}{nz} \cdot \frac{4}{dcell4} \cdot \frac{\varepsilon cell4}{Uhc4_{mcase}}\right) \cdot yzkhc4c7h14_{iz}$$

$$yzkhc4ch4_{iz+1} = \left(1 - keffhc4c1\left(Thc_{mcase}, zhc4_{iz}\right) \cdot \frac{Lhc}{nz} \cdot \frac{4}{dcell4} \cdot \frac{\varepsilon cell4}{Uhc4_{mcase}}\right) \cdot yzkhc4ch4_{iz}$$

Case specific

mcase = 5

$yzkhc4c7h14_{nz} = 7.281 \cdot 10^{-5}$ $yzkhc4c7h14_0 = 0.0005$

$yzkhc4ch4_{nz} = 0.003$ $yzkhc4ch4_0 = 0.005$ $\frac{yzkhc4c7h14_{nz}}{yzkhc4c7h14_0} = 1.456 \cdot 10^{-1}$ $\frac{yzkhc4ch4_{nz}}{yzkhc4ch4_0} = 0.5959$

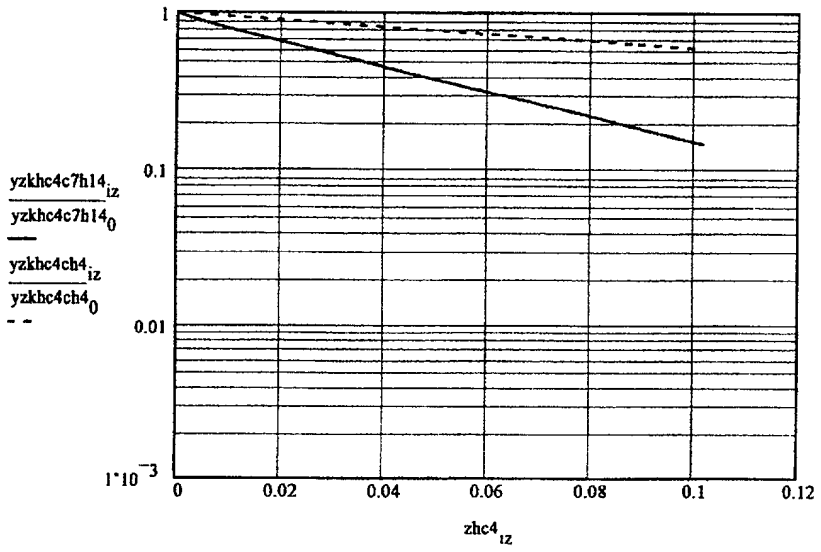

Case specific mcase = 5

Conversion of C7H14 under case 5 (full power) is 99.4% [vs. 99.6% via averaged integrated formulas] with about 1-inch entry length. Conversion of CH4 (and also CO) is very high (>99.99%) within about 3.5-inch.

This result shows that the averaged integrated values for CH4, C7H14, and CO conversions are very good approximations and can be used for different values of fuel and CO concentrations.

****

Defines transport restricted rate constant function given catalyst effective first order rate constant, k0T, methane or cyclohexane concentration, x, and surface temperature, T

PdO Catalyst Rate Constants

$Erpd0 := 12800 \cdot K$ $Erpd1 := 4900 \cdot K$ $Erpd3 := 15000 \cdot K$

Region0 - low T PdO to 625K ignores inhibition by H2O and CO2 **Region1 - Intermediate T 625K to 909K** **Region2 - Flat 909K to 1048K decomposition** **Region3 - Pd metal**

$Apd0 := 2.4 \cdot 10^{3} \cdot 200 \cdot gm^{-1} \cdot sec^{-1}$ $Apd1 := Apd0 \cdot \exp\left(-\frac{Erpd0}{625 \cdot K} + \frac{Erpd1}{625 \cdot K}\right)$ $Apd2 := Apd1 \cdot \exp\left(\frac{-Erpd1}{909.1 \cdot K}\right)$

Interpolation formula for the four PdO+Pd rate constants

$Apd3 := Apd2 \cdot \exp\left(\frac{Erpd3}{1048.1 \cdot K}\right)$

$$kpd(T) := \left[Apd3^{2} \cdot \exp\left(-\frac{2 \cdot Erpd3}{T}\right) + \frac{1}{\left(Apd2^{-2} + Apd1^{-2} \cdot \exp\left(\frac{2 \cdot Erpd1}{T}\right) + Apd0^{-2} \cdot \exp\left(\frac{2 \cdot Erpd0}{T}\right)\right)} \right]^{0.5}$$

Add expression for Pt(.5%)Pd(3.0%) catalyst with C3H8 here, use x2 for estimated rate constant with C7H14:

Rate constant via crushed powder results for C3H8

$$kptpdC3(T) := 6.9 \cdot 10^{4} \cdot \exp\left(-\frac{10760 \cdot K}{T}\right) \cdot gm^{-1} \cdot sec^{-1}$$

$10 \cdot kpd(900 \cdot K) = 49.2392 \cdot kg^{-1} \cdot sec^{-1}$

$2 \cdot kptpdC3(900 \cdot K) = 886.4358 \cdot kg^{-1} \cdot sec^{-1}$

****

$nx := 0, 1 .. 41$ $T_{nx} := 500 \cdot K + nx \cdot 25 \cdot K$

CATALYTIC RATE CONSTANT vs TEMPERATURE (mol/atmCHx/s/gcat)

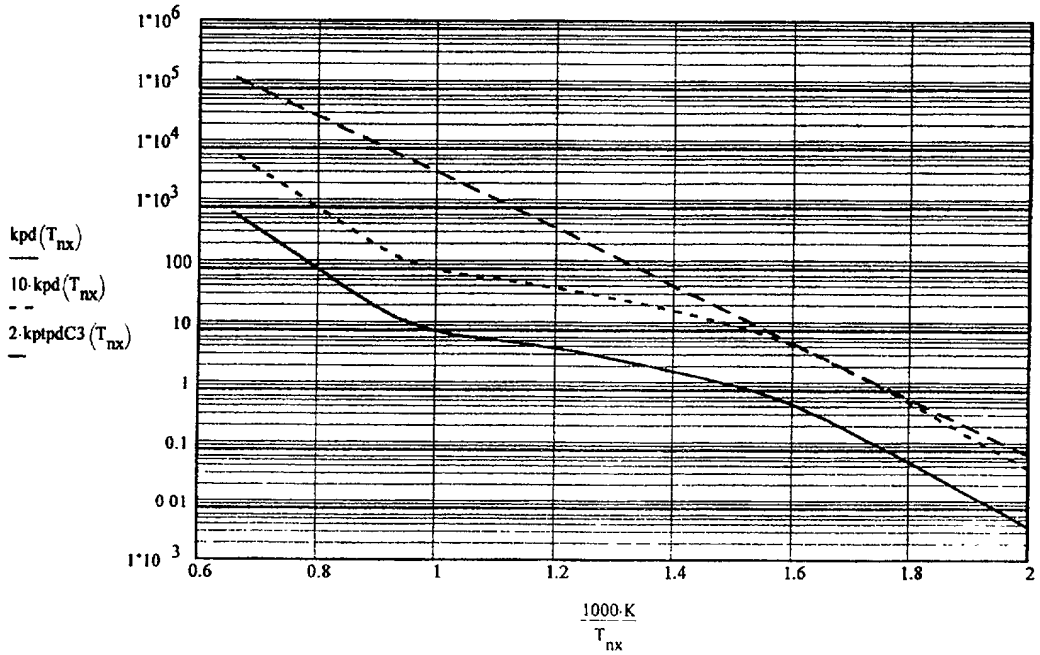

B4

$$keffrec6c1(T,z) = \frac{1}{\left(\frac{1}{RatekCH4(kpd(T),T)\cdot Lcat}\right) + \frac{1}{kgpbl6c1(T,z)}}$$

$$kgpbl6c1\left(Tavg_{ncase}, \frac{Lrec}{2}\right) = 35.3023\cdot sec^{-1}\cdot cm$$

$$keffrec6c1\left(Tavg_{ncase}, \frac{Lrec}{2}\right) = 0.7922\cdot sec^{-1}\cdot cm \qquad RatekCH4\left(kpd\left(Tavg_{ncase}\right), Tavg_{ncase}\right)\cdot Lcat = 0.8104\cdot sec^{-1}\cdot cm$$

$$keffrec6c7(T,z) = \frac{1}{\left(\frac{1}{RatekC7H14(2\cdot kptpdC3(T),T)\cdot Lcat}\right) + \frac{1}{kgpbl6c7(T,z)}}$$

$$kgpbl6c7\left(Tavg_{ncase}, \frac{Lrec}{2}\right) = 10.1756\cdot sec^{-1}\cdot cm$$

$$keffrec6c7\left(Tavg_{ncase}, \frac{Lrec}{2}\right) = 7.4067\cdot sec^{-1}\cdot cm \qquad RatekC7H14\left(2\cdot kptpdC3\left(Tavg_{ncase}\right), Tavg_{ncase}\right)\cdot Lcat = 27.2196\cdot sec^{-1}\cdot$$

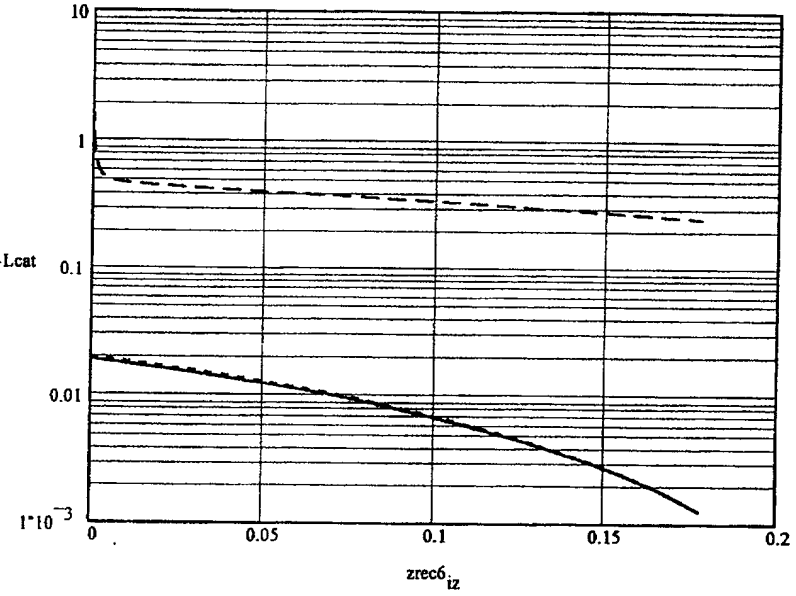

Case specific ncase = 5

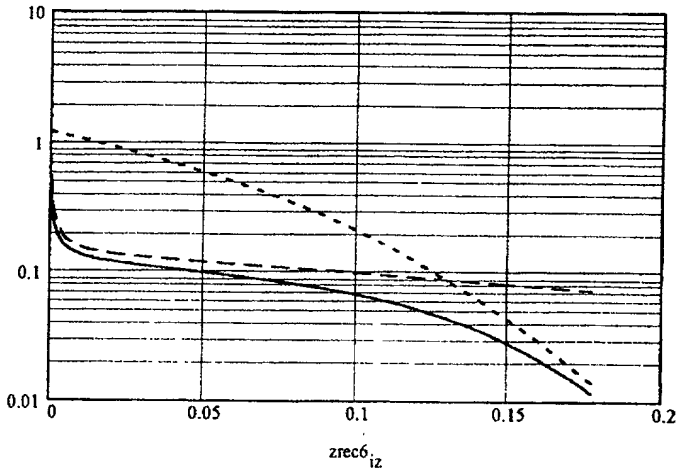

Determine conversion of fuels with transport-limited finite catalytic combustion rates:

$$Trecz_{iz} := Trecin_{ncase} - \frac{Trecin_{ncase} - Trecout_{ncase}}{nz} \cdot iz$$

Case specific ncase = 5

$Trecz_{nz} = 630.3722 \cdot K$ $Trecout_{ncase} = 630.3722 \cdot K$

$yzkc7h14_0 := yc7h140$ $yzkch4_0 := ych40$

$$yzkc7h14_{iz+1} := \left(1 - keffrec6c7\left(Trecz_{iz}, zrec6_{iz}\right) \cdot \frac{Lrec}{nz} \cdot 1.1 \cdot \frac{4}{dcell6} \cdot \frac{\varepsilon cell6}{Urec_{ncase}} \cdot \frac{Trecin_5}{Trecz_{iz}}\right) \cdot yzkc7h14_{iz}$$

Case specific

ncase = 5

$$yzkch4_{iz+1} := \left(1 - keffrec6c1\left(Trecz_{iz}, zrec6_{iz}\right) \cdot \frac{Lrec}{nz} \cdot 1.1 \cdot \frac{4}{dcell6} \cdot \frac{\varepsilon cell6}{Urec_{ncase}} \cdot \frac{Trecin_5}{Trecz_{iz}}\right) \cdot yzkch4_{iz}$$

Case specific

$yzkc7h14_{nz} = 1.802 \cdot 10^{-5}$ $yzkc7h14_0 = 0.0005$ $\frac{yzkc7h14_{nz}}{yzkc7h14_0} = 3.603 \cdot 10^{-2}$ $\frac{yzkch4_{nz}}{yzkch4_0} = 0.6838$

$yzkch4_{nz} = 0.0034$ $yzkch4_0 = 0.005$

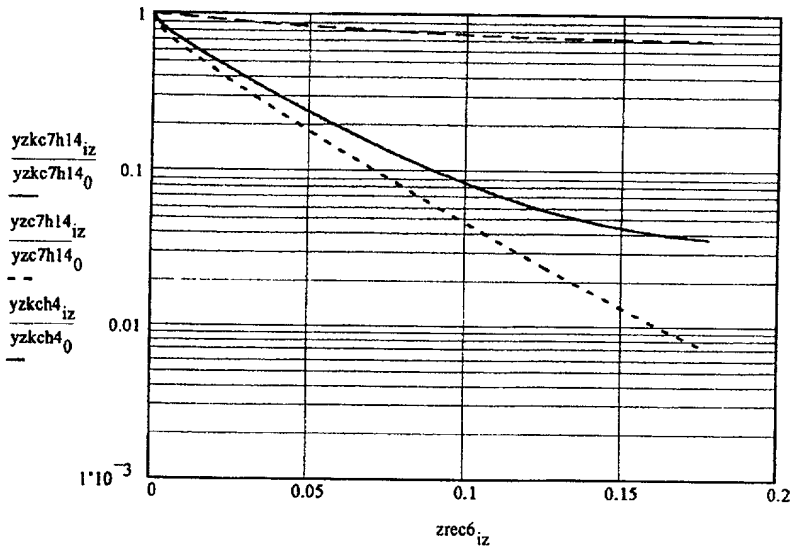

Case specific ncase = 5

Conversion of C7H14 under case 5 (full power) is 97.4% with estimated catalytic rates and transport limitations [vs. 99.6% for the maximum BL transport-limited conversion]. Conversion of CH4 is very poor (32%). CO conversion is probably very high given higher catalytic and transport rates than with C7H14.

This result shows that the specific rates of catalytic oxidation of all added components needs to be measured as applied to a recuperator. The use of a recuperator for emission control would appear to be greatly enhanced with higher exhaust (recuperator) temperatures.

In the following section, the conversion of C7H14, CH4 and CO is considered for various honeycomb monliths

$Thc_{jcase+1} := Trecin_{jcase+1}$ $\rho mixhc_{jcase+1} := \rho mixrec(Trecin_{jcase+1})$

$Ghc2_{jcase+1} := \frac{mf_{jcase+1}}{Shc \cdot \varepsilon cell2}$ $Ghc4_{jcase+1} := \frac{mf_{jcase+1}}{Shc \cdot \varepsilon cell4}$ $Ghc6_{jcase+1} := \frac{mf_{jcase+1}}{Shc \cdot \varepsilon cell6}$

$$Uhc2 = \begin{bmatrix} 0 \\ 3.058 \\ 3.9753 \\ 4.801 \\ 5.8101 \\ 10.0353 \end{bmatrix} \cdot m \cdot sec^{-1} \qquad Uhc4 = \begin{bmatrix} 0 \\ 3.2157 \\ 4.1804 \\ 5.0487 \\ 6.1098 \\ 10.553 \end{bmatrix} \cdot m \cdot sec^{-1} \qquad Uhc6 = \begin{bmatrix} 0 \\ 3.1706 \\ 4.1218 \\ 4.9779 \\ 6.0242 \\ 10.4051 \end{bmatrix} \cdot m \cdot sec^{-1}$$

Evaluate Reynolds numbers for use in calculating the momentum, heat, and mass transfer functions:

$Rehc2_{jcase+1} := \frac{Ghc2_{jcase+1} \cdot dcell2}{\mu mixT(Thc_{jcase+1})}$ $Rehc4_{jcase+1} := \frac{Ghc4_{jcase+1} \cdot dcell4}{\mu mixT(Thc_{jcase+1})}$ $Rehc6_{jcase+1} := \frac{Ghc6_{jcase+1} \cdot dcell6}{\mu mixT(Thc_{jcase+1})}$

$$Rehc2 = \begin{bmatrix} 0 \\ 43.776 \\ 56.9088 \\ 68.7283 \\ 83.1744 \\ 167.4548 \end{bmatrix} \qquad Rehc4 = \begin{bmatrix} 0 \\ 31.7427 \\ 41.2655 \\ 49.836 \\ 60.3111 \\ 121.4242 \end{bmatrix} \qquad Rehc6 = \begin{bmatrix} 0 \\ 25.7355 \\ 33.4562 \\ 40.4048 \\ 48.8975 \\ 98.4453 \end{bmatrix}$$

$$cfrichc2(j,z) := \frac{14.227}{Rehc2_j} \cdot \left[1 + 0.046263 \cdot \left(Rehc2_j \cdot \frac{dcell2}{z}\right)\right]^{0.45363}$$

$$cfrichc4(j,z) := \frac{14.227}{Rehc4_j} \cdot \left[1 + 0.046263 \cdot \left(Rehc4_j \cdot \frac{dcell4}{z}\right)\right]^{0.45363}$$

Average coefficients of friction for smooth square channels

$$cfrichc6(j,z) := \frac{14.227}{Rehc6_j} \cdot \left[1 + 0.046263 \cdot \left(Rehc6_j \cdot \frac{dcell6}{z}\right)\right]^{0.45363}$$

Calculate monolith pressure drop in recuperator with entrance effect:

$$\Delta Phc2_{jcase+1} := 4\cdot cfrichc2(jcase+1, Lhc)\cdot\frac{\left(Uhc2_{jcase+1}\right)^2}{2}\cdot\rho mixhc_{jcase+1}\cdot\frac{Lhc}{dcell2}$$

$$\Delta Phc4_{jcase+1} := 4\cdot cfrichc4(jcase+1, Lhc)\cdot\frac{\left(Uhc4_{jcase+1}\right)^2}{2}\cdot\rho mixhc_{jcase+1}\cdot\frac{Lhc}{dcell4}$$

$$\Delta Phc6_{jcase+1} := 4\cdot cfrichc6(jcase+1, Lhc)\cdot\frac{\left(Uhc6_{jcase+1}\right)^2}{2}\cdot\rho mixhc_{jcase+1}\cdot\frac{Lhc}{dcell6}$$

$$\frac{\Delta Phc2}{Phc} = \begin{bmatrix}0\\0.0013\\0.0017\\0.002\\0.0024\\0.0041\end{bmatrix} \quad \frac{\Delta Phc4}{Phc} = \begin{bmatrix}0\\0.0028\\0.0036\\0.0044\\0.0053\\0.0088\end{bmatrix} \quad \frac{\Delta Phc6}{Phc} = \begin{bmatrix}0\\0.004\\0.0053\\0.0064\\0.0077\\0.0127\end{bmatrix} \quad \frac{3.5}{4}\cdot\frac{\Delta Phc6}{Phc} = \begin{bmatrix}0\\0.0035\\0.0046\\0.0056\\0.0068\\0.0111\end{bmatrix} \quad \Delta Phcmax\_P = \begin{bmatrix}0\\0.003\\0.004\\0.005\\0.006\\0.011\end{bmatrix}$$

Chose 600 cells per in2 honeycombs but reduce length to 3.5in via estimated ΔP

$Lhc = 3.5\cdot in$

Use 600 cells/in2 in honeycomb monolith for calculation of CH4, C7H14, and CO conversions

Find mass transfer rates via Nusselt formulas:

$$Numavghc6c1_{jcase+1} := 2.976\cdot\left[1+\left(\frac{7.6\cdot Lhc}{Rehc6_{jcase+1}\cdot Sc1T\left(Thc_{jcase+1}\right)\cdot dcell6}\right)^{-\frac{8}{3}}\right]^{\frac{1}{8}} \qquad Numavghc6c1 = \begin{bmatrix}0\\2.976\\2.976\\2.9761\\2.9761\\2.9767\end{bmatrix}$$

$$Numavghc6co_{jcase+1} := 2.976\cdot\left[1+\left(\frac{7.6\cdot Lhc}{Rehc6_{jcase+1}\cdot SccoT\left(Thc_{jcase+1}\right)\cdot dcell6}\right)^{-\frac{8}{3}}\right]^{\frac{1}{8}} \qquad Numavghc6co = \begin{bmatrix}0\\2.976\\2.976\\2.9761\\2.9761\\2.9769\end{bmatrix}$$

$$Numavghc6c7_{jcase+1} = 2.976\cdot\left[1+\left(\frac{7.6\cdot Lhc}{Rehc6_{jcase+1}\cdot Sc7T\left(Thc_{jcase+1}\right)\cdot dcell6}\right)^{\frac{8}{3}}\right]^{\frac{1}{8}}$$

$$Numavghc6c7 = \begin{bmatrix} 0 \\ 2.9765 \\ 2.977 \\ 2.9777 \\ 2.9788 \\ 2.994 \end{bmatrix}$$

Once again the entrance effects within monoliths are generally small

****

Now determine the maximum possible CH4, C7H14, and CO conversions in a 600 cells per in2 monolith

ych40 := 0.005 yc7h140 := 0.0005 yco0 := 0.005

$$ych4hc6_{jcase+1} = ych40\cdot\exp\left(\frac{-4\cdot Lhc\cdot Numavghc6c1_{jcase+1}}{Rehc6_{jcase+1}\cdot Sc1T\left(Thc_{jcase+1}\right)\cdot dcell6}\right)$$

$$\frac{-4\cdot Lhc\cdot Numavghc6c1_{jcase+1}}{Rehc6_{jcase+1}\cdot Sc1T\left(Thc_{jcase+1}\right)\cdot dcell6}$$

-64.0074
-49.2367
-40.7696
-33.689
-16.7076

$$\frac{ych4hc6}{ych40} = \begin{bmatrix} 0 \\ 0 \\ 0 \\ 0 \\ 2.339\cdot 10^{-15} \\ 5.5463\cdot 10^{-8} \end{bmatrix}$$

$$ycohc6_{jcase+1} = yco0\cdot\exp\left(\frac{-4\cdot Lhc\cdot Numavghc6co_{jcase+1}}{Rehc6_{jcase+1}\cdot SccoT\left(Thc_{jcase+1}\right)\cdot dcell6}\right)$$

$$\frac{ycohc6}{yco0} = \begin{bmatrix} 0 \\ 0 \\ 0 \\ 0 \\ 4.7906\cdot 10^{-14} \\ 2.445\cdot 10^{-7} \end{bmatrix}$$

$$\frac{-4\cdot Lhc\cdot Numavghc6co_{jcase+1}}{Rehc6_{jcase+1}\cdot SccoT\left(Thc_{jcase+1}\right)\cdot dcell6}$$

-58.27
-44.8234
-37.1153
-30.6695
-15.2241

$$yc7h14hc6_{jcase+1} = yc7h140 \cdot \exp\left(\frac{-3.5 \cdot Lhc \cdot Numavghc6c7_{jcase+1}}{Rehc6_{jcase+1} \cdot Sc7T\left(Thc_{jcase+1}\right) \cdot dcell6}\right) \qquad \frac{-3.5 \cdot Lhc \cdot Numavghc6c7_{jcase+1}}{Rehc6_{jcase+1} \cdot Sc7T\left(Thc_{jcase+1}\right) \cdot dcell6}$$

-16.2974
-12.5386
-10.3846
-8.5841
-4.2631

$$\frac{yc7h14hc6}{yc7h140} = \begin{bmatrix} 0 \\ 8.3588 \cdot 10^{-8} \\ 3.5856 \cdot 10^{-6} \\ 3.0905 \cdot 10^{-5} \\ 0.0002 \\ 0.0141 \end{bmatrix}$$

Only for C7H14 and only in case 5 (maximum power) does the BL transport-only calculated conversion (98.6%) fall below 99.9% with a 600 cells/in2 monolith With 50 ppm C7H14 in the exhaust in this case, the exit concentration would be 0.7 ppm.

For the final analysis, consider the finite catalytic conversion of C7H14 and CH4 in a monolith: mcase = 5

$$zzcharhc6c7_{jcase+1} = \frac{Rehc6_{jcase+1} \cdot Sc7T\left(Thc_{jcase+1}\right) \cdot dcell6}{2} \qquad \frac{Lhc}{zzcharhc6c7_{mcase}} = 0.8137$$

$$zzcharhc6c1_{jcase+1} = \frac{Rehc6_{jcase+1} \cdot Sc1T\left(Trecin_{jcase+1}\right) \cdot dcell6}{2} \qquad \frac{Lhc}{zzcharhc6c1_{mcase}} = 2.8064$$

$nz = 400$ $Lhc = 8.89 \cdot cm$ $dcell6 = 0.0961 \cdot cm$

$$zhc6_{iz} = iz \cdot \frac{Lhc}{nz} + dwall6 \qquad zzhc6c7_{iz} = \frac{zhc6_{iz}}{zzcharhc6c7_{mcase}} \qquad zzhc6c1_{iz} = \frac{zhc6_{iz}}{zzcharhc6c1_{mcase}}$$

$$zzcharhc6c7 = \begin{bmatrix} 0 \\ 2.8414 \\ 3.6938 \\ 4.461 \\ 5.3986 \\ 10.926 \end{bmatrix} \cdot cm$$

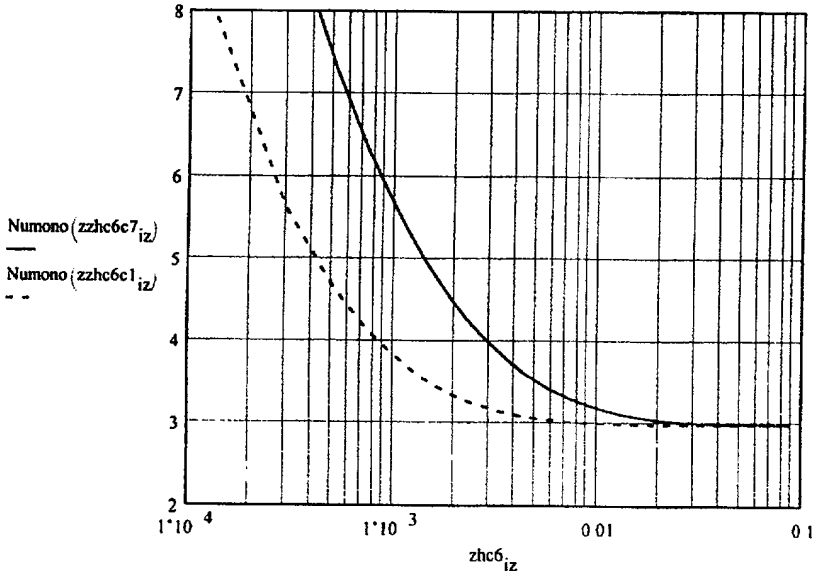

$$kgpblhc6c7(T,z) := \frac{Dc7h14T(T)\cdot Numono\left(\frac{z}{zzcharhc6c7_{mcase}}\right)}{dcell6}$$

Case specific $mcase = 5$

$$kgpblhc6c7(Thc_{mcase}, Lhc) = 13.6172\cdot sec^{-1}\cdot cm$$

$$kgpblhc6c1(T,z) := \frac{Dch4T(T)\cdot Numono\left(\frac{z}{zzcharhc6c1_{mcase}}\right)}{dcell6}$$

$$kgpblhc6c1(Thc_{mcase}, Lhc) = 46.9581\cdot sec^{-1}\cdot cm$$

$$keffhc6c1(T,z) := \frac{1}{\left(\frac{1}{RatekCH4(kpd(T),T)\cdot Lcat}\right) + \frac{1}{kgpblhc6c1(T,z)}}$$

$$kgpblhc6c1\left(Thc_{mcase}, \frac{Lhc}{2}\right) = 46.9589\cdot sec^{-1}\cdot cm$$

$$keffhc6c1\left(Thc_{mcase}, \frac{Lrec}{2}\right) = 1.8693\cdot sec^{-1}\cdot cm$$

$$RatekCH4\left(kpd\left(Thc_{mcase}\right), Thc_{mcase}\right)\cdot Lcat = 1.9467\cdot sec^{-1}\cdot cm$$

$$keffhc6c7(T,z) := \frac{1}{\left(\frac{1}{RatekC7H14(2\cdot kptpdC3(T),T)\cdot Lcat}\right) + \frac{1}{kgpblhc6c7(T,z)}}$$

$$kgpblhc6c7\left(Thc_{mcase}, \frac{Lhc}{2}\right) = 13.6468\cdot sec^{-1}\cdot cm$$

$$keffhc6c7\left(Thc_{mcase}, \frac{Lhc}{2}\right) = 12.2537\cdot sec^{-1}\cdot cm$$

$$RatekC7H14\left(2\cdot kptpdC3\left(Thc_{mcase}\right), Thc_{mcase}\right)\cdot Lcat = 120.0371\cdot sec^{-1}\cdot cm$$

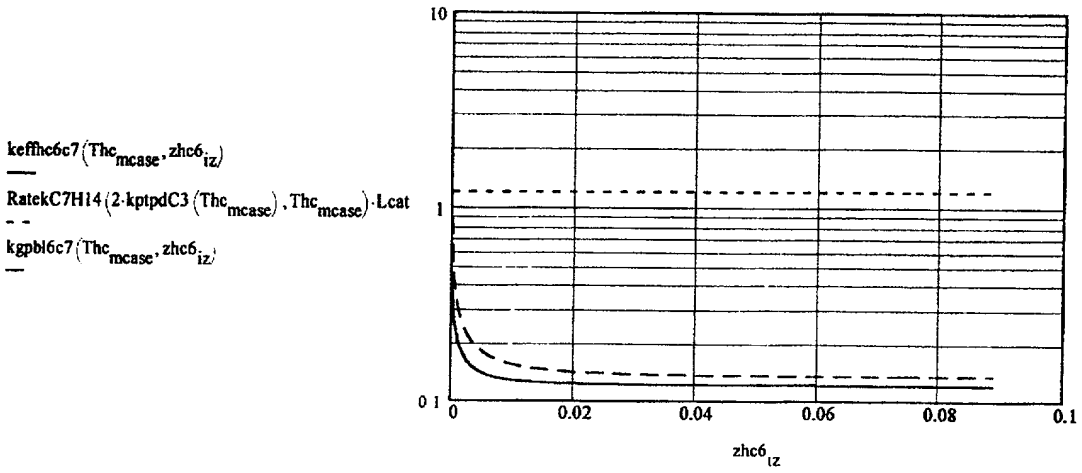

Determine conversion of fuels with transport-limited finite catalytic combustion rates:

Case specific mcase = 5

$yzkhc6c7h14_0 := yc7h140$ $yzkhc6ch4_0 := ych40$

$$Thc := \begin{bmatrix} 0 \\ 1005.3722 \\ 1005.3722 \\ 1005.3722 \\ 1005.3722 \\ 916.4833 \end{bmatrix} \cdot K$$

$$yzkhc6c7h14_{iz+1} := \left(1 - keffhc6c7\left(Thc_{mcase}, zhc6_{iz}\right) \cdot \frac{Lhc}{nz} \cdot \frac{4}{dcell6} \cdot \frac{\varepsilon cell6}{Uhc6_{mcase}}\right) \cdot yzkhc6c7h14_{iz}$$

$$yzkhc6ch4_{iz+1} := \left(1 - keffhc6c1\left(Thc_{mcase}, zhc6_{iz}\right) \cdot \frac{Lhc}{nz} \cdot \frac{4}{dcell6} \cdot \frac{\varepsilon cell4}{Uhc6_{mcase}}\right) \cdot yzkhc6ch4_{iz}$$

Case specific

mcase = 5

$yzkhc6c7h14_{nz} = 9.964 \cdot 10^{-6}$ $yzkhc6c7h14_0 = 0.0005$

$yzkhc6ch4_{nz} = 0.0028$ $yzkhc6ch4_0 = 0.005$ $\frac{yzkhc6c7h14_{nz}}{yzkhc6c7h14_0} = 1.993 \cdot 10^{-2}$ $\frac{yzkhc6ch4_{nz}}{yzkhc6ch4_0} = 0.5693$

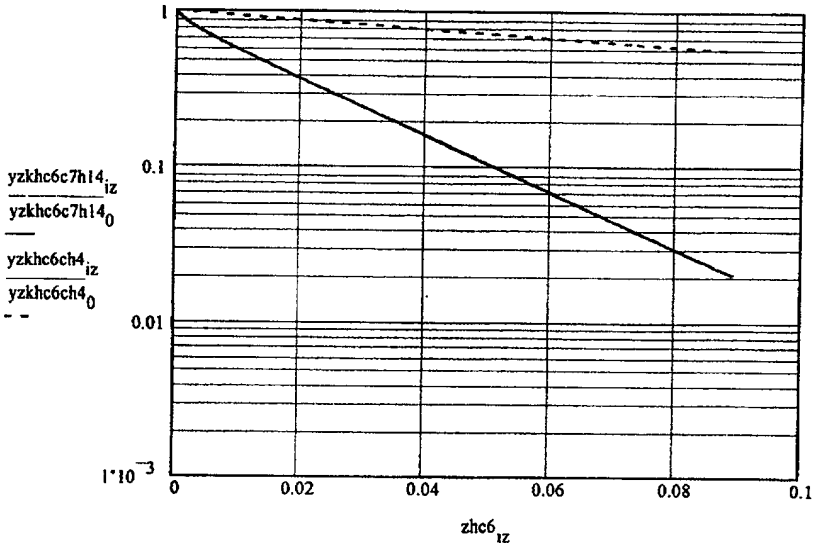

Case specific mcase = 5

Conversion of C7H14 under case 5 (full power) with 600 cells/in2 x 3.5-in length and extrapolated catalytic rates (via C3H8 at 400C) is 98.0% [vs. 99.6% via averaged integrated formulas, 99.3% with temperature dependent transport, and 98.6% with 400 cells/in2 and 4-in length. Conversion of CH4 is limited by slow kinetics and CO is expected to be very high (>99.99%).

Gas Properties and Constants

$cm \equiv 0.01 \cdot m$ $J \equiv kg \cdot m^2 \cdot sec^{-2}$ $W \equiv J \cdot sec^{-1}$ $Pref = 1 \cdot atm$

$N \equiv kg \cdot m \cdot sec^{-2}$ $Pa \equiv N \cdot m^{-2}$ $atm \equiv 101300 \cdot Pa$ $\mu m \equiv 0.000001 \cdot m$

$R = 8.3143 \cdot \frac{J}{K}$ $Rc = 8.3143 \cdot J \cdot mole^{-1} \cdot K^{-1}$

n	Gas	MolWt	σ(LJ)	ε(LJ)
1	CH4	$MW_0 = 16.044 \cdot gm$	$\sigma_0 = 3.785 \cdot 10^{-10} \cdot m$	$\varepsilon_0 = 148.6 \cdot K$
2	O2	$MW_1 = 31.999 \cdot gm$	$\sigma_1 = 3.464 \cdot 10^{-10} \cdot m$	$\varepsilon_1 = 106.7 \cdot K$
3	N2	$MW_2 = 28.018 \cdot gm$	$\sigma_2 = 3.798 \cdot 10^{-10} \cdot m$	$\varepsilon_2 = 71.4 \cdot K$
4	CO2	$MW_3 = 44.010 \cdot gm$	$\sigma_3 = 3.941 \cdot 10^{-10} \cdot m$	$\varepsilon_3 = 195.2 \cdot K$
5	H2O	$MW_4 = 18.015 \cdot gm$	$\sigma_4 = 2.641 \cdot 10^{-10} \cdot m$	$\varepsilon_4 = 809.1 \cdot K$

Define transport integrals:

Constants:

$\sigma\mu a_0 = 1.16145$	$\sigma\mu b_0 = 0.14874$	$\sigma Da_0 = 1.06036$	$\sigma Db_0 = 0.1561$
$\sigma\mu a_1 = 0.52487$	$\sigma\mu b_1 = 0.7732$	$\sigma Da_1 = 0.193$	$\sigma Db_1 = 0.47635$
$\sigma\mu a_2 = 2.16178$	$\sigma\mu b_2 = 2.43787$	$\sigma Da_2 = 1.03587$	$\sigma Db_2 = 1.52996$
		$\sigma Da_3 = 1.76474$	$\sigma Db_3 = 3.89411$

Functions:

$$\Omega\mu(T) = \sigma\mu a_0 \cdot \exp\left[-\left(\sigma\mu b_0 \cdot \ln(T)\right)\right] + \sum_{i\mu=1}^{2} \sigma\mu a_{i\mu} \cdot \exp\left(-\sigma\mu b_{i\mu} \cdot T\right) \qquad \Omega\mu(3) = 1.0394$$

$$\Omega D(T) = \sigma Da_0 \cdot \exp\left[-\left(\sigma Db_0 \cdot \ln(T)\right)\right] + \sum_{iD=1}^{3} \sigma Da_{iD} \cdot \exp\left(-\sigma Db_{iD} \cdot T\right) \qquad \Omega D(3) = 0.95002$$

B5
~~B4~~

****

Set Inlet Conditions:

$P = 1.0 \cdot atm$ $\quad$ $ych40 = 0.035$

Define gas composition w/r methane using moist (3%) air:

$$y(x) := \begin{bmatrix} x \\ (1 - ych40)\cdot 0.2 - 2\cdot ych40 + 2\cdot x \\ (1 - ych40)\cdot 0.77 \\ ych40 - x \\ (1 - ych40)\cdot 0.03 + 2\cdot ych40 - 2\cdot x \end{bmatrix} \qquad y(0.02) = \begin{bmatrix} 0.02 \\ 0.163 \\ 0.743 \\ 0.015 \\ 0.059 \end{bmatrix}$$

****

****

Define viscosity function

$$\mu(T) = \begin{bmatrix} 2.6693\cdot 10^{-26}\cdot \dfrac{(MW_0\cdot T)^{0.5}}{(\sigma_0)^2\cdot \Omega\mu\left(\frac{T}{\varepsilon_0}\right)}\cdot \dfrac{10^5\cdot cm}{sec}\cdot \left(\dfrac{gm}{K}\right)^{0.5} \\ \dfrac{(MW_1\cdot T)^{0.5}}{(\sigma_1)^2\cdot \Omega\mu\left(\frac{T}{\varepsilon_1}\right)}\cdot \left[2.6693\cdot 10^{-26}\cdot \left(\dfrac{10^5\cdot cm}{sec}\right)\cdot \left(\dfrac{gm}{K}\right)^{0.5}\right] \\ \dfrac{(MW_2\cdot T)^{0.5}}{(\sigma_2)^2\cdot \Omega\mu\left(\frac{T}{\varepsilon_2}\right)}\cdot \left[2.6693\cdot 10^{-26}\cdot \left(\dfrac{10^5\cdot cm}{sec}\right)\cdot \left(\dfrac{gm}{K}\right)^{0.5}\right] \\ \dfrac{(MW_3\cdot T)^{0.5}}{(\sigma_3)^2\cdot \Omega\mu\left(\frac{T}{\varepsilon_3}\right)}\cdot \left[2.6693\cdot 10^{-26}\cdot \left(\dfrac{10^5\cdot cm}{sec}\right)\cdot \left(\dfrac{gm}{K}\right)^{0.5}\right] \\ \dfrac{1.116\cdot (MW_4\cdot T)^{0.5}}{(3.115\cdot 10^{-8}\cdot cm)^2\cdot \Omega\mu\left(\frac{T}{514\cdot K}\right)}\cdot \left[2.6693\cdot 10^{-26}\cdot \left(\dfrac{10^5\cdot cm}{sec}\right)\cdot \left(\dfrac{gm}{K}\right)^{0.5}\right] \end{bmatrix} \qquad \mu(300\cdot K) = \begin{bmatrix} 1.103\cdot 10^{-5} \\ 2.06\cdot 10^{-5} \\ 1.77\cdot 10^{-5} \\ 1.519\cdot 10^{-5} \\ 1.068\cdot 10^{-5} \end{bmatrix} \cdot kg\cdot m^{-1}\cdot sec^{-1}$$

$$\mu mix(x,T) = \sum_{n=0}^{4} \frac{y(x)_n \cdot (\mu(T))_n}{\sum_{m=0}^{4} y(x)_m \cdot \left[\frac{\left[1+\left(\frac{\mu(T)_n}{\mu(T)_m}\right)^{0.5}\cdot\left(\frac{MW_m}{MW_n}\right)^{0.25}\right]^2}{\left[8\cdot\left(1+\frac{MW_n}{MW_m}\right)\right]^{0.5}}\right]} \qquad y(0.02) = \begin{bmatrix} 0.02 \\ 0.163 \\ 0.743 \\ 0.015 \\ 0.059 \end{bmatrix}$$

$\mu mix(0.02, 300\cdot K) = 1.759\cdot 10^{-5}\cdot kg\cdot m^{-1}\cdot sec^{-1}$

****

Define thermal conductivity functions

igas := 0, 1 .. 4

CH4
O2
N2
CO2
H2O

$$a\lambda = \begin{bmatrix} -1.869 \\ -.3273 \\ 0.3919 \\ -7.215 \\ 7.341 \end{bmatrix} \quad b\lambda = \begin{bmatrix} 0.08727 \\ 0.09966 \\ 0.09816 \\ 0.08015 \\ -0.01013 \end{bmatrix} \quad c\lambda = \begin{bmatrix} 1.179\cdot 10^{-4} \\ -(3.743\cdot 10^{-5}) \\ -(5.067\cdot 10^{-5}) \\ 5.477\cdot 10^{-6} \\ 1.801\cdot 10^{-4} \end{bmatrix} \quad d\lambda = \begin{bmatrix} -(3.614\cdot 10^{-8}) \\ 9.732\cdot 10^{-9} \\ 1.504\cdot 10^{-8} \\ -(1.053\cdot 10^{-8}) \\ -(9.1\cdot 10^{-8}) \end{bmatrix}$$

$$\lambda(i,T) = \left[a\lambda_i + b\lambda_i\cdot\frac{T}{K} + c\lambda_i\cdot\left(\frac{T}{K}\right)^2 + d\lambda_i\cdot\left(\frac{T}{K}\right)^3\right]\cdot 0.00001\cdot\frac{W}{cm\cdot K} \quad W/cm/K$$

$\lambda(igas, 1000\cdot K)$

$0.16716\cdot kg\cdot m\cdot sec^{-3}\cdot K^{-1}$
$0.07163\cdot kg\cdot m\cdot sec^{-3}\cdot K^{-1}$
$0.06292\cdot kg\cdot m\cdot sec^{-3}\cdot K^{-1}$
$0.06788\cdot kg\cdot m\cdot sec^{-3}\cdot K^{-1}$
$0.08631\cdot kg\cdot m\cdot sec^{-3}\cdot K^{-1}$

$$\lambda mix(x,T) = \sum_{i=0}^{4} \frac{y(x)_i \cdot \lambda(i,T)}{\sum_{j=0}^{4} y(x)_j \cdot \left[\frac{\left[1+\left(\frac{\mu(T)_i}{\mu(T)_j}\right)^{0.5}\cdot\left(\frac{MW_j}{MW_i}\right)^{0.25}\right]^2}{\left[8\cdot\left(1+\frac{MW_i}{MW_j}\right)\right]^{0.5}}\right]}$$

$\lambda mix(.0, 1000\cdot K) = 6.64\cdot 10^{-4}\cdot\frac{W}{cm\cdot K}$

****

Define thermal conductivity of alumina and SS321

$$Altc = \begin{bmatrix} 83.71 \\ 224.898 \\ 255.842 \\ 132.727 \\ 25.9695 \end{bmatrix}$$

The parameter set Altc_n was determined from published values of the thermal conductivity. Ref: HCP

λAl2O3(x) is the thermal conductivity function (of x with unit K) while λ1 is its derivative w/r to temperature.

$$\lambda Al2O3(x) := \sum_{n=0}^{4} Altc_n \cdot \left(\frac{x}{1000 \cdot K}\right)^n \cdot \frac{W}{m \cdot K} \qquad \lambda 1(x) := \sum_{n=1}^{4} \frac{Altc_n}{1000 \cdot K} \cdot n \cdot \left(\frac{x}{1000 \cdot K}\right)^{n-1} \cdot \frac{W}{m \cdot K}$$

$$S321tc = \begin{bmatrix} 4.69312 \\ 4.9812 \\ -0.33357 \\ 0 \\ 0 \end{bmatrix}$$

The parameter set S321tc_n was determined from published values of the thermal conductivity. Ref: Handbook of Metals 8th Ed. Vol. 1 p. 423

$$\lambda ss321(x) := \sum_{n=0}^{4} S321tc_n \cdot \left(\frac{x}{1000 \cdot K}\right)^n \cdot \frac{W}{m \cdot K}$$

$$\lambda ss321(1000 \cdot K) = 9.341 \cdot \frac{W}{m \cdot K} \qquad \lambda Al2O3(1000 \cdot K) = 7.897 \cdot \frac{W}{m \cdot K} \qquad \lambda 1(1000 \cdot K) \cdot 1000 \cdot K = -7.517 \cdot \frac{W}{m \cdot K}$$

$i := 30, 31 .. 200 \qquad Ta_i := 10 \cdot i \cdot K$

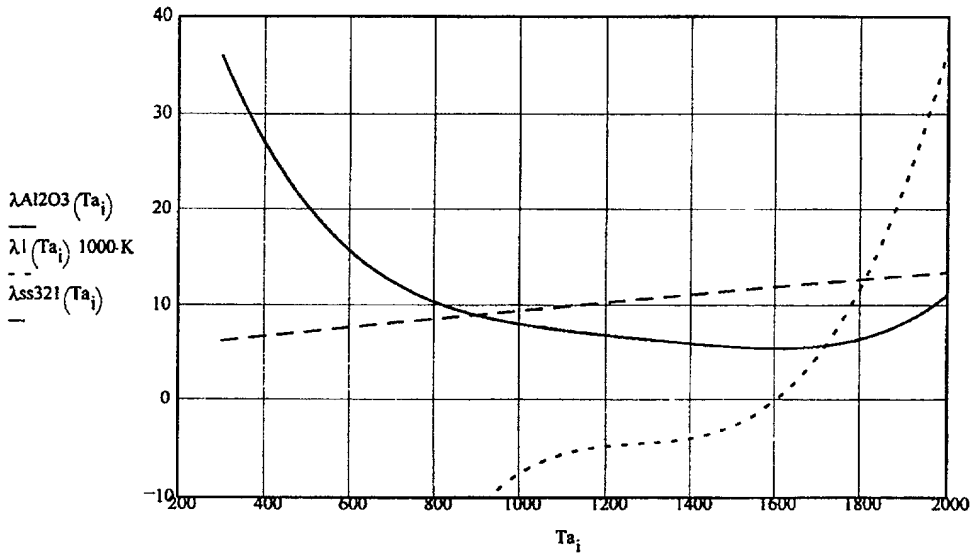

$x := 1500 \cdot K$ x0 root(λ1(x),x) $x0 = 1.588 \cdot 10^{3} \cdot K$

$\lambda ss321(300 \cdot K) = 6.157 \cdot \frac{W}{m \cdot K}$ $0.003 \cdot in = 7.62 \cdot 10^{-3} \cdot cm$

$\lambda Al2O3(300 \cdot K) = 0.359 \cdot \frac{W}{cm \cdot K}$ $\lambda Al2O3(200 \cdot K) = 0.479 \cdot \frac{W}{cm \cdot K}$

$\lambda Al2O3(800 \cdot K) = 0.102 \cdot \frac{W}{cm \cdot K}$ $\lambda Al2O3(x0) = 0.054 \cdot \frac{W}{cm \cdot K}$ Minimum thermal conductivity

****

****

Determine thermal conductivity of porous wall:

Ref: RHG - Handbook Chpt 6 for effective thermal conductivity including convection and radiative terms

$\varepsilon rad := 0.6$ $\varepsilon := 0.42$ $dp := 0.00005 \cdot cm$ $dp = 5 \cdot 10^{-7} \cdot m$

$$\lambda wc(x,T) := \lambda mix(x,T) \cdot \left[0.0931 + 2 \cdot 0.9069 \cdot \left(\frac{\lambda Al2O3(T)}{\lambda Al2O3(T) - \lambda mix(x,T)} \right)^2 \cdot \left(\ln\left(\frac{\lambda Al2O3(T)}{\lambda mix(x,T)} \right) - 1 \right) \right] \ldots + 0.229 \cdot 10^{-6} \cdot \frac{W}{m^2 \cdot K^4} \cdot \varepsilon \cdot dp \cdot \varepsilon rad \cdot T^3 \cdot \left[\varepsilon + \frac{1 - \varepsilon}{\left(\frac{0.229 \cdot 10^{-6} \cdot \frac{W}{m^2 \cdot K^4} \cdot \varepsilon \cdot dp \cdot \varepsilon rad \cdot T^3}{\lambda Al2O3(T)} + 1 \right)} \right]$$

$$\lambda wcnr(x,T) := \lambda mix(x,T) \cdot \left[0.0931 + 2 \cdot 0.9069 \cdot \left(\frac{\lambda Al2O3(T)}{\lambda Al2O3(T) - \lambda mix(x,T)} \right)^2 \cdot \left(\ln\left(\frac{\lambda Al2O3(T)}{\lambda mix(x,T)} \right) - 1 \right) \right]$$

$\lambda wc(0.01, 1000 \cdot K) = 0.473 \cdot \frac{W}{m \cdot K}$ $\lambda wcnr(0.01, 1000 \cdot K) = 0.473 \cdot \frac{W}{m \cdot K}$ Radiation component negligible with such small particles in the washcoat

$\lambda mix(0.01, 1000 \cdot K) = 0.067 \cdot \frac{W}{m \cdot K}$ $\lambda Al2O3(700 \cdot K) = 12.354 \cdot \frac{W}{m \cdot K}$ $\lambda ss321(1000 \cdot K) = 9.341 \cdot \frac{W}{m \cdot K}$

$\frac{\lambda Al2O3(1000\cdot K)}{\lambda mix(0.01,1000\cdot K)} = 117.74$ $\frac{\lambda wc(0.01,1000\cdot K)}{\lambda mix(0.01,1000\cdot K)} = 7.046$

The thermal conductivity of the wash coat is about 7 times greater at 1000K than the gas phase conductivity

$\frac{\lambda wc(0.01,1000\cdot K)}{\lambda ss321(1000\cdot K)} = 0.051$ $\frac{\frac{\lambda wc(0.01,1000\cdot K)}{0.001\cdot cm} + \frac{\lambda ss321(1000\cdot K)}{0.003\cdot in}}{\frac{\lambda ss321(1000\cdot K)}{0.003\cdot in}} = 1.386$

The washcoat increases the thermal conductance of the wall by about 39%

$\frac{\lambda ss321(1000\cdot K)}{\lambda mix(0.01,1000\cdot K)} = 139.275$

For a Nusselt no. of 2.976 (dcell8 = 0.0961*cm) for developed flow in the recuperator (full power) the mean heat transfer boundary layer thickness is much greater than either the SS321 wall thickness or the washcoat thickness.

$\delta gprecup = \frac{0.0961\cdot cm}{2.976}$ $\delta gprecup = 0.032\cdot cm$

$$hrecavg(T) = \frac{1}{\left(\frac{2}{\frac{\lambda mix(0.01,T)}{\delta gprecup}}\right) + \frac{1}{\frac{\lambda ss321(1000\cdot K)}{0.003\cdot in}}}$$

Overall local heat transfer coefficient for the recuperator (assuming gas phase conductivities are about the same

$$hrecavgwc(T) = \frac{1}{\left[\frac{1}{\frac{\lambda mix(0.01,T)}{\delta gprecup - \frac{2\cdot 0.001\cdot cm}{2.976}}}\right] + \left(\frac{1}{\frac{\lambda mix(0.01,T)}{\delta gprecup}}\right) + \left(\frac{1}{\frac{\lambda ss321(1000\cdot K)}{0.003\cdot in}}\right) + \frac{1}{\frac{\lambda wc(0.01,T)}{0.001\cdot cm}}}$$

Effect of wash coat on heat transfer doefficient

$hrecavg(1000\cdot K) = 0.01038\cdot\frac{W}{cm^2\cdot K}$ $hrecavgwc(1000\cdot K) = 0.01046\cdot\frac{W}{cm^2\cdot K}$

The wash coat makes about 0.1% increase in heat transfer coefficient because of the slightly decreased cell size and greater thermal conductivity of the washcoat vs. gas phase.

****

Hi.

APPENDIX C

[redacted] COMBUSTION CATALYSTS FOR [redacted] TURBINES

Introduction

[redacted] I described possible alternative combustion catalyst configurations and detailed analysis of relevant performance factors, i.e., mass-transfer limited hydrocarbon conversions, pressure drop, catalyst temperatures, post combustion conversion of hydrocarbons and CO, etc. This report represents a comprehensive collection of my findings and comments. Attached are the final MathSoft Mathcad 6 analyses of the suggested alternative combustion catalyst configurations.

Alternative Combustion Catalyst Configurations

Two approaches are suggested for the catalytic combustion of gasoline vapors in air. These approaches represent more conventional and perhaps less expensive alternatives to the PCI Microlith™ technology. They are summarized as follows:

- **Monolith with bypass air** -- A standard 3.5", corrugated FeCrAl alloy, 600 cells/in^2 monolith should be able to reach ≈ 86% (naphtha) to >99.8% (natural gas) fuel conversions. Using an air by-pass would allow longer residence time and higher adiabatic temperature rise (which is probably necessary for natural gas but may not be for diesel fuel or naphtha) within the combustor to ensure fast catalytic reaction rates. Higher temperatures within and at the exit of the catalyst monolith would also increase homogeneous combustion reactions, and help convert residual fuel vapors in the region immediately downstream of the catalyst but upstream of the turbine. A controller for bypass flow could help with turn-down, startup, and tuning steady-state conversions.

- **Radial flow catalyst bed** -- Provided that the flow rate can be reduced to < 3 m/s, a thin packed bed of catalyst beads or granules may also achieve conversions similar to those of the monolith and PCI Microlith™ catalyst screens at equivalent pressure drop. The bed might intrude upon your fuel injection and premixing zone, but this could actually benefit combustion (within limits, e.g., ±30% fuel/air ratio) by providing locally higher adiabatic temperatures. A packed bed has fairly good thermal conductivity and is virtually immune to thermal shock problems. A screened frame and possibly metal plates (or alternatively for robustness, silica-coated silicon carbide) could be located within the bed to guide the flow. Downstream hydrocarbon and CO conversion also would be necessary for low emissions as in the case of the monolith.

C1

1/9

- **Exhaust converter** -- A 400 cells/in^2 post combustion monolith located just ahead of the regenerator exhaust stream inlet could provide a very significant reduction in hydrocarbon emissions regardless of the configuration and performance of the combustion catalyst. An emission control monolith should remove about 99% of the residual unburned fuel components and > 99.9% of the CO.

Analysis of Catalyst Performance

Mathsoft's Mathcad 6.0 Plus Professional program was used to perform detailed calculations of pressure drop and conversion of C_1, C_5, C_7, and C_9 hydrocarbons (methane, isopentane, cycloheptane and nonene) and CO. The analyses generally assume catalytic rates are fast under Capstone's specified combustion conditions. The analyses use various catalyst parameters such as particle/channel size and bed length for the two upstream (monolith and fixed bed) configurations. Only monoliths were considered for the downstream 1-atm conversion of residual CO and hydrocarbons.

Gas Properties

Initially the Mathcad document describes and defines various gas component and mixture properties and functions (pp. 1-13) that are used in the subsequent calculations. The gas and vapor components are identified with their physical parameters (p. 1) and the composition of combustion mixtures as a function of fuel conversion are defined (pp. 2-3). Mixture densities, diffusivities of individual fuel component in the mixtures, viscosity, and thermal conductivity are then defined and plotted as functions of composition and temperature (pp. 4-9). The composition of various fuel mixtures is shown to minimally effect mixture physical properties (< 0.5% under such lean conditions). These properties are then redefined as empirical functions of temperature for simplification of subsequent analysis (pp. 6-9). Heat capacities, heats of combustion and enthalpy functions of the mixtures are similarly defined (pp. 9-11), and the initial composition necessary for

an adiabatic temperature rise of 511°F are determined for each of the four fuel components (p. 11 and re-entered on p. 2). Finally, transport functions, e.g., Prandtl Number, Schmidt Number, thermal diffusivity, momentum diffusivity, etc., are defined (pp. 12-13) prior to definitions of the catalyst configurations, geometry, and flow conditions.

Catalyst Configurations

The physical parameters of several catalyst configurations (honeycomb monoliths and packed beds) and the appropriate flow conditions are described (p. 14) and used in the subsequent analyses.

Combustion Monolith Performance

The pressure drop values for (standard) 3.5 or 4.0 inch length 400 and 600 cells/in^2 monoliths are determined as functions of flow rate (pp. 15-16, and see figure on p. 16). Heat and mass Nusselt functions are defined and used to calculate single-pass fuel conversion vs. monolith depth (p. 17-19). It is possible to determine laminar flow hydrothermal Nusselt functions for square or sinusoidal channels (which may be more representative of actual monolith channel shapes), but this was not included in the current analysis. Accordingly the Nusselt functions cannot be considered more accurate than about ± 30%.

The results of the performance analysis for the monoliths are summarized in a table (p. 18) for the two cell densities, the two lengths, and 0, 20, and 40% by-pass air. The transport-limiting conversion of fuel components is plotted as a function of pressure drop for constant flow rate but extended monolith length (p. 19). High fuel conversions (≈ 99.5%) are possible with the 600 cells/in^2 monolith at 1% pressure drop (but it requires 10 inches length).

Post Combustion Converter

Analysis of post-combustion downstream (1-atm vs. 3-atm upstream) conversion of CO and fuels and the pressure drop in 400 and 600 cpi monoliths shows excellent results for such a wide area monolith (pp. 20-25). After defining component diffusivity functions and describing monolith configuration (pp. 20-21), the pressure drop and conversions of CO and fuel vapors are calculated and plotted as functions of monolith depth (pp. 21-23). Finally, the results of an analysis of the overall conversions of individual hydrocarbons and CO including upstream combustor, homogeneous combustion, and the exhaust converter are tabulated (p. 23).

Differential (Local) Nusselt Analysis

A different analysis, where the local hydrothermal Nusselt functions are defined and integrated over the length of a monolith (pp. 24-25), are used to check the integral formulas.

These values (p. 25), which are derived from different sources (Kays and Crawford, "Convection Heat and Mass Transfer," 3rd, 1993, vs. Rosner, "Transport Processes in Chemically Reacting Systems", 1986) show higher conversions than the integrated values, e.g., 94% conversion for C_7H_{14} vs. 86% with the integral expression. This difference appears to be caused by the greater effect of hydrothermal entrance (as opposed to hydrodynamically developed flow with thermal entrance) and shows the integral formulas to be conservative by a factor of about two.

Combustion with Packed Beds

Pressure drop and fuel conversion functions are defined and used to analyze the performance of packed beds (pp. 26-31). Pressure drop is a strong function of the superficial flow rate, nearly second order (pressure drops are calculated and plotted against superficial linear flow velocity for various sizes of catalyst particles on p. 27). Gas to particle Nusselt numbers for packed beds are developed plotted for methane, isopentane, cycloheptane and nonene for three sizes of catalyst granules (pp. 27-28). Shape factors are not included in this analysis, so the results represent values for packed spheres with equivalent effect on ΔP, not with equivalent diameter. The conversion of fuel components (again assuming very fast catalytic rates) is determined (pp. 28-29) for the oblique flow geometry (which is defined on p. 16).

For full perpendicular flow such as with an annular cylindrical packed bed rather than the conical bed , the pressure drop function is much greater for equivalent conversion of fuel components. This is caused by the higher power dependence of ΔP on flow velocities (form drag), while the conversion per unit depth of bed increases almost linearly with increasing flow rate. At flows higher than about 2 m/s the catalyst granules begin to act as bluff bodies which cause the flow to accelerate around them. While this increases backmixing which helps convection, it causes a greater effect on the pressure drop. Conversions for methane and cycloheptane are plotted as a function of pressure drop for beds of 1-mm and 1/8-in. granules (pp. 29-31). For oblique flow (2.5 m/s superficial velocity through the conical bed) with the small granules, C_7H_{14} conversions are calculated to be very high (> 99.99%) at 1% pressure drop, while for perpendicular flow (8.2 m/s) with the 1/8-in. pellets, C_7H_{14} conversions are calculated to be very low ($\approx$ 62%) at 2% pressure drop. Clearly some radial configuration must be used to achieve high conversions with the packed beds without a pressure drop penalty.

Required Catalytic Rates

Finally, the specific catalytic rate constants required for conversions of methane and cycloheptane in a 600 cells/in^2 monolith are determined (pp. 32-35) for Capstone's conditions.

The effect of gas diffusional restrictions within the macroporous (pores between agglomerated washcoat particles within a catalyst layer) and microporous (within the porous particles) is defined for CH_4 and C_7H_{14} (pp. 32-33). The effect of rate constant on surface temperature (for a point at the entry to the channel) is determined (p. 34) and shows the rates necessary to move fully into the transport limited regime, i.e., when the concentration of fuel near the surface approaches zero and temperature approaches a limit. This analysis could be turned around by calculating the conversion for a given catalytic rate constant.

But, further analysis of the expected conversions requires measurements of the actual rate of the washcoated catalysts and catalyst beds. The analysis concludes with a complex rate expression for methane combustion by supported PdO that was based on measured rates (in the absence of transport limitations). This rate was based on PdO, an hexa-aluminate support ($LaAl_{11}O_{18}$) with a much lower surface area than the La-stabilized supported used in the Capstone monoliths and pellets. The interception of the curve showing the surface temperature as a function of catalytic rate constant (as on p. 35) and the curve showing the actual rate constant of the catalyst as a function of catalyst temperature (plotted on p. 37) given the actual performance of the catalyst.

[redacted]

More detailed calculations would integrate the conversion through the monolith or packed bed and it would include the thermal conduction along the monolith channel or within the bed. This would represent a one-dimensional calculation (axial surface and gas phase temperatures) which is only an approximation to the actual two- or three-dimensional convective transport and reaction problem. Such calculations could provide estimates of extinction conditions for specific catalysts. Such calculations and further analyses are beyond the scope of the current comments, but could be performed by extending the current Mathcad 6 program.

Conclusions

Catalyst Performance

Several conclusions can be drawn about the transport limiting performance of a catalysts used to combustion gasoline and methane fuels for Capstone's 24 kW microturbine:

1) Commercially available small cell (600 cells/in^2) honeycomb monoliths should be seriously considered as an alternative to the PCI Microlith technology. A catalytic monolith configured as annular flow 600 cells/in^2 honeycomb can achieve very high conversion of methane (99.99%) and

[redacted]

modest conversion for gasoline (94% for cycloheptane) etc. with low pressure drop.

2) If the fuel air mixing can be moved upstream sufficiently to allow use of a longer catalyst monoliths, significantly lower emission could result without unacceptable (> 1%) pressure drop ratio. For 1% $\Delta P/P$ drop (with greater monolith length), transport limited conversion of C_7H_{14} should reach 99.5% in an active 600 cells/in^2 honeycomb monolith.

3) Post combustion monolith catalysts should be considered for use in EZEV turbines, regardless of the method of fuel conversion during combustion. A short 400 cells/in^2 Alpha-IV metal monolith coated with a layer of supported Pt located at the inlet to the recuperator can give very significant emission reductions for CO and all hydrocarbons because of the lower linear velocities, high exhaust temperature, greater diffusivities at 1-atm. Conversions of CO and CH_4 can be very high, while conversions with C_7H_{14} and other gasoline fuels is less, it still can bring the gasoline range fuel components in the exhaust to a few ppm with the assumption that only a modest degree of homogeneous combustion occurs upstream of the turbine.

4) Provided that significant homogeneous combustion occurs within the channels and downstream of the monolith ($\approx$ 80% conversion giving 60 ppm C_7H_{14} and 840 ppm CO leaving the turbine) and that a 400 cells/in^2 post combustion hydrocarbon oxidation catalyst was used downstream, gasoline emissions should fall below 0.5 ppm.

5) The oblique flow/conical catalyst packed bed could also be considered as an option to the Microlith™ and honeycomb monolith catalysts. The performance of the packed beds can be very good in terms of fuel conversion with the smaller catalyst granules. Yet, these beds must have some element of radial flow as the pressure drop for a flow linear flow rate will cause excessive pressure drop. A word of caution here, packed beds are more susceptible to flash back caused by the higher degree of backmixing and regions where local residence times can be quite long relative to the screens and monoliths.

Catalyst Durability, Robustness, and Costs

1) [redacted] concerns were expressed about the tolerance of combustion catalysts to momentarily high fuel/air ratios and local unmixedness. While clearly high degrees of F/A control and uniformly premixed combustion gases are desired, the combustion catalysts should show robustness sufficient to survive short excursions of off-specification F/A ratio conditions as well as showing the durability necessary for long active life under normal operation at high temperatures.

2) The greater the thermal mass of the catalyst, the greater its robustness in the face of locally or globally high F/A. In this regard the packed beds would be

[redacted]

superior to the fine screens of the Microlith™ and the thin walled metal monoliths.

3) A packed bed also has greater ability to disperse locally high F/A mixtures to a greater extent than the Microlith™ and to a much greater than the honeycomb channels. High thermal conductivity also improves robustness in locally high F/A (hot spot) conditions. Here the packed bed is perhaps superior to the metal monolith because of it greater radial conductivity, while the screens have very little ability (radiation) to disperse heat from locally hot zones.

4) The Alpha-IV alloy honeycomb should be much more resistant to fast overheating to high temperatures than the PCI microlith. The Alzeta/Grace electrically heated monolith previously examined by Capstone (Nomac) had entrance channels too large to give high conversion except with long length and smaller channels downstream, hence the large volume and weight.

5) Packed beds represent the least cost catalyst for combustion because they use configurations and materials common with commercial VOC incineration catalysts. The metal monoliths have low costs because of their widespread acceptance and increasing use in automobile catalytic converters and as VOC catalysts. The premixed, gasoline-fueled, and recuperated nature of the combustion process for Capstone's microturbines is a good fit (with a slight push to higher pressure, higher throughput, low pressure drop, and greater robustness) with the commercial VOC catalysts available from several sources, including Prototech/United Catalysts. It would not appear necessary to develop new catalyst and catalytic engineered combustors for Capstone' microturbine combustion applications.

The following table summarizes the findings of this analysis:

Property	Ranking				
Fuel Conversion	Packed Beds	>	Screens	>	Monoliths
Pressure Drop	Monoliths	>	Screens	>	Packed Beds
Durability	Packed Beds	≈	Monoliths	≈	Screens
Robustness	Packed Beds	>	Monoliths	>	Screens
Cost & Availability	Packed Beds	>	Monoliths	>	Screens

[redacted]

United States Patent & Trademark Office

Office of Initial Patent Examination -- Scanning Division

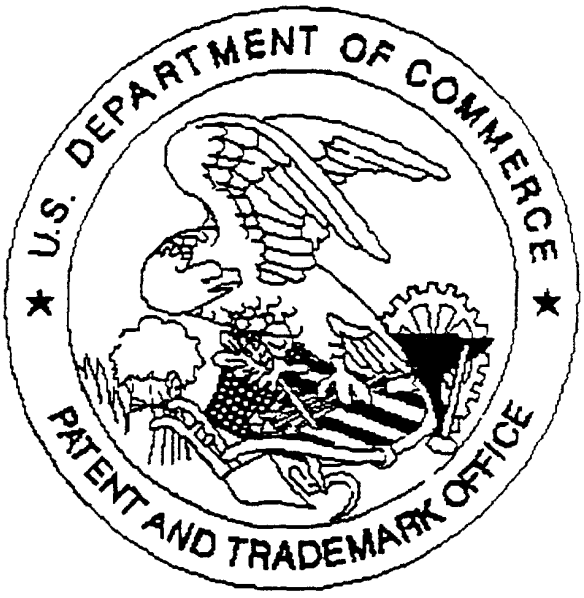

Application deficiencies found during scanning:

☐ Page(s)_____of_____ were not present for scanning. (Document title)

☐ Page(s)_____of_____were not present for scanning. (Document title)

☑ ***Scanned copy is best available.*** Appendix

Final Recommendations

Use of Catalysts in Existing Engines

The following recommendations are made on the basis of improving the *existing* microturbine catalytic combustion performance:

1) Install 400 cells/in^2 1-atm monolith with a Pt-based catalyst for post combustion CO and hydrocarbon removal. This unit should provide the greatest improvement in emissions with little effect on pressure drop at modest cost (≈ $200/unit installed). It could be used with all catalytic and even with non-catalytic burners to reduce CO and hydrocarbon emissions. However, it cannot be effective in reducing NOx emissions from non-catalytic burners.

2) Use a 600 cells/in^2 Alpha-IV alloy metal monolith of 4-in. length with premixed fuel and air as a lower pressure drop alternative to the PCI Microlith™ system. Fuel conversion may be lower than the PCI unit, but with lower pressure drop; at equivalent ΔP/P, the monolith should show superior fuel conversion. A small amount of by-pass air could help with turn-down and could be used to improve emissions during normal operation by increasing residence time and allowing higher temperatures in the homogeneous zones within the channels and immediately downstream of the combustor.

Use of Catalysts in Advanced Engines

For *advanced* combustion systems, the fuel air mixing could be moved upstream of its current position to allow great premixing and to give greater volume for the catalyst.

1) Nominally 1-mm to 1/16-in. packed beds in a conical configuration with about 2-3 m/s linear superficial bed velocity could give good performance, especially with a small bypass air stream for post catalyst hydrocarbon reduction. An inconel screen could be located upstream to suppress flashback and ceramic foams or honeycomb monoliths could be used as mechanical supports to increase robustness.

2) A longer 600 cells/in^2 Alpha-IV alloy metal monolith (from 3.5- to 8- or 10-in.) could also decrease hydrocarbon and CO emissions with acceptable ΔP/P by relocating the F/A mixing zone upstream.

Additional Catalytic R&D Activities

Additional Analysis -- Fuel combustion rates can be measured for specific catalysts under Capstone's combustion conditions. The rates can be incorporated in an extended analysis of

combustor performance for use in predicting fuel conversion, specifying required catalyst activity maintenance (e.g., Is it close to extinction at 1000°F inlet temperature?), and assisting in the design of current and next generation combustors (e.g., How much by-pass air is necessary? What are the limited on F/A ratios?, etc.).

Advanced Materials - [redacted] more robust units could be developed with ceramic structural components and state-of-the-art catalysts capable of resisting short (a few seconds) temperature excursions to 3000°F (1650°C). The attrition resistance and crush strength of the Norton SA 6576 catalyst pellets supplied to Capstone by SRI International also need improvement (their very large specific volume of macropores, while desirable, leads to poor mechanical strength), and other catalysts (e.g., 1.5-mm extruded, Pt-promoted, Mn-substituted hexa-aluminates) could be examined for activity and attrition resistance.

In the longer-term, [redacted] SRI could coat steels with chromium and aluminum (*in situ* preparation of FeCrAl alloy films) to prepare inexpensive, high-performance recuperators and monoliths for use in advanced higher temperature engines.

Systems -- Additional engineering analysis and catalyst preparation and testing could provide Capstone with cost effective assistance in the design of EZEV turbogenerators with alternative fuels such as LPG, CNG, and diesel for hybrid vehicles. LPG could be used in the current designs with combustion and exhaust converter monoliths; CNG could be used with combustion and exhaust converter monoliths, but with by-pass air to increase F/A ratios and catalyst temperatures; and diesel fuel could require upstream mixing with long combustion monoliths or conical beds and longer exhaust converter monoliths.

[redacted]

Appendix C

CAPSTONE MOL [redacted]

Gas Properties and Constants

$cm \equiv 0.01 \cdot m$ $\quad J \equiv kg \cdot m^2 \cdot sec^{-2}$ $\quad W \equiv J \cdot sec^{-1}$ $\quad Pref = 1 \cdot atm$

$N \equiv kg \cdot m \cdot sec^{-2}$ $\quad Pa \equiv N \cdot m^{-2}$ $\quad atm \equiv 101300 \cdot Pa$ $\quad \mu m \equiv 0.000001 \cdot m$

$R := 8.3143 \cdot \frac{J}{K}$ $\quad Rc := 8.3143 \cdot J \cdot mole^{-1} \cdot K^{-1}$

n	Gas	MolWt	σ(LJ)	ε(LJ)
1	CH4	$MW_0 = 16.044 \cdot gm$	$\sigma_0 = 3.785 \cdot 10^{-10} \cdot m$	$\varepsilon_0 = 148.6 \cdot K$
2	O2	$MW_1 = 31.999 \cdot gm$	$\sigma_1 = 3.464 \cdot 10^{-10} \cdot m$	$\varepsilon_1 = 106.7 \cdot K$
3	N2	$MW_2 = 28.018 \cdot gm$	$\sigma_2 = 3.798 \cdot 10^{-10} \cdot m$	$\varepsilon_2 = 71.4 \cdot K$
4	CO2	$MW_3 = 44.010 \cdot gm$	$\sigma_3 = 3.941 \cdot 10^{-10} \cdot m$	$\varepsilon_3 = 195.2 \cdot K$
5	H2O	$MW_4 = 18.015 \cdot gm$	$\sigma_4 = 2.641 \cdot 10^{-10} \cdot m$	$\varepsilon_4 = 809.1 \cdot K$

6 C5H12 2-methyl-butane

$Tb5 = 301 \cdot K$ $\quad Tc5 = 460.4 \cdot K$ $\quad Pc5 = 3.39 \cdot 10^6 \cdot Pa$ $\quad Vc5 = 306$

$\varepsilon_5 = \frac{Tc5}{1.2593}$ $\quad \sigma_5 = Vc5^{\frac{1}{3}} \cdot 10^{-10} \cdot m$

$MW_5 = 72.151 \cdot gm$ $\quad \varepsilon_5 = 365.59994 \cdot K$ $\quad \sigma_5 = 6.73866 \cdot 10^{-10} \cdot m$

7 C7H14 methyl-cyclohexane

$Tc7 = 572.2 \cdot K$ $\quad Tb7 = 374.1 \cdot K$ $\quad Pc7 = 3.47 \cdot 10^6 \cdot Pa$ $\quad Vc7 = 368$

$\varepsilon_6 := \frac{Tc7}{1.2593}$ $\quad \sigma_6 := Vc7^{\frac{1}{3}} \cdot 10^{-10} \cdot m$

$MW_6 = 98.189 \cdot gm$ $\quad \sigma_6 = 7.1661 \cdot 10^{-10} \cdot m$ $\quad \varepsilon_6 = 454.37942 \cdot K$

8 C9H18 1-nonene

$Tc9 = 592 \cdot K$ $\quad Tb9 = 420 \cdot K$ $\quad Vc9 = 580$ $\quad Pc9 = 2.34 \cdot 10^6 \cdot Pa$

$\varepsilon_7 = \frac{Tc9}{1.2593}$ $\quad \sigma_7 = Vc9^{\frac{1}{3}} \cdot 10^{-10} \cdot m$

$MW_7 = 126.243 \cdot gm$ $\quad \sigma_7 = 8.33955 \cdot 10^{-10} \cdot m$ $\quad \varepsilon_7 = 470.10244 \cdot K$

9 CO

$\varepsilon_8 = 91.7 \cdot K$ $\quad \sigma_8 = 3.69 \cdot 10^{-10} \cdot m$

$MW_8 = 28.01 \cdot gm$

CAPSTONE MOD [redacted]

****

Define constants for transport integrals:

$\sigma\mu a_0 := 1.16145$ $\sigma\mu b_0 := 0.14874$ $\sigma Da_0 := 1.06036$ $\sigma Db_0 := 0.1561$

$\sigma\mu a_1 := 0.52487$ $\sigma\mu b_1 := 0.7732$ $\sigma Da_1 := 0.193$ $\sigma Db_1 := 0.47635$

$\sigma\mu a_2 := 2.16178$ $\sigma\mu b_2 := 2.43787$ $\sigma Da_2 := 1.03587$ $\sigma Db_2 := 1.52996$

$\sigma Da_3 := 1.76474$ $\sigma Db_3 := 3.89411$

Define transport integrals:

$$\Omega\mu(T) := \sigma\mu a_0 \cdot \exp\left[-\left(\sigma\mu b_0 \cdot \ln(T)\right)\right] + \sum_{i\mu=1}^{2} \sigma\mu a_{i\mu} \cdot \exp\left(-\sigma\mu b_{i\mu} \cdot T\right) \qquad \Omega\mu(3) = 1.0394$$

$$\Omega D(T) := \sigma Da_0 \cdot \exp\left[-\left(\sigma Db_0 \cdot \ln(T)\right)\right] + \sum_{i\mu=1}^{3} \sigma Da_{i\mu} \cdot \exp\left(-\sigma Db_{i\mu} \cdot T\right) \qquad \Omega D(3) = 0.95002$$

****

Set Inlet Conditions: $P := 3 \cdot atm$

$ych40 := 0.01183$ $y0c5h12 := 0.0028968$

$y0c7h14 := 0.0021859$ $y0c9h18 := 0.0016878$

These values for y0i have been determined via enthalpy functions on p. 11 for temperature rise from 1000F to 1511F.

$CH_4 + H_2O + O_2 + N_2 \rightarrow CO_2 + H_2O + O_2 + N_2$

Define gas composition w/r methane using moist (2%) air:

$$y(y0,x) := \begin{bmatrix} y0\cdot(1-x) \\ (1-y0)\cdot 0.205 - 2\cdot ych40\cdot x \\ (1-y0)\cdot 0.775 \\ y0\cdot x \\ (1-y0)\cdot 0.02 + 2\cdot y0\cdot x \\ 0 \\ 0 \\ 0 \end{bmatrix} \begin{matrix} fuel \\ O_2 \\ N_2 \\ CO_2 \\ H_2O \end{matrix}$$

$$y(ych40, 0.1) = \begin{bmatrix} 0.0106 \\ 0.2002 \\ 0.7658 \\ 0.0012 \\ 0.0221 \\ 0 \\ 0 \\ 0 \end{bmatrix}$$

$\sum y(ych40, 0.5) = 1$

(y_{stoic}, x)

CAPSTONE MIX [redacted]

Define function for calculating stoichiometric gas composition for combustion of 2-methyl-butane using moist (2%) air:

C_5H_{12}

$$y5(y0,x) := \frac{\begin{bmatrix} 0 \\ (1-y0)\cdot 0.205 - 8\cdot y0\cdot x \\ (1-y0)\cdot 0.775 \\ 5\cdot(y0\cdot x) \\ (1-y0)\cdot 0.02 + 6\cdot y0\cdot x \\ y0\cdot(1-x) \\ 0 \\ 0 \end{bmatrix}}{1+2\cdot y0\cdot x} \quad \begin{matrix} \text{Butane} \\ O_2 \\ N_2 \\ CO_2 \\ H_2O \\ C_5H_{12} \end{matrix}$$

$$y5(y0c5h12,0.5) = \begin{bmatrix} 0 \\ 0.192262 \\ 0.770523 \\ 0.007221 \\ 0.02855 \\ 0.001444 \\ 0 \\ 0 \end{bmatrix}$$

$\sum y5(y0c5h12,0.5) = 1$

Define function for calculating stoichiometric gas composition for combustion of methyl-cyclohexane using moist (2%) air:

C_7H_{14}

$$y7(y0,x) := \frac{\begin{bmatrix} 0 \\ (1-y0)\cdot 0.205 - 10.5\cdot y0\cdot x \\ (1-y0)\cdot 0.775 \\ 7\cdot(y0\cdot x) \\ (1-y0)\cdot 0.02 + 7\cdot y0\cdot x \\ 0 \\ y0\cdot(1-x) \\ 0 \end{bmatrix}}{1+2.5\cdot y0\cdot x} \quad \begin{matrix} CH_4 \\ \\ \\ \\ \\ C_5H_{12} \\ C_7H_{14} \\ \end{matrix}$$

$$y7(y0c7h14,0.5) = \begin{bmatrix} 0 \\ 0.19255 \\ 0.771199 \\ 0.00763 \\ 0.027532 \\ 0 \\ 0.00109 \\ 0 \end{bmatrix}$$

$\sum y7(y0c7h14,0.5) = 1$

Define function for calculating stoichiometric gas composition for combustion of 1-nonene using moist (2%) air:

C_9H_{18}

$$y9(y0,x) := \frac{\begin{bmatrix} 0 \\ (1-y0)\cdot 0.205 - 13.5\cdot y0\cdot x \\ (1-y0)\cdot 0.775 \\ 9\cdot(y0\cdot x) \\ (1-y0)\cdot 0.02 + 9\cdot y0\cdot x \\ 0 \\ 0 \\ y0\cdot(1-x) \end{bmatrix}}{1+3.5\cdot y0\cdot x} \quad C_9H_{18}$$

$$y9(y0c9h18,0.5) = \begin{bmatrix} 0 \\ 0.192692 \\ 0.771413 \\ 0.007573 \\ 0.02748 \\ 0 \\ 0 \\ 8.414148\cdot 10^{-4} \end{bmatrix}$$

$\sum y9(y0c9h18,0.5) = 1$

****

CAPSTONE MOD [redacted]

****

Define functions for evaluation of mixture properties (ideal gas) given fractional fuel conversion and temperature.

Density and average molecular weight:

$$\rho mix(x,T) := \left(\sum_{kk=0}^{7} y(ych40,x)_{kk} \cdot MW_{kk} \right) \cdot \frac{P}{R \cdot T} \qquad MWmix(x) := \left(\sum_{kk=0}^{7} y(ych40,x)_{kk} \cdot MW_{kk} \right)$$

$\rho mix(1,300 \cdot K) = 3.470573 \cdot kg \cdot m^{-3}$ $\qquad$ $MWmix(1) = 28.485 \cdot gm$

Define diffusion coefficients for specific binary diffusion pairs:

$$Diff(n,m,T) := 1.8829 \cdot 10^{-27} \cdot \frac{\left[\left(\frac{1}{MW_n} + \frac{1}{MW_m} \right) \cdot T^3 \right]^{0.5}}{\left(\frac{\sigma_n + \sigma_m}{2} \right)^2 \cdot \Omega D \left[\frac{T}{(\varepsilon_n \cdot \varepsilon_m)^{0.5}} \right] \cdot \frac{P}{Pref}} \cdot 10^8 \cdot gm^{0.5} \cdot cm^4 \cdot sec^{-1} \cdot K^{1.5}$$

$Diff(0,2,300 \cdot K) = 0.07417 \cdot sec^{-1} \cdot cm^2$ $\qquad$ $Diff(2,7,300 \cdot K) = 0.01597 \cdot sec^{-1} \cdot cm^2$

Define functions for use with various fuel air mixtures:

$$Dch4(x,T) := \frac{1 - y(ych40,x)_0}{\sum_{jgas=1}^{7} \frac{y(ych40,x)_{jgas}}{Diff(0,jgas,T)}}$$

$Dch4(0.5,298 \cdot K) = 7.31327 \cdot 10^{-6} \cdot m^2 \cdot sec^{-1}$

$$Dc5h12(x,T) := \frac{1 - y5(y0c5h12,x)_0}{\sum_{jgas=1}^{7} \frac{y5(y0c5h12,x)_{jgas}}{Diff(5,jgas,T)}}$$

$Dc5h12(0.5,298 \cdot K) = 2.28466 \cdot 10^{-6} \cdot m^2 \cdot sec^{-1}$

$$Dc7h14(x,T) := \frac{1 - y7(y0c7h14,x)_0}{\sum_{jgas=1}^{7} \frac{y7(y0c7h14,x)_{jgas}}{Diff(6,jgas,T)}}$$

$Dc7h14(0.5,298 \cdot K) = 1.94254 \cdot 10^{-6} \cdot m^2 \cdot sec^{-1}$

$$Dc9h18(x,T) := \frac{1 - y9(y0c9h18,x)_0}{\sum_{jgas=1}^{7} \frac{y9(y0c9h18,x)_{jgas}}{Diff(7,jgas,T)}}$$

$Dc9h18(0.5,298 \cdot K) = 1.53123 \cdot 10^{-6} \cdot m^2 \cdot sec^{-1}$

****

CAPSTONE MOD [redacted]

****

Display gas mixture properties

$idsp := 0..9$ $\quad Tdsp_{idsp} := (750 + 50 \cdot idsp) \cdot K$

$Tin := \left[(1000 - 32) \cdot \frac{5}{9} + 273.15\right] \cdot K \quad Tin = 810.92778 \cdot K \quad Tout := \left[(1511 - 32) \cdot \frac{5}{9} + 273.15\right] \cdot K \quad Tout = 1094.81667 \cdot K$

Plots (below) of Di for CH4, C5H12, etc. show large gap between CH4 and the other hydrocarbons and show very little effect of fuel conversion (even for methane) on Di because the fuels are so dilute.

Therefore we can choose methyl cyclohexane as the molecule representative of naphtha and ignore the effect of conversion on gas properties

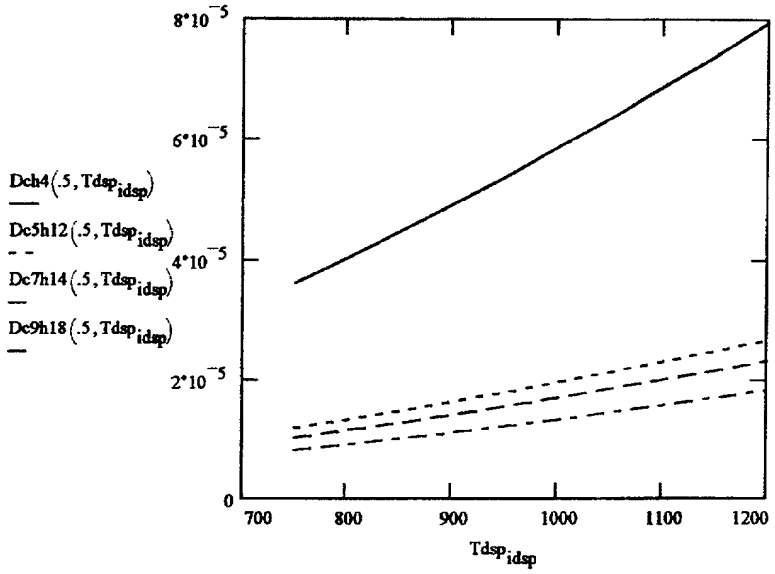

$Tdsp_{idsp}$	$Dch4(.5, Tdsp_{idsp})$
$7.5 \cdot 10^2 \cdot K$	$3.61119 \cdot 10^{-5} \cdot m^2 \cdot sec^{-1}$
$8 \cdot 10^2 \cdot K$	$4.02644 \cdot 10^{-5} \cdot m^2 \cdot sec^{-1}$
$8.5 \cdot 10^2 \cdot K$	$4.45884 \cdot 10^{-5} \cdot m^2 \cdot sec^{-1}$
$9 \cdot 10^2 \cdot K$	$4.90801 \cdot 10^{-5} \cdot m^2 \cdot sec^{-1}$
$9.5 \cdot 10^2 \cdot K$	$5.37357 \cdot 10^{-5} \cdot m^2 \cdot sec^{-1}$
$1 \cdot 10^3 \cdot K$	$5.85522 \cdot 10^{-5} \cdot m^2 \cdot sec^{-1}$
$1.05 \cdot 10^3 \cdot K$	$6.35265 \cdot 10^{-5} \cdot m^2 \cdot sec^{-1}$
$1.1 \cdot 10^3 \cdot K$	$6.8656 \cdot 10^{-5} \cdot m^2 \cdot sec^{-1}$
$1.15 \cdot 10^3 \cdot K$	$7.39384 \cdot 10^{-5} \cdot m^2 \cdot sec^{-1}$
$1.2 \cdot 10^3 \cdot K$	$7.93712 \cdot 10^{-5} \cdot m^2 \cdot sec^{-1}$

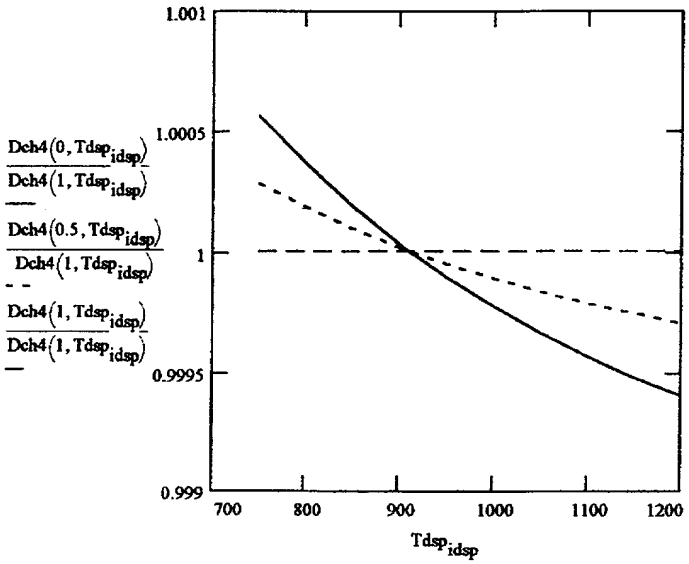

$Tdsp_{idsp}$	$Dc7h14(.5, Tdsp_{idsp})$
$7.5 \cdot 10^2 \cdot K$	$1.03475 \cdot 10^{-5} \cdot m^2 \cdot sec^{-1}$
$8 \cdot 10^2 \cdot K$	$1.15717 \cdot 10^{-5} \cdot m^2 \cdot sec^{-1}$
$8.5 \cdot 10^2 \cdot K$	$1.28482 \cdot 10^{-5} \cdot m^2 \cdot sec^{-1}$
$9 \cdot 10^2 \cdot K$	$1.41758 \cdot 10^{-5} \cdot m^2 \cdot sec^{-1}$
$9.5 \cdot 10^2 \cdot K$	$1.55533 \cdot 10^{-5} \cdot m^2 \cdot sec^{-1}$
$1 \cdot 10^3 \cdot K$	$1.69798 \cdot 10^{-5} \cdot m^2 \cdot sec^{-1}$
$1.05 \cdot 10^3 \cdot K$	$1.84541 \cdot 10^{-5} \cdot m^2 \cdot sec^{-1}$
$1.1 \cdot 10^3 \cdot K$	$1.99755 \cdot 10^{-5} \cdot m^2 \cdot sec^{-1}$
$1.15 \cdot 10^3 \cdot K$	$2.15429 \cdot 10^{-5} \cdot m^2 \cdot sec^{-1}$
$1.2 \cdot 10^3 \cdot K$	$2.31555 \cdot 10^{-5} \cdot m^2 \cdot sec^{-1}$

CAPSTONE M.C.

Define interpolation formulas for Dch4 and Dc7h14 vs. T(K) at x=0.5 via Jandel Scientific's Tablecurve program

$$Dch4T(T) := \exp\left(-11.718527 + 1.6257167\cdot\ln\left(\frac{T}{K}\right) - \frac{46.77509\cdot K}{T}\right)\cdot\frac{cm^2}{sec}$$

$Dch4(.5, 1000\cdot K) = 0.585522\cdot sec^{-1}\cdot cm^2$

$Dch4T(1000\cdot K) = 0.585523\cdot sec^{-1}\cdot cm^2$

$$Dc7h14T(T) := \exp\left(-12.923061 + 1.6260558\cdot\ln\left(\frac{T}{K}\right) - \frac{82.480098\cdot K}{T}\right)\cdot\frac{cm^2}{sec}$$

$Dc7h14(.5, 1000\cdot K) = 0.169798\cdot sec^{-1}\cdot cm$

$Dc7h14T(1000\cdot K) = 0.169798\cdot sec^{-1}\cdot cm^2$

****

Define viscosity functions for major constituents:

$$\mu(T) := \begin{bmatrix} 2.6693\cdot10^{-26}\cdot\frac{(MW_0\cdot T)^{0.5}}{(\sigma_0)^2\cdot\Omega\mu\left(\frac{T}{\varepsilon_0}\right)}\cdot\frac{10^5\cdot cm}{sec}\cdot\left(\frac{gm}{K}\right)^{0.5} \\ \frac{(MW_1\cdot T)^{0.5}}{(\sigma_1)^2\cdot\Omega\mu\left(\frac{T}{\varepsilon_1}\right)}\cdot\left[2.6693\cdot10^{-26}\cdot\left(\frac{10^5\cdot cm}{sec}\right)\cdot\left(\frac{gm}{K}\right)^{0.5}\right] \\ \frac{(MW_2\cdot T)^{0.5}}{(\sigma_2)^2\cdot\Omega\mu\left(\frac{T}{\varepsilon_2}\right)}\cdot\left[2.6693\cdot10^{-26}\cdot\left(\frac{10^5\cdot cm}{sec}\right)\cdot\left(\frac{gm}{K}\right)^{0.5}\right] \\ \frac{(MW_3\cdot T)^{0.5}}{(\sigma_3)^2\cdot\Omega\mu\left(\frac{T}{\varepsilon_3}\right)}\cdot\left[2.6693\cdot10^{-26}\cdot\left(\frac{10^5\cdot cm}{sec}\right)\cdot\left(\frac{gm}{K}\right)^{0.5}\right] \\ \frac{1.116\cdot(MW_4\cdot T)^{0.5}}{(3.115\cdot10^{-8}\cdot cm)^2\cdot\Omega\mu\left(\frac{T}{514\cdot K}\right)}\cdot\left[2.6693\cdot10^{-26}\cdot\left(\frac{10^5\cdot cm}{sec}\right)\cdot\left(\frac{gm}{K}\right)^{0.5}\right] \end{bmatrix}$$

$$\mu(300\cdot K) = \begin{bmatrix} 1.10281\cdot10^{-5} \\ 2.0603\cdot10^{-5} \\ 1.76981\cdot10^{-5} \\ 1.51851\cdot10^{-5} \\ 1.06784\cdot10^{-5} \end{bmatrix}\cdot kg\cdot m^{-1}\cdot sec^{-1}$$

$$\mu mix(x, T) := \sum_{n=0}^{4}\frac{y(ych40, x)_n\cdot\mu(T)_n}{\sum_{m=0}^{4} y(ych40, x)_m\cdot\left[\frac{\left[1+\left(\frac{\mu(T)_n}{\mu(T)_m}\right)^{0.5}\cdot\left(\frac{MW_m}{MW_n}\right)^{0.25}\right]^2}{\left[8\cdot\left(1+\frac{MW_n}{MW_m}\right)\right]^{0.5}}\right]}$$

$$y(ych40, 0.5) = \begin{bmatrix} 0.00592 \\ 0.19074 \\ 0.76583 \\ 0.00592 \\ 0.03159 \\ 0 \\ 0 \\ 0 \end{bmatrix}$$

$\mu mix(0.5, 300\cdot K) = 0.00002\cdot kg\cdot m^{-1}\cdot sec^{-1}$

$ych40 = 0.01183$

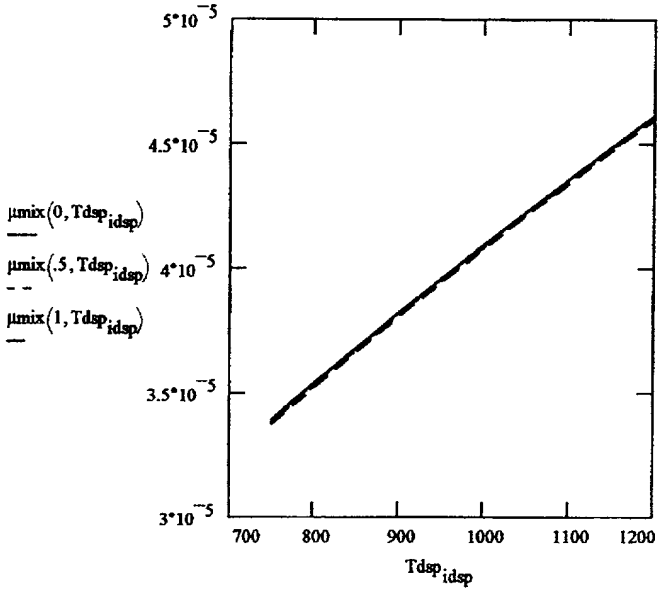

The viscosity of the CH4 - air mixtures vary little with composition (< 0.5%), again because the fuel is so dilute. We can therefore neglect the effect of composition by chosing x=0.5 in all cases.

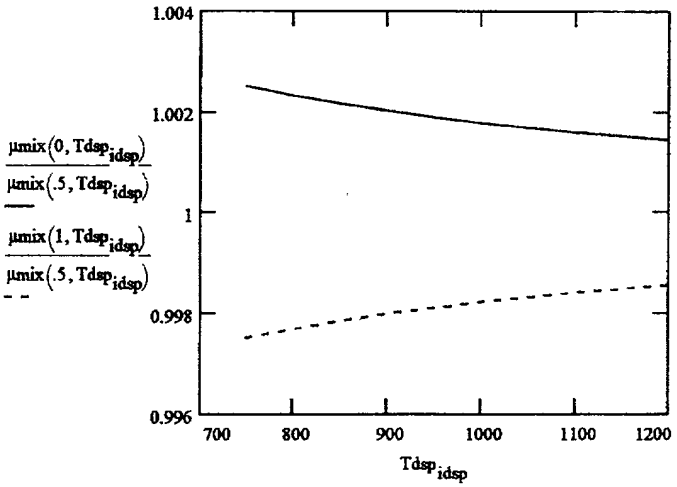

$Tdsp_{idsp}$	$\mu mix(0.5, Tdsp_{idsp})$
$7.5 \cdot 10^2 \cdot K$	$3.38338 \cdot 10^{-5} \cdot kg \cdot m^{-1} \cdot sec^{-1}$
$8 \cdot 10^2 \cdot K$	$3.53056 \cdot 10^{-5} \cdot kg \cdot m^{-1} \cdot sec^{-1}$
$8.5 \cdot 10^2 \cdot K$	$3.67429 \cdot 10^{-5} \cdot kg \cdot m^{-1} \cdot sec^{-1}$
$9 \cdot 10^2 \cdot K$	$3.81491 \cdot 10^{-5} \cdot kg \cdot m^{-1} \cdot sec^{-1}$
$9.5 \cdot 10^2 \cdot K$	$3.95267 \cdot 10^{-5} \cdot kg \cdot m^{-1} \cdot sec^{-1}$
$1 \cdot 10^3 \cdot K$	$4.08779 \cdot 10^{-5} \cdot kg \cdot m^{-1} \cdot sec^{-1}$
$1.05 \cdot 10^3 \cdot K$	$4.22047 \cdot 10^{-5} \cdot kg \cdot m^{-1} \cdot sec^{-1}$
$1.1 \cdot 10^3 \cdot K$	$4.35088 \cdot 10^{-5} \cdot kg \cdot m^{-1} \cdot sec^{-1}$
$1.15 \cdot 10^3 \cdot K$	$4.47917 \cdot 10^{-5} \cdot kg \cdot m^{-1} \cdot sec^{-1}$
$1.2 \cdot 10^3 \cdot K$	$4.60547 \cdot 10^{-5} \cdot kg \cdot m^{-1} \cdot sec^{-1}$

$$\mu mixT(T) := \exp\left(-0.70216045 + 0.640874 \cdot \ln\left(\frac{T}{K}\right) + \frac{-14.24382 \cdot K}{T}\right) \cdot 10^{-6} \cdot kg \cdot m^{-1} \cdot sec^{-1}$$

$\mu mix(.5, 1000 \cdot K) = 4.08779 \cdot 10^{-5} \cdot kg \cdot m^{-1} \cdot sec^{-1}$

$\mu mixT(1000 \cdot K) = 4.08782 \cdot 10^{-5} \cdot kg \cdot m^{-1} \cdot sec^{-1}$

****

Define thermal conductivity functions for light molecules

$igas := 0, 1 .. 4$

CH4
O2
N2
CO2
H2O

$$a\lambda := \begin{bmatrix} -1.869 \\ -.3273 \\ 0.3919 \\ -7.215 \\ 7.341 \end{bmatrix} \quad b\lambda = \begin{bmatrix} 0.08727 \\ 0.09966 \\ 0.09816 \\ 0.08015 \\ -0.01013 \end{bmatrix} \quad c\lambda = \begin{bmatrix} 1.179\cdot10^{-4} \\ -(3.743\cdot10^{-5}) \\ -(5.067\cdot10^{-5}) \\ 5.477\cdot10^{-6} \\ 1.801\cdot10^{-4} \end{bmatrix} \quad d\lambda = \begin{bmatrix} -(3.614\cdot10^{-8}) \\ 9.732\cdot10^{-9} \\ 1.504\cdot10^{-8} \\ -(1.053\cdot10^{-8}) \\ -(9.1\cdot10^{-8}) \end{bmatrix}$$

$$\lambda(i,T) := \left[a\lambda_i + b\lambda_i \cdot \frac{T}{K} + c\lambda_i \cdot \left(\frac{T}{K}\right)^2 + d\lambda_i \cdot \left(\frac{T}{K}\right)^3 \right] \cdot 0.00001 \cdot \frac{W}{cm \cdot K}$$

$\lambda(igas, 1000\cdot K)$ W/cm/K

$0.16716\cdot kg\cdot m\cdot sec^{-3}\cdot K^{-1}$
$0.07163\cdot kg\cdot m\cdot sec^{-3}\cdot K^{-1}$
$0.06292\cdot kg\cdot m\cdot sec^{-3}\cdot K^{-1}$
$0.06788\cdot kg\cdot m\cdot sec^{-3}\cdot K^{-1}$
$0.08631\cdot kg\cdot m\cdot sec^{-3}\cdot K^{-1}$

$$\lambda mix(x,T) := \sum_{i=0}^{4} \frac{y(ych40,x)_i \cdot \lambda(i,T)}{\sum_{j=0}^{4} y(ych40,x)_j \cdot \left[\frac{\left[1 + \left(\frac{\mu(T)_i}{\mu(T)_j} \right)^{0.5} \cdot \left(\frac{MW_j}{MW_i} \right)^{0.25} \right]^2}{\left[8 \cdot \left(1 + \frac{MW_i}{MW_j} \right) \right]^{0.5}} \right]}$$

$$\lambda mix(.0, 1000\cdot K) = 0.00066 \cdot \frac{W}{cm \cdot K}$$

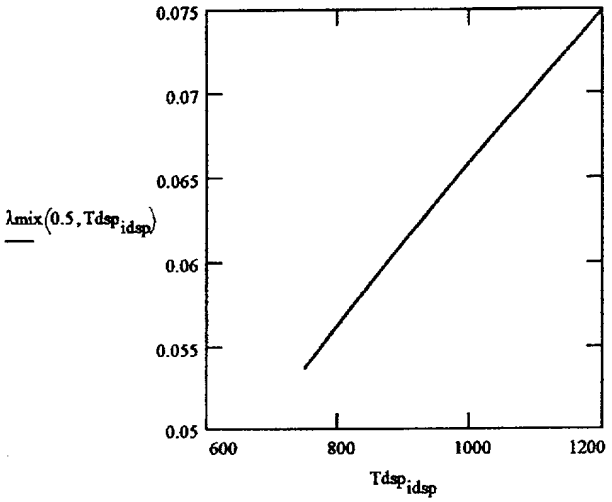

$Tdsp_{idsp}$	$\lambda mix(0.5, Tdsp_{idsp})$
$7.5\cdot10^2\cdot K$	$0.05362\cdot kg\cdot m\cdot sec^{-3}\cdot K^{-1}$
$8\cdot10^2\cdot K$	$0.05621\cdot kg\cdot m\cdot sec^{-3}\cdot K^{-1}$
$8.5\cdot10^2\cdot K$	$0.05872\cdot kg\cdot m\cdot sec^{-3}\cdot K^{-1}$
$9\cdot10^2\cdot K$	$0.06117\cdot kg\cdot m\cdot sec^{-3}\cdot K^{-1}$
$9.5\cdot10^2\cdot K$	$0.06355\cdot kg\cdot m\cdot sec^{-3}\cdot K^{-1}$
$1\cdot10^3\cdot K$	$0.06589\cdot kg\cdot m\cdot sec^{-3}\cdot K^{-1}$
$1.05\cdot10^3\cdot K$	$0.06818\cdot kg\cdot m\cdot sec^{-3}\cdot K^{-1}$
$1.1\cdot10^3\cdot K$	$0.07043\cdot kg\cdot m\cdot sec^{-3}\cdot K^{-1}$
$1.15\cdot10^3\cdot K$	$0.07266\cdot kg\cdot m\cdot sec^{-3}\cdot K^{-1}$
$1.2\cdot10^3\cdot K$	$0.07488\cdot kg\cdot m\cdot sec^{-3}\cdot K^{-1}$

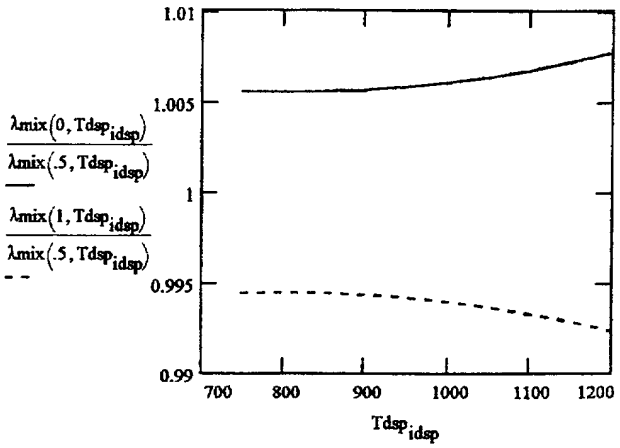

The thermal conductivity varies > 1% with conversion. Selection of 50% conversion gives and error range of +.5-.5% at 1000K. This is likely to be smaller than the accuracy of measured thermal conductivity. Therefore we again define a composition independent formula to increase speed in calculating derived transport properties

$$\lambda mixT(T) := \exp\left(-7.073383 + 0.6397005\cdot\ln\left(\frac{T}{K}\right) + \frac{-65.2387\cdot K}{T}\right)\cdot W\cdot m^{-1}\cdot K^{-1}$$

$\lambda mix(.5, 1000\cdot K) = 0.06589\cdot m^{-1}\cdot K^{-1}\cdot W$ $\lambda mixT(1000\cdot K) = 0.06589\cdot m^{-1}\cdot K^{-1}\cdot W$

****

Determine the heat capacity and enthalpy functions of the fuel-air mixtures for the evaluation of temperature rise

Define heat capacities and heat of combustion:

$$Cpcoef := \begin{bmatrix} 19.25 & .05213 & 0.00001197 & -0.00000001132 \\ 28.11 & -0.000368 & 0.00001746 & -0.00000001065 \\ 31.15 & -0.01357 & 0.0000268 & -0.00000001168 \\ 19.8 & 0.07344 & -0.00005602 & 0.00000001715 \\ 32.24 & 0.001924 & 0.00001055 & -0.000000003596 \\ -9.52 & 0.5066 & -0.0002729 & 0.00000005723 \\ -76.19 & 0.7867 & -0.0004204 & 0.00000007516 \\ -37.18 & 0.8122 & -0.0004509 & 0.00000009705 \end{bmatrix}$$

$$Cp(igas, T) := \sum_{jj=0}^{3} Cpcoef_{igas,jj}\cdot\left(\frac{T}{K}\right)^{jj}\cdot\frac{J}{K}$$

J/mol/K

$Cp(0, 300\cdot K) = 35.66066\cdot K^{-1}\cdot J$ $Cp(5, 300\cdot K) = 119.44421\cdot K^{-1}\cdot J$

$Cp(6, 300\cdot K) = 124.01332\cdot K^{-1}\cdot J$ $Cp(7, 300\cdot K) = 168.51935\cdot K^{-1}\cdot J$

$$y(ych40, 0.5) = \begin{bmatrix} 0.00592 \\ 0.19074 \\ 0.76583 \\ 0.00592 \\ 0.03159 \\ 0 \\ 0 \\ 0 \end{bmatrix}$$

$$Cpmix(x, T) := \sum_{jk=0}^{4} Cp(jk, T)\cdot y(ych40, x)_{jk}$$

$Cpmix(0.5, 998\cdot K) = 33.66993\cdot J\cdot K^{-1}$

CAPSTONE.MCD [redacted]

Define heats of combustion

$\Delta Cpcomb(T) := (Cp(3,T) + 2\cdot Cp(4,T)) - (Cp(0,T) + 2\cdot Cp(1,T))$ CH4 + 2O2 ==> CO2 + 2H2O

$\Delta Cpcomb5(T) := (5\cdot Cp(3,T) + 6\cdot Cp(4,T)) - (Cp(5,T) + 8\cdot Cp(1,T))$ C5H12 + 8O2 ==> 5CO2 + 6H2O

$\Delta Cpcomb7(T) := (7\cdot Cp(3,T) + 7\cdot Cp(4,T)) - (Cp(6,T) + 10.5\cdot Cp(1,T))$ C7H14 + 10.5O2 ==> 7CO2 + 7H2O

$\Delta Cpcomb9(T) := (9\cdot Cp(3,T) + 9\cdot Cp(4,T)) - (Cp(7,T) + 13.5\cdot Cp(1,T))$ C9H18 = 13.5O2 ==> 9CO2 + 9H2O

$$\Delta Hf := \begin{bmatrix} -74900\cdot J \\ 0\cdot J \\ 0\cdot J \\ -393800\cdot J \\ -242000\cdot J \\ -154600\cdot J \\ -119400\cdot J \\ -103600\cdot J \end{bmatrix}$$

$\Delta Cpcomb(298\cdot K) = 10.38812\cdot K^{-1}\cdot J$

$\frac{\Delta Cpcomb5(298\cdot K)}{5} = 6.97449\cdot kg\cdot m^2\cdot sec^{-2}\cdot K^{-1}$

$\frac{\Delta Cpcomb7(298\cdot K)}{7} = 9.35823\cdot K^{-1}\cdot J$

$\frac{\Delta Cpcomb9(298\cdot K)}{9} = 8.3177\cdot K^{-1}\cdot J$

Define enthalpy function for individual components and ΔH for fuels:

$$Hf(nn,T) := \Delta Hf_{nn} + \int_{298\cdot K}^{T} Cp(nn,Tx)\,dTx$$

Hf(igas, 1000·K)

$-36559.44819\cdot kg\cdot m^2\cdot sec^{-2}$
$22590.03871\cdot kg\cdot m^2\cdot sec^{-2}$
$21484.78794\cdot kg\cdot m^2\cdot sec^{-2}$
$-3.60367\cdot 10^5\cdot kg\cdot m^2\cdot sec^{-2}$
$-2.15959\cdot 10^5\cdot kg\cdot m^2\cdot sec^{-2}$

$$\Delta Hcomb(T) := \left[\left(\Delta Hf_3 + 2\cdot\Delta Hf_4\right) - \left(\Delta Hf_0 + 2\cdot\Delta Hf_1\right)\right] + \int_{298\cdot K}^{T} \Delta Cpcomb(Tx)\,dTx$$

$$\Delta Hcomb5(T) := \left[\left[(5\cdot\Delta Hf)_3 + 6\cdot\Delta Hf_4\right] - \left(\Delta Hf_0 + 8\cdot\Delta Hf_1\right)\right] + \int_{298\cdot K}^{T} \Delta Cpcomb5(Tx)\,dTx$$

$$\Delta Hcomb7(T) := \left[\left[(7\cdot\Delta Hf)_3 + 7\cdot\Delta Hf_4\right] - \left(\Delta Hf_0 + 10.5\cdot\Delta Hf_1\right)\right] + \int_{298\cdot K}^{T} \Delta Cpcomb7(Tx)\,dTx$$

$$\Delta Hcomb9(T) := \left[\left[(9\cdot\Delta Hf)_3 + 9\cdot\Delta Hf_4\right] - \left(\Delta Hf_0 + 13.5\cdot\Delta Hf_1\right)\right] + \int_{298\cdot K}^{T} \Delta Cpcomb9(Tx)\,dTx$$

Evaluate a few values of ΔH for CH4, C5H12, C7H14, and C9H18:

$\Delta Hcomb(800\cdot K) = -8.00306\cdot 10^5\cdot J$

$\frac{\Delta Hcomb5(800\cdot K)}{5} = -6.69221\cdot 10^5\cdot J$

$\frac{\Delta Hcomb7(800\cdot K)}{7} = -6.2472\cdot 10^5\cdot J$

$\frac{\Delta Hcomb9(800\cdot K)}{9} = -6.26002\cdot 10^5\cdot J$

****

CAPSTONE MAC [redacted]

****

Define the mixture enthalpies and determine the fuel composition needed for 511F temperature rise from 1000F.

igas := 0, 1 .. 7

$$Hmix(x,T) := \sum_{kgas=0}^{7} y(ych40,x)_{kgas} \cdot Hf(kgas,T)$$

ych40 = 0.01183

Hmix(0, 810.93·K) = 1.006514·10^4 ·J Hmix(1, 1094.82·K) = 1.006518·10^4 ·J

Determines CH4 inlet concentration

$$Hmix5(x,T) := \sum_{kgas=0}^{7} y5(y0c5h12,x)_{kgas} \cdot Hf(kgas,T)$$

y0c5h12 = 0.0028968

Determines C5H12 inlet concentration

Hmix5(0, 810.93·K) = 1.058499·10^4 ·J Hmix5(1, 1094.82·K) = 1.058492·10^4 ·J

$$Hmix7(x,T) := \sum_{kgas=0}^{7} y7(y0c7h14,x)_{kgas} \cdot Hf(kgas,T)$$

y0c7h14 := 0.0021859

Determines C7H14 inlet concentration

Hmix7(0, 810.93·K) = 1.075807·10^4 ·J Hmix7(1, 1094.82·K) = 1.075812·10^4 ·J

$$Hmix9(x,T) := \sum_{kgas=0}^{7} y9(y0c9h18,x)_{kgas} \cdot Hf(kgas,T)$$

y0c9h18 := 0.0016878

Determines C9H18 inlet concentration

Hmix9(0, 810.93·K) = 1.083024·10^4 ·J Hmix9(1, 1094.82·K) = 1.083028·10^4 ·J

****

[redacted]

****

Define momentum and thermal difusivities:

$P = 3.039 \cdot 10^5 \cdot Pa$

$\alpha(igas, T) := \frac{\lambda(igas, T) \cdot R \cdot T}{Cp(igas, T) \cdot P}$ $\quad \alpha(0, 300 \cdot K) = 0.07813 \cdot sec^{-1} \cdot cm^2$

$\alpha mix(x, T) := \frac{\lambda mix(x, T) \cdot R \cdot T}{Cpmix(x, T) \cdot P}$ $\quad \alpha mix(.5, 1000 \cdot K) = 0.5352 \cdot sec^{-1} \cdot cm^2$

$\upsilon mix(x, T) := \frac{\mu mix(x, T)}{\rho mix(x, T)}$ $\quad \rho mix(.5, 1000 \cdot K) = 1.04117 \cdot 10^{-3} \cdot gm \cdot cm^{-3}$

$\upsilon mix(.5, 1000 \cdot K) = 0.3926 \cdot sec^{-1} \cdot cm^2$

$Dch4(.5, 1000 \cdot K) = 0.5855 \cdot sec^{-1} \cdot cm^2$ $\quad Dc5h12(.5, 1000 \cdot K) = 0.1957 \cdot sec^{-1} \cdot cm^2$

$Dc7h14(0.5, 1000 \cdot K) = 0.1698 \cdot sec^{-1} \cdot cm^2$ $\quad Dc9h18(.5, 1000 \cdot K) = 0.13431 \cdot sec^{-1} \cdot cm^2$

Define Prandl, Schmidt, and Lewis numbers

$Pr(x, T) := \frac{\upsilon mix(x, T)}{\alpha mix(x, T)}$ $\quad Pr(.5, 1000 \cdot K) = 0.73359$

$Sc(x, T) := \frac{\upsilon mix(x, T)}{Dch4(x, T)}$ $\quad Sc(.5, 1000 \cdot K) = 0.67054$ $\quad Sc5(x, T) := \frac{\upsilon mix(x, T)}{Dc5h12(x, T)}$ $\quad Sc5(.5, 1000 \cdot K) = 2.00639$

$Sc7(x, T) := \frac{\upsilon mix(x, T)}{Dc7h14(x, T)}$ $\quad Sc7(.5, 1000 \cdot K) = 2.31224$ $\quad Sc9(x, T) := \frac{\upsilon mix(x, T)}{Dc9h18(x, T)}$ $\quad Sc9(.5, 1000 \cdot K) = 2.92325$

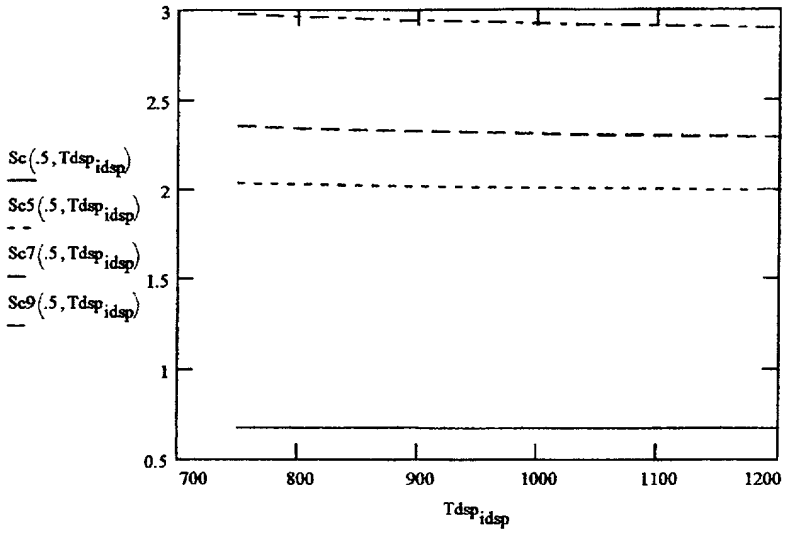

These relations have weak temperature dependence and (presumably) very weak dependence on composition

$$Le(x,T) := \frac{Dch4(x,T)}{\alpha mix(x,T)} \quad Le(.5,1000\cdot K) = 1.09404 \qquad Le5(x,T) := \frac{Dc5h12(x,T)}{\alpha mix(x,T)} \quad Le5(.5,1000\cdot K) = 0.36563$$

$$Le7(x,T) := \frac{Dc7h14(x,T)}{\alpha mix(x,T)} \quad Le7(.5,1000\cdot K) = 0.31726 \qquad Le9(x,T) := \frac{Dc9h18(x,T)}{\alpha mix(x,T)} \quad Le9(.5,1000\cdot K) = 0.25095$$

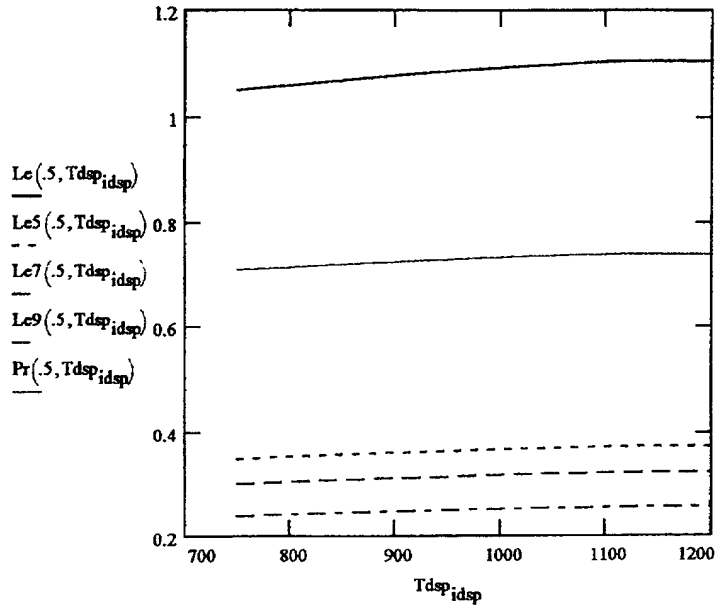

The Lewis numbers show approximately the temperature rise at the wall of an active catalyst relative to the adiabatic temperature rise at that point.

Clearly temperature (and composition) have little influence on the ΔT at the wall, while the nature of the fuel molecule has a strong effect (from 0.25*ΔTadiab for C9 to 1.1*ΔTadiab for CH4)

****

Can remove compositional dependence for most property fundctions

$$\rho mixT(T) := MWmix(0.5)\cdot\frac{P}{R\cdot T} \qquad \upsilon mixT(T) := \frac{\mu mixT(T)}{\rho mixT(T)}$$

$$ScT(T) := \frac{\mu mixT(T)}{Dch4T(T)\cdot\rho mix(0.5,T)} \qquad Sc7T(T) := \frac{\mu mixT(T)}{Dc7h14T(T)\cdot\rho mix(0.5,T)}$$

These functions speed calculations of Nu numbers and heat and mass transfer coefficients

This ends the extended section that defines gas properties for the combustion of several fuel air mixtures.

****

CAPSTONE [redacted]

****

Define honeycomb configurations

$Diao := 9 \cdot in$ $Diao = 22.86 \cdot cm$ $Diai := 4 \cdot in$ $Diai = 10.16 \cdot cm$ $Lhc := 3.5 \cdot in$ $Lhc = 8.89 \cdot cm$

With bypass change Diao to 8.5 in $Bypass := 0$ Bypass - 0, 0.2, 0.4 Lhc - 3.5, 4 in

Honeycombs: Represent as square channel metal alloy wall 0.05 mm, uncoated

$Cells1 := 100 \cdot in^{-2}$ $dwall1 := 0.009 \cdot cm$ $Cells2 := 200 \cdot in^{-2}$ $dwall2 := 0.009 \cdot cm$

$dcell1 := (Cells1)^{-0.5} - dwall1$ $dcell2 := (Cells2)^{-0.5} - dwall2$

Describe 100 and 200 cpi dimensions, although not expected to be used

$dcell1 = 0.245 \cdot cm$ $ks1 := 0.002 \cdot cm$ $dcell2 = 0.17061 \cdot cm$ $ks2 := 0.002 \cdot cm$

$\varepsilon cell1 := dcell1^2 \cdot Cells1$ $\varepsilon cell1 = 0.93039$ $\varepsilon cell2 := dcell2^2 \cdot Cells2$ $\varepsilon cell2 = 0.90229$

$Cells4 := 400 \cdot in^{-2}$ $dwall4 := 0.007 \cdot cm$ $Cells6 := 600 \cdot in^{-2}$ $dwall6 := 0.007 \cdot cm$

$dcell4 := (Cells4)^{-0.5} - dwall4$ $dcell4 = 0.12 \cdot cm$ $dcell6 := (Cells6)^{-0.5} - dwall6$ $dcell6 = 0.0967 \cdot cm$

$dcell4 = 0.12 \cdot cm$ $ks4 := 0.001 \cdot cm$ $dcell6 = 0.0967 \cdot cm$ $ks6 := 0.001 \cdot cm$

$\varepsilon cell4 := dcell4^2 \cdot Cells4$ $\varepsilon cell4 = 0.8928$ $\varepsilon cell6 := dcell6^2 \cdot Cells6$ $\varepsilon cell6 = 0.86955$

Packed Beds: Cylindrical (conical) geometry

$Dinr := 6 \cdot in$ $Dinr = 15.24 \cdot cm$ $Doutr := 7 \cdot in$ $Doutr = 17.78 \cdot cm$ $Wbed := 7 \cdot in$ $Wbed = 17.78 \cdot cm$ $Lbed := 0.75 \cdot in$

? to sheyer angle

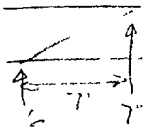

$Smono := \frac{\pi}{4} \cdot (Diao^2 - Diai^2)$ $Sbed := \pi \cdot \left(\frac{Dinr + Doutr}{2}\right) \cdot Wbed$ $\frac{Smono}{Sbed} = 0.35714$

****

Define initial combustion conditions Adjust U0 to fit U(Tin)=7 m/sec w/o bypass flow

$Uref := 7 \cdot \frac{m}{sec}$ $Tin := (537.778 + 273.15) \cdot K$ $Tin = 810.928 \cdot K$ $P = 3.039 \cdot 10^5 \cdot kg \cdot m^{-1} \cdot sec^{-2}$

$M0 := Uref \cdot \rho mix(0, Tin) \cdot \left[\frac{\pi}{4} \cdot ((9 \cdot in)^2 - (4 \cdot in)^2)\right]$ $M0 = 0.29601 \cdot kg \cdot sec^{-1}$ $Tout := (821.667 + 273.15) \cdot K$

$Tout = 1094.817 \cdot K$

$U0 := \frac{M0 \cdot (1 - Bypass)}{\rho mix(0, Tin)} \cdot \frac{1}{\frac{\pi}{4} \cdot (Diao^2 - Diai^2)}$

$U(T) := U0 \cdot \frac{T}{Tin}$ $U(Tin) = 7 \cdot m \cdot sec^{-1}$ $G0 := U(Tin) \cdot \rho mix(0, Tin)$

$Ubed(T) := \frac{M0}{\rho mix(0, Tin) \cdot Sbed}$ $Ubed(Tin) = 2.5 \cdot m \cdot sec^{-1}$ $G0 = 8.98749 \cdot kg \cdot m^{-2} \cdot sec^{-1}$

****

Evaluate Reynolds numbers for use in calculating the momentum, heat, and mass transfer functions:

$$Rehc4(T) := \frac{G0 \cdot dcell4}{\varepsilon cell4 \cdot \mu mixT(T)} \qquad Rehc4(Tin) = 339.11451$$

$$Rehc6(T) := \frac{G0 \cdot dcell6}{\varepsilon cell6 \cdot \mu mixT(T)} \qquad Rehc6(Tin) = 280.56407$$

For laminar flow with entrance effect (adapted from Kays & Crawford, "Convective Heat and Mass Transfer"):

$$cfric4(T,z) := \frac{14.227}{Rehc4(T)} \cdot \left[1 + 0.046263 \cdot \left(Rehc4(T) \cdot \frac{dcell4}{z}\right)\right]^{0.45363}$$

$$cfric6(T,z) := \frac{14.227}{Rehc6(T)} \cdot \left[1 + 0.046263 \cdot \left(Rehc6(T) \cdot \frac{dcell6}{z}\right)\right]^{0.45363}$$ Average coefficient of friction

Calculate monolith pressure drop in several monoliths with entrance effect:

$$z_{idsp} := 0.5 \cdot cm + 1 \cdot idsp \cdot cm \qquad Udsp_{idsp} = (4 + idsp) \cdot m \cdot sec^{-1}$$

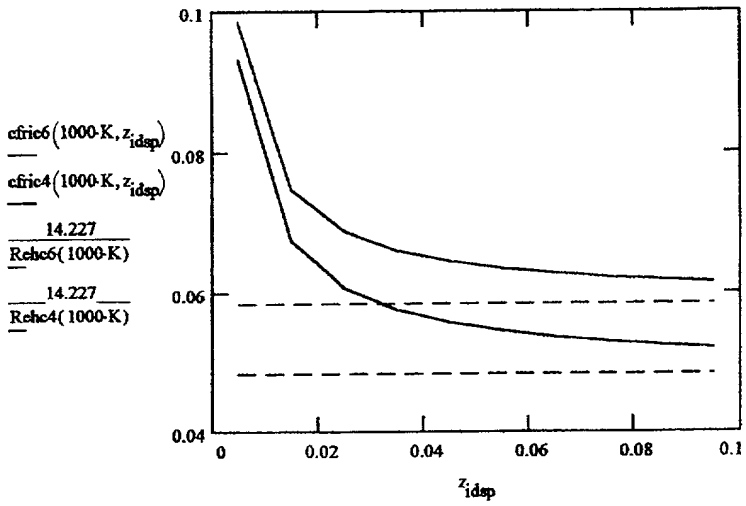

The entrance effect for ΔP of a channel in laminar flow is significant even to 3.5 in. length.

[redacted]

$$Tavg := \frac{Tin + Tout}{2} \qquad cficx(x,z) := \frac{14.227}{x}\cdot(1 + 0.0462363\cdot(x\cdot z))^{0.45363}$$

$$Rex6_{idsp} := \frac{dcell6}{\varepsilon cell6}\cdot\frac{Udsp_{idsp}}{\upsilon mixT(Tavg)} \qquad Rex4_{idsp} := \frac{dcell4}{\varepsilon cell4}\cdot\frac{Udsp_{idsp}}{\upsilon mixT(Tavg)}$$

$$\Delta Px4_{idsp} := 4\cdot cficx\left(Rex4_{idsp}, \frac{dcell4}{Lhc}\right)\cdot\frac{\rho mixT(Tavg)}{2}\cdot\left(\frac{Udsp_{idsp}}{\varepsilon cell4}\right)^2\cdot\frac{Lhc}{dcell4}$$

$$\Delta Px6_{idsp} := 4\cdot cficx\left(Rex6_{idsp}, \frac{dcell6}{Lhc}\right)\cdot\frac{\rho mixT(Tavg)}{2}\cdot\left(\frac{Udsp_{idsp}}{\varepsilon cell6}\right)^2\cdot\frac{Lhc}{dcell6}$$

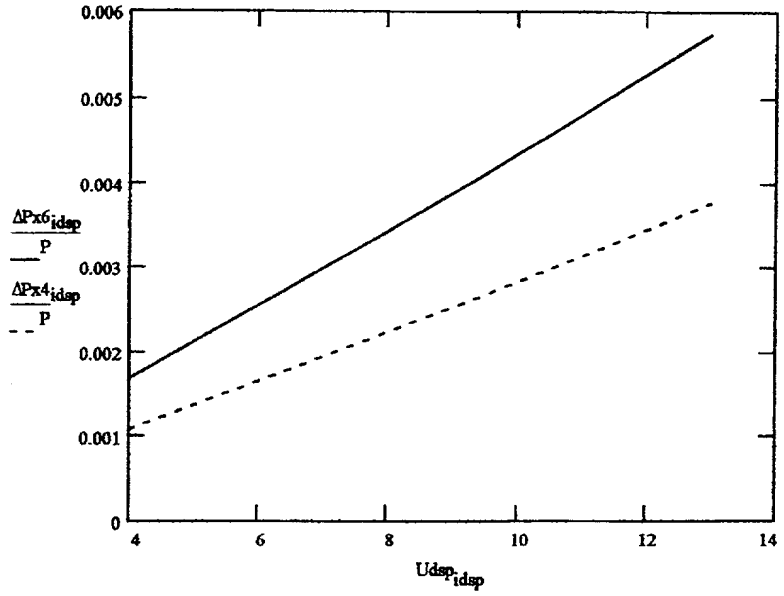

ΔP/P < 0.5% to about 11 m/sec

$$\Delta Phc6(T) := 4\cdot cfric6(T,Lhc)\cdot\frac{\rho mixT(T)\cdot\left(\frac{U(T)}{\varepsilon cell6}\right)^2}{2}\cdot\frac{Lhc}{dcell6} \qquad Tavg = 952.8725\cdot K \qquad U(Tavg) = 8.22528\cdot m\cdot sec^{-1}$$

$$\frac{\Delta Phc6(Tin)}{P} = 0.00271 \qquad \frac{\Delta Phc6(Tout)}{P} = 0.00441 \qquad \frac{\Delta Phc6(Tavg)}{P} = 0.00352$$

$$\Delta Phc4(T) := 4\cdot cfric4(T,Lhc)\cdot\frac{\rho mixT(T)\cdot\left(\frac{U(T)}{\varepsilon cell4}\right)^2}{2}\cdot\frac{Lhc}{dcell4} \qquad \frac{\Delta Phc4(Tavg)}{P} = 0.00228$$

CAPSTONE MAT [redacted]

****

Find 1-D heat and mass transfer rates via Nusselt formulas

Averaged Nu for 600 cpi square channels (fully developed laminar flow) taken from Rosner:

$$\frac{7.6\cdot(2\cdot cm)}{Rehc6(Tavg)\cdot Pr(.5,Tavg)\cdot dcell6} = 0.85369$$

$$NuhavgR6(z) := 2.976\cdot\left[1+\left(\frac{7.6\cdot z}{Rehc6(Tavg)\cdot Pr(.5,Tavg)\cdot dcell6}\right)^{-\frac{8}{3}}\right]^{\frac{1}{8}} \qquad NuhavgR6(Lhc) = 2.98649$$

$$NumavgR6(z) := 2.976\cdot\left[1+\left(\frac{7.6\cdot z}{Rehc6(Tavg)\cdot ScT(Tavg)\cdot dcell6}\right)^{-\frac{8}{3}}\right]^{\frac{1}{8}} \qquad NumavgR6(Lhc) = 2.98441$$

$$Num5avgR6(z) := 2.976\cdot\left[1+\left(\frac{7.6\cdot z}{Rehc6(Tavg)\cdot Sc5(.5,Tavg)\cdot dcell6}\right)^{-\frac{8}{3}}\right]^{\frac{1}{8}} \qquad Num5avgR6(Lhc) = 3.11102$$

$$Num7avgR6(z) := 2.976\cdot\left[1+\left(\frac{7.6\cdot z}{Rehc6(Tavg)\cdot Sc7T(Tavg)\cdot dcell6}\right)^{-\frac{8}{3}}\right]^{\frac{1}{8}} \qquad Num7avgR6(Lhc) = 3.16167$$

$$Num7avgR4(z) := 2.976\cdot\left[1+\left(\frac{7.6\cdot z}{Rehc4(Tavg)\cdot Sc7T(Tavg)\cdot dcell4}\right)^{-\frac{8}{3}}\right]^{\frac{1}{8}} \qquad Num7avgR4(Lhc) = 3.3902$$

$$Num9avgR6(z) := 2.976\cdot\left[1+\left(\frac{7.6\cdot z}{Rehc6(Tavg)\cdot Sc9(.5,Tavg)\cdot dcell6}\right)^{-\frac{8}{3}}\right]^{\frac{1}{8}} \qquad Num9avgR6(Lhc) = 3.2775$$

The Nusselt numbers for mass transfer show small (< 5%) compensation for the low diffusivity of the higher hydrocarbons.

****

[redacted]

Use exponential functions implied by the definition of average (integrated) Num functions to calculate exit mole fractions.

$$yc7h14(T,z) := y0c7h14 \cdot \exp\left(\frac{-4 \cdot z \cdot Num7avgR6(z)}{Rehc6(T) \cdot Sc7T(T) \cdot dcell6}\right)$$

$$\frac{yc7h14(Tavg, Lhc)}{y0c7h14} = 0.13705$$

$$ych4(T,z) := ych40 \cdot \exp\left(\frac{-4 \cdot z \cdot NumavgR6(z)}{Rehc6(T) \cdot ScT(T) \cdot dcell6}\right)$$

$$\frac{ych4(Tavg, Lhc)}{ych40} = 0.001533$$

$$yc5h12(T,z) := y0c5h12 \cdot \exp\left(\frac{-4 \cdot z \cdot Num7avgR6(z)}{Rehc6(T) \cdot Sc5(0.5,T) \cdot dcell6}\right)$$

$$\frac{yc5h12(Tavg, Lhc)}{y0c5h12} = 0.10114$$

$$yc9h18(T,z) := y0c9h18 \cdot \exp\left(\frac{-4 \cdot z \cdot Num9avgR6(z)}{Rehc6(T) \cdot Sc9(0.5,T) \cdot dcell6}\right)$$

$$\frac{yc9h18(Tavg, Lhc)}{y0c9h18} = 0.19604$$

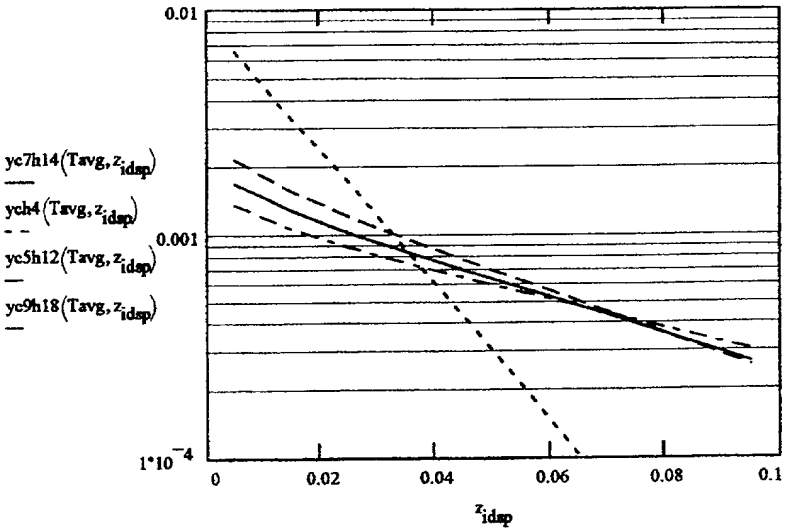

$z_9 = 0.095 \cdot m$

$z_9 = 3.74016 \cdot in$

Summary if 600 cpi Metal Monolith Performance

%Bypass	Length(in)	Diao(in)	Yout/Yin C7H14	Yout/Yin CH4	ΔP/P
0	3.5	9.0	0.13705	0.001533	0.00352
0	4	9.0	0.10679	0.000611	0.00400
20	3.5	8.5	0.11888	0.000906	0.00324
20	4	8.5	0.09055	0.000335	0.00368
40	3.5	8.5	0.06266	0.000089	0.00240
40	4	8.5	0.04317	0.000023	0.00273

Bypass = 0
Lhc = 3.5 ·in
Diao = 9 ·in

These values are conservative and do not account for the higher average temperature with the higher F/A ratios and do not account for hydrothermal entry.

[redacted]

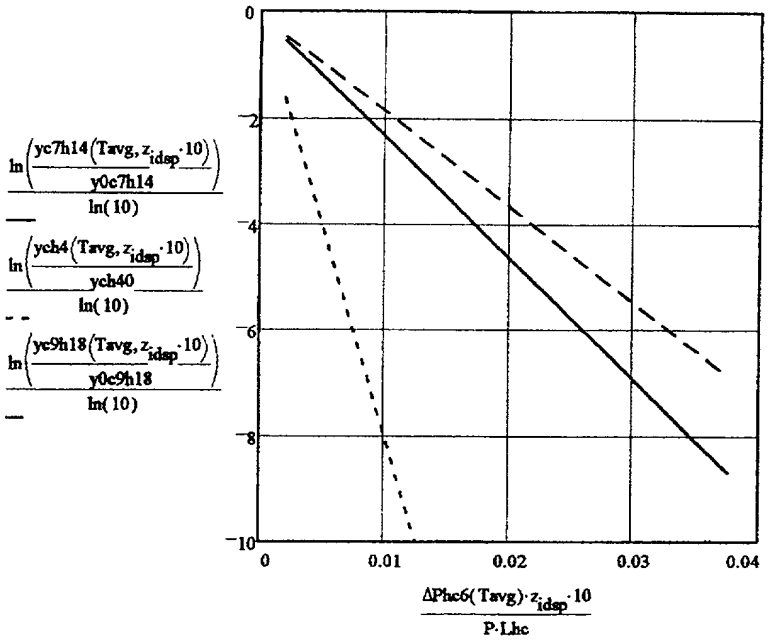

Constant Flow 8.2 m/sec
Variable Length to 89 cm

$U(Tavg) = 8.22528\cdot m\cdot sec^{-1}$

$10\cdot Lhc = 88.9\cdot cm$

Conversions at ΔP/P=0.01
CH4 = 1.06*10^-8
C7H14=4.8*10^-3
C9H18=1.44*10^-2
z=25.25 cm

$zx := 25.25\cdot cm$

$\frac{\Delta Phc6(Tavg)\cdot zx}{P\cdot Lhc} = 0.01000$ $\quad$ $\frac{yc7h14(Tavg, zx)}{y0c7h14} = 4.80371\cdot 10^{-3}$

$\frac{ych4(Tavg, zx)}{ych40} = 1.06492\cdot 10^{-8}$ $\quad$ $\frac{yc9h18(Tavg, zx)}{y0c9h18} = 1.44218\cdot 10^{-2}$

Conversions at ΔP/P=0.02
CH4 = 1.14*10^-16
C7H14=2.41*10^-5
C9H18=2.21*10^-4
z=50.5 cm

The 600 cpi monolith has low pressure drop at 8.89 cm length. If it's length were extended to give 1.0% and 2.0% fractional pressure drop, then C7H14 conversions would increase to 99.5% and 99.998% respectively

[redacted]

****

Set up properties for CO to calculate the conversion of dilute CO and hydrocarbons downstream of the turbine

$$Dco1(x,T) := \frac{\frac{P}{Pref}}{\sum_{jgas=0}^{7} \frac{y(ych40,x)_{jgas}}{Diff(8,jgas,T)}}$$

$Dco1(.5,Tin) = 1.12854 \cdot sec^{-1} \cdot cm^2$ $Pref = 1 \cdot atm$

$Dch4(.5,Tin) = 0.41195 \cdot sec^{-1} \cdot cm^2$ $P = 3 \cdot atm$

$$Dco7(x,T) := \frac{\frac{P}{Pref}}{\sum_{jgas=0}^{7} \frac{y7(y0c7h14,x)_{jgas}}{Diff(8,jgas,T)}}$$

$Dco7(.5,Tin) = 1.12396 \cdot sec^{-1} \cdot cm^2$ $Pref = 1 \cdot atm$

$Dc7h14(.5,Tin) = 0.11846 \cdot sec^{-1} \cdot cm^2$ $P = 3 \cdot atm$

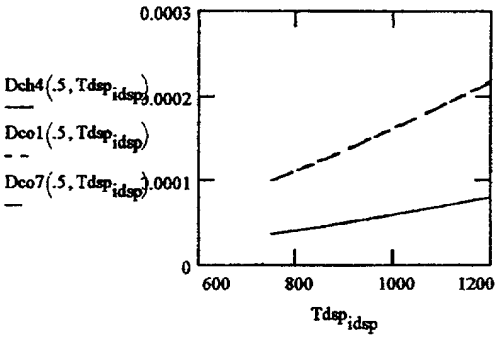

$Tdsp_{idsp}$	$Dco1(.5, Tdsp_{idsp})$
750·K	$9.90331 \cdot 10^{-5} \cdot m^2 \cdot sec^{-1}$
800·K	$1.10324 \cdot 10^{-4} \cdot m^2 \cdot sec^{-1}$
850·K	$1.2208 \cdot 10^{-4} \cdot m^2 \cdot sec^{-1}$
900·K	$1.34291 \cdot 10^{-4} \cdot m^2 \cdot sec^{-1}$
950·K	$1.46949 \cdot 10^{-4} \cdot m^2 \cdot sec^{-1}$
1000·K	$1.60044 \cdot 10^{-4} \cdot m^2 \cdot sec^{-1}$
1050·K	$1.73572 \cdot 10^{-4} \cdot m^2 \cdot sec^{-1}$
1100·K	$1.87523 \cdot 10^{-4} \cdot m^2 \cdot sec^{-1}$
1150·K	$2.01893 \cdot 10^{-4} \cdot m^2 \cdot sec^{-1}$
1200·K	$2.16675 \cdot 10^{-4} \cdot m^2 \cdot sec^{-1}$

$$DcoT(T) := \exp\left[\left(-10.80086 + 1.6357427 \cdot \ln\left(\frac{T}{K}\right)\right) - 28.157906 \cdot \frac{K}{T}\right] \cdot 10^{-4} \cdot m^2 \cdot sec^{-1}$$

$Dco1(.5,Tavg) = 1.47689 \cdot sec^{-1} \cdot cm^2$

$DcoT(Tavg) = 1.47689 \cdot sec^{-1} \cdot cm^2$

$dreco := 17 \cdot in$ $dreco = 43.18 \cdot cm$ $Lrec = 3.5 \cdot in$

$dreci := 6 \cdot in$ $dreci = 15.24 \cdot cm$ $Lrec = 8.89 \cdot cm$

$M0 = 0.29601 \cdot kg \cdot sec^{-1}$ $Arecup := \pi \cdot \frac{dreco^2 - dreci^2}{4}$ $Arecup = 0.1282 \cdot m^2$

$Greco := \frac{M0}{Arecup}$ $Greco = 2.30904 \cdot kg \cdot m^{-2} \cdot sec^{-1}$ $G0 = 8.98749 \cdot kg \cdot m^{-2} \cdot sec^{-1}$

$Prec := 1 \cdot atm$ $\rho mixrec(T) := \frac{MWmix(0.5) \cdot Prec}{R \cdot T}$ $\rho mixrec(Tavg) = 0.36422 \cdot kg \cdot m^{-3}$

$$Urec(T) := \frac{Grec0}{\rho mixrec(T)} \qquad Urec(Tavg) = 6.33964 \cdot m \cdot sec^{-1} \qquad SccoT(T) := \frac{\mu mixT(T)}{DcoT(T) \cdot \rho mixrec(T)}$$

$$Rerec4(T) := \frac{Grec0 \cdot dcell4}{\mu mixT(T)} \qquad Rerec4(Tavg) = 69.96214$$

Schmidt numbers are independent of pressure

$$Rerec6(T) := \frac{Grec0 \cdot dcell6}{\mu mixT(T)} \qquad Rerec6(Tavg) = 56.37495 \qquad Tavg = 952.8725 \cdot K$$

$$cfricrec4(T,z) := \frac{14.227}{Rerec4(T)} \cdot \left[1 + 0.046263 \cdot \left(Rerec4(T) \cdot \frac{dcell4}{z}\right)\right]^{0.45363}$$

$$cfricrec6(T,z) := \frac{14.227}{Rerec6(T)} \cdot \left[1 + 0.046263 \cdot \left(Rerec6(T) \cdot \frac{dcell6}{z}\right)\right]^{0.45363}$$

Calculate monolith pressure drop in several monoliths with entrance effect:

$$\Delta Prec4(T) := 4 \cdot cfricrec4(T, Lrec) \cdot \frac{\rho mixrec(T) \cdot \left(\frac{Urec(T)}{\varepsilon cell4}\right)^2}{2} \cdot \frac{Lrec}{dcell4} \qquad \frac{\Delta Prec4(Tavg)}{Prec} = 0.00557$$

$$\Delta Prec6(T) := 4 \cdot cfricrec6(T, Lrec) \cdot \frac{\rho mixrec(T) \cdot \left(\frac{Urec(T)}{\varepsilon cell6}\right)^2}{2} \cdot \frac{Lrec}{dcell6} \qquad \frac{\Delta Prec6(Tavg)}{Prec} = 0.00898$$

$$Numavgrec6(z) := 2.976 \cdot \left[1 + \left(\frac{7.6 \cdot z}{Rerec6(Tavg) \cdot ScT(Tavg) \cdot dcell6}\right)^{-\frac{8}{3}}\right]^{\frac{1}{8}} \qquad Numavgrec6(Lrec) = 2.97616$$

$$Numavgrec4(z) := 2.976 \cdot \left[1 + \left(\frac{7.6 \cdot z}{Rerec4(Tavg) \cdot ScT(Tavg) \cdot dcell4}\right)^{-\frac{8}{3}}\right]^{\frac{1}{8}} \qquad Numavgrec4(Lrec) = 2.97649$$

$$Numavgrec7R6(z) := 2.976 \cdot \left[1 + \left(\frac{7.6 \cdot z}{Rerec6(Tavg) \cdot Sc7T(Tavg) \cdot dcell6}\right)^{-\frac{8}{3}}\right]^{\frac{1}{8}} \qquad Numavgrec7R6(Lrec) = 2.98024$$

CAPSTONE [redacted]

$$Numavgrec7R4(z) := 2.976\cdot\left[1+\left(\frac{7.6\cdot z}{Rerec4(Tavg)\cdot Sc7T(Tavg)\cdot dcell4}\right)^{-\frac{8}{3}}\right]^{\frac{1}{8}} \qquad Numavgrec7R6(Lrec) = 2.98024$$

$$NumavgreccoR6(z) := 2.976\cdot\left[1+\left(\frac{7.6\cdot z}{Rerec6(Tavg)\cdot SccoT(Tavg)\cdot dcell6}\right)^{-\frac{8}{3}}\right]^{\frac{1}{8}} \qquad NumavgR6(Lrec) = 2.98441$$

$$NumavgreccoR4(z) := 2.976\cdot\left[1+\left(\frac{7.6\cdot z}{Rerec4(Tavg)\cdot SccoT(Tavg)\cdot dcell4}\right)^{-\frac{8}{3}}\right]^{\frac{1}{8}} \qquad NumavgreccoR4(Lrec) = 2.97663$$

The average (integral) Nusselt numbers at 1-atm with the larger flwo cross section show very little contribution of the therma entry length, i.e. the flow velocities and heat and mass transfer coefficients have values close to those in long channels.

Now determine CH4, C7H14, and CO conversions in 400 and 600 cpi honeycombs, assuming 80% C7H14 conversion downstream of the combustion monolith and upstream of the turbine

$$ych4rec6(T,z) := ych4(Tavg,Lhc)\cdot\exp\left(\frac{-4\cdot z\cdot Numavgrec6(z)}{Rerec6(T)\cdot ScT(T)\cdot dcell6}\right) \qquad \frac{ych4rec6(Tavg,Lrec)}{ych4(Tavg,Lhc)} = 2.733018\cdot 10^{-13}$$

$ych4rec6(Tin,Lrec) = 0$ $ych4(Tavg,Lhc) = 1.81356\cdot 10^{-5}$ $Bypass = 0$ $Lhc = 3.5\cdot in$ $Diao = 9\cdot in$

$$yc7h14rec6(T,z) := 0.2\cdot yc7h14(Tavg,Lhc)\cdot\exp\left(\frac{-4\cdot z\cdot Numavgrec7R6(z)}{Rerec6(T)\cdot Sc7T(T)\cdot dcell6}\right) \qquad \frac{yc7h14rec6(Tin,Lrec)}{0.2\cdot yc7h14(Tavg,Lhc)} = 0.00057$$

$yc7h14rec6(Tin,Lrec) = 3.42819\cdot 10^{-8}$ $0.2\cdot yc7h14(Tavg,Lhc) = 5.99172\cdot 10^{-5}$

$$ych4rec4(T,z) := ych4(Tavg,Lhc)\cdot\exp\left(\frac{-4\cdot z\cdot Numavgrec4(z)}{Rerec4(T)\cdot ScT(T)\cdot dcell4}\right) \qquad \frac{ych4rec4(Tavg,Lrec)}{ych4(Tavg,Lhc)} = 6.945016\cdot 10^{-9}$$

$ych4rec4(Tin,Lrec) = 8.84152\cdot 10^{-13}$

$$yc7h14rec4(T,z) := 0.2\cdot yc7h14(Tavg,Lhc)\cdot\exp\left(\frac{-4\cdot z\cdot Numavgrec7R4(z)}{Rerec4(T)\cdot Sc7T(T)\cdot dcell4}\right) \qquad \frac{yc7h14rec4(Tin,Lrec)}{0.2\cdot yc7h14(Tavg,Lhc)} = 0.00773$$

$yc7h14rec4(Tin,Lrec) = 4.63263\cdot 10^{-7}$ $0.2\cdot yc7h14(Tavg,Lhc) = 5.99172\cdot 10^{-5}$ $0.4\cdot 7\cdot yc7h14(Tavg,Lhc) = 8.3884\cdot 10^{-4}$

$$ycorec4(T,z) := 0.4\cdot 7\cdot yc7h14(Tavg,Lhc)\cdot \exp\left(\frac{-4\cdot z\cdot NumavgreccoR4(z)}{Rerec4(T)\cdot SccoT(T)\cdot dcell4}\right) \qquad ycorec4(Tavg,Lrec) = 3.06761\cdot 10^{-11}$$

$$ycorec6(T,z) := 0.4\cdot 7\cdot yc7h14(Tavg,Lhc)\cdot \exp\left(\frac{-4\cdot z\cdot NumavgreccoR6(z)}{Rerec6(T)\cdot SccoT(T)\cdot dcell6}\right) \qquad ycorec6(Tavg,Lrec) = 2.9626\cdot 10^{-15}$$

$$zx_{idsp} := (idsp + 0.05)\cdot cm$$

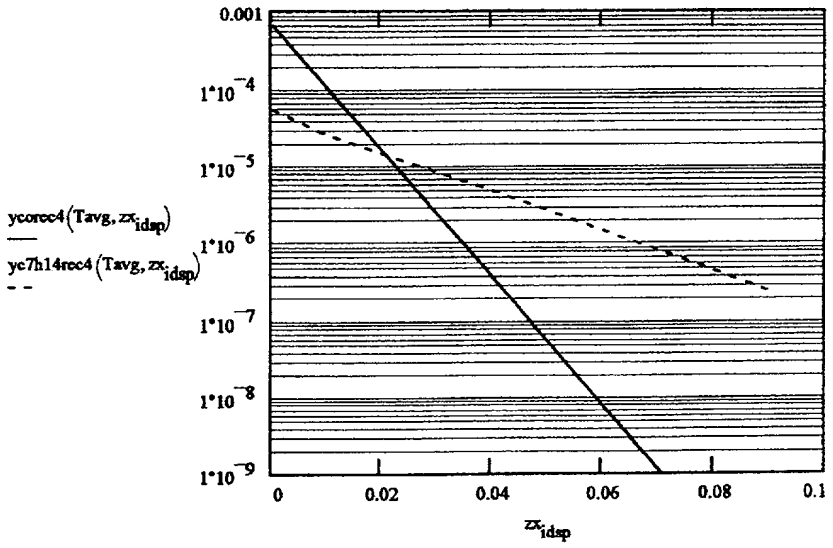

$Sc7T(Tavg) = 2.31842$

$SccoT(Tavg) = 0.73627$

$ScT(Tavg) = 0.67113$

$$\frac{ycorec4(Tavg,Lrec)}{(0.4\cdot 7\cdot yc7h14(Tavg,Lhc))} = 3.65696\cdot 10^{-8}$$

$$\frac{ycorec6(Tavg,Lrec)}{(0.4\cdot 7\cdot yc7h14(Tavg,Lhc))} = 3.53178\cdot 10^{-12}$$

This analysis assumes 80% homogeneous conversion of fuel exiting a 3.5in. 600 cpi monolith without bypass flow and assuming 40% production of CO in the post combustion monolith region.

CO conversion in a 400 cpi recuperator monolith is >99.99%, while cyclohexane conversion is 99.2%.

The final CO and C7H14 levels are < 1 ppb and .5 ppm while post turbine concentrations are taken as 840 and 60 ppm respectively. CH4 conversion also should be very high and use of a 600 cpi or longer monolith would give higher HC conversions (x20 for 600 cpi).

Post turbine pre recuperation monolith pressure drops are modest: 0.56% for 400 cpi and 0.90% for 600 cpi monoliths.

[redacted]

An alternative method of calculating performance uses local Nusselt numbers for heat and mass transfer to determine the wall temperature and combustion rates at the wall. First we define the local Nu function then check conversion assuming fast kinetics and compare with the previous averaged (integrated) Nu formula.

Local Nu(x) taken from Kays & Crawford for hydro & thermal entrance laminar with circular channel:

$Numono(z) := (1 + \exp(-1.09689 - 0.381402 \cdot \ln(z) - 8.287774 \cdot z^{0.5})) \cdot 3.66$ $Numono(0.1152163) = 3.82723$

$zzchar6 := \frac{Rehc6(Tavg) \cdot Pr(.5, Tavg) \cdot dcell6}{2}$ $zzchar6 = 8.90257 \cdot cm$ $\frac{Lhc}{zzchar6} = 0.99859$

$Rehc6(Tavg) = 252.34858$

$itest := 0..50$ $dcell6 = 0.0967 \cdot cm$

$ztest_{itest} := itest \cdot 0.05 \cdot cm + 0.05 \cdot cm$ $zz_{itest} := \frac{ztest_{itest} + dwall6}{zzchar6}$

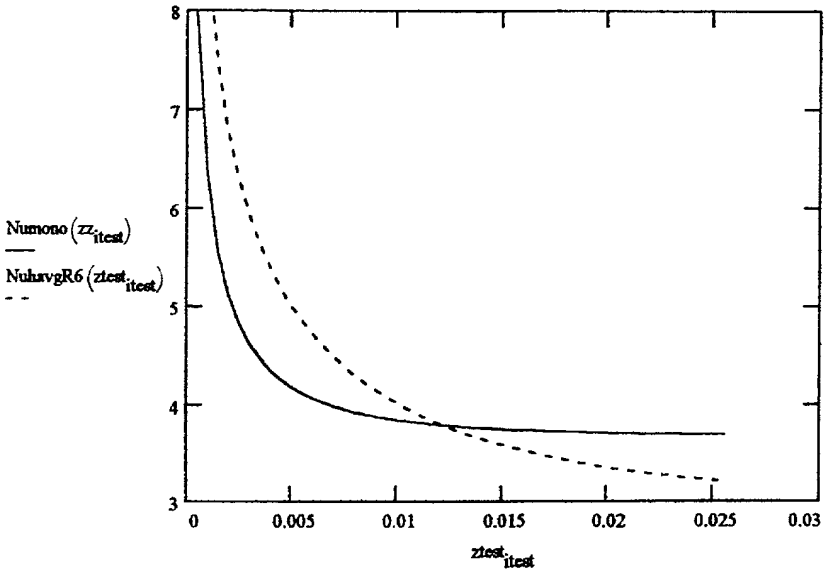

$Rehc6(Tavg) = 252.34858$ $dcell6 = 0.0967 \cdot cm$ $zz6ch4 := \frac{Rehc6(Tavg) \cdot ScT(Tavg) \cdot dcell6}{2}$

$Pr(.5, Tavg) = 0.72969$

$Rehc6(Tavg) \cdot Pr(.5, Tavg) \cdot dcell6 = 17.80513 \cdot cm$

$zz6c7h14 := \frac{Rehc6(Tavg) \cdot Sc7T(Tavg) \cdot dcell6}{2}$

$h(T,z) := \frac{\lambda mixT(T) \cdot Numono\left(\frac{z}{zzchar6}\right)}{dcell6}$

$kgpb(T,z) := \frac{Dch4T(T) \cdot Numono\left(\frac{z}{zz6ch4}\right)}{dcell6}$ $kgpb(Tin, Lhc) = 15.5934 \cdot sec^{-1} \cdot cm$

$$kgpb7(T,z) := \frac{Dc7h14T(T)\cdot Numono\left(\frac{z}{zz6c7h14}\right)}{dcell6} \qquad kgpb7(Tin,Lhc) = 4.50626\cdot sec^{-1}\cdot cm$$

Prater Temperature for CH4 at the inlet with fully developed flow

$$kgpb(Tin,Lhc)\cdot\frac{P}{R\cdot Tin}\cdot\frac{ych40\cdot -\Delta Hcomb(Tin)}{h(Tin,Lhc)} = 309.73474\cdot K$$

Prater Temperature for C7H14 at the inlet with fully developed flow

$$kgpb7(Tin,Lhc)\cdot\frac{P}{R\cdot Tin}\cdot\frac{y0c7h14\cdot -\Delta Hcomb7(Tin)}{h(Tin,10\cdot cm)} = 90.38489\cdot K$$

****

Determine maximum conversion of fuels with very fast catalytic combustion rates (zero fuel concentration at the wall)

$iz := 0..100 \qquad ych46_0 := ych40 \qquad yc7h146_0 := y0c7h14 \qquad Tavg := \frac{Tin + Tout}{2}$

$$z6_{iz} := dwall6 + iz\cdot\frac{Lhc}{100}\cdot\frac{7}{7}$$

$$Lhc\cdot\frac{7}{7} = 8.89\cdot cm$$

3.5 & 4-in. monolith length

$$ych46_{iz+1} := \left(1 - kgpb\left(Tavg, z6_{iz}\right)\cdot\frac{Lhc}{100}\cdot\frac{7}{7}\cdot\frac{4}{dcell6}\cdot\frac{\varepsilon cell6}{U(Tavg)}\right)\cdot ych46_{iz}$$

$$\frac{ych46_{101}}{ych40} = 1.2447\cdot 10^{-4}$$

$$\frac{ych4\left(Tavg, Lhc\cdot\frac{7}{7}\right)}{ych40} = 0.00153$$

$$yc7h146_{iz+1} := \left(1 - kgpb7\left(Tavg, z6_{iz}\right)\cdot\frac{Lhc}{100}\cdot\frac{7}{7}\cdot\frac{4}{dcell6}\cdot\frac{\varepsilon cell6}{U(Tavg)}\right)\cdot yc7h146_{iz}$$

$$\frac{yc7h146_{101}}{y0c7h14} = 0.06145$$

****

By-pass	length	yC7H14out/yin	yCH4out/yin
0	3.5·in	0.06145	$1.2447\cdot 10^{-4}$
0	4·in	0.04256	$3.288\cdot 10^{-5}$
0.2	3.5·in	0.0502	$5.96324\cdot 10^{-5}$
0.2	4·in	0.03374	$1.3974\cdot 10^{-5}$
0.4	3.5·in	0.02054	$2.17587\cdot 10^{-6}$
0.4	3.5·in	0.01207	$2.92928\cdot 10^{-7}$

$Tavg = 952.8725\cdot K$

$Lhc = 3.5\cdot in$

$Diao = 9\cdot in$

$Bypass = 0$

Nu function with circular channel hydothermal entry length shows 93.9% to 98.8% conversion of C7H14

****

Packed bed

[redacted]

****

Pressure Drop Calcuations for a Packed Bed

given: ε - void fraction;
dp - effective particle diameter
U - mean superficial velocity
ν - kinematic viscocity
ρ - density

$$fbed(x) := \frac{150}{x} + 1.75$$

x = Reynolds #

****

1161 F

At T = 900K and 10 atm pressure,

$\rho mix(0.0, 300 \cdot K) = 3.47058 \cdot kg \cdot m^{-3}$

$\rho mix(.5, Tavg) = 1.09267 \cdot kg \cdot m^{-3}$ $\quad \upsilon mix(.5, Tavg) = 0.00004 \cdot m^2 \cdot sec^{-1}$

$j := 0..3$

$dp_j := \frac{.125}{j+1} \cdot in$ $\quad Lbed = 0.75 \cdot in$ $\quad dp = \begin{bmatrix} 0.3175 \\ 0.15875 \\ 0.10583 \\ 0.07938 \end{bmatrix} \cdot cm$

$\varepsilon := 0.5$ $\quad \upsilon 0 := \upsilon mix(.5, Tavg)$

$i := 1..10$

$Utx_i := i \cdot m \cdot sec^{-1}$ $\quad \rho 0 := \rho mix(.5, Tavg)$ $\quad Rebed_{i,j} := Utx_i \frac{dp_j}{\upsilon 0 \cdot (1 - \varepsilon)}$

$$\Delta P_{i,j} := Lbed \cdot fbed\left(Rebed_{i,j}\right) \cdot \frac{1 - \varepsilon}{\varepsilon^3} \frac{\rho 0 \cdot \left(Utx_i\right)^2}{dp_j}$$

$Utx =$

0	
1	
2	
3	
4	
5	$\cdot m \cdot sec^{-1}$
6	
7	
8	
9	
10	

$Rebed =$

0	0	0	0	
1	175.19103	87.59551	58.39701	43.79776
2	350.38206	175.19103	116.79402	87.59551
3	525.57309	262.78654	175.19103	131.39327
4	700.76412	350.38206	233.58804	175.19103
5	875.95515	437.97757	291.98505	218.98879
6	1051.14617	525.57309	350.38206	262.78654
7	1226.3372	613.1686	408.77907	306.5843
8	1401.52823	700.76412	467.17608	350.38206
9	1576.71926	788.35963	525.57309	394.17982
10	1751.91029	875.95515	583.9701	437.97757

$\Delta P =$

0	0	0	0	
1	0.00067	0.00179	0.00335	0.00536
2	0.00226	0.0054	0.00943	0.01434
3	0.00474	0.01081	0.01822	0.02695
4	0.00814	0.01804	0.02972	0.04318
5	0.01243	0.02708	0.04395	0.06304
6	0.01764	0.03794	0.0609	0.08651
7	0.02375	0.0506	0.08056	0.11362
8	0.03077	0.06508	0.10294	0.14435
9	0.03869	0.08137	0.12804	0.1787
10	0.04752	0.09947	0.15586	0.21668

$\cdot atm$

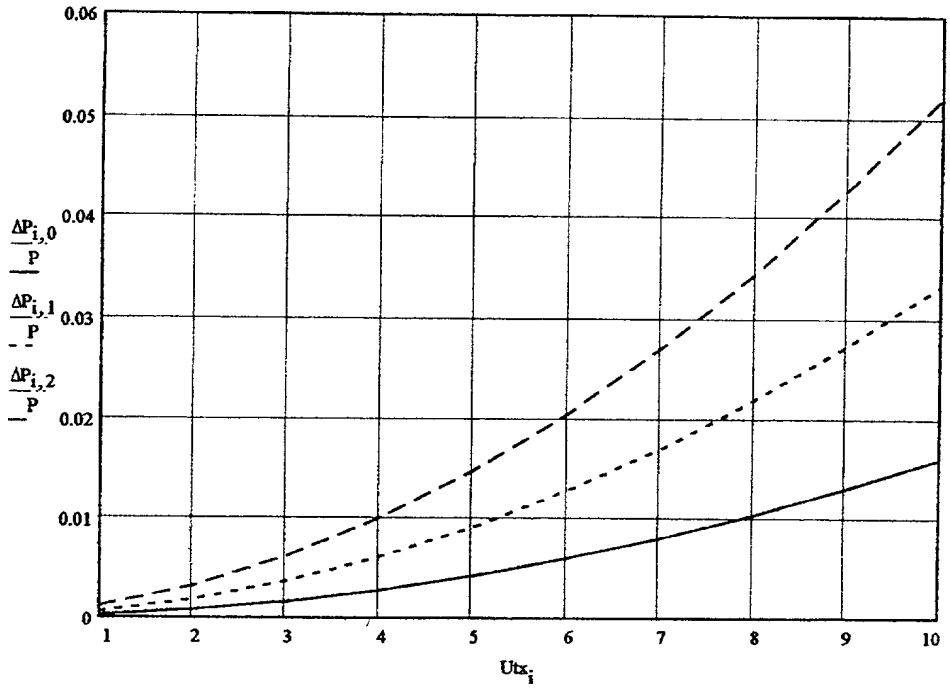

Particle diameters

$dp_2 = 0.04167 \cdot in$ 1/24"

Smack 1mm

$dp_1 = 0.0625 \cdot in$ 1/16"

$dp_0 = 0.125 \cdot in$ 1/8"

$Lbed = 0.75 \cdot in$

$$\Delta P(\varepsilon, T, z) := z \cdot fbed\left[\frac{Ubed(T) \cdot dp_j}{\upsilon 0 \cdot (1-\varepsilon)}\right] \cdot \frac{1-\varepsilon}{\varepsilon^3} \cdot \frac{\rho 0 \cdot (Ubed(T))^2}{dp_j} \qquad \varepsilon := 0.45$$

$$dp = \begin{bmatrix} 0.3175 \\ 0.15875 \\ 0.10583 \\ 0.07938 \end{bmatrix} \cdot cm$$

$\frac{\Delta P(.45, Tavg, Lbed)}{P}$
0.00173
0.00407
0.00703
0.0106

$\frac{\Delta P(.5, Tavg, Lbed)}{P}$
0.00113
0.00263
0.00449
0.00673

$Ubed(Tavg) = 2.5 \cdot m \cdot sec^{-1}$

For larger particles use axial beds with greater length 1/8"

$k = 0$ $\quad dp_0 = 0.125 \cdot in$ = 1/8" which we have

$U(Tavg) = 8.22528 \cdot m \cdot sec^{-1}$

$$\Delta Paxial(\varepsilon, T, z) := z \cdot fbed\left[\frac{U(T) \cdot dp_k}{\upsilon 0 \cdot (1-\varepsilon)}\right] \cdot \frac{1-\varepsilon}{\varepsilon^3} \cdot \frac{\rho 0 \cdot (U(T))^2}{dp_k}$$

$\Delta Paxial(\varepsilon, Tavg, 1 \cdot in) = 0.0657 \cdot atm$

$P = 3 \cdot atm$ $\quad \frac{\Delta Paxial(\varepsilon, Tavg, 1 \cdot in)}{P} = 0.0219$ 1/8th inch pellets give about 2% pressure drop per inch

****

CAPSTONE [redacted]

****

Determine Nu values for heat and mass transfer between particles and the gas phase in the bed

$$Repart(T) := \frac{Ubed(T)\cdot dp}{\upsilon mixT(T)\cdot(1-\varepsilon)} \qquad dp = \begin{bmatrix} 0.3175 \\ 0.15875 \\ 0.10583 \\ 0.07938 \end{bmatrix} \cdot cm \qquad \varepsilon = 0.45$$

$$Repart(Tavg) = \begin{bmatrix} 398.16156 \\ 199.08078 \\ 132.72052 \\ 99.54039 \end{bmatrix} \qquad Pr(.5, Tavg) = 0.72969 \qquad Sc(.5, Tavg) = 0.67112$$

$$k := 0$$

$$NuhpartR(T) := 1.34\cdot\left[Pr(.5,T)^{0.4}\cdot\left[0.4\cdot\left(Repart(T)_k\right)^{0.5} + 0.2\cdot\left(Repart(T)_k\right)^{\frac{2}{3}}\right]\right] \qquad NuhpartR(Tavg) = 22.21552$$

$$havgpart(T) := \frac{\lambda mixT(T)\cdot NuhpartR(T)}{dp_k} \qquad havgpart(Tavg) = 445.59219\cdot m^{-2}\cdot K^{-1}\cdot W$$

Effective boundary layer thickness:

$$\frac{dp_k}{NuhpartR(Tavg)} = 142.9181\cdot\mu m \qquad \frac{dcell6}{NuhavgR6(Lhc)} = 323.77508\cdot\mu m$$

$$dp_k = 0.3175\cdot cm \qquad dcell6 = 0.0967\cdot cm$$

****

$$NumpartR(T) := 1.34\cdot ScT(T)^{0.4}\cdot\left[0.4\cdot\left(Repart(T)_k\right)^{1} + 0.2\cdot\left(Repart(T)_k\right)^{\frac{2}{3}}\right] \qquad NumpartR(Tavg) = 21.48438$$

$$kgpart(T) := \frac{Dch4T(T)\cdot NumpartR(T)}{\varepsilon\cdot dp_k} \qquad kgpart(Tin) = 72.76151\cdot sec^{-1}\cdot cm$$

$$Nupart7R(T) := 1.34\cdot Sc7T(T)^{0.4}\cdot\left[0.4\cdot\left(Repart(T)_k\right)^{0.5} + 0.2\cdot\left(Repart(T)_k\right)^{\frac{2}{3}}\right] \qquad Nupart7R(Tavg) = 35.27582$$

$$kgfb7(T) := \frac{Dc7h14T(T)\cdot Nupart7R(T)}{\varepsilon\cdot dp_k} \qquad kgfb7(Tin) = 34.44665\cdot sec^{-1}\cdot cm$$

CAPSTONE MOD

$$ych46_{iz+1} := \left[1 - kgpart(Tavg)\cdot\frac{Lbed}{50}\cdot\frac{6\cdot(1-\varepsilon)^2}{dp_k}\cdot\frac{1}{Ubed(Tavg)}\right]\cdot ych46_{iz} \qquad \frac{ych46_{51}}{ych46_0} = 0.02369771$$

$$ych4p(T,z) := ych40\cdot\exp\left[-6\cdot(1-\varepsilon)\cdot\frac{NumpartR(T)}{\varepsilon\cdot Repart(T)_k\cdot ScT(T)}\cdot\frac{z}{dp_k}\right] \qquad \frac{ych4p(Tavg,Lbed)}{ych40} = 0.02908261$$

$$yc7h14(T,z) := y0c7h14\cdot\exp\left[-6\cdot(1-\varepsilon)\cdot\frac{Nupart7R(T)}{\varepsilon\cdot Repart(T)_k\cdot Sc7T(T)}\cdot\frac{z}{dp_k}\right] \qquad \frac{yc7h14(Tavg,Lbed)}{y0c7h14} = 0.18611$$

[redacted]

dpart(cm)	yout/yinC7H14	yout/yinCH4	ΔP/P
0.3175	0.18611	0.02908261	0.00113
0.15875	0.0116	0.0000846	0.00263

[redacted]

$dp_k = 0.3175\cdot cm$

$Ubed(Tavg) = 2.5\cdot m\cdot sec^{-1}$

$\varepsilon = 0.45$

$Wbed = 17.78\cdot cm$

$Lbed = 1.905\cdot cm$

****

****

Determine hydrocarbon conversions in the packed beds vs pressure to estimate effective conversion at equivalent pressure drop

$$yc7h14dp2(T,z) := y0c7h14\cdot\exp\left[-6\cdot(1-\varepsilon)\cdot\frac{1.34\cdot Sc7T(T)^{0.4}\cdot\left[0.4\cdot\left(Repart(T)_2\right)^{\frac{1}{2}} + 0.2\cdot\left(Repart(T)_2\right)^{\frac{2}{3}}\right]}{\varepsilon\cdot Repart(T)_2\cdot Sc7T(T)}\cdot\frac{z}{dp_2}\right]$$

$$ych4dp2(T,z) := ych40\cdot\exp\left[-6\cdot(1-\varepsilon)\cdot\frac{1.34\cdot ScT(T)^{0.4}\cdot\left[0.4\cdot\left(Repart(T)_2\right)^{\frac{1}{2}} + 0.2\cdot\left(Repart(T)_2\right)^{\frac{2}{3}}\right]}{\varepsilon\cdot Repart(T)_2\cdot ScT(T)}\cdot\frac{z}{dp_2}\right]$$

$$\Delta Pdp2(Tavg,z) := z\cdot fbed\left(Repart(Tavg)_2\right)\cdot\frac{1-\varepsilon}{\varepsilon^3}\cdot\frac{\rho 0\cdot(Ubed(Tavg))^2}{dp_2}$$

$Ubed(Tavg) = 2.5\cdot m\cdot sec^{-1}$

[redacted]

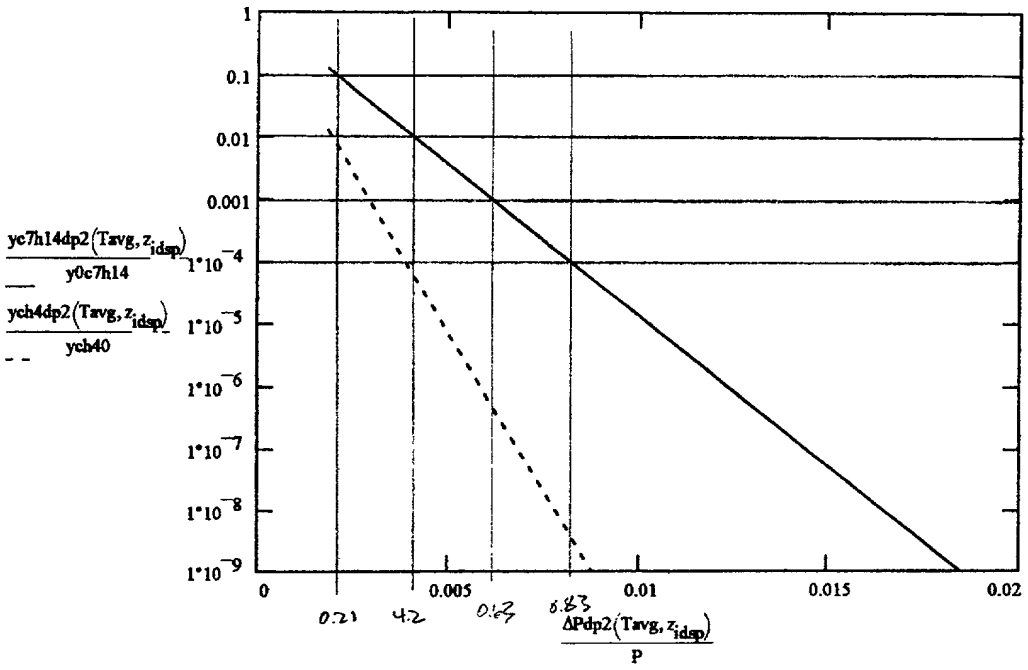

Small

$dp_2 = 0.10583 \cdot cm$

$dp_2 = 0.04167 \cdot in$

$z_9 = 3.74016 \cdot in$

$Lbed = 0.75 \cdot in$

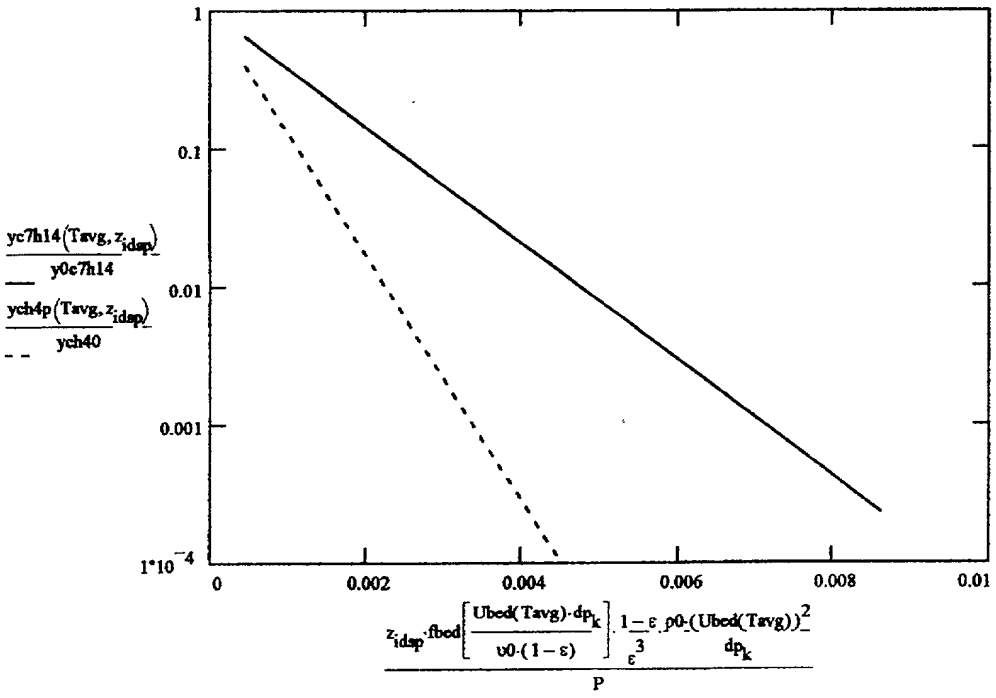

Large

$dp_0 = 0.3175 \cdot cm$

$dp_0 = 0.125 \cdot in$

$z_9 = 3.74016 \cdot in$

$Lbed = 0.75 \cdot in$

$Ubed(Tavg) = 2.5 \cdot m \cdot sec^{-1}$

For oblique flow through cone-shaped beds, large particles give a very low ΔP (even with thick beds) and high conversion

CAPSTONE PLOT

[redacted]

$zxx := 2.71 \cdot cm$

$\frac{\Delta Pdp2(Tavg, zxx)}{P} = 0.01000$ $\quad \frac{yc7h14dp2(Tavg, zxx)}{y0c7h14} = 1.32434 \cdot 10^{-5}$ $\quad \frac{ych4dp2(Tavg, zxx)}{ych40} = 5.45793 \cdot 10^{-11}$

For ΔP/P = 1%, C7H14 conversion = 99.9987% with fine particles, dp = 1.06 mm

$zy := 2.0 \cdot cm$

$Repaxial(T) := \frac{U(T) \cdot dp_0}{\upsilon mixT(T) \cdot (1 - \varepsilon)}$ $\quad Numpaxial(T) := 1.34 \cdot ScT(T)^{0.4} \cdot \left[0.4 \cdot (Repaxial(T))^{\frac{1}{2}} + 0.2 \cdot (Repaxial(T))^{\frac{2}{3}}\right]$

$Nump7axial(T) := 1.34 \cdot Sc7T(T)^{0.4} \cdot \left[0.4 \cdot (Repaxial(T))^{\frac{1}{2}} + 0.2 \cdot (Repaxial(T))^{\frac{2}{3}}\right]$

$ych4paxial(T, z) := ych40 \cdot \exp\left[-6 \cdot (1 - \varepsilon) \cdot \frac{Numpaxial(T)}{\varepsilon \cdot Repaxial(T) \cdot ScT(T)} \cdot \frac{z}{dp_0}\right]$

$yc7h14paxial(T, z) := y0c7h14 \cdot \exp\left[-6 \cdot (1 - \varepsilon) \cdot \frac{Nump7axial(T)}{\varepsilon \cdot Repaxial(T) \cdot Sc7T(T)} \cdot \frac{z}{dp_0}\right]$

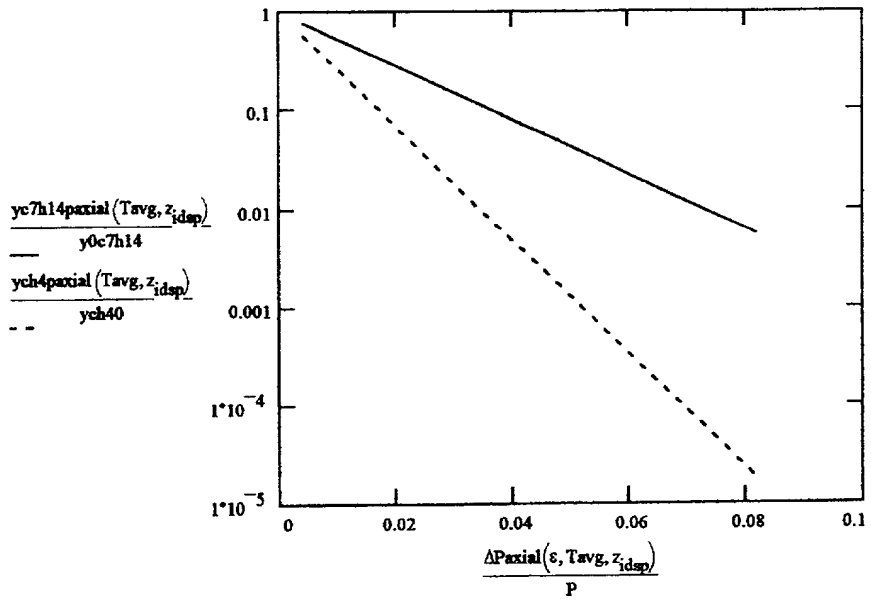

Pressure drop increases approximately with thesquare of flow velocity while conversion decreases exponentially

$U(Tavg) = 8.22528 \cdot m \cdot sec^{-1}$ $\quad zy := 2.32 \cdot cm$

$\frac{\Delta Paxial(\varepsilon, Tavg, zy)}{P} = 0.02000$ $\quad \frac{ych4paxial(Tavg, zy)}{ych40} = 0.06888284$ $\quad \frac{yc7h14paxial(Tavg, zy)}{y0c7h14} = 0.28038$

For flow perpendicular to the fixed bed, even with large catalyst particles, the equivalent pressure drop for high C7H14 conversion is very high. Even with ΔP/P = 2%, the C7H14 conversion is only 72%. For high conversion with practical fixed beds, the superficial bed flow rate must lower than about 3 m/sec to give high conversion with low ΔP

****

CAPSTONE PAGE [redacted]

****

Define Catalyst Functions:

$R = 82.07601 \cdot K^{-1} \cdot atm \cdot cm^3$ atm*cm3/mol*K

$TOL := 0.0001$ $Rcm := 83143000 \cdot gm \cdot cm^2 \cdot sec^{-2} \cdot K^{-1}$

$$\eta sph(\phi) := \frac{3}{\phi} \cdot \left(\frac{1}{\tanh(\phi)} - \frac{1}{\phi} \right)$$

$$\eta fpl(\phi) := \frac{\tanh(\phi)}{\phi}$$

****

Physical Properties for Pd/Al2O3 Washcoated cCatalyst

$Scat := 85 \cdot m^2 \cdot gm^{-1}$ $\rho catpart := 2.5 \cdot gm \cdot cm^{-3}$

$V\mu pore := 0.15 \cdot cm^3 \cdot gm^{-1}$

$Loat := 0.0020 \cdot cm$ $dpcat := 0.0002 \cdot cm$

Washcoat thickness - 20 microns Size of γ-Al2O3 particle within washcoat - 2 microns

$$d\mu pore := 6 \cdot \frac{V\mu pore}{Scat}$$ $\varepsilon\mu pore := 0.375$ $d\mu pore = 1.05882 \cdot 10^{-6} \cdot cm$

$\tau\mu pore := 3.0$

****

$$DeffCH4(x,T) := \frac{\frac{\varepsilon\mu pore}{\tau\mu pore}}{\left[\frac{1}{Dch4(x,T)} + \frac{3}{d\mu pore \cdot \sqrt{\frac{8}{\pi} \cdot \frac{R \cdot T}{MW_0}}} \right]}$$

$$d\mu pore \cdot \sqrt{\frac{8}{\pi} \cdot \frac{R \cdot Tin}{MW_0}} = 0.10953 \cdot sec^{-1} \cdot cm^2$$

$Dch4(.5, Tin) = 0.41195 \cdot sec^{-1} \cdot cm^2$

$DeffCH4(.5, Tin) = 0.00419 \cdot sec^{-1} \cdot cm^2$

$$DeffC7H14(x,T) := \frac{\frac{\varepsilon\mu pore}{\tau\mu pore}}{\left[\frac{1}{Dc7h14(x,T)} + \frac{3}{d\mu pore \cdot \sqrt{\frac{8}{\pi} \cdot \frac{R \cdot T}{MW_6}}} \right]}$$

$$d\mu pore \cdot \sqrt{\frac{8}{\pi} \cdot \frac{R \cdot Tin}{MW_6}} = 0.04428 \cdot sec^{-1} \cdot cm^2$$

$Dc7h14(.5, Tin) = 0.11846 \cdot sec^{-1} \cdot cm^2$

$DeffC7H14(0.5, Tin) = 0.00164 \cdot sec^{-1} \cdot cm^2$

$$DmacCH4(x,T) := \frac{0.4}{2.5} \cdot Dch4(x,T) \qquad DmacCH4(.5,800\cdot K) = 0.06442 \cdot sec^{-1} \cdot cm^2$$

$$DmacC7H14(x,T) := \frac{0.4}{2.5} \cdot Dc7h14(x,T) \qquad DmacC7H14(.5,800\cdot K) = 0.01851 \cdot sec^{-1} \cdot cm^2$$

$k0T := 0.01 \cdot gm^{-1} \cdot sec^{-1}$ Test value for k0T

Macropore porosity - 0.4 and tortuousity - 2.5

Microscopic Thiele Modulus for CH4

$$\phi\mu(k0T,x,T) := \sqrt{\left[\rho catpart \cdot \left(\frac{R\cdot T}{Pref}\right) \cdot \frac{k0T}{DeffCH4(x,T)}\right]} \cdot \frac{dpcat}{6} \qquad \phi\mu(k0T,.5,Tin) = 0.021$$

Macroscopic Thiele Modulus for CH4

$$\Phi mac(k0T,x,T) := \sqrt{\left[\rho catpart \cdot \left(\frac{R\cdot T}{Pref}\right) \cdot k0T\right] \cdot \frac{\eta sph(\phi\mu(k0T,x,T))}{DmacCH4(x,T)}} \cdot Lcat \qquad \Phi mac(k0T,ych40,Tin) = 0.31774$$

Microscopic Thiele Modulus for C7H14

$$\phi\mu7(k0T,x,T) := \sqrt{\left[\rho catpart \cdot \left(\frac{R\cdot T}{Pref}\right) \cdot \frac{k0T}{DeffC7H14(x,T)}\right]} \cdot \frac{dpcat}{6} \qquad \phi\mu7(k0T,.5,Tin) = 0.03357$$

Macroscopic Thiele Modulus for C7H14

$$\Phi mac7(k0T,x,T) := \sqrt{\left[\rho catpart \cdot \left(\frac{R\cdot T}{Pref}\right) \cdot k0T\right] \cdot \frac{\eta sph(\phi\mu7(k0T,x,T))}{DmacC7H14(x,T)}} \cdot Lcat \qquad \Phi mac7(k0T,ych40,Tin) = 0.59265$$

$$RatekCH4(k0T,x,T) := -\eta sph(\phi\mu(k0T,x,T)) \cdot \eta fpl(\Phi mac(k0T,x,T)) \cdot \left[\rho catpart \cdot \left(\frac{R\cdot T}{Pref}\right) \cdot k0T\right]$$

$$RatekCH4(k0T,0,Tin) = -1610.07113 \cdot sec^{-1}$$

$$RatekC7H14(k0T,x,T) := -\eta sph(\phi\mu7(k0T,x,T)) \cdot \eta fpl(\Phi mac7(k0T,x,T)) \cdot \left[\rho catpart \cdot \left(\frac{R\cdot T}{Pref}\right) \cdot k0T\right]$$

$$RatekC7H14(k0T,0,Tin) = -1492.98186 \cdot sec^{-1}$$

Defines transport restricted rate constant function given catalyst effective first order rate constant - k0T, methane or cyclohexane conversion - x, and surface temperature - T

****

[redacted]

****

$Ts := Tin$ $k0T = 0.01 \cdot sec^{-1} \cdot gm^{-1}$ $Tavg = 952.8725 \cdot K$

$kgpb(Tin, 0.1 \cdot cm) = 26.77306 \cdot sec^{-1} \cdot cm$ $RatekCH4(k0T, 0, Ts) = -1610.07113 \cdot sec^{-1}$ $Lcat = 0.002 \cdot cm$

$$Tin + \frac{kgpb(Tavg, 0.1 \cdot cm)}{\left[\left(\frac{kgpb(Tavg, .1 \cdot cm)}{-RatekCH4(k0T, 0, Ts) \cdot Lcat}\right) + 1\right]} \cdot \frac{ych40 \cdot -\Delta Hcomb(Tavg)}{h(Tavg, .1 \cdot cm)} \cdot \frac{P}{R \cdot Ts} = 840.46756 \cdot K$$

$Tout = 1094.817 \cdot K$

$xs := ych40$ $xs = 0.01183$ $Tin = 810.928 \cdot K$

$Rk := 6.33 \cdot m^{-2} \cdot sec^{-1}$ $Ratech4 := 0.036 \cdot m^{-2} \cdot sec^{-1}$ $k0T = 10 \cdot kg^{-1} \cdot sec^{-1}$

Set up subroutine/function to solve for the surface temperature given a rate constant

$TOL := 0.0001$ $ych40 = 0.01183$ $x := 0.01$

$Ts := 1673 \cdot K$ $Ts7 := 1473 \cdot K$

Given

$$Ts = Tin + \frac{y(ych40, x)_0 \cdot \frac{P}{R \cdot Ts}}{\frac{1}{-RatekCH4(k0T, x, Ts) \cdot Lcat} + \frac{1}{kgpb\left(Tin, \frac{Lhc}{100}\right)}} \cdot \frac{-\Delta Hcomb(Ts)}{h\left(Tin, \frac{Lhc}{100}\right)}$$

$Tshi(k0T) := Find(Ts)$ $Tshi(100 \cdot k0T) = 1010.10631 \cdot K$

Given

$$Ts7 = Tin + \frac{y7(y0c7h14, x)_6 \cdot \frac{P}{R \cdot Ts}}{\frac{1}{-RatekC7H14(k0T, x, Ts) \cdot Lcat} + \frac{1}{kgpb7\left(Tin, \frac{Lhc}{100}\right)}} \cdot \frac{-\Delta Hcomb7(Ts)}{h\left(Tin, \frac{Lhc}{100}\right)}$$

$Tshi7(k0T) := Find(Ts7)$ $Tshi7(100 \cdot k0T) = 873.32275 \cdot K$

$Rk := -RatekCH4(k0T, xs, Ts) \cdot Lcat$ $Rk7 := -RatekC7H14(k0T, xs, Ts) \cdot Lcat$

$Rk = 6.72632 \cdot sec^{-1} \cdot cm$ $Rk7 = 6.41773 \cdot sec^{-1} \cdot cm$ $k0T = 10 \cdot kg^{-1} \cdot sec^{-1}$

$$Ratech4 := \frac{xs \cdot \frac{P}{R \cdot Ts}}{\frac{1}{Rk} + \frac{1}{kgpb(Tin, Lhc)}}$$

$kgpb(Tin, Lhc) = 15.5934 \cdot sec^{-1} \cdot cm$ $Ratech4 = 0.01215 \cdot m^{-2} \cdot sec^{-1}$

$kgpb7(Tin, Lhc) = 4.50626 \cdot sec^{-1} \cdot cm$

$$Ts := Tin + Ratech4 \cdot \frac{-\Delta Hcomb(Ts)}{h(Tin, Lhc)} \cdot ych40$$

$Ratech4 = 0.01215 \cdot m^{-2} \cdot sec^{-1}$

$Rk = 6.72632 \cdot sec^{-1} \cdot cm$

$$xs := \frac{Ratech4}{Rk}$$

$Ts = 811.4626 \cdot K$ $xs = 0.18057 \cdot m^{-3}$ $Tin = 810.928 \cdot K$

$k0T = 10 \cdot kg^{-1} \cdot sec^{-1}$ $Tshi(100 \cdot k0T) = 1010.10631 \cdot K$ $Tshi(0.01 \cdot kg^{-1} \cdot sec^{-1}) = 810.96346 \cdot K$

$Tshi7(100 \cdot k0T) = 873.32275 \cdot K$ $Tshi7(0.01 \cdot kg^{-1} \cdot sec^{-1}) = 810.96393 \cdot K$

$xn := 0, 1 .. 30$

$k0Tcalc_{xn} := 10^{-1+\frac{xn}{5}} \cdot kg^{-1} \cdot sec^{-1}$ $Tsurf_{xn} = Tshi(k0Tcalc_{xn})$ $Tsurf7_{xn} = Tshi7(k0Tcalc_{xn})$

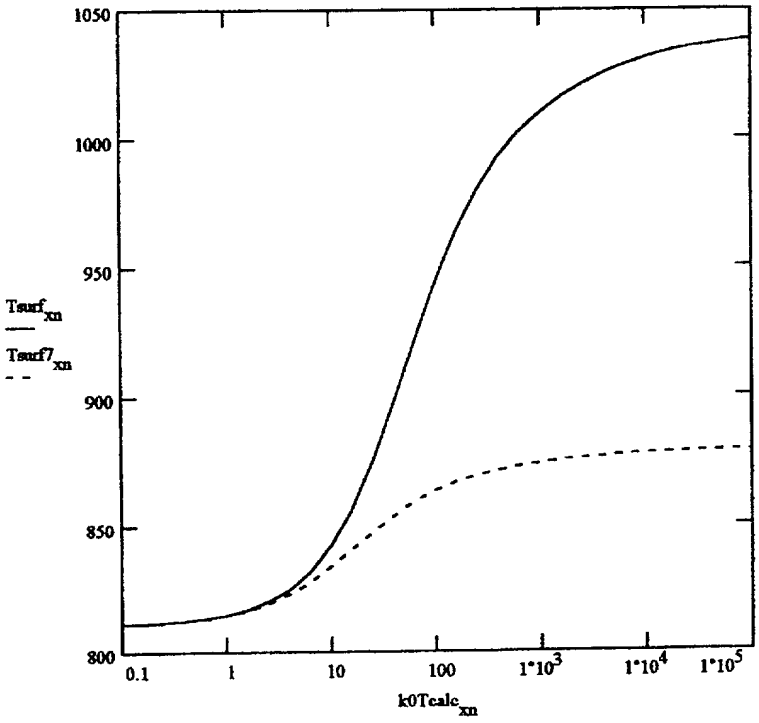

This plot shows the surface temperature within a honeycomb channel as a function of the specific catalytic rate constant for methane and methylcyclohexane combustion at a location within 1-mm of the leading edge

Takes into account the internal pore diffusion (micro- and macropores) and boundary layer heat and mass transport. Upper surface temperature limit approaches the adiabatic temperature for methane and a much lower (Prater) temperature for C7H14

k0 unit - sec^-1 per kg washcoat
T unit - K

We can also determine the actual effective first order rate constants for methane, propane, and other fuels and estimate the temperatures required for catalytic light-off and extinction, with roughly estimated Nu numbers.

Other factors, such as the upstream surface temperature and gas phase radial temperature profile and thermal conduction of the catalyst wall, can also effect the light-off and and the critical extinction points. These calculations are beyond the scope of the current analysis.

****

CAPSTONE MCU [redacted]

****

PdO Catalyst Rate Constants

$Erpd0 := 12800 \cdot K$ $Erpd1 := 4900 \cdot K$ $Erpd3 := 15000 \cdot K$

Region0 - low T PdO to 625K ignores inhibition by H2O and CO2

Region1 - Intermediate T 625K to 909K

Region2 - Flat 909K to 1048K decomposition

Region3 - Pd metal

$$Apd0 := 2.4 \cdot 10^3 \cdot 200 \cdot gm^{-1} \cdot sec^{-1}$$

$$Apd1 := Apd0 \cdot \exp\left(-\frac{Erpd0}{625 \cdot K} + \frac{Erpd1}{625 \cdot K}\right) \qquad Apd2 := Apd1 \cdot \exp\left(\frac{-Erpd1}{909.1 \cdot K}\right)$$

$$Apd3 := Apd2 \cdot \exp\left(\frac{Erpd3}{1048.1 \cdot K}\right)$$

Interpolation formula for the four PdO+Pd rate constants

$$kpd(T) := \left[Apd3^2 \cdot \exp\left(-\frac{2 \cdot Erpd3}{T}\right) + \frac{1}{\left(Apd2^{-2} + Apd1^{-2} \cdot \exp\left(\frac{2 \cdot Erpd1}{T}\right) + Apd0^{-2} \cdot \exp\left(\frac{2 \cdot Erpd0}{T}\right)\right)} \right]^{0.5}$$

****

$nx := 0, 1 .. 41$ $T_{nx} := 500 \cdot K + nx \cdot 25 \cdot K$

CATALYTIC RATE CONSTANT NEEDED FOR HEAT BALANCE IN A MONOLITH WITH FULLY DEVELOPED FLOW

Compared with extrapolated but measured rate constants (mol/atmCH4/s/gcat)

$Lcat = 0.00002 \cdot m$

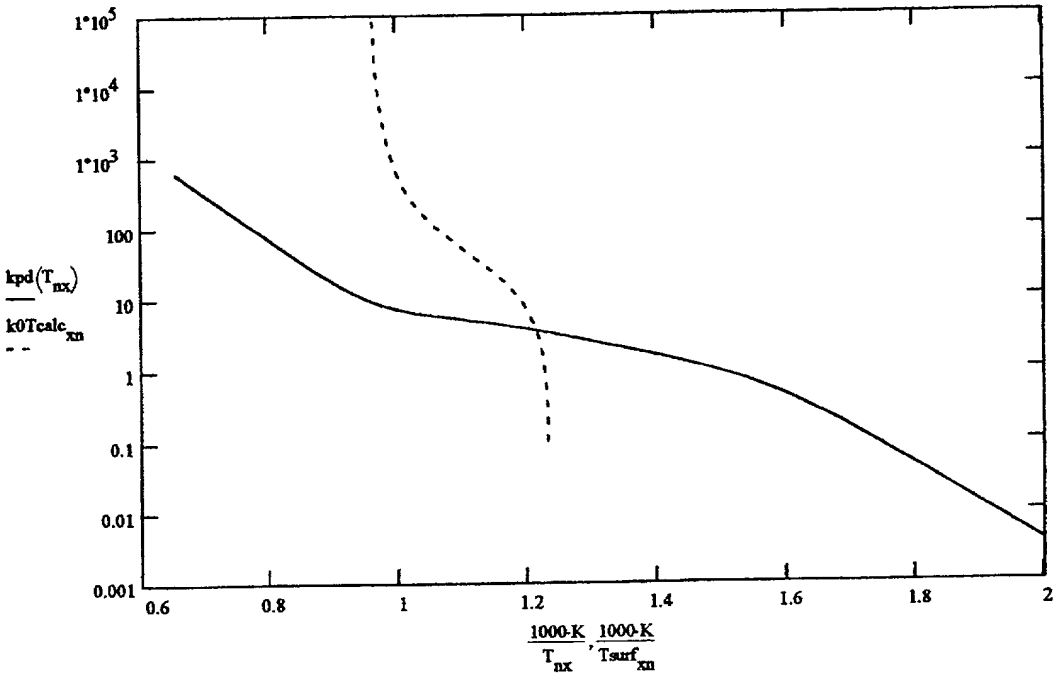

[redacted]

Compared with extrapolated and estimated rate constants for C7H14 (10x mol/atmCH4/s/gcat)

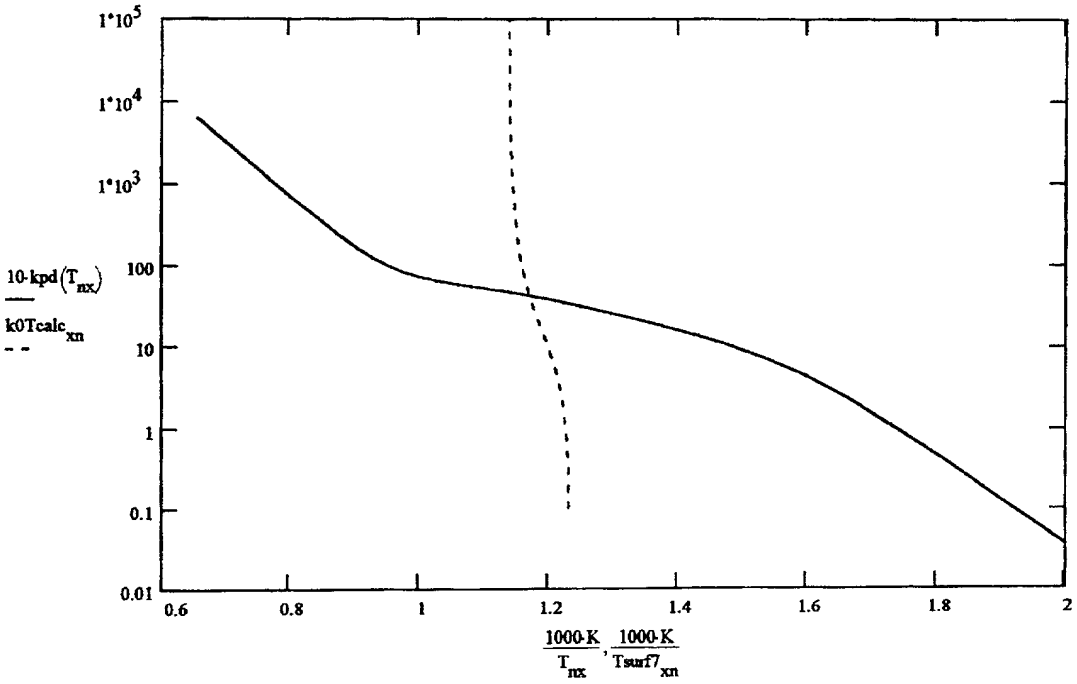

Define functions to calculate surface temperature profiles given gas temperature and composition

TOL := 0.1 Ts = 811.4626·K

Tsx := 1500·K Tsx7 := 1400·K

x = 0.01

$$\frac{1}{-\text{RatekCH4}(\text{kpd}(\text{Tsx}),x,\text{Tsx})\cdot\text{Lcat}}+\frac{1}{\text{kgpb}(\text{Tin},\text{Lhc})}=7.01896\cdot m^{-1}\cdot s$$

Given

$$\text{Tsx}=\text{Tin}+\frac{y(\text{ych40},x)_0\cdot\frac{P}{R\cdot\text{Tsx}}}{\frac{1}{-\text{RatekCH4}(\text{kpd}(\text{Tsx}),x,\text{Tsx})\cdot\text{Lcat}}+\frac{1}{\text{kgpb}(\text{Tin},z)}}\cdot\frac{-\Delta\text{Hcomb}(\text{Tsx})}{h(\text{Tin},z)}$$

Tsrf(Tin, x, z) := Find(Tsx)

Tsch4x := Tsrf(Tin, x, 0.1·cm) Z inlet = 0.1 cm

Tsch4x = 823.23891·K Tin = 810.928·K x = 0.01 Lcat = 0.002·cm $y(\text{ych40},x)_0 = 0.01171$

kpd(Tsch4x) = 3.51311·kg^-1·sec^-1

kgpb(Tin, 0.1·cm) = 26.77306·sec^-1·cm -RatekCH4(kpd(Tsch4x), x, Tsch4x)·Lcat = 1.17316·sec^-1·cm

[redacted]

Given

$$Tsx7 = Tin + \frac{y7(y0c7h14,x)_6 \cdot \frac{P}{R \cdot Tsx7}}{\frac{1}{-RatekC7H14(10 \cdot kpd(Tsx7),x,Tsx7) \cdot Lcat} + \frac{1}{kgpb7(Tin,z)}} \cdot \frac{-\Delta Hcomb7(Tsx7)}{h(Tin,z)}$$

$Tsrf7(Tin,x,z) := Find(Tsx7)$

$Tsc7h14x := Tsrf7(Tin,x,0.1 \cdot cm)$ Z inlet = 0.1 cm

$Tsc7h14x = 871.51735 \cdot K$ $Tin = 810.928 \cdot K$ $x = 0.01$ $Lcat = 0.002 \cdot cm$ $y(ych40,x)_0 = 0.01171$

$10 \cdot kpd(Tsc7h14x) = 44.23122 \cdot kg^{-1} \cdot sec^{-1}$ $-RatekC7H14(10 \cdot kpd(Tsch4x),x,Tsc7h14x) \cdot Lcat = 9.21644 \cdot sec^{-1} \cdot cm$

$kgpb7(Tin,0.1 \cdot cm) = 12.3599 \cdot sec^{-1} \cdot cm$

Assuming the rate constant for C7H14 combustion is ten times the rate constant for CH4 combustion, the surface temperature near the inlet (1-mm in) is 871.5 K (1100F) and near the transport limit for C7H14 and 823.2K (1050F) and surface rate controlled for CH4. If this calculation is repeated for a series of steps downstream with corrections to the gas phase concentrations and temperatures, new surface temperatures and rates can be calculated throught the length of the monolith.

****